DIRECT DESIGN FOR

MULTIPLE LOAD CASES

(Reinforced and Partially Prestressed Concrete Beams

Under Combined Bending and Torsional Loads)

by

JALEL MOUSSA

Ingenieur en Genie Civil

Ecole Nationale Polytechnique d' Alger.

A Thesis Submitted for the Degree of

Master of Science.

Department of Civil Engineering,

University of Glasgow.

January, 1988.

بسم الله الرحمن الرحيم

IN THE NAME OF ALLAH, THE MOST MERCIFUL,

THE MOST GRACIOUS

E R R A T U M

PAGE	LINE	READ	INSTEAD OF
4	7	Web	Face
7	3	Subsequently	Consequently
8	11	For	Of
13	28	Forces	Results
51	23	According	Owing
66	16	Partially prestressed	Partially
85	10	Length	Dimension
85	18	Cases	Case

TO MY PARENTS

CONTENTS

ACKNOWLEDGEMENTS

The work described herein was carried out in the Department of Civil Engineering at the University of Glasgow, under the general guidance of Professor A. Coull.

The author would like to express his appreciation to Professor A. Coull and Dr. D. R. Green for the facilities of the department.

The author is greatly indebted to Dr. P. Bhatt for his valuable supervision, encouragement and advice during the course of this study.

My grateful thanks are also due to:

* The laboratory technicians for assisting in the experimental work and for all the tedious work involved in the preparation of the test specimens. In particular, Messrs A. Burnett, J. Tompson, R. Thornton, I. Todd, R. Hawthorn, B. Tompson, A. Yuill, R. Rodrick, I. Gardner and A. Gray.

* My friend R. Saadi for his help in the experimental work and with the computer program.

* My friends Z. Merouani, M. Souici, A. Bouazza, S. Murthi, F.Abidi for their useful discussions and comments.

* My friends A. Dlim, D. Abderrahmane, R.M Seridi, R. Manaa, T.Boumerfeg, M. Benredouane, M. Bendahgane, and S. Djellab for their encouragement.

* The C.N.E.R.I.B. and the British Council for the financial support during the period of the research.

* The staff of the general direction of C.N.E.R.I.B. for their encouragement and trust.

* Dar El Arkam's family.

Finally, my special thanks are reserved for my family for their boundless patience and continuous encouragement throughout the years.

SUMMARY

This thesis reports experimental and theoretical investigations on reinforced and partially prestressed concrete beams subjected to multiple combinations of bending and torsional loads. The beams were idealised as hollow beams with the walls in a state of plane stress. Elastic stress field at ultimate load in conjuction with a yield criterion was used to obtain the required quantities of reinforcement. The type of yield criteria adopted in this study is the classical ultimate limit capacity concept originated by Nielsen.

The experimental study consisted of testing four reinforced concrete beams and two partially prestressed concrete beams. All the beams were 300mm square and hollow. The parameters investigated were load combinations and load history. The test results indicate that the adopted approach satisfactorily predicts the ultimate strength of the beams under multiple combinations of bending and torsional loads. A plane stress finite element program was used to carry out a non–linear analysis of the experimental test beams. Good agreement was obtained between theoretical results assuming monotonic proportional loading and the overall behaviour of tested beams.

LIST OF NOTATIONS

A_o	Cross-sectional area enclosed by centre-line of stirrups or beam wall
A_1	Area bounded by the lines connecting the centres of the corner longitudinal bars
A_2	Area bounded by the centreline of the shear flow
A_s	Cross-sectional area of one stringer
A_{sl}	Total cross-sectional area of longitudinal steel
Asl,t	Cross-sectional area of top longitudinal steel
$A_{sl,b}$	Cross-sectional area of bottom longitudinal steel
A_{sv}	Area of stirrup leg
A_x	Area of steel per unit length in x direction
A_{xp}	Area of prestressing wires
A_{xr}	Area of additional reinforcement
A_y , A_{yr}	Area of steel per unit length in y direction
a_{cr}	Depth of crack to surface of nearest longitudunal bar
a'	Distance from compression face to point at which crackwidth is considered
[B]	Strain matrix
$[B]^T$	Transpose of strain matrix
b_t	Width of the section at the centroid of the tension steel
C	Torsional second moment of inertia
c	Concrete cover
c_{min}	Minimum concrete cover to tension steel
[D]	Material elastic property matrix
d	Effective depth
d_f	Displacement on front web of beam
d_r	Displacement on rear web of beam

$\{d\}$	Nodal displacement
E_c	Modulus of elasticity of concrete
E_s	Elastic modulus of steel
$E_c.I_{cr}$	Flexural rigidity
e	Eccentricity
F	force
F(T)	Stringer force due to torsion
F(M)	Stringer force due to bending
$\{F^{ex}\}$	Remedial force vector
f_{cu}	Compressive cube strength of concrete
f_c'	Compressive cylinder strength of concrete
f_{pe}	effective stress of prestressing wires
f_{py}	Yield stress of steel in prestressing wires
f_t	Tensile strength of concrete
f_s	Yield stress of steel in tension
f_s'	Yield stress of steel in compression
f_{yl}	Yield stress of longitudinal steel (stringers)
f_{yv}	Yield stress of stirrups
f_x, f_y	Yield stress of steel in x and y axis
f_r	Modulus of rupture for concrete
G	Shear modulus of concrete
GC	Pre-cracking torsional rigidity
GC_{cr}	Post-cracking torsional rigidity
H	Force in longitudinal bars
I_{eff}	Effective second moment of inertia
I_g	Gross second moment of inertia
I_{cr}	Post-cracking flexural second moment of inertia
K	Ratio of depth in compression/depth of the section
[K]	Structural stiffness matrix
$[K^{-1}]$	Inverse of structural stiffness matrix

K_o	Constant depending on loading and end constraint condition of beam
K^*	Ratio of depth in compression to total depth of section
K_{MM}	Flexural rigidity due to bending
K_{MT}	Flexural rigidity due to torsion
K_{TT}	Torsional rigidity
L	Span of beam
M	Applied bending moment
M_{cr}	Bending moment at first cracking
M_u	Ultimate bending moment
M_x	Midspan moment
m	Ratio of tensile to compressive strength of concrete
N_x	Applied in-plane force per unit width in x direction
N_x^s	Steel force in x direction
N_{xy}	Applied shear force per unit width
N_y	Applied in-plane force per unit width in y direction
N_y^s	Steel force in y direction
n	Modular ratio
n^*	Effective modular ratio
P	Axial load
{P}	External load vector
$\{P_{n+1}\}$	Load vector at present stage of loading
P_d	Design load
q	Shear flow
R_f	Diagonal compression resultant force on flange of beam
R_w	Diagonal compression resultant force on web of beam
1/R	Curvature
r	Ratio of area of longitudinal/transverse steel in section
r_L	Ratio of area of top/bottom flange longitudinal bars

S_v	Spacing of stirrups
T	Applied torsion
T_b	Bending component of applied torsion
T_t	Torsional component of applied torque
T_c	Torque resisted by concrete
T_u	Ultimate torsion
t	Thickness of element or beam wall
u	Perimeter of stirrup centreline
W_{max}	Maximum crackwidth
d^2w/dz^2	Curvature
x	Width of rectangular beam section
x_1	Width of stirrup centre-line for rectangular beam section
X,Y,Z	Global coordinates
y	Depth of rectangular beam section
y_1	Depth of stirrup centre-line for rectangular beam section
y_o	Distance from extreme compression fibre to neutral axis
y_t	Distance from the neutral axis to the tension face
z	Distance along beam length
α	St Venant's coefficient
α_p	Nadai's coefficient
α_t	$0.66 + 0.33.y_1/x_1 \leqslant 1.5$
β	Angle of inclination of concrete struts
Δ	Vertical displacement
$\{\Delta P\}$	Incremental load vector
$\{\Delta\delta_i\},\{\Delta\delta_n\}$	Incremental displacement vector
$\{\delta_{i+1}\},\{\delta_{n+1}\}$	Total displacement vector at present loading
$\{\Delta\epsilon_i\},\{\Delta\epsilon_n\}$	Incremental strain vector i^{th} & n^{th} iteration
$\{\Delta\sigma_i\},\{\Delta\sigma_n\}$	Incremental stress vector i^{th} & n^{th} iteration
ϵ	Strain
ϵ_l	Longitudinal steel strain

$\epsilon_{l,av}$	Average longitudinal steel strain
$\epsilon_{l,b}$	Bottom flange longitudinal steel strain
$\epsilon_{l,t}$	Top flange longitudinal steel strain
ϵ_v	Stirrup strains
ϵ_m	Average strain with stiffening effect of concrete at the tension zone
ϵ_1	Strain at the level considered, calculated ignoring the stiffening effect of the concrete in the tension zone
$\{\epsilon_0\}$	Initial strain vector
$\{\epsilon_i\},\{\epsilon_n\}$	Strain vector at previous loading i^{th} & n^{th} iteration
$\{\epsilon_{i+1}\},\{\epsilon_{n+1}\}$	Total strain vector at present loading
θ	Angle of cracks to beam axis
σ	Normal stress
σ_x, σ_y	Normal in-plane stress in x and y directions
σ_1, σ_2	Major and minor principal stress
σ_c	Diagonal concrete stress
$\{\sigma_0\}$	Initial stress vector
$\{\sigma_i\},\{\sigma_n\}$	Stress vector at previous loading i^{th} & n^{th} iteration
$\{\sigma_{i+1}\},\{\sigma_{n+1}\}$	Total stress vector at present loading
σ_{pb}	Prestressing stress in bottom flange
σ_{pt}	Prestressing stress in top flange
τ	Shear stress
τ_t	Maximum torsional shear stress
τ_{xy}	Shear stress in x-y axis
Φ	Ratio of torsion to bending moment
ψ	Angle of twist
$d\psi/dz$	Rate of twist

CHAPTER 1

INTRODUCTION

Beams in practice are subjected to many types of loads like axial and shear forces, bending and twisting moments, etc. In general the beam is subjected to multiple load cases which result in non-proportional load sequences. However strength determination in usual structural engineering practice is based on failure under monotonically increasing, proportional loadings. The effects of non proportional load sequences are largely ignored.

In the case of beams subjected to combined bending and torsion, considerable work has been done using proportional loading. The aim of the present study is to extend this to non proportional combined bending and torsional load cases.

The study was confined to a short experimental programme of tests on 300mm square hollow beams subjected to non proportional combined bending and torsional load cases. The beams were designed according to the classical limit state concept such that the beams resisted any combination of non proportional loads. Both reinforced and partially prestressed concrete beams were tested. The results appear to indicate that the classical limit state concept called Direct Design Approach is adequate for the design of beams subjected to non proportional loads.

The thesis is organized in seven chapters. Chapter two is a review of torsion and torsion combined with bending applied to reinforced concrete beams. In chapter three is presented the method of design adopted, and its application for designing beams subjected to non proportional combination of bending and torsional load cases. Experimental set up and test programme are described in chapter four. The experimental results and their discussion are presented in chapter five. In chapter six is presented the 2-D non linear finite element program used to analyse the reinforced concrete beams tested. The analysis to determine the overall behaviour of beams under multiple loading was done assuming monotonically

increasing, proportional loadings. Finally, conclusions and recommendations for future work are presented in chapter seven.

CHAPTER 2

REVIEW OF PREVIOUS INVESTIGATIONS

2.1 INTRODUCTION

Considerable amount of work has been done on beams subjected to torsion and torsion combined with bending. A detailed review of the state of the art is given in publications by Cowan[7] and Hsu[1].

In this chapter is presented a brief summary of research findings dealing with torsion and torsion combined with bending.

2.2 TORSION

Torsion is a major factor to consider in the design of many kinds of reinforced concrete structures, especially reinforced concrete beams. Torsion is generally a secondary effect in reinforced and prestressed concrete buildings, it occurs as a consequence of compatibility requirements as in grid systems. The reduction of torsional stiffness due to cracking does not necessarily lead to collapse but merely to a redistribution of the loads in the structure. When torsion arises as a primary effect, redistribution of load paths is not possible. It is therefore necessary to design the member to resist the effect of torsional forces.

2.2.1 *Experimental Investigations*

During the past five decades, detailed experimental programmes were undertaken to understand the behaviour of members subjected to torsion. Hsu and Mo[17,18,19] listed 108 tests on reinforced concrete beams and 50 tests on prestressed concrete beams subjected to torsion available in the literature.

Before cracking, torsion is resisted by plain concrete alone. Failure was generally assumed to occur when the maximum tensile stress due to shear reaches

the tensile strength of concrete. In plain concrete members subjected to pure torsion, the beam fails by the formation of helical cracks inclined at 45° as shown in figure 2.1.(a). Hsu reexamined the mechanism of failure with the aid of a high–speed movie camera at a speed of 1,200 frames per second. The film projection speed was 20 frames per second, thus the failure process was slowed down and clearly observed. The movie showed that the first crack, which is inclined at 45° to the axis of the beam, appeared on the front face. It gradually widened and progressed accross the top of the beam. Until, finally, the concrete crushed on the back face. This failure process and the study of the failure surface as shown in figure 2.1.(b) revealed a bending–type failure.

For reinforced concrete beams, the stiffness of the section decreases rapidly after cracking. But the ultimate strength is considerably increased over that of plain concrete beams and large plastic deformations has been observed[1]. The post–cracking stiffness of reinforced concrete beams depends on the amount and disposition of the reinforcing steel.

2.2.2 *Theoretical Approach*

2.2.2.1 *Pre–cracking strength of section subjected to pure torsion*

The study of the behaviour of reinforced concrete beams under torsion at pre–cracking is based on plain concrete sections, because the contribution of reinforcing steel at this stage is negligeable. Three theories are used to predict the torsional strength of plain concrete members. These are the elastic theory, the plastic theory and the skew–bending theory.

a) Elastic Theory [1,7]

St.Venant's classical solution predicts reasonably well the torsional strength of plain concrete beams. In applying this theory, it is assumed that torsional failure of plain concrete member occurs when the maximum principal tensile stress equals

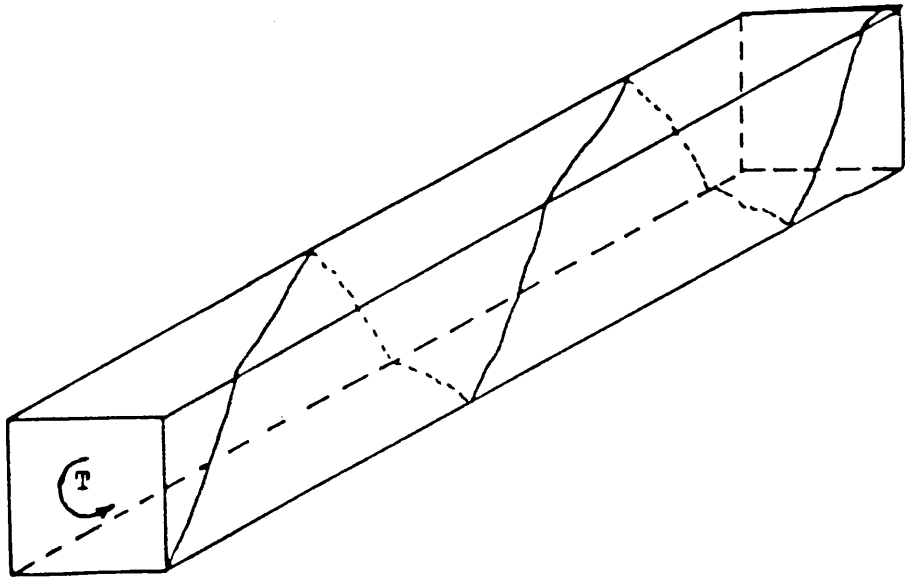

Figure 2.1.a Helical Crack on plain Concrete Beam under pure Torsion .

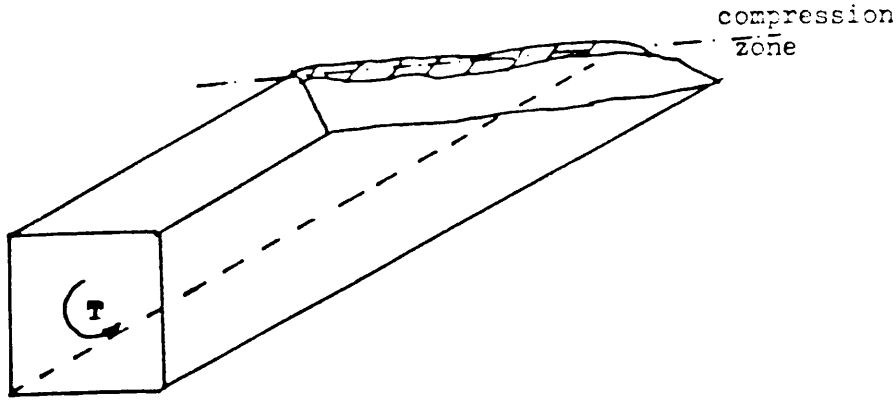

Figure 2.1.b Skew Bending surface of rectangular section subjected to pure Torsion .

the tensile strength or torsional shear strength of concrete. In a rectangular section, the maximum shear stresses occur on the periphery at the middle of the longer sides of the beam. The applied torque is expressed as :

$$T = \alpha.x^2.y.\tau_t$$

where α = St.Venant's coefficient depending on the ratio y/x .

x,y = cross–sectional dimensions $y > x$.

τ_t = maximum torsional shear stress.

The elastic theory when compared with test results indicate that the theory underestimates the ultimate strength of plain concrete members. The test strength is approximately 50 % greater than that predicted by theory[1]. This is due to the limited ductility of concrete which allows a certain amount of redistribution of stresses.

b) Plastic Theory [1]

In this case we assume that concrete is a ductile material, then the strength of concrete beams can be estimated from plastic analysis. Similar to elastic theory, failure was assumed to occur when maximum principal tensile stress reaches the tensile strength of concrete. Assuming full plasticity, the plastic failure torque, T, can be expressed by :

$$T = \alpha_p.x^2.y.t \qquad (2.2)$$

Where $\alpha_p = (0.5 - x/(6.y))$, α_p is approximately 50 % greater than α used in the elastic theory. Thus the plastic theory explains the reason for the extra strength underestimated by the elastic theory.

The plastic theory, however has the following weaknesses :

1) Principal tension is the cause of torsional beam failure, but no significant plastic behaviour has been observed in test of tensile strength of concrete.

2) Torsional failure of plain concrete members is quite brittle. There is no sign of a plastic rotation.

3) The theory cannot account for a size effect. Tests results indicate that for small sections, the calculated plastic torques are smaller than test values, whereas the

opposite is the case for large sections.

c) Skew–Bending Theory [1]

The previous theories are unsatisfactory because they do not predict the ultimate strength of plain concrete beams under torsion. Hsu surmised that the failure criterion used in these theories may be incorrect. Consequently he developed a new theory based on the observed skew–bending failure. He assumed that failure is reached when the tensile stress induced by a 45° bending component of torque on the wider face of beam is equal to the modulus of rupture of the material. Figure 2.2 shows the applied torque resolved into two components acting on the failure surface. These are the bending component, T_b , which is assumed to be responsible for the observed bending type failure and the torsional component, T_t. According to Skew–Bending theory. T_b can be defined as follow :

$$T_b = T.\cos\theta = (x^2.y/6).\mathrm{cosec}\,\theta.f_r \qquad (2.3)$$

Where θ = angle between tensile cracks on wider face and axis of beam.

f_r = modulus of rupture of concrete.

$$T = (x^2.y/3).f_r.\mathrm{cosec}2\theta \qquad (2.4)$$

To find the minimum torsional strength, we differentiate equation (2.4) with respect to θ and equate it to zero :

$$dT/d\theta = (x^2.y/3).f_r.(2.\cot 2\theta.\mathrm{cosec}2\theta) = 0$$

A minimum value is obtained when $\theta = 45°$. Therefore substituting $\theta = 45°$ into equation (2.4)

$$T = (x^2.y/3).f_r \qquad (2.5)$$

It is noticed in equation (2.5) that the effect of the twisting component, T_t , is not considered. According to tests by McHenry and Kerni[8], a perpendicular compressive stress of equal magnitude due to T_t will reduce the tensile strength of concrete by 15%. Since bending failure in plain concrete is due to tension, the modulus of rupture in equation (2.5) should also be reduced by 15%. Thus equation (2.5) becomes :

$$T = (x^2.y/3).(0.85.f_r) \qquad (2.6)$$

Comparison of the equations provided by these three theories shows that they all are functions of the same parameter $x^2.y$. They differ only in the non dimensional coefficients (α,α_p) and in the material constants. In the elastic and plastic theories, the material constant is the direct tensile strength of concrete, f_t . In the Skew–Bending theory, it is the reduced modulus of rupture ($0.85f_r$). A comparison of the coefficients is shown in figure 2.3. It can be seen that the St.Venant's coefficient in the elastic theory and Nadai's coefficient in the plastic theory are functions of y/x . Whereas the coefficient in the Skew–Bending theory is a constant of 1/3 which lies between St.Venant's and Nadai's coefficients.

d) Thin Walled Tube Theory [21]

The shear stress near the perimeter is mainly responsible of the torsional resistance of a member, because it has the largest lever arm. For this reason it is helpful to approximate the solid section as a thin–walled hollow tube. According to Bredt's thin tube theory, the maximum torque to be resisted by the section can be expressed as :

$$T = 2.A_o.t.\tau_t \qquad (2.7)$$

Where A_o = area enclosed by the 'centreline' of cross–section of the tube.

t = thickness of the tube wall.

If the tube has re– entrant corners as shown in figure 2.4, then a considerable stress concentration may take place at the corners, but equation 2.7 ignores this fact. The stiffness relationship for the thin–walled section is given as :

$$T = G.C.d\psi/dz \qquad (2.8)$$

In which C = torsional inertia defined as $4.A_o^2.t/u$

u = perimeter of the section centreline.

G = shear modulus of concrete.

$d\psi/dz$ = rate of twist.

z = distance along the beam.

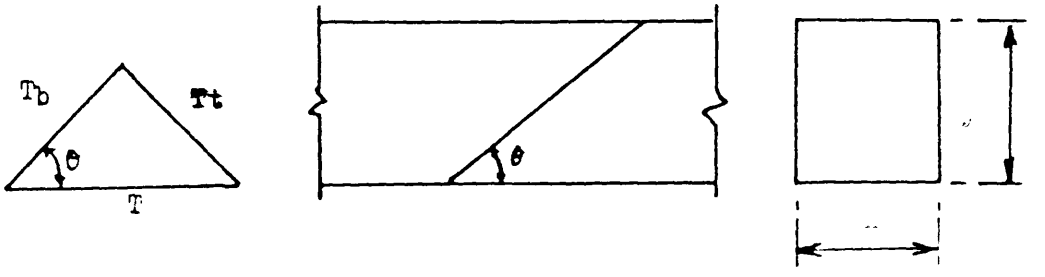

Figure 2.2 Components of applied Torque. (a) Tb - Bending component (b) Tt - Torsion component.

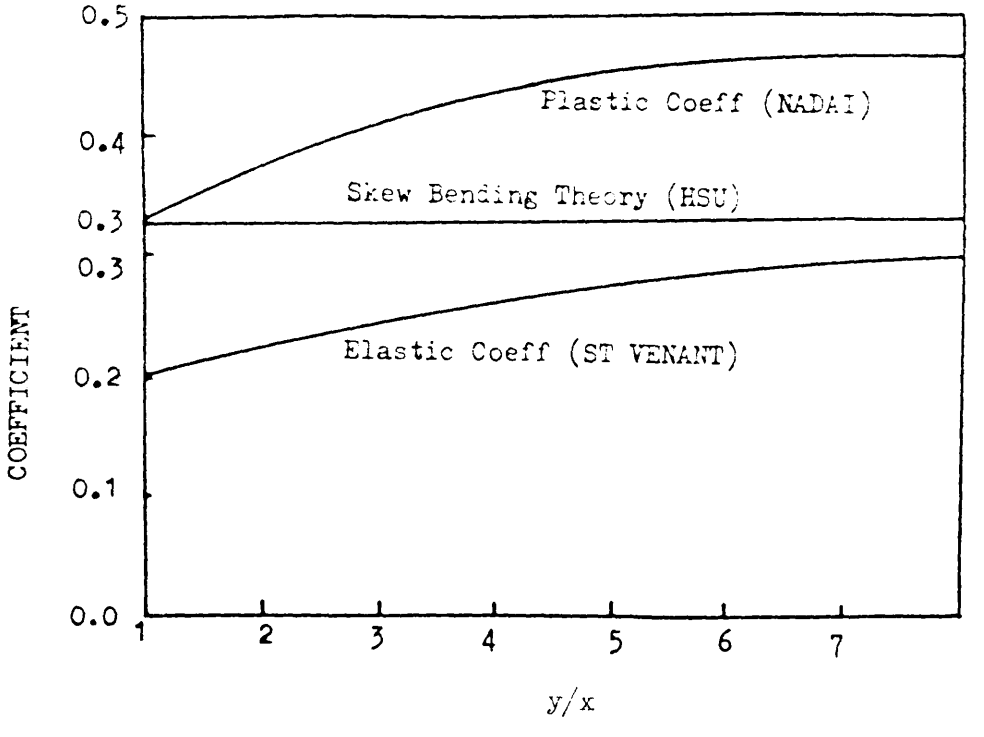

Figure 2.3 Comparison of Stress coefficient for Elastic, Plastic and Skew Bending Theories.

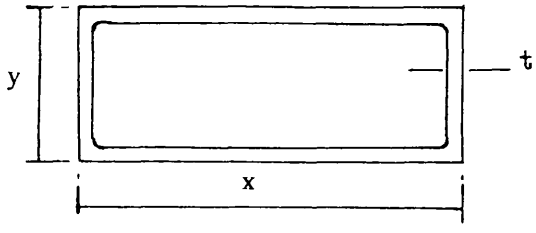

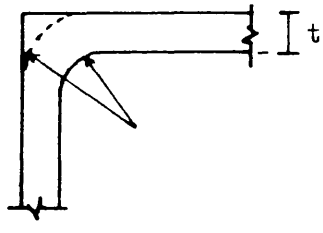

Figure 2.4 Rectangular Tube with re–entrant corners.

2.2.2.2 *Post cracking behaviour of beams subjected to torsion*

In practice, the shear reinforcement is provided most conveniently in the form of longitudinal bars and vertical stirrups. The stirrups resist the vertical component of the diagonal tension, and the longitudinal bars resist the horizontal component as shown in figure 2.5, while concrete sustains diagonal compressive forces parallel to the cracks. This behaviour is similar to that of the classical space truss model. Tests carried out till now are in good agreement with the fact that reinforcing steel in association with concrete is required to resist torsion i.e the diagonal concrete struts are needed. This approach forms the basis of the British code (BS 8110)[9] recommendations for torsional design.

Many models have been developed for calculating the torsional strength of members with both longitudinal steel and stirrups. These models can be divided in two types: The truss analogy model and the skew–bending model.

A) Space Truss Model [10,11,12,13]

The space truss method is based on the idealisation of a reinforced concrete beam as a space truss, consisting of longitudinal bars called stringers acting as compression or tension chords, and stirrups called ties. The cracked concrete acts as compression diagonals. Figure 2.6 shows a typical space truss model.

The space truss model is based on the following assumptions :

1. Longitudinal and transverse steel carry only axial tension; i.e., the shear forces carried by dowel action of the reinforcement are neglected.
2. The tensile strength of concrete is neglected.
3. For a solid section subjected to torsion, the concrete core does not contribute to the torsional resistance.
4. All reinforcing steel passing through the failure surface have reached their respective yield strength.

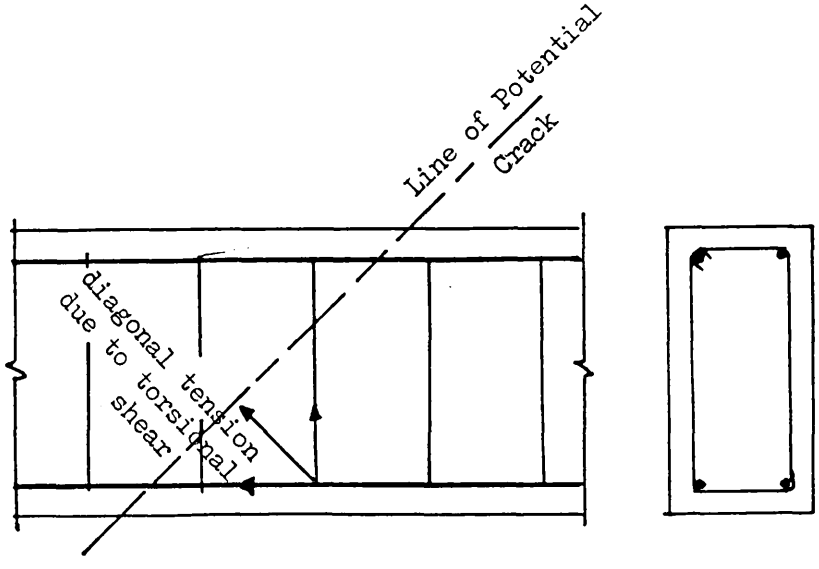

Figure 2.5 Vertical hoops and longitudinal bars used as torsional shear reinforcement. The longitudinal bars resist the horizontal component and the hoops the vertical component of the diagonal tension.

To obtain a lower bound solution for any applied load, a statically admissible state of stress not violating the yield criterion should exist. This means that the applied and resisting forces in the reinforcing steel cannot exceed the yield forces nor can the stress in the concrete strut be greater than the compressive stress of concrete f_{cu}.

Consider the freebody diagrams shown in figure 2.6. The cross–section is considered to be symmetrical about the Z– axis. The longitudinal steel forces are assumed to be concentrated in the stringers with force ($H = A_s.f_{yl}$) at the corners. The stirrup reinforcement is taken to be constant on all sides of the beam.

Under torsion, a constant shear flow q, will develop in the wall of the box section. It can be expressed as :

$$q = T/(2.A_o) \qquad (2.9)$$

The uniformly distributed concrete stress σ_c is inclined at an angle θ to beam axis, see figure 2.6.a . The diagonal stress is represented by a compression resultant force R_f and R_w on the flange and web of the beam respectively.

The resultant force R_w is given in terms of shear flow q as :

$$R_w.\sin\theta = q.y_1$$

$$R_w = q.y_1/\sin\theta \qquad (2.10.a)$$

Similarly, R_f is obtained as

$$R_f = q.x_1/\sin\theta$$

Where y_1 , x_1 are the depth and width of stirrup legs.

Taking a section perpendicular to the struts, from equilibrium the following relations are obtained :

$$R_w = \sigma_c.t.y_1.\cos\theta$$

$$\sigma_c = R_w/(t.y_1.\cos\theta) = q.y_1/(t.y_1.\cos\theta.\sin\theta)$$

$$\sigma_c.t = q/(\sin\theta.\cos\theta) \qquad (2.10.b)$$

Assuming all the stringers are equal in cross–sectional area, the force in each stringer H is obtained from the contribution of horizontal components of results R_f and R_w on the flange and web of the section respectively.

$$H = (1/2)(R_w + R_f).\cos\theta$$

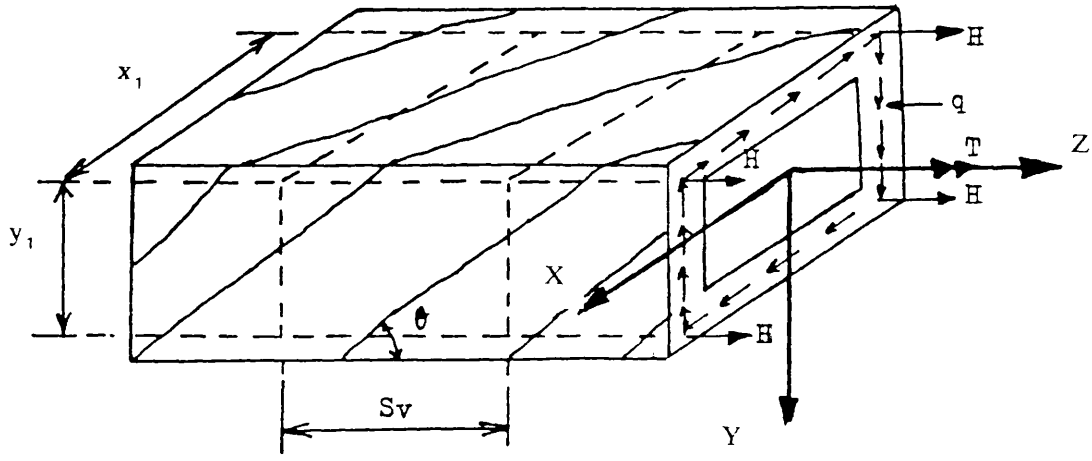

Figure 2.6 Space Truss Model for Torsion.

But $R_w = q.y_1/\sin\theta$, $R_f = q.x_1/\sin\theta$ (equation 2.10.a)

Hence

$H = (1/2).q.(y_1 + x_1).\cos\theta/\sin\theta$

$H = A_s.f_{yl} = (1/2).(y_1 + x_1).q.\cot\theta$ (2.11)

Where A_s, f_{yl} : Area and yield stress of one stringer.

According to figure 2.6.b , the force in a stirrup is expressed as :

$\sigma_c.t.\sin^2\theta.s_v = A_{sv}.f_{yv}$

Where A_{sv}, f_{yv} : Area and yield stress of stirrup leg

s_v : Spacing of stirrups

Substituting for $\sigma_c.t$ from equa 2.10.a we get

$(q.\sin^2\theta/\sin\theta.\cos\theta).s_v = A_{sv}.f_{yv}$

Therefore

$A_{sv}.f_{yv} = q.s_v.\tan\theta$ (2.12.a)

From equation 2.12.a, we can deduce the angle of inclination of the diagonals to the beam axis as :

$$\tan\theta = (A_{sv}.f_{yv})/(q.s_v) \qquad (2.12.b)$$

If now we consider the entire cross–section, the total force in the stringers is four times the value found in equation 2.11. It can be expressed as :

$\Sigma.H = 4.A_s.f_{yl} = q.2.(x_1 + y_1).\cot\theta$ (2. 13)

Where $u = 2(x_1 + y_1)$ = perimeter of stirrup centreline.

A_{sl} = total area of stringers.

Also substituting for q from equa 2.9, we obtain stirrup force in equa 2. 12.a as :

$A_{sv}.\ f_{yv} = (T.s_v/2.\ A_o).\tan\theta$ (2.14)

Similarly, the diagonal stress σ_c (equation 2. 10.b) can be expressed as :

$\sigma_c = (T/2.A_o.\ t).1/(\sin\theta.\cos\theta)$ (2.15)

The state of stress described by equations 2.13, 2.14 and 2.15 is statically admissible, i.e. it fullfills all equilibrium equations. Assuming an underreinforced cross–section, i.e. yielding of the steel will take place prior to crushing of the concrete, the strength of the section will be determined by the yield forces in the stringers and stirrups. The ultimate torsional resistance T_u of the section is reached if both the

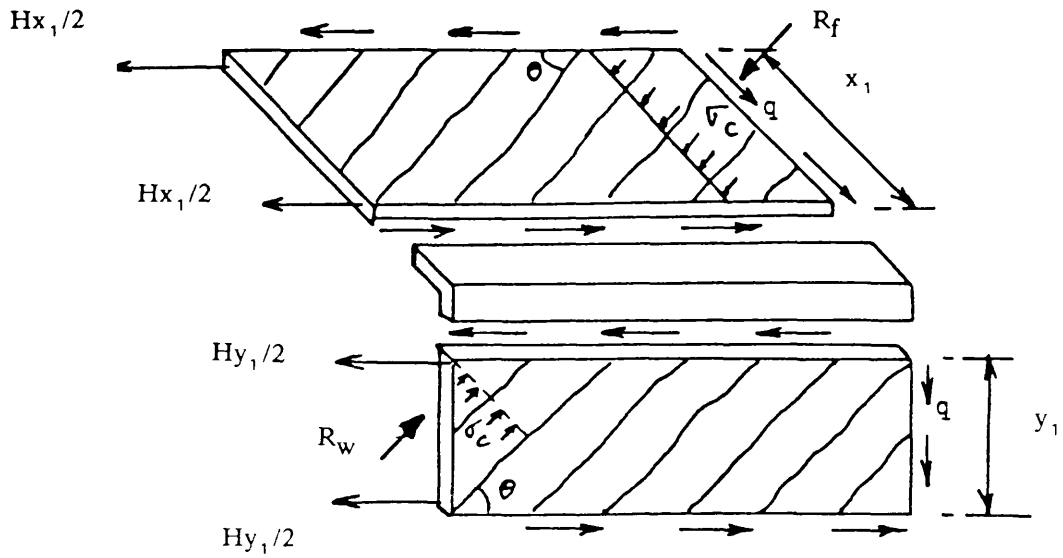

Figure2.6.a Forces in Beam Wall

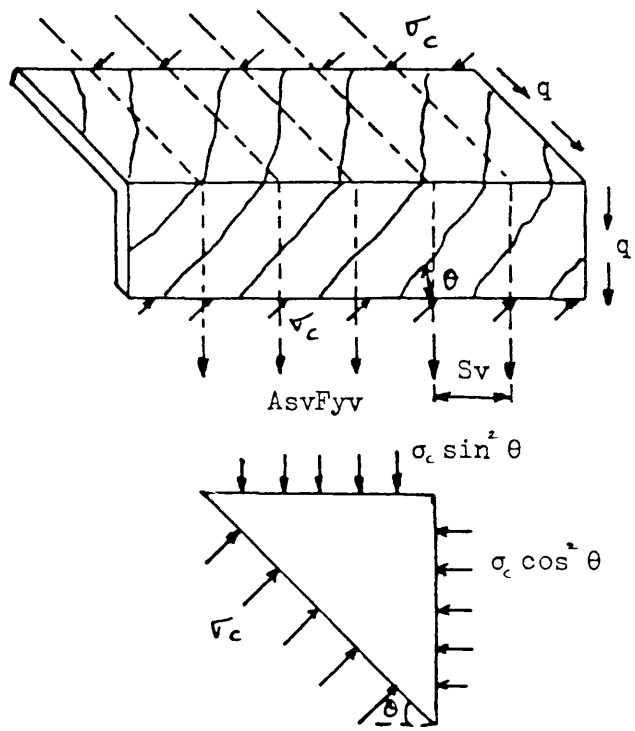

Figure 2.6.b Forces in Beam corner

stringers and stirrups yield. Equations 2.13 and 2.14 give :

$$T_u = (2.A_o.A_{sl}.f_{yl}\ /u).\tan\theta \qquad (2.16.a)$$

$$T_u = (2.A_o.s_v.f_{yv}\ /s_v\ ).\cot\theta \qquad (2.16.b)$$

Eliminating T_u or θ the final expressions are obtained :

$$\tan\theta = [\ (A_{sv}.f_{yv}\ /s_v\ ).u/(A_{sl}.f_{yl})\ ]^{\frac{1}{2}} \qquad (2.17)$$

$$T_u = 2.A_o.[\ (A_{sv}.f_{yv}/s_v\ ).(A_{sl}.f_{yl}\ /u)\ ]^{\frac{1}{2}} \qquad (2.18.a)$$

If the ratio of transverse to longitudinal steel is equal to unity, equation 2.17 gives $\tan\theta = 1.0$, hence $\theta = 45°$; and equation 2.18.a reduces to :

$$T_u = (2.A_o.A_{sv}.f_{yv}\ /s_v\ ) = (2.A_o.A_{sl}.f_{yl}\ /u) \qquad (2.18.b)$$

Comparison with test carried out at various research establishments indicate very good agreement between the observed ultimate strength and the predictions of equation 2.18.a .

B) Skew Bending Model [1,11]

The concept of the skew bending theory is based on the observed failure mechanism characterised by the yielding of tension reinforcement on the three faces of the beam and formation of compression 'hinge' on the fourth face. Figure 2.7 shows a skew bending failure model.

The skew bending model is based on the following assumptions :

1. Longitudinal and transverse steel carry only axial tension; i.e, the shear force carried by dowel action of the reinforcement is neglected.
2. The tensile strength of concrete is neglected.
3. Both the longitudinal bars and stirrups, which intersect the failure surface, yield at failure of the beam.
4. The width of compression struts is very small compared to the overall dimension of the section.

From equilibrium conditions at a failure surface, the following equations for ultimate torque are derived :

In the first equilibrium condition it is assumed that the compression zone is very

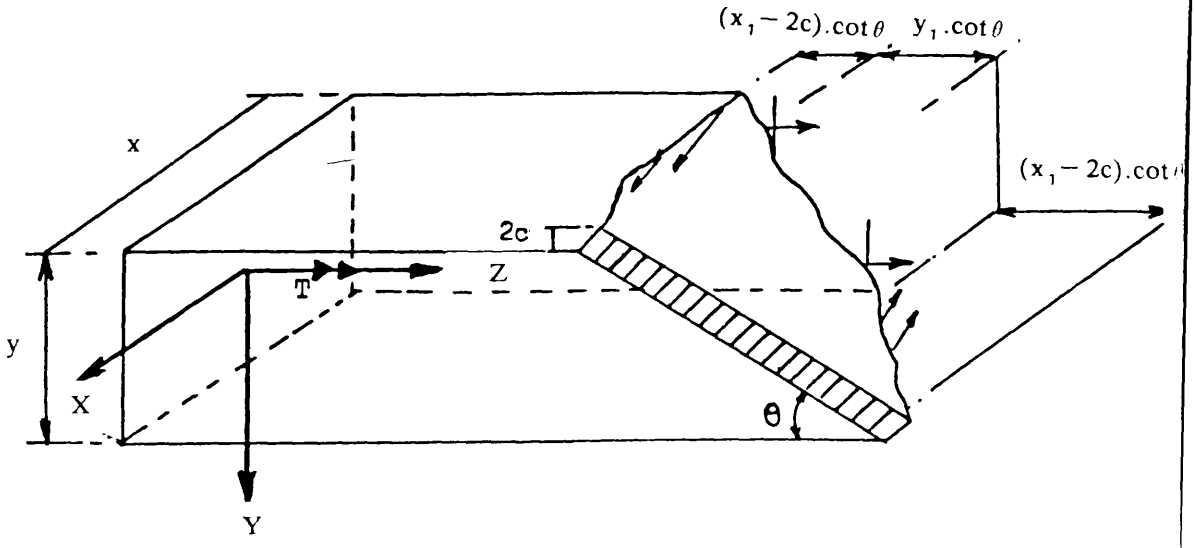

FAILURE SURFACE

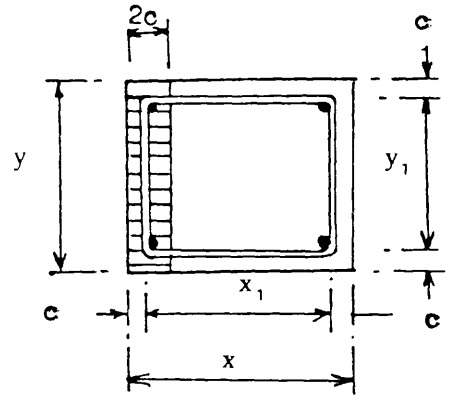

SECTION

Figure 2.7 Skew Bending idealisation for Beam under pure Torsion.

small, therefore internal lever arm is taken as $x - 2c = x_1$. The torsional moment is then given by :

$$T = A_{sv}.f_{yv}.(y_1.\cot\theta/s_v).x_1 + A_{sv}.f_{yv}.(x_1.\cot\theta/s_v).y_1$$

Where A_{sv} , f_{yv} = area and yield stress of stirrup.

x_1 , y_1 = width and depth of stirrup.

c = concrete cover.

s_v = spacing of stirrups.

Introducing enclosed area of stirrup $A_o = x_1.y_1$ into the above expressions gives :

$$T = 2.A_o.(A_{sv}.f_{yv}/s_v).\cot\theta \qquad (2.19)$$

Equation 2.19 expresses the fact that torque is resisted by tensile forces in the stirrups. These tensile stirrups, however, also cause an internal bending moment :

$$M = A_{sv}.f_{yv}.(x_1.\cot\theta/s_v).(y_1 + x_1).\cot\theta \qquad (2.20.a)$$

The function of the longitudinal bars is to neutralise the internal bending moment in equation 2.20.a, thus making internal equilibrium possible. Moment from the longitudinal bar is given as :

$$M = (y_1 / u).A_{sl}.f_{yl}.x_1 + 2.(x_1/u).A_{sl}.f_{yl}.(x_1/2)$$

$$M = (1/2).A_{sl}.f_{yl}.x_1 \qquad (2.20.b)$$

In which

A_{sl} , f_{yl} = area and yield stress of longitudinal bars.

$u = 2.(x_1 + y_1)$, perimeter of the centreline of stirrups.

Therefore the following condition must be satisfied :

$$M = A_{sv}.f_{yv}.(x_1.\cot\theta/s_v).(y_1 + x_1).\cot\theta = (1/2).A_{sl}.f_{yl}.x_1$$

This gives :

$$\cot^2\theta = (A_{sl}.f_{yl}/u).s_v/(A_{sv}.f_{yv})$$

$$\tan^2\theta = (A_{sv}.f_{yv}/s_v).u/(A_{sl}.f_{yl}) \qquad (2.21)$$

Substituting this equation (2.21) into 2.19 , we get :

$$T_u = 2.A_o.[(A_{sl}.f_{yl}/u).(A_{sv}.f_{yv}/s_v)]^{\frac{1}{2}} \qquad (2.22)$$

T_u : ultimate torque

For 'equal steel area'

i.e $(A_{sv}.f_{yv}/s_v) = (A_{sl}.f_{yl}/u)$; $\tan\theta = 1$ and $\theta = 45°$

Accordingly, equation 2.22 reduces to :

$$T_u = 2.A_o.(A_{sv}.f_{yv}/s_v) = 2.A_o.(A_{sl}.f_{yl}/u) \qquad (2.23)$$

Equations 2.21 and 2.22 obtained in the skew bending model are identical to equations 2.17 and 2.18.a derived by truss theory.

After description of these two theories, the following observations are made :

1. The quality of concrete plays no part in the ultimate torque. The ultimate torque equations hold only for underreinforced beams, i.e. crushing of concrete is avoided.

2. Altough both methods are based on different idealised failure surface, they lead to the same ultimate strength solution.

Thurlimann[12,13] has introduced limitations on the value of $\tan\theta$. To avoid the problem of excessive cracking due to crushing of diagonal compression struts before yielding of reinforced steel, such limits are required. The limit deduced from experimental tests is given by

$$1/2 \leqslant \tan\theta \leqslant 2 \qquad (2.24)$$

If large cracks develop, then the aggregate interlock desintegrates. At lower limit $\tan\theta = 1/2$ the crack strain and the stirrup strain are equal to 5 and 4 times the longitudinal strain, respectively. Hence, it can be expected that yielding of the stirrups alone will lead to a shear failure without yielding of the longitudinal steel. The opposite holds for $\tan\theta = 2$. In this case the stirrups will no longer yield and a bending failure will result.

The prediction from the theoretical models have been compared to experimental model. It is observed that the actual torsional strength of a member is overestimated.

The ultimate torque expression for a beam with 45^0 crack angle is given as:

$$T_u = 2.A_o.A_{sv}.f_{yv}/s_v \qquad (2.25)$$

Equation 2.25 was derived by Rausch in 1929. Since then efforts have been made to modify this equation. The modifications suggested to improve this prediction are:

a) The addition of an efficiency factor for reinforcement.

b) An arbitrary definition for the centreline of the shear flow.

c) The deletion of the concrete cover.

d) Use of a new stress strain curve for softened concrete.

The assumption in the first modification is that the reinforcement is only partially efficient. An efficiency factor, which less than unity, was incorporated in Eq.2.25 so that the constant 2 is reduced. In the ACI code the torsional strength of an underreinforced concrete member is expressed as :

$$T_u = T_c + \alpha_t . A_o . A_{sv} . f_{yv} / s_v \qquad (2.26)$$

where $\alpha_t = 0.66 + 0.33\ y_1/x_1 \leqslant 1.5$

T_c = torque resisted by concrete.

The equation 2.26 gives a torsional strength considerably less than predicted by Eq.2.25.

The second modification is to reduce the area A_o by making an arbitrary definition for the centreline of the shear flow. It is assumed that the centreline of the shear flow coincides with the lines connecting the centres of the corner longitudinal bars. This approach was first suggested by Lampert and Thurlimann in 1968 and was adopted by the CEB–FIP Model code.[25] In the CEB–FIP model code, T_u, is expressed as :

$$T_u = T_{cv} + 2.A_1 . A_{sv} . f_{yv} . \cot\beta / s_v \qquad (2.27)$$

where A_1 = the area bounded by the lines connecting the centres of the corner longitudinal bars.

β = angle of inclination of the concrete struts.

$T_{cv} = T_c$ when $T_u \leqslant T_c$

$T_{cv} = 0$ when $T_u \geqslant 3.T_c$

Since the longitudinal bars are always placed within the stirrups, A_1 will always be less than A_o. For practical purpose T from Eq.2.27 will be less than T from Eq.2.25.

The third modification was suggested by Collins and Mitchell in 1980.[22] This approach also tries to reduce the area A_o by making an arbitrary assumption. The equation proposed is

$$T_u = 2.A_2 . A_{sv} . f_{yv} . \cot\beta / s_v \qquad (2.28)$$

where A_2 is the area bounded by the centreline of the shear flow. This centreline of the shear flow is assumed to coincide with the centroidal line of the equivalent compression stress block in the concrete struts. Thus the concrete cover outside the centreline of a hoop bar is assumed to be ineffective. Tests indicate that this is true especially at the corners.

Actually, the strength of concrete struts is greatly reduced by the diagonal crack. This phenomenon is called the softening of concrete. The compression capacity of the concrete in the longitudinal direction is reduced by the transverse tension in the reinforcement. The stress–strain curve of the softened concrete has approximately the same shape as that of nonsoftened concrete, except that the stress has been proportionally scaled down.

The fourth modification was suggested by Hsu and Mo[17,18,19]. Using the softening effect of concrete, they presented a new theory which predicts the torsional behaviour of 108 test beams available from the literature. This approach will not be presented in this investigation, more details can be found in references (17,18,19).

In the first three approaches an arbitrary assumption is necessary to bring the theory closer to the test results. In the fourth approach there is no need to make arbitrary assumptions, however, the theory presented in this approach is too complex and is unsuitable for design practice. Therefore several simplifications and design limitations are necessary for design practice.

2.2.2.3 *Post–cracking Torsional Stiffness*

The post– cracking torque–twist relationship can be expressed as :

$$T = G.C_{cr}.d\Psi/dz \qquad (2.29)$$

where $G.C_{cr}$ = post– cracking torsional rigidity.

It has been shown[1,2] that the behaviour and strength of a solid section after cracking are identical to that of hollow section with the same overall dimension, material and steel arrangement. In other words, a solid section can be idealised as

a hollow section for the purpose of determining post–cracking stiffness. Post–cracking torsional rigidity is given as.[1,2,21]

$$G.C_{cr} = (4.E_s.A_o^2.A_{sv} /(u.s_v)).(r/r+1) \qquad (2.30)$$

where $r = (A_{sl} /A_{sv}).(s_v / u) = \cot^2\theta$ of Eq 2.17 if $f_{yl} = f_{yv}$

E_s = elastic modulus of steel.

Equation 2.30 is only true for the case of underreinforced section, because ultimate failure is reached after yielding of steel and not crushing of concrete. The drop in torsional stiffness after cracking may be characterized by the ratio of cracked rigidity $G.C_{cr}$ to uncracked rigidity G.C. From equation 2.8, uncracked rigidity of a hollow section G.C is defined as : $4.A_o^2.t.G/u$

$G = 0.5\ E_c$, if we assume that Poisson ratio equal zero.

$$G.C_{cr} /G.C = (E_s.A_{sv}.\ (r/r+1)) \ /\ (0.5.E_c.s_v.t)$$

$$= (2.n.A_{sv})/(t.s_v).(r/r+1) \qquad (2.31)$$

Where E_c = Young modulus of concrete.

$n = E_s / E_c$, modular ratio .

2.3 TORSION COMBINED WITH BENDING MOMENT

Both the theoretical and the experimental results show that a moderate amount of bending does not decrease the torsional strength, but on the contrary increases it. The mode of failure of reinforced concrete beams subjected to combined torsion and bending moment is difficult to predict, because failure patterns associated with pure bending or pure torsion only are very different from each other. Many parameters control the mode of failure. These parameters are the ratio of bending to torsional moment, strength of concrete, ratio of cross–sectional dimensions and quantity and disposition of reinforcing steel.

2.3.1 *Experimental Investigations*

Beams provided with both longitudinal and transverse reinforcing steel

generally behave similar to plain concrete beams before cracking. However, after cracking the longitudinal and transverse steel become stressed, while the concrete sustains diagonal compressive forces parallel to the cracks.

This increase in the reinforcing bars stresses is due to the redistribution of stresses after cracking. A complicated cracking pattern with evidence of flexure and torsional influence has been observed. Failure of the beam is caused by yielding of steel and not crushing of concrete.

2.3.2 *Theoretical Approach*

2.3.2.1 *Post cracking Behaviour of Beams under combined Torsion and Bending*

There are two main approaches to assess the ultimate strength of reinforced concrete beams subjected to combined torsion and bending. These are the skew bending model and the space truss model. Figures 2.8 and 2.9 shows typical space truss and skew bending failure models. Using the postulated failure mechanism and adopting some simplifying assumption discussed in section 2.2.2.2 for the case of pure torsion, ultimate strength equations are established from equilibrium consideration for combined loading.

Figure 2.10 shows the superposition of the longitudinal bar forces F(T) and F(M) induced by torsion and bending. It can be seen that the forces in the bottom stringers due to torsion and bending are additive, whereas the forces in the top stringer are substractive. The transverse reinforcement contribute to the torsional resistance. Failure of hollow section subjected to torsion and bending may occur in two modes. The first mode is caused by the yielding of the bottom longitudinal bars and the transverse steel. The second mode is caused by the yielding of the top longitudinal bars and the transverse steel.

A simplified generalised derivation of ultimate strength under torsion and bending is given as follows :

From the ultimate strength of beams under pure torsion, assuming $\theta = 45°$,

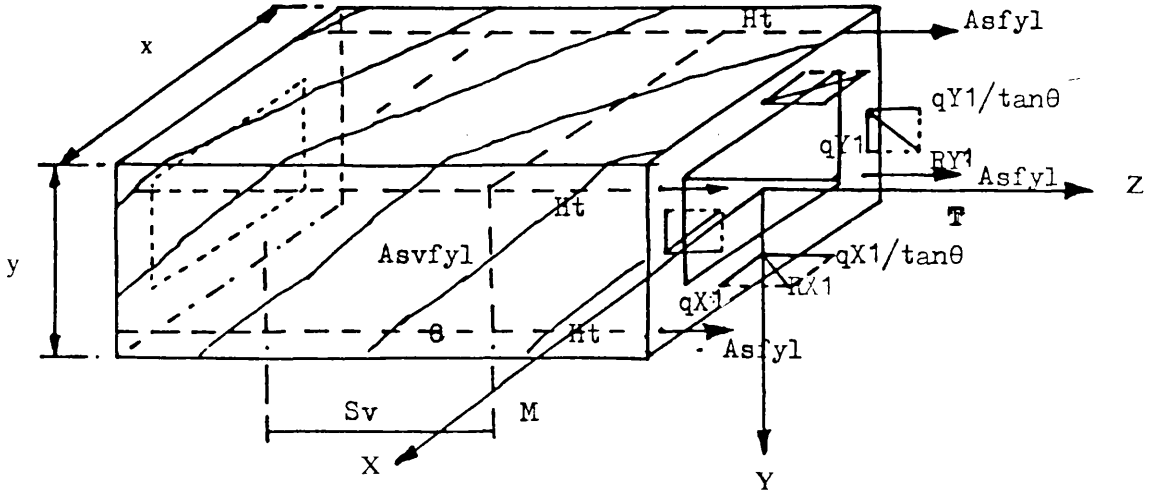

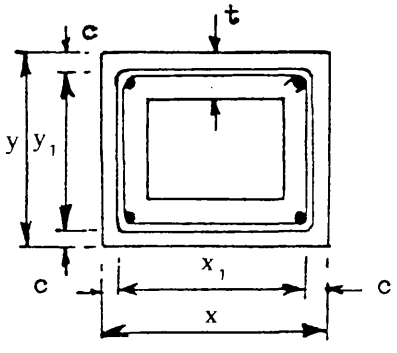

CROSS-SECTION OF BEAM

Figure 2.8 Space Truss Model for Beam under combined Torsion and Bending.

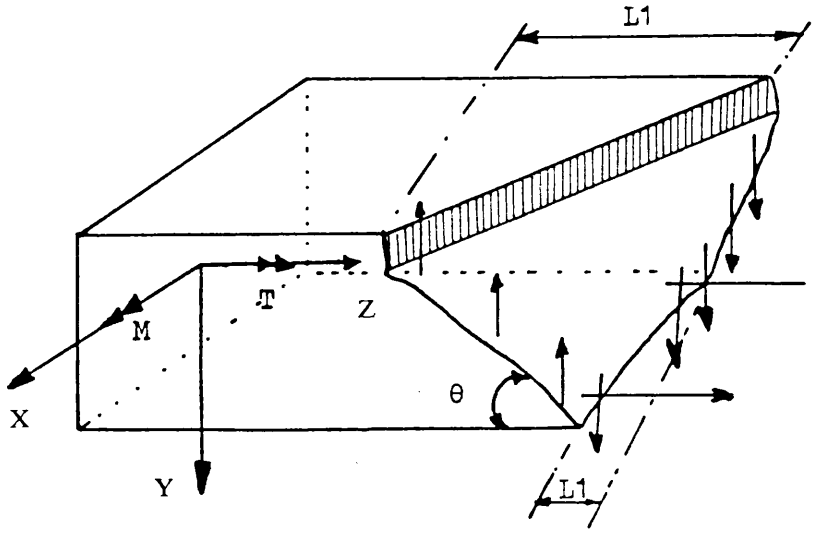

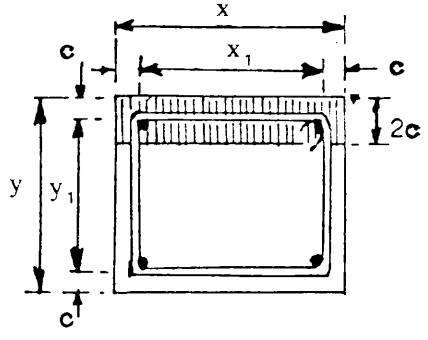

SECTION

Figure 2.9.a Failure Surface for Combined Torsion and Bending in Skew bending model. (Bending dominated)

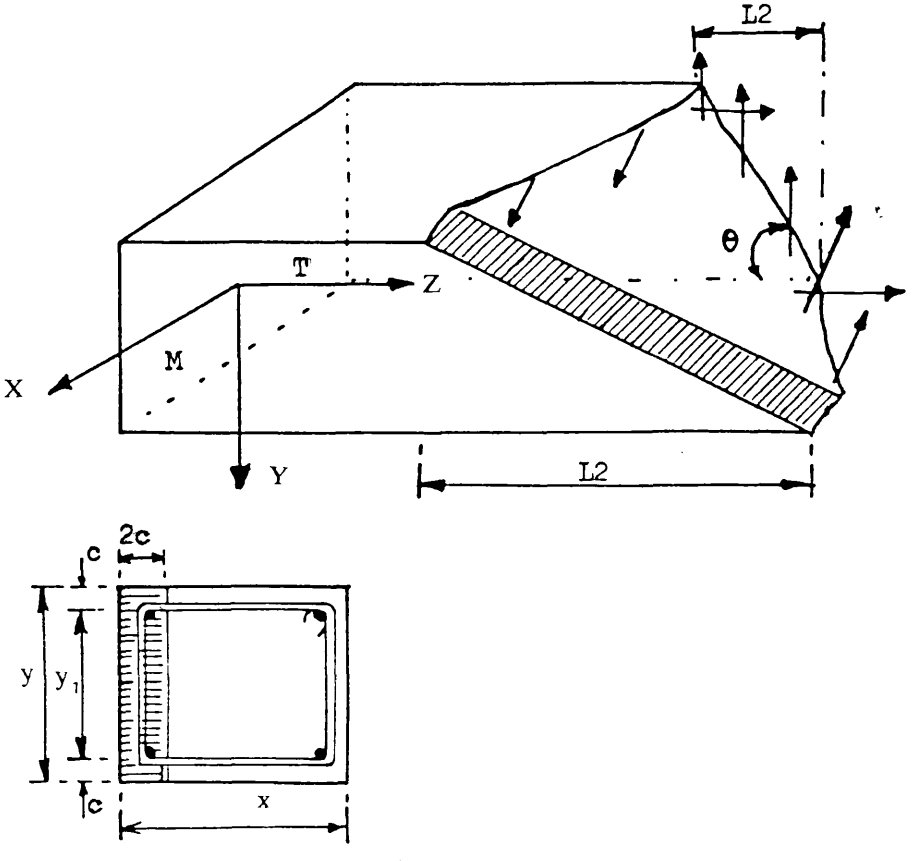

Figure 2.9.b Failure Surface for Combined Torsion and Bending in Skew bending approach. (Torsion dominated)

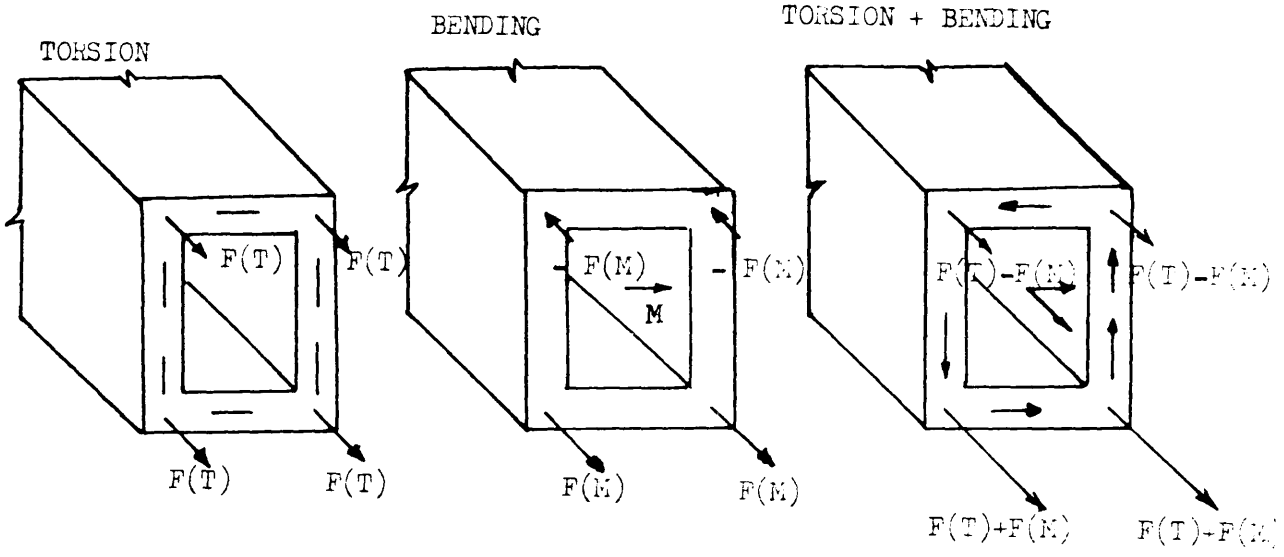

Figure 2.10 Superposition of Torsion and Bending.

we obtain :

From consideration of stirrups

$$T_u = 2.A_o.(A_{sv}.f_{yv} /s_v) \qquad (2.32)$$

and from consideration of the corresponding longitudinal steel

$$T_u = 2.A_o.(A_{sl}.f_{yl} /u) \qquad (2.33)$$

Half of the total area of the longitudinal steel is distributed at the bottom of the beam, while the other half is distributed at the top. Therefore top or bottom longitudinal steel equal to :

$$A_{sl} /2 = (A_{sl,t})_{torsion} = (1/2).[(T_u.u)/(2.A_o.f_{yl})] \qquad (2.34)$$

$$A_{sl} /2 = (A_{sl,b})_{torsion} = (1/2).[(T_u.u)/(2.A_o.f_{yl})] \qquad (2.35)$$

Where $A_{sl,t}$ and $A_{sl,b}$: top and bottom longitudinal reinforcement respectively.

In the case of pure bending, longitudinal bottom steel area required to resist applied bending moment M is :

$$(A_{sl,b})_{bending} = M/(f_{yl}.y_1) \qquad (2.36)$$

In which y_1 = lever arm.

In the state of combined torsion and bending, if we consider the first mode of failure viz yielding of the bottom bars, we obtain total area of longitudinal steel as :

$$(A_{sl})_b = M/(f_{yl}.y_1) + (T_u /(2.A_o.f_{yl})).(u/2) \qquad (2.37)$$

$$(A_{sl,b}.f_{yl}.y_1) = M_u = M + (T_u.y_1 /(2.A_o)).(u/2)$$

where M_u = ultimate strength in pure bending moment

Hence ultimate bending moment equal

$$M_u = M + T_u.y_1 /(2.x_1.y_1).(x_1 + y_1) \qquad (2.38)$$

and applied bending moment is given as :

$$M = M_u - (T/2).(1 + (y_1 /x_1)) \qquad (2.39)$$

The second mode of failure is now considered. the tensile force due to torsion in the top longitudinal bar is counteracted by the compression due to bending. Total area of steel at the top is equal :

$$A_{sl,t} = -M/(f_{yl}.y_1) + (T_u /(2.A_o.f_{yl})).(u/2) \qquad (2.40)$$

As in the case of first mode of failure, further simplification of equation 2.38 gives

$$M = -M_u + (T/2).(1 + (y_1 / x_1)) \qquad (2.41)$$

Where $-M_u$ = negative ultimate pure bending moment.

Based on the above derivation of the ultimate strength for reinforced concrete beams under torsion and bending, the following observations can be made :

1. Generally, the total area of steel is made up of the summation of separate design for pure torsion and bending (equations 2.37 and 2.40). However, in the bending compression zone, the longitudinal torsional steel may be reduced because the tensile force due to torsion is counteracted by the compression due to bending. The transverse steel for pure torsion is unchanged by combined loading and is required on all sides of beam as usual.

2. To avoid the crushing of diagonal compression struts before yielding of reinforcing steel, limitation is imposed on the inclination angle θ of the compression diagonal to beam axis. Thurlimann[12,13] suggested the following limit to θ as :

$$1/2 < \tan\theta < 2$$

$\tan\theta$ is a function of the ratio of transverse to longitudinal reinforcing steel. Therefore a limit is set on the total amount of steel as well as the ratio of transverse to longitudinal steel.

3. Equations 2.39 and 2.41 show that an interaction exists between torsion and bending moment. The former equation shows that the bending moment of a section is reduced when a torsional moment T is added. Whereas, the latter equation shows that the presence of a small moment M, can increase the torsional capacity of a section.

The equations derived in the above theoretical investigation seldom easily lead themselves to design office use, even if the comparison between theory and experiment shows a fairly satisfactory prediction of ultimate strength under combined loading.

2.3.2.2 *Post–cracking stiffness under combined loading*

$d\Psi/dz = (u/2.A_o).(\epsilon_l + \epsilon_v)$ (2.42)

And from the difference between the bottom and top longitudinal steel strains, curvature can be defined as :

$1/R = (\epsilon_{l,b} - \epsilon_{l,t})/y_1$ (2.43)

$\epsilon_{l,b}$ = bottom flange longitudinal strain.

$\epsilon_{l,t}$ = top flange longitudinal strain.

y_l = depth of the section.

Under combined loading, post–cracking stiffness will depend on the ratio of torsion to bending moment Φ. The interaction relationship is therefore broadly classified into two regions.

a) Range 1 – Torsion dominates ($T/M > \Phi_{limit}$)

b) range 2 – Bending dominates ($T/M < \Phi_{limit}$)

The value of Φ_{limit} between the two ranges is characterised by zero stress condition in the top bars. By substituting $A_{sl,t} = 0$ in equation 2.40, we obtain :

$\Phi_{limit} = 2.A_o/(y_1.(u/2)) = 2/(1+(y_1/x_1))$ (2.44)

1) Post–cracking rate of curvature :

Post–cracking rate of curvature can be expressed in a general form as :

$d^2w/dz^2 = M/K_{MM} + T/K_{MT}$ (2.45)

K_{MM} and K_{MT} are the post–cracking rigidities due to bending and torsion respectively. Their value depends on the range.

a) Range 1 – Torsion dominates ($T/M > \Phi_{limit}$)

$K_{MM} = E_s.y_1^2 . A_{sl,b} .(r_L/(r_L + 1))$

$K_{MT} = (4.A_o.y_1.E_s.A_{sl,b}/u).(r_L/(r_L - 1))$

$r_L = A_{sl,t}/A_{sl,b}$ (ratio of area of top to bottom longitudinal bars)

b) Range 2 – Bending dominates ($T/M > \Phi_{limit}$)

$K_{MM} = E_c.I_{cr}$ (flexural rigidity in pure bending)

$K_{MT} = \Phi_{limit}.E_c.I_{cr}/[(E_c.I_{cr}) - 1]$

$K_{MM} = E_s.y_1^2 . A_{sl,b}/2$ (flexural rigidity when $T/M = \Phi_{limit}$)

Where E_c = Young modulus of concrete

I_{cr} = moment of inertia of cracked section (see equation 2.48)

Where E_c = Young modulus of concrete

I_{cr} = moment of inertia of cracked section (see equation 2.48)

2) Post– cracking rate of twist :

The post– cracking rate of twist is obtained from equation (2.42) as :

$$d\Psi/dz = T/K_{TT} + M/K_{MT} \qquad (2.46)$$

The values of torsional rigidities K_{TT} , and K_{MT} depends on the range.

a) Range 1 – Torsion dominates ($T/M > \Phi_{limit}$)

$K_{TT} = G.C_{cr} = (4.E_S.A_o^2 . A_{sv} /(u.s_v)).(r/(r+1))$ (torsional rigidity in pure torsion)

where r = ratio of area of longitudinal/transverse steel in section

$K_{TM} = K_{MT} = (4.A_o.y_1.E_s.A_{sl,b} /u).(r_L /(r_L - 1))$

where r_L = ratio of area of top/bottom flange longitudinal bars

If $0 < r_L < 1.0$, the influence of the bending term in equation 2.46 will be insignificant. Therefore, post– cracking rate of twist in this range can be safely approximated to the case of pure torsion.

b) Range 2 – Bending dominates ($T/M < \Phi_{limit}$)

It is not possible to establish post– cracking rate of twist in this range directly because contribution of uncracked compression zone to the stiffness is unknown. The effect of bending is neglected in this range, hence post– cracking rate of twist is approximated to the case of pure torsion.

2.4 SERVICEABILITY LIMIT STATE OF REINFORCED CONCRETE BEAMS

It has been recognized that the design approach for reinforced concrete, ideally should combine the best features of ultimate strength and working stress design. Early in 1964 the European concrete committee proposed that a structure must be designed with reference to several limit states . The most important limit states are : strength at ultimate load, deflection at service load and crack widths at service load. Thus to ensure a satisfactory design, the crack widths and deflections at service load must be checked to make certain that they lie within reasonable

limiting values. This check requires the use of 'elastic theory'. The estimation of the service load behaviour is complicated by the inelastic behaviour of concrete. In the short–term, cracking of concrete in tensile zone is the main source of non linearity. Cracking and deflection are inter–related problems but for simplicity it is usual to treat them separately.

2.4.1 *Deflection*

During the pre–cracking stage, concrete is assumed to be linear elastic and therefore deflections are evaluated using the elastic theory with the moment of inertia of gross section I_g , i.e. that steel is neglected. After cracking, in the short term, a modular ratio approach is considered in the elastic analysis. The tensile concrete contribution to the stiffness of the beam is ignored. Branson[14] defined the effective second moment of area after cracking as :

$$I_{eff} = (M_{cr} / M_{max})^3 . I_g + (1 - (M_{cr} / M_{max})^3) . I_{cr} \qquad (2.47)$$

Where I_{eff} = effective second moment of area.

I_g = gross second moment of area before cracking.

I_{cr} = second moment of area of cracked section.

M_{max} = maximum applied moment.

M_{cr} = moment at first cracking.

The second moment of area of the cracked section can be estimated from elastic analysis of the fully cracked rectangular simply supported beam as :

$$I_{cr} = (x.y^3/3).(K^3 + 3.n.p.(1-K^2)) \qquad (2.48)$$

$K = y_o / y$ = ratio of depth in compression to depth of the section.

In which x and y = breadth and depth of section respectively.

$$K = [(n.p)^2 + 2.n.p - n.p]^{\frac{1}{2}}$$

n = modular ratio

p = ratio of steel in section.

For ordinary reinforced beams, the cracking moment can be computed as :

$$M_{cr} = f_r . I_g / y_t \qquad (2.49)$$

Where f_r = modulus of rupture of concrete.

y_t = depth from neutral axis to the tension face.

For ordinary reinforced concrete beams, short term deflection can be defined in the form :

$$\Delta = K_o.M_x.L^2 /(E_c.I_{eff}) \qquad (2.50)$$

in which K_o = constant depending on loading and end restraints.

M_x = midspan moment.

L = span of beam.

E_c = elastic modulus of concrete.

Gilbert[15] in his analysis introduced a new modular ratio, to take into account the stiffening effect of intact concrete between cracks in the tensile zone after cracking. This is possible by considering the effective area of tensile concrete A_{eff} located at the level of steel.

$$A_{eff} = (0.21.y - n.A_{sl}).(M_{cr} /M_{max})^2 \qquad (2.51)$$

Accordingly the modified modular ratio n^* is :

$$n^* = n + A_{eff} /A_{sl,b} \qquad (2.52)$$

This value of n^* instead of n should be used in calculating K and I_{cr} in Eq.2.48.

The Branson's approach forms the basis of the American code (ACI 318–77) ACI435 . The British code BS8110[9] requires that the final deflection (including the effect of temperature, creep or shrinkage) should not exceed span/250 for the case of horizontal members (floors,beams,roof) where partitions and finishes will not be affected by deflection. For the situation where partitions and finishes will be affected, the deflection limit is span/350 or 20 mm whichever is the lesser.

2.4.2 *Cracks* [16,23]

With the frequent use of high strength steel tendency toward ultimate load and limit theory designs, control of cracking becomes as important as control of deflection in reinforced concrete. Cracks form when the tensile stress in the concrete exceeds its strength. Immediately after the formation of the first crack, the stress in the concrete at the cracking zone is reduced to zero and is resisted by the reinforcement.

Many variables affect the development and characteristics of cracks. The major ones are percentage of reinforcement, bond characteristics and size of bar, concrete cover, distribution of reinforcement and strength of concrete.

The most commonly used theories for assessing crack widths are :

a) Classical theory : This approach is based on slip concept which assumes that crackwidth depends on the bond slip between concrete and steel. Crackwidth is expressed in terms of steel stresses.

b) No–slip theory : Assumes a condition of no slip of the steel relative to concrete. Crack is therefore considered to have a zero width at surface of the steel bar and increases gradually as the surface of the member is approached. This means that crackwidth is dependent on deformation of the surronding concrete.

The British code BS8110[9] recommendations for estimating crackwidth of beams and one way slabs is based on Beeby's approach[16] . He observed that crack spacing and width increased with the distance from the bar and reaches a constant value at a certain distance from the bar. This value is dependent on the crack depth rather than the distance from the bar. The design surface crackwidth, which should not exceed 0.3 mm (BS8110 , part 2 , clause 3.2.4) may be calculated from the following equation :

$$W_{max} = (3.a_{cr}.\epsilon_m)/[(1 + 2.(a_{cr} - c_{min})/(h-x)] \qquad (2.53)$$

Where a_{cr} = distance from the point considered to the surface of the nearest longitudinal bar.

c_{min} = minimum cover to the tension steel.

h = overall depth of the member.

x = depth of the neutral axis.

ϵ_m = average strain at the level where the cracking is being considered.

ϵ_m may be calculated on the basis of the assumption given in clause 3.6 BS8110 part 2 .

$$\epsilon_m = \epsilon_1 - [b_t.(h-x).(a'-x)] / [3.E_s A_{sl,b}.(d-x)]$$

In which

ϵ_1 = strain at the level considered, calculated ignoring the stiffening effect

of the concrete in the tension zone.

b_t = width of the section at the centroid of the tension steel.

a' = distance from the compression face to the point at which the crack width is being calculated.

E_s = modulus of elasticity of the reinforcement.

$A_{sl,b}$ = area of tension reinforcement.

d = effective depth.

The proposed method described above can evaluate crackwidths with reasonable accuracy.

2.5 BEHAVIOUR OF CONCRETE UNDER MULTIPLE LOADING

Strength determination in usual structural engineering practice is based on failure under monotonically increasing, proportional loadings. The effects of non proportional load sequences are largely ignored. To the author's knowledge no work has been done on beams subjected to multiple loading.

Even in perfectly–plastic structures, where the strength can be represented by an envelope enclosing all possible load histories, specific load sequences below failure can cause incremental deformations that lead to unacceptably high displacements and associated instabilities. Gerstle and Cook[24] report that the design rules for assessing the strength of tall steel building frames are based on tests under monotonically increasing axial loads, P, and bending moment, M. Actually, axial columns forces are primarly due to gravity loads, while bending moments occur primarly under wind or seismic loads. It therefore appears more appropriate to anticipate axial forces applied first, followed by moments which may suffer reversal, as shown in figure 2.11 . Gerstle[20] has also conducted tests involving multiaxial load histories applied on 10 cm concrete cubes. These tests have no immediate bearing on the present investigation, nevertheless it is interesting to show some curves concerning these tests. Figure 2.12 shows the loading and unloading in concrete. Figure 2.13 and 2.14 show the major principal stress versus principal

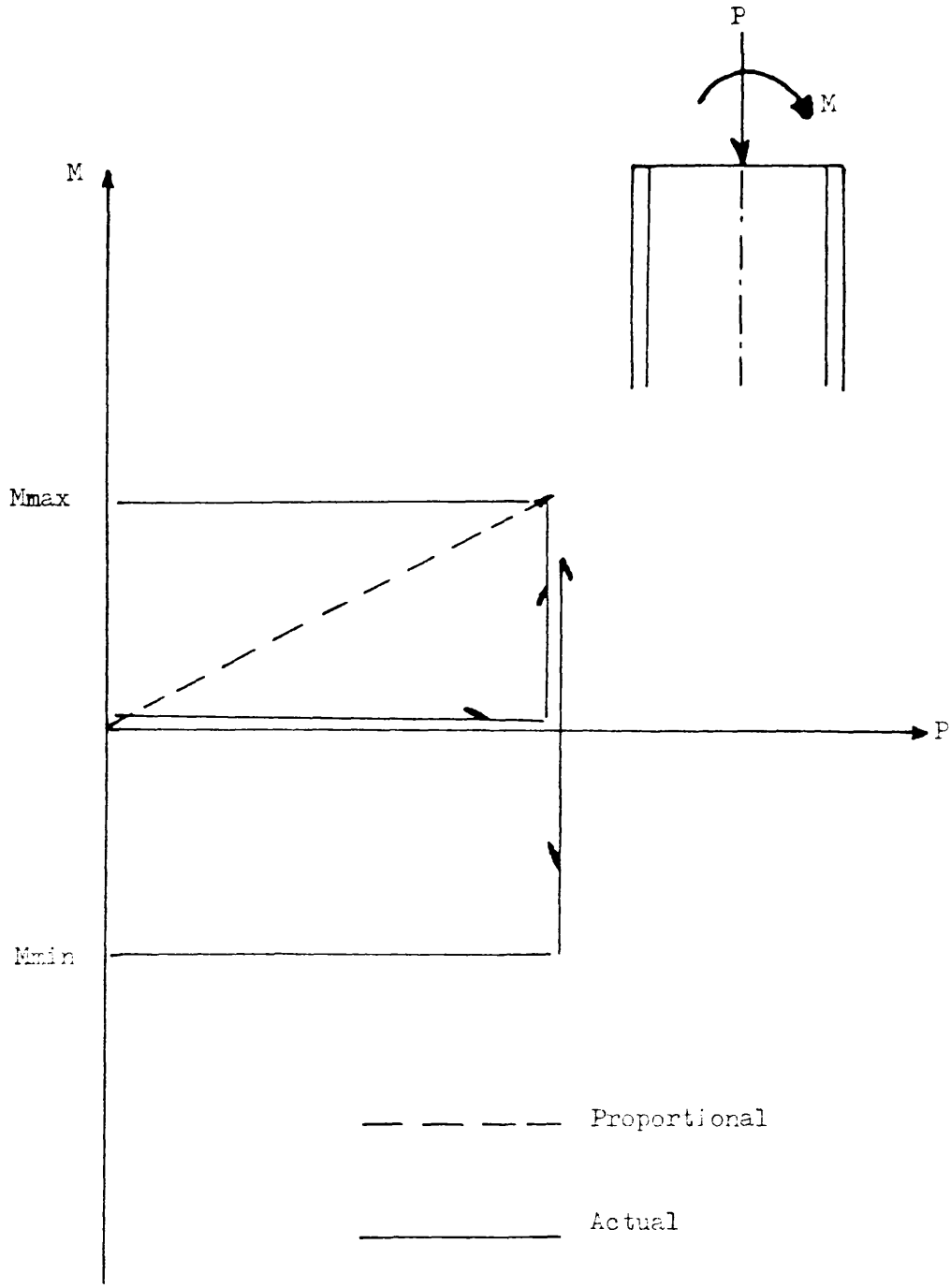

Figure 2.11 Assumed and actual load paths.

strains for the case of load history.

This brief summary of research dealing with multiple loading shows that this kind of loading must be studied in the future for a better understanding of the behaviour of reinforced concrete members under such loading and to find out if the existing design recommendations are valid for this case of loading.

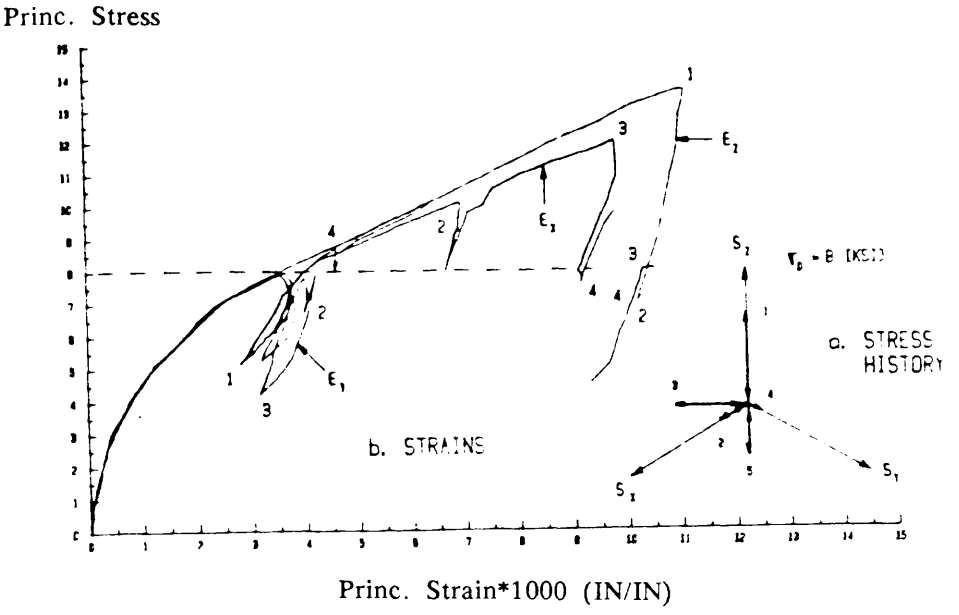

Fig 2.12 Loading and unloading in concrete

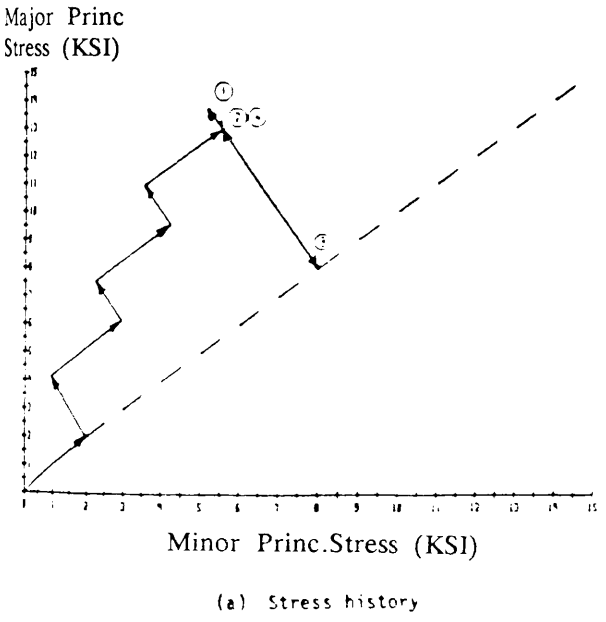

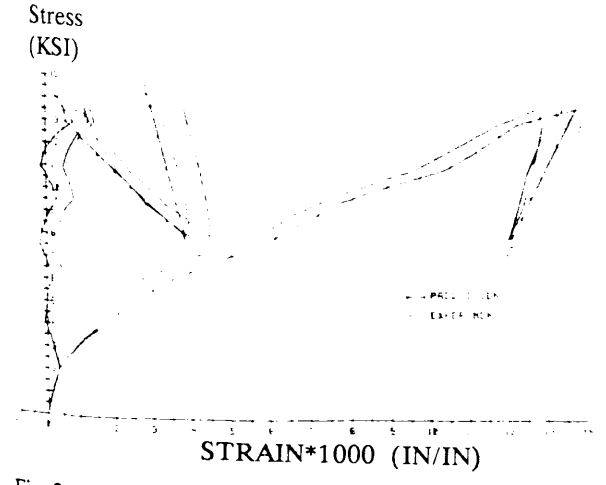

Fig 2.13 Major principal stress versus principal strains for stairstep load history

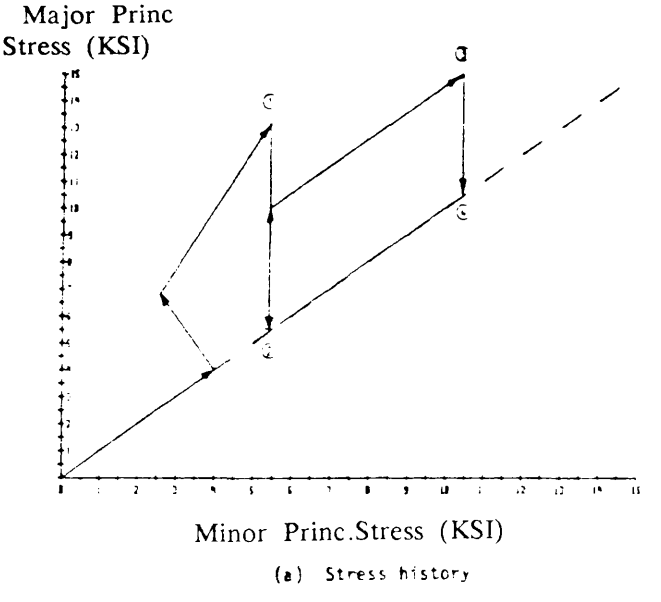

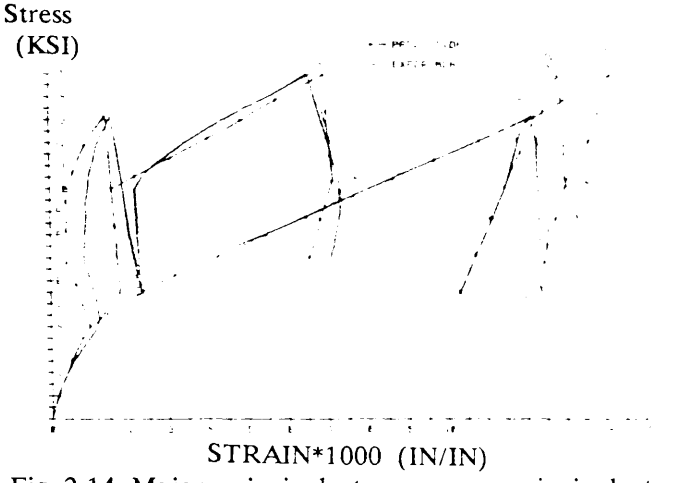

Fig 2.14 Major principal stress versus principal strains for general axisymmetric load history

CHAPTER 3

DESIGN PHILOSOPHY

3.1 INTRODUCTION

The object of structural design is to reach acceptable probability that the structure during its design life, will fulfill the function for which it was designed. The requirements that a structure has to satisfy are stated as limit states. If the limit state of a structure is exceeded, then the structure is deemed to be unfit for use. There are two types of limit states :

1) Ultimate limit state (ULS) : This requires that the structure, or part of structure should not collapse at ultimate design load. The ultimate limit state should not be reached by rupture of any section, by overturning or by buckling under the worst combination of ultimate loads as stated in BS 8110[26]. Collapse is associated with the inability of the structure to carry any additional load.

2) Serviceability limit state (SLS) : This requires that the structure should not suffer from excessive deflection, cracking and vibration under service load conditions. Deflection due to gravity loading should not adversaly affect its efficiency or appearence[26]. Cracking should be kept within reasonable bounds by attention to detail[26].

The usual practice in reinforced concrete design is to design for the ultimate limit state and then check for serviceability limit state. The opposite procedure is often followed in prestressed concrete design.

In order to study experimentally the strength of reinforced and partially prestressed concrete beams under multiple loading consisting of various combinations of combined bending and torsional loads. Large scale reinforced and partially prestressed concrete models were chosen. This chapter details the procedure and philosophy adopted in the design of models. In general, if a beam is subjected to torsion and bending the following stresses exist : σ_x, σ_y, τ_{xy} (figure 3.2), or alternatively as principal stresses σ_1 and σ_2, with an orientation θ. This applied set

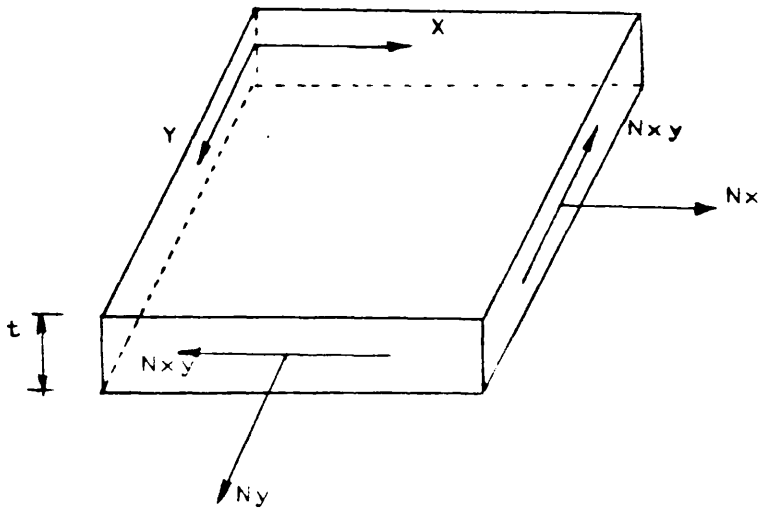

Figure(3.1) Element Under In-Plane Loading.

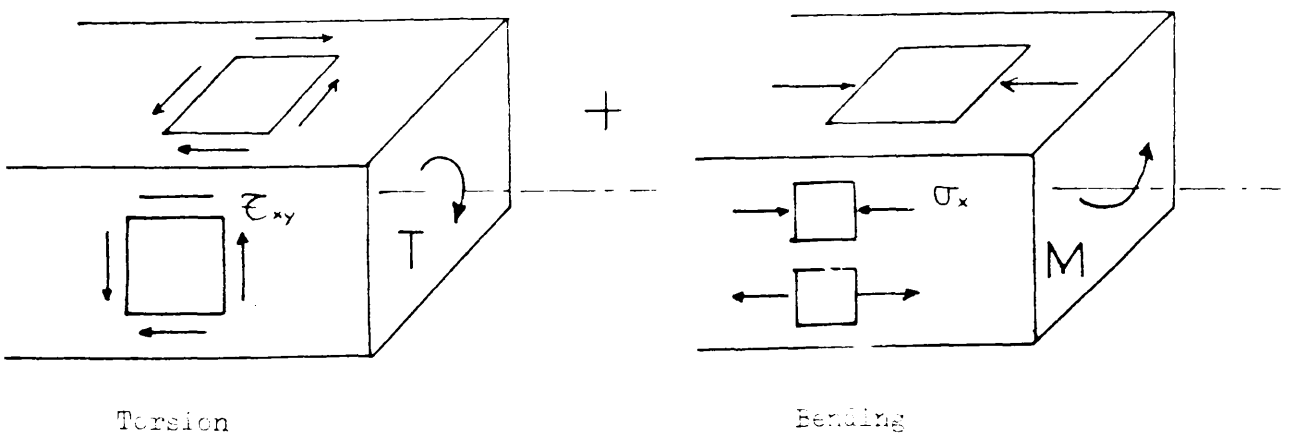

Torsion

Bending

Figure(3.2) Beam subjected to torsion and bending.

of stresses are resisted by a combination of stresses in concrete and steel reinforcement. The object of design is to ensure that the combined strength of concrete and the associated steel reinforcement area can safely resist the applied loads. The basic approach is known as the 'Direct Design Method', and was suggested for flexural members by Wood[3] and extended by Armer[4], and for in plane stresses by Nielsen[5] and Clark[6]. Hago[27], Memon[28], El– Nounou[29], Ebireri[2] and Abdelhafiz[30] have used this procedure to design and test various type of reinforced concrete structures. This chapter describes the basic features of this approach and how this method can be used for the design of beams under multiple loading. More details about this approach are found in references (4,29).

The proposed ultimate limit direct design method is based on the theory of plasticity, thus the structure must satisfy the three basic conditions at ultimate load inherent in the classical plasticity theory :

1– Equilibrium condition : The externally applied loads must be in equilibrium with internal stresses.

2– Yield criterion : At no point in the structure should the set of stresses exceeds the yield criterion.

3– Mechanism condition : Under ultimate load, the structure should develop sufficient 'plastic' regions to transform it into mechanism.

Reinforced concrete does not exhibit perfectly plastic response. Therefore a collapse may occur in the concrete before yielding has redistributed the stresses. One way of overcoming this defect is to reduce the ductility demands to ensure minimum redistribution such that most of the critical sections of the structure yield simultaneously.

3.2 PROPOSED ULTIMATE LIMIT STATE DIRECT DESIGN APPROACH

The direct design approach provides optimum reinforcement to resist predetermined stress field in reinforced concrete structures.

In this approach, a section is designed to resist a given set of forces using

elastic stress field and yield criteria for reinforced concrete subjected to in–plane and / or out of plane forces. The approach satisfies the classical conditions of plasticity theory as follows :

1) Equilibrium condition :

The distribution of stresses in the reinforced concrete structure is obtained by elastic analysis, using say the finite element or any other technique. Since these methods of analysis are derived from equilibrium equations, this condition is automatically satisfied.

2) Yield criterion :

In reinforced concrete structures, the external applied loads have to be resisted either by concrete alone or by combination of concrete and steel. In addition to reinforcement requirements based on stress / strength considerations there are often practical constraints on the direction in which the reinforcement may lie; on the proportion of steel which may be provided. An efficient design is achieved by minimizing the total amount of reinforcement required by the design criteria within the bounds of these practical constraints.

For in–plane forces Nielsen [5] has presented the yield criterion for section having orthogonal reinforcement in tension only. This approach has been extended by Clark[6] to cover the possibility that compression steel or skew tension reinforcement may be required. The required equations are derived in section 3.3

3) Mechanism condition :

Because the necessary resistance is made equal to the calculated stress at every point in the structure, it is expected that all parts of the structure will attain their ultimate strength under the design load. Accordingly, with minimum redistribution of the stresses, every point will yield at the ultimate load, thus converting the structure into a mechanism.

3.3 DESIGN OF ORTHOGONAL REINFORCEMENT TO RESIST IN-PLANE FORCES

The design of reinforcement for a given set of stresses in the case of concrete beams has been solved by the classical ultimate limit capacity concept of Nielsen[5]. The main problem is to find the optimum reinforcement area and thickness of concrete.

The design equations are based on the following assumptions :

1– The reinforcement is assumed to be symmetrically positioned with respect to the middle surface of the section and to be in two orthogonal directions, as shown in figure 3.5.

2–The reinforcement can carry only uniaxial stress in their original bar direction. This means kinking of the bars and contribution by dowel action of the bars in resisting shear is neglected.

3– The bar spacing is assumed to be small in comparison with the overall structure dimensions so that the reinforcement can be considered in terms of area per unit width rather than as individual bars.

4– The concrete is assumed to have zero tensile strength, to exhibit the square yield criterion shown in figure 3.3 for in–plane stress and to be elastic perfectly plastic when yielding.

5– The reinforcement bars are also assumed to exhibit perfect elastic/plastic behaviour and to yield at stress of f_s in tension and f_s' in compression, as shown in figure 3.4

6– Instability failures, bond failures are assumed to be prevented by proper detailing and choice of the section.

3.3.1 *Theory*

Figure 3.1 represents a thin– walled reinforced concrete element subjected to in–plane forces N_x, N_y and N_{xy}, which is resisted by a combination of stress in concrete and steel, as shown in figure 3.6 .

Equilibrium conditions

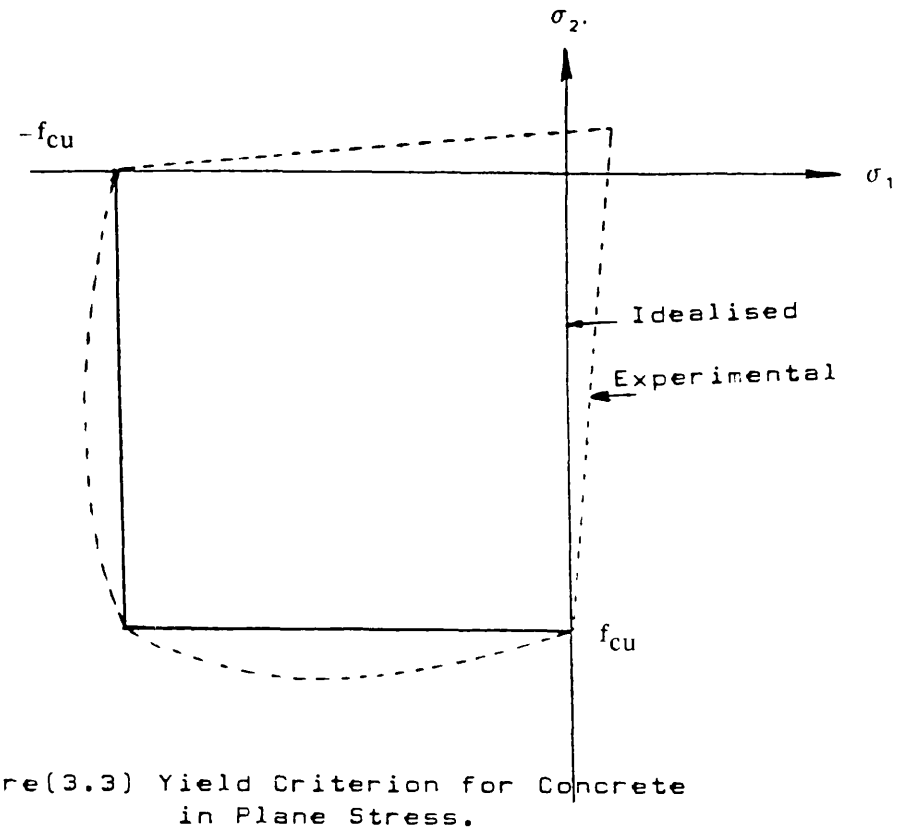

Figure(3.3) Yield Criterion for Concrete in Plane Stress.

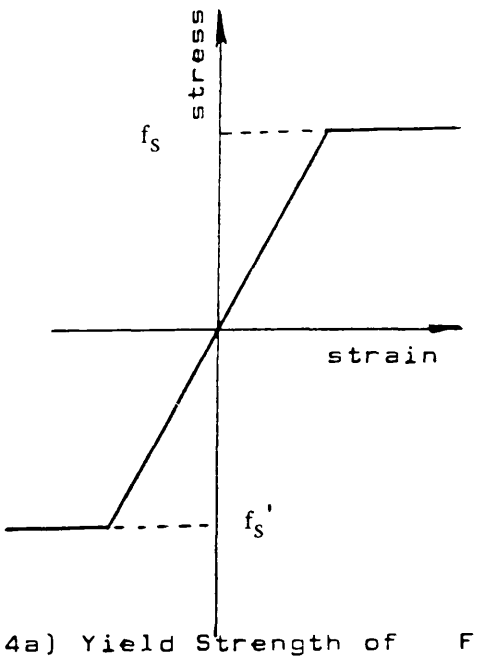

Figure(3.4a) Yield Strength of Reinforcing Steel in Tension and Compression

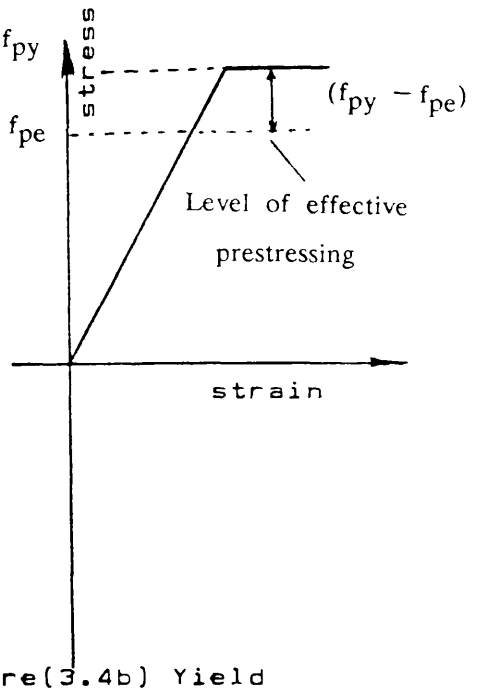

Figure(3.4b) Yield Strength of Prestressing Steel in Tension.

a) Concrete

The principal concrete stresses are taken to be σ_1 and σ_2 with the major principal stress σ_1 at an angle θ to the X axis. σ_1 is always numerically greater than σ_2. All stresses are taken to be tension positive.

From figure 3.6(b) the concrete resistance is given as :

$$\sigma_x = \sigma_1.\cos^2\theta + \sigma_2.\sin^2\theta \qquad (3.1.a)$$

$$\sigma_y = \sigma_1.\sin^2\theta + \sigma_2.\cos^2\theta \qquad (3.1.b)$$

$$\tau_{xy} = (\sigma_1 - \sigma_2)\cos\theta.\sin\theta \qquad (3.1.c)$$

b) Steel

Let the area of reinforcement in the X and Y direction be A_x and A_y respectively and their associated stresses f_x and f_y. From figure 3.6(c) the steel resistance in the X and Y directions is given as :

$$\sigma_x = A_x.f_x/t \qquad (3.2.a)$$

$$\sigma_y = A_y.f_y/t \qquad (3.2.b)$$

Where t is the thickness of the element.

By equating the applied stresses to combined resisting stresses, the following three equations of equilibrium can be written.

$$N_x = A_x.f_x + \sigma_1.t.\cos^2\theta + \sigma_2.t.\sin^2\theta \qquad (3.3.a)$$

$$N_y = A_y.f_y + \sigma_1.t.\sin^2\theta + \sigma_2.t.\cos^2\theta \qquad (3.3.b)$$

$$N_{xy} = (\sigma_1 - \sigma_2)\cos\theta\ \sin\theta \qquad (3.3.c)$$

where $N_x = \sigma_x.t$, $N_y = \sigma_y.t$ and $N_{xy} = \tau_{xy}.t$

In each direction, tension reinforcement, compression reinforcement or no reinforcement may be required. Figure 3.7 summarises the four possible combinations from the 2–D situation, originally proposed by Nielsen [5] These four possible combination are derived as follows. Let us consider the major principal stress σ_1 as tensile. Since concrete cannot carry any tension, we set the value of $\sigma_1 = 0$. Equation (3.3.a) to (3.3.c) gives

$$N_x - A_x.f_x = \sigma_2.t.\sin^2\theta \qquad (3.4.a)$$

$$N_y - A_y.f_y = \sigma_2.t.\cos^2\theta \qquad (3.4.b)$$

$$N_{xy} = -\sigma_2.t.\cos\theta\ \sin\theta \qquad (3.4.c)$$

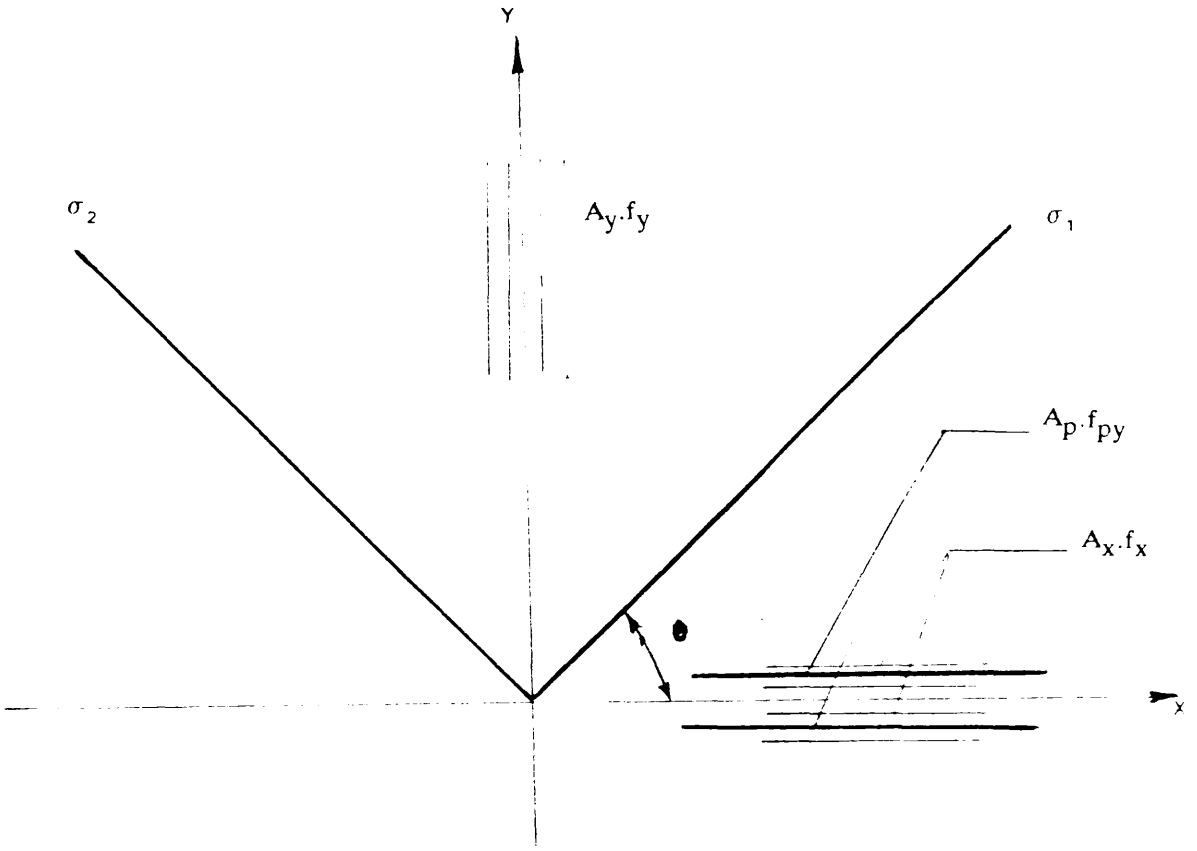

Figure(3.5) Direction of Reinforcing Steel and Principal Stress in Concrete.

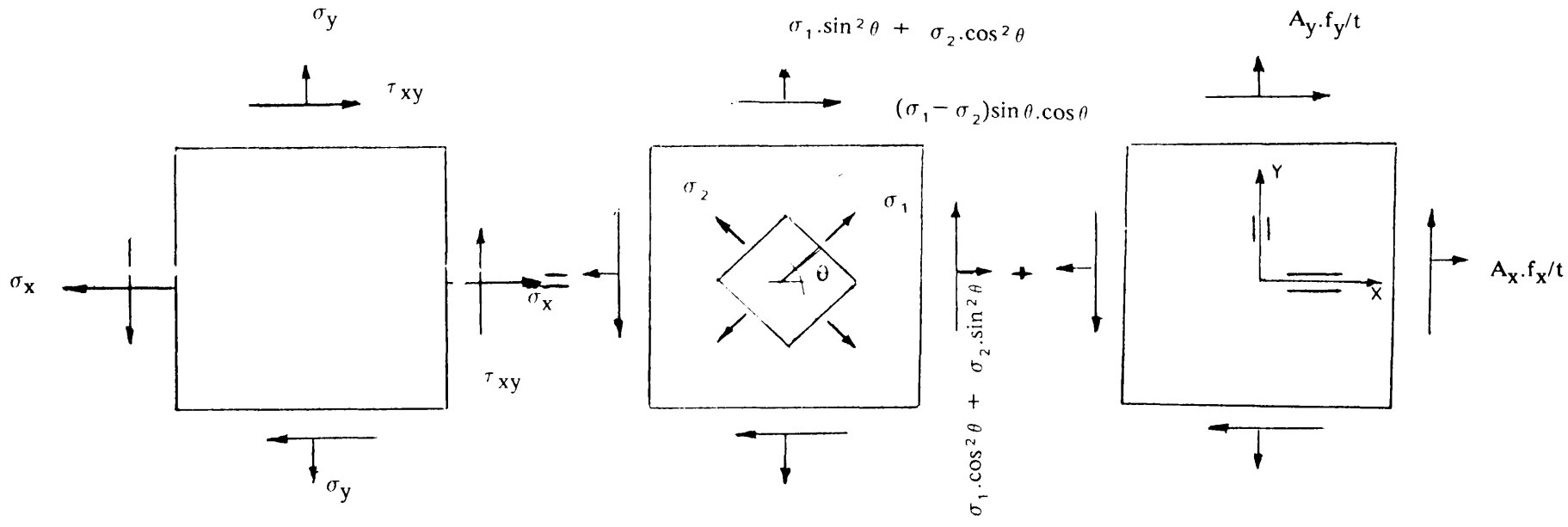

Figure(3.6) Equilibrum of Element under In-Plane Forces.

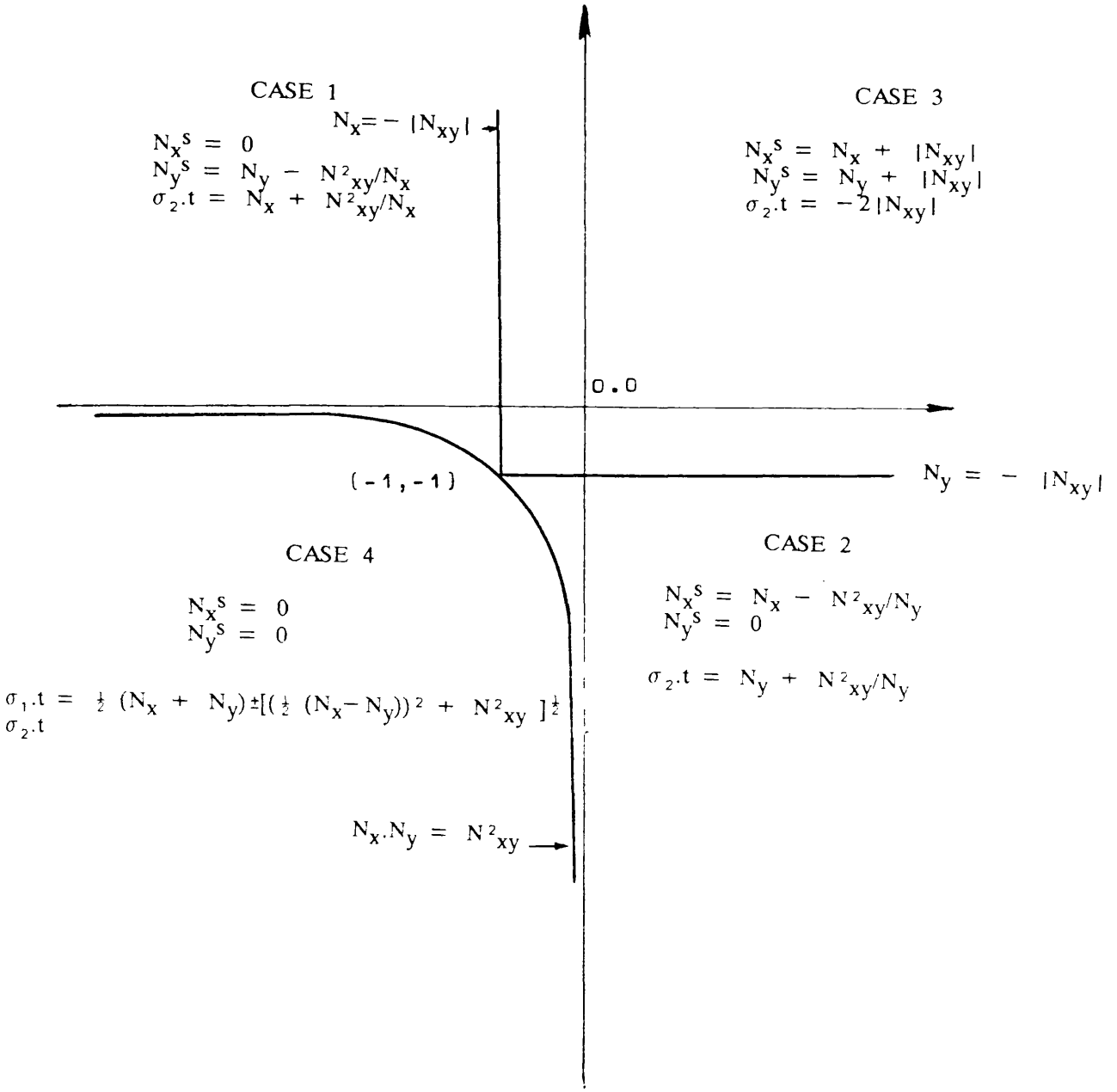

Figure(3.7) Graphical Representation of Four Cases of Reinforcement.

Using the notations

$$A_x f_x = N_x^s \qquad (3.4)$$

$$A_y f_y = N_y^s \qquad (3.5)$$

Eliminating θ and σ_2 from equation (3.4.a) to (3.4.c), we get

$$(N_x^s - N_x)(N_y^s - N_y) = N^2_{xy} \qquad (3.6)$$

This equation represents the yield criterion for reinforced concrete element under in–plane loads. Nielsen based his design equations on the assumptions that

$\sigma_2 < 0$

$|\sigma_2| \leqslant f_{cu}$, so that compression steel is never required, i.e N_x^s and $N_y^s > 0$

From equation (3.4.a) to (3.5)

Case 1 :

If $N_x^s = 0$, and $N_y^s \neq 0$

Then from equatiom (3.6) $N_y^s = (N_y - N^2_{xy} / N_x)$

$\sigma_2.t.\sin^2\theta = N_x$

$-\sigma_2.t.\sin\theta.\cos\theta = N_{xy}$

$\tan\theta = - N_x / N_{xy}$

$\sigma_2.t = N_x + N^2_{xy} / N_x \qquad (3.7)$

If $|\sigma_2| > f_{cu}$, the section is redesigned with increased thickness t.

Case 2 :

If $N_y^s = 0$ and $N_x^s \neq 0$

Then from equation (3.6) $N_x^s = (N_x - N^2_{xy} / N_y)$

$\sigma_2.t.\cos^2\theta = N_y$

$-\sigma_2 t.\sin\theta.\cos\theta = N_{xy}$

$\tan\theta = - N_{xy} / N_y$

$\sigma_2.t = N_y + N^2_{xy} / N_y \qquad (3.8)$

Again if $|\sigma_2| > f_{cu}$, we redesign the thickness of the section.

Case 3 :

If N_x^s and $N_y^s \neq 0$, in this case we minimise total quantity of steel $(N_x^s + N_y^s)$. From the yield criterion in equation (3.6)

$N_y^s = N_y + N^2_{xy} / (N_x^s - N_x)$

$N_x^s + N_y^s = N_x^s + N_y + N^2_{xy} / (N_x^s - N_x)$

Minimising the sum of the steel in both directions;

$d(N_x^s + N_y^s)/dN_x^s = 0$

$d[N_x^s + N_y + N^2_{xy} / (N_x^s - N_x)]/dN_x^s = 1 - N^2_{xy} / (N_x^s - N_x)^2 = 0$

Rearranging the above equation we get

$N_x^s - N_x = \pm |N_{xy}|$

As $N_x^s - N_x > 0$, we choose the positive root

$$N_x^s = N_x + |N_{xy}| \qquad (3.9)$$

Substituting for the yield criterion for N_x^s , we have

$$N_y^s = N_y + |N_{xy}| \qquad (3.10)$$

$\tan^2\theta = (N_x - N_x^s)/(N_y - N_y^s) = 1$

$\theta = 45^0$

$\sigma_2.t = -2|N_{xy}|$

We can deduce from equation (3.9) and (3.10) that

$N_x^s = 0$ if $N_x = - |N_{xy}|$

and

$N_y^s = 0$ if $N_y = - |N_{xy}|$

Case 4 :

If both principal stresses σ_1 and σ_2 in equation (3.3.a) to (3.3.c) are compressive, no steel reinforcement is required, in this case σ_1 and σ_2 are given by

$$\sigma_1.t = \tfrac{1}{2}(N_x + N_y) \pm [(\tfrac{1}{2}(N_x - N_y))^2 + N^2_{xy}]^{\frac{1}{2}} \qquad (3.12)$$

$\sigma_2.t$

Owing to Nielsen assumptions, compression steel is never required. However in certain situations, compression reinforcement is required in one or both direction. Accordingly, reinforcement can either be in tension, compression or no reinforcement required. These situations have increased the number of cases of reinforcement from original four to nine. Table 3.1 shows the 9 possible combinations of reinforcement . In the design for multiple loading in the present study , we limited ourselves to the four cases proposed by Nielsen, as use of compression steel is rarely an economical proposition.

Table 3.1 – Summary of possible combination of reinforcement

case	Reinforcement	Known values	Method of solution
1	x and y tension	$f_x=f_y=f_s$; $\sigma_1 = 0$	Minimisation of $(A_x + A_y)$
2	zero x,y tension	$f_y=f_s$; $f_x=0$	Direct solution
3	zero y, x tension	$f_x=f_s$; $f_y=0$; $\sigma_1 = 0$	Direct solution
4	x & y compression	$f_x=f_y=f_s'$; $\sigma_2 = f_{cu}$	Minimisation of $(A_x + A_y)$
5	zero x, y compression	$f_x=f_y'$; $f_x=0$; $\sigma_2 = f_{cu}$	Direct solution
6	zero y, x compression	$f_x=f_s'$; $f_y=0$; $\sigma_2 = f_{cu}$	Direct solution
7	x tension, y compression	$f_x=f_s$; $f_y=f_s'$ $\sigma_1=0$; $\sigma_2=f_{cu}$	Direct solution
8	y tension, x compression	$f_x=f_s'$; $f_y=f_s$ $\sigma_1=0$; $\sigma_2=f_{cu}$	Direct solution
9	No reinforcement	$f_x=f_y=0$	Direct solution

3.4 DIRECT DESIGN FOR MULTIPLE LOADING CASES

In this section is presented an application of the 'Direct Design Method' to design reinforcement to resist multiple loading. The yield criteria is given by equation (3.6).

$(N_x^S - N_x)(N_y^S - N_y) - N^2_{xy} = 0$

In the case of multiple loading, the design procedure can be as follows.

1. Using the design equations (as shown in figure 3.8), for each load case, calculate the corresponding N^S_{xi} and N^S_{yi}.

2. Calculate the maximum of all the N^S_{xi} and N^S_{yi} taking into consideration all the load cases. Let these be N^S_{x-max} and N^S_{y-max}.

Evidently if we use these as the design stresses, then we will get a safe design but not necessarily an optimum design. So we can move towards an optimum design as follows.

3. Assume that in the X direction we provide N^S_{x-max} , but in the Y direction we provide N_y^S so as to satisfy the yield criterion in each case.

N_y^S is given for each case by

$$N^S_{yi} = N_{yi} + N^2_{xyi} / (N^S_{x-max} - N_{xi}) \qquad (3.13)$$

Calculate the maximum of all these N^S_{yi}. Evidently a safe design is produced if we use N^S_{x-max} in conjuction with the maximum N^S_{yi} determined so as to satisfy the yield criteria.

4. A similar procedure to 3 above can be done if we choose N^S_{y-max} as the design stress in Y direction and calculate the N^S_{xi} for each load case so as to satisfy the yield criterion and choose the maximum of all the N^S_{xi} to determine the design moment in the X direction,

$$N^S_{xi} = N_{xi} + N^2_{xyi} / (N^S_{y-max} - N_{yi}) \qquad (3.14)$$

Therefore a better design is to choose that set of design stress where the

$(N_x^S + N_y^S)$ is the smallest.

We can stop at this stage but if need be we can improve on this by assuming that other combinations are possible and use a simple search technique (i.e examining

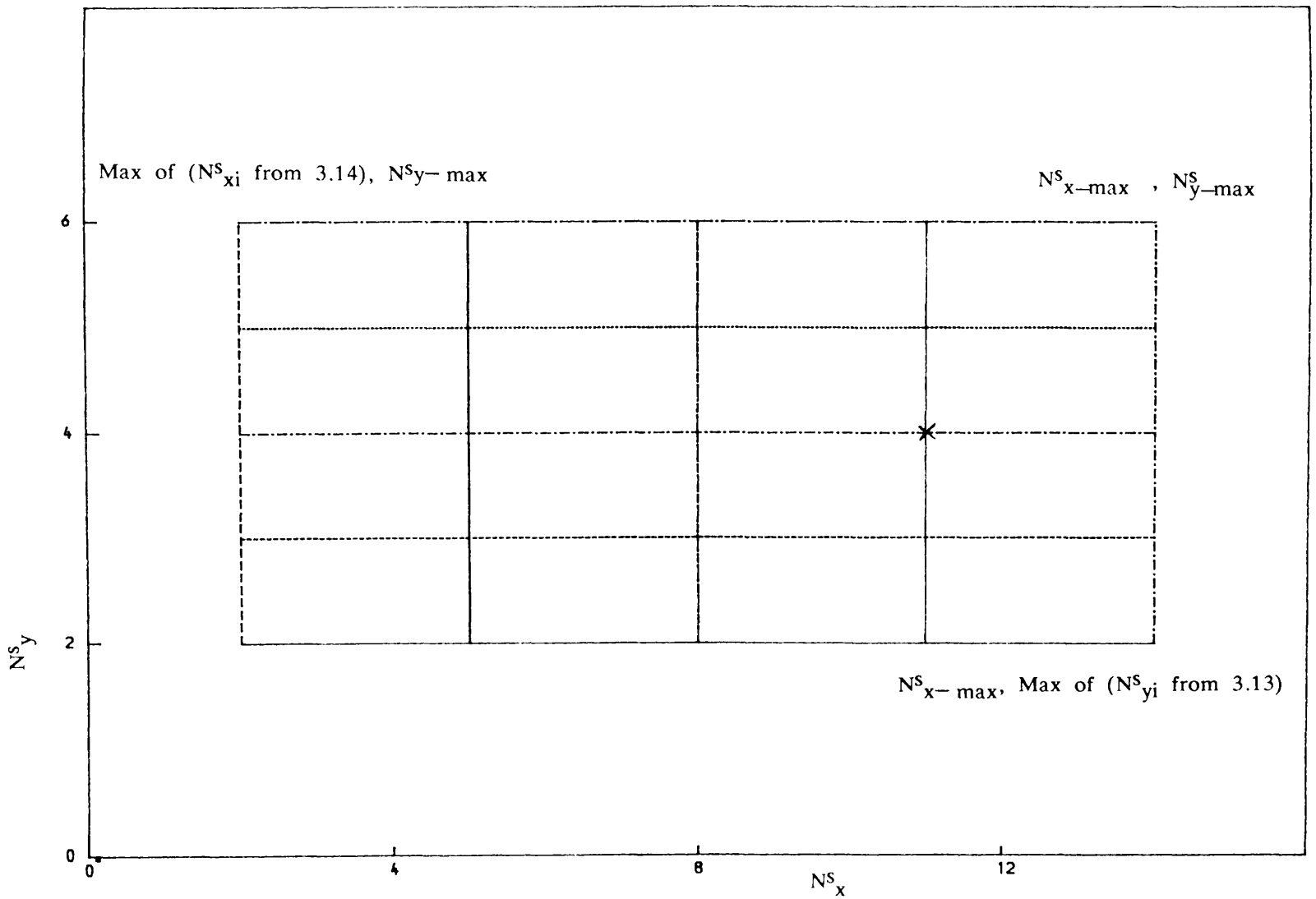

FIGURE 3.8 DESIGN REGION FOR MULTIPLE LOADCASES

the feasable design region as shown in figure 3.8). For each load case, we see if the design stresses at the grid points is a better minimum. If it is not, we reject it. If it is, we check to see if it violates the yield criterion for the load cases considered. If it does, we reject it. If not, we see at which grid point we can get minimum of ($N_x^s + N_y^s$). This give us the optimum design stresses. This results in a large number of simple calculations. In the next section, is presented a simple computer program to accomplish the task.

3.4.1 *Program*

For a given geometrical and mechanical characteristics of a concrete beam and for different combinations of bending and torsional moments, do the following.

1. Calculate the flexural direct stress and torsional shear stress, the flexural stress is calculated at different points in the section, but the shear stress is constant.
2. Evaluate :

$A = N_x / N_{xy}$ and $B = N_y / N_{xy}$.

3. Determine in which of the four regions in figure 3.7 the given stress state lies.
4. Calculate the corresponding value of the principal stress σ_2 , if $|\sigma_2| > f_{cu}$, then the concrete thickness must be increased.
5. Evaluate the forces in the reinforcement N_x^s and N_y^s ,
6. Check the validity of the Nielsen yield criterion equation for different combinations of (N_x^s , N_y^s) varying from their minimal values to their maximal values and for different combinations of (N_x , N_y , N_{xy}).
7. Deduce the optimum reinforcement for the given section of the beam to withstand multiple loading.

3.4.2 *Design application for multiple loadcases*

(Application for designing beams subjected to non proportional combination of bending and torsional load cases)

The computer program described above gives the optimum values of (N_x^S, N_y^S) for the six regions shown in figure 3.9. N_x^S and N_y^S are the theoretical steel values. This section shows how these theoretical steel values are converted to actual steel values.

3.4.2.1 Reinforced concrete beams

The actual steel values for the case of reinforced concrete beams are obtained as follows:

$A_x.f_x = N_x^S.t$

$A_y.f_y = N_y^S.t$

From the above equations the actual steel values A_x and A_y are deduced as:

$A_x = N_x^S.t/f_x$

$A_y = N_x^S.t/f_y$, A_y is the same for the six regions

a) Top flange (region 1)

$A_{x1} = (N^S_{x1}.t/f_x).b$

where b = width of the top flange

b) Side webs (regions 2– 5)

$A_{x2-5} = (N^S_{x2-5}.t/_xf).t$

c) Bottom flange (region 6)

$A_{x6} = (N^S_{x6}.t/f_x).b$

Numerical application for maximum loads of $T_{max}= 32.0$ kN/m and

$M_{max}= 32.0$ kN/m.

$N^S_{x1}= 6$ N/mm, $N^S_{x2}= 6$ N/mm, $N^S_{x3}= 6$ N/mm, $N^S_{x4}= 7$ N/mm, $N^S_{x5}= 10$ N/mm,

$N^S_{x6}= 11.5$ N/mm

$N_y^S= 5.1$ N/mm

Assuming t= 50mm, b= 300mm, assuming high yield steel $f_x=f_y= 540$ N/mm^2,

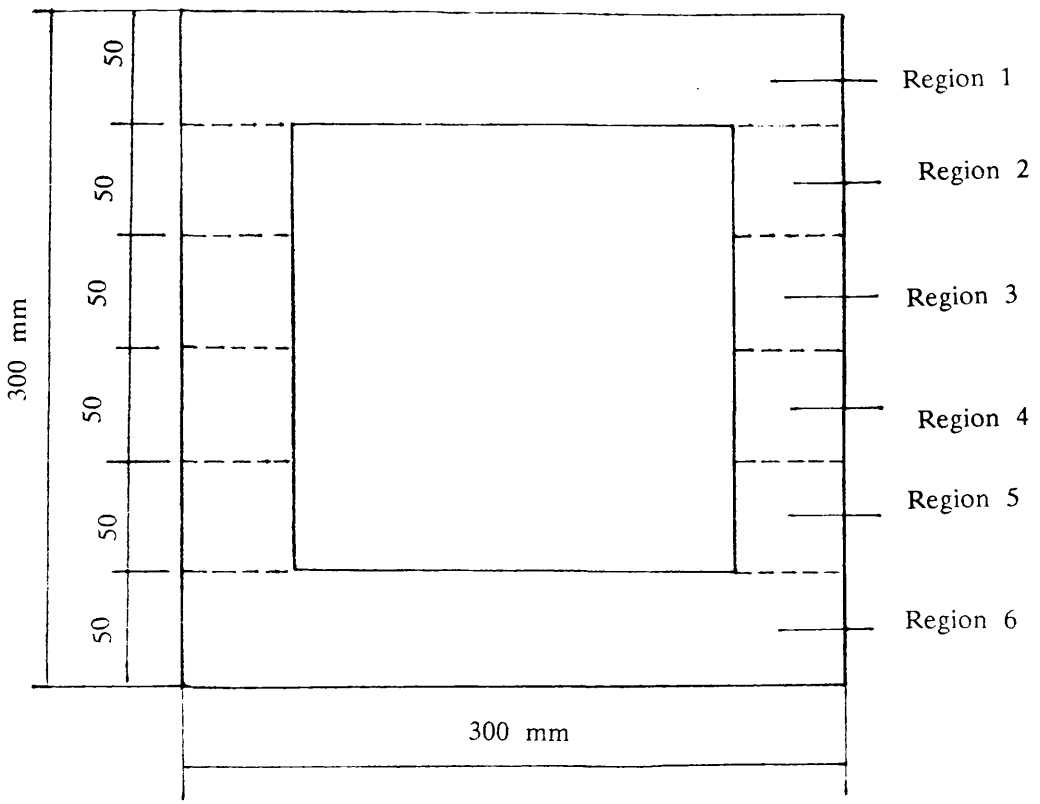

Figure 3.9 The six regions of the beam section considered in the design

Then

x steel : $A_{x1} = 167mm^2$, $A_{x2} = 56mm^2$, $A_{x3} = 56mm^2$, $A_{x4} = 65mm^2$, $A_{x5} = 93mm^2$, $A_{x6} = 320mm^2$

y steel : $A_y = 474mm^2$

Longitudinal steel adopted :

from $A_{x1} = 167mm^2$, use 2 10mm bars in the top flange

from $A_{x2} + A_{x3} = 112mm^2$, use 2 08mm bars in the webs (top half)

from $A_{x4} + A_{x5} = 158mm^2$, use 2 10mm bars in the webs (bottom half)

from $A_{x6} = 320mm^2$, use 2 08mm and 3 10mm bars in the bottom flange

Transverse steel adopted :

from $A_y = 474mm^2$, use 08mm stirrup at 105mm

Figure 3.10 shows details of reinforced concrete beam cross-sectional reinforcement.

3.4.2.2 Partially prestressed concrete beams

The prestressing wires have an effective prestressing stress f_{pe} of their yield stress f_{py}. Then the remaining stress $(f_{py} - f_{pe})$ is availible to act as ordinary reinforcement.

The actual steel values for the case of reinforced concrete beams are obtained as follow :

From figure 3.4.b the following expression can be expressed

$$A_x.f_x = N_x^s.t = A_{xr}.f_x + A_{xp}.(f_{py} - f_{pe})$$

$$A_y.f_y = N_y^s.t$$

where A_{xr} = area of additional reinforcement needed

A_{xp} = area of prestressing wires per unit width

f_{py} = yield stress of prestressing wires

f_{pe} = effective stress of prestressing wires

f_x = yield stress of steel in x direction

From the above equations the actual steel values of A_{xr} and A_y are deduced

$$A_{xr} = [\, N_x^s.t - A_{xp}.(f_{py} - f_{pe})]/f_x$$

$A_y = N_y^s.t/f_s$, A_y is the same for the six regions

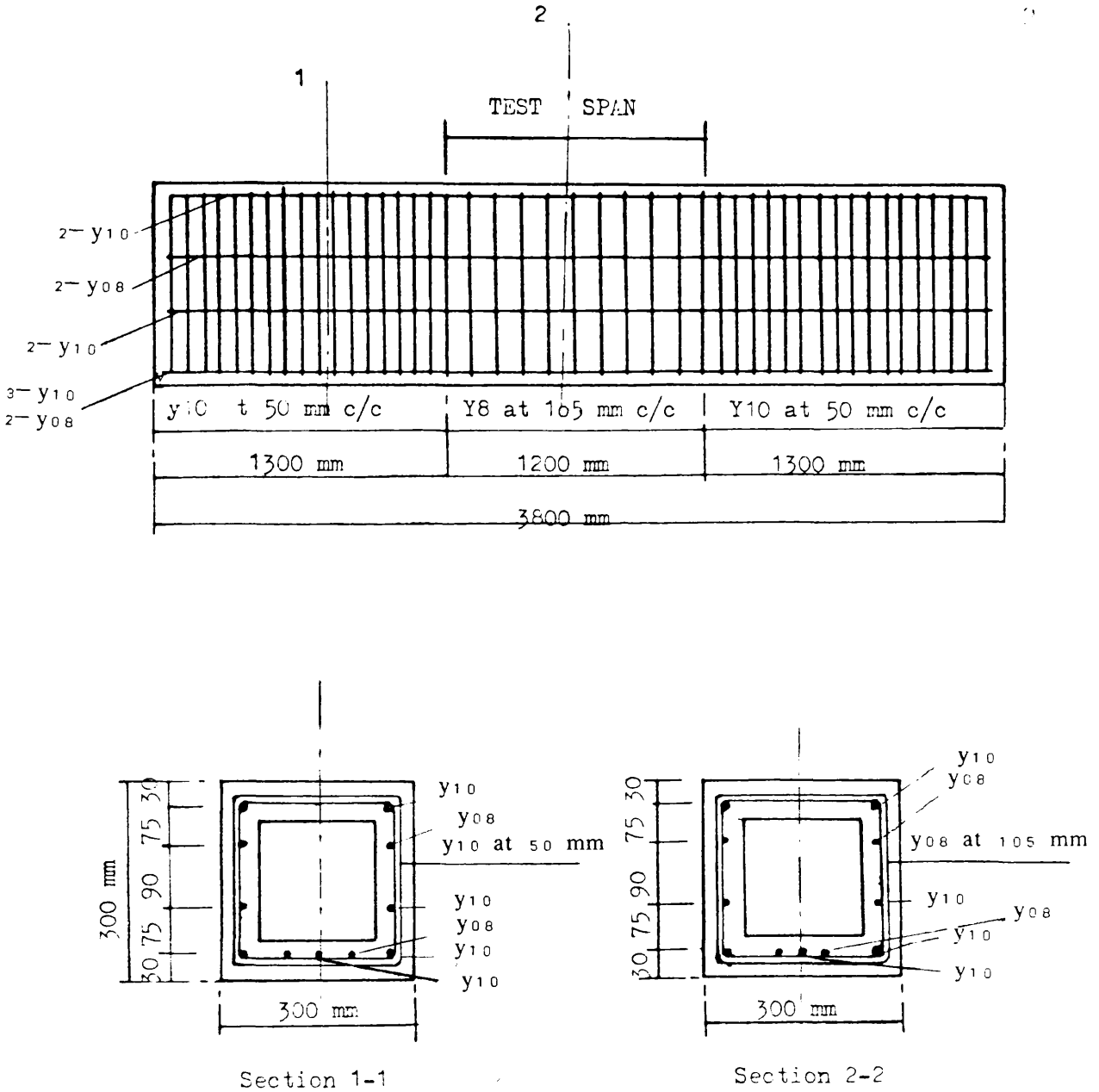

Figure 3.10 Reinforcement details of beams in series A.

1) Top flange (region 1)

$A_{xr_1} = [(N^S_{x_1}.t - A_{xp_1}.(f_{py} - f_{pe}))/f_x].b$

2) Side webs (region 2– 5)

$A_{xr_{2-5}} = [(N^S_{x_{2-5}} . t - A_{xp_{2-5}} . (fpy - f_{pe})) / f_x].t$

3) Bottom flange (region 6)

$A_{xr_6} = [(N^S_{x_6}.t - A_{xp_6}.(f_{py} - f_{pe}))/f_x].b$

Numerical application for maximum load of $M_{max}= 32.0$ kN.m and $T_{max}= 32.0$ kN.m

Five prestressing wires of 5mm diameter were chosen, 3 in the bottom flange and 2 in the webs (bottom half).

$N^S_{x_1}= 5.2$ N/mm, $N^S_{x_2}= 4.7$ N/mm, $N^S_{x_3}= 4.2$ N/mm, $N^S_{x_4}= 5.1$ N/mm,

$N^S_{x_5}= 7.1$ N/mm, $N^S_{x_6}= 9.2$ N/mm

$N_y^S= 5.1$ N/mm,

Assuming t= 50mm, b= 300mm, $f_{py}= 1522$ N/mm^2, $f_{pe}= 585$ N/mm^2, $f_x= 540$ N/mm^2

$A_{xp_1}= 0$, $A_{xp_2}= 0$, $A_{xp_3}= 0$, $A_{xp_4}= 0$, $A_{xp_5}= 0.8$ (2 wires of area 40mm^2/t), $A_{xp_6}= 0.2$ (3 wires of area 60mm^2/b)

Then

x steel: $A_{xr_1}= 144$mm^2, $A_{xr_2}= 44$mm^2, $A_{xr_3}= 39$mm^2, $A_{xr_4}= 47$mm^2, $A_{xr_5}= 0$, $A_{xr_6}= 151$mm^2

y steel : $A_y = 474$mm^2

Longitudinal steel :

from $A_{xr_1}= 144$mm^2, use 2 10mm bars in the top flange

from $A_{xr_2} + A_{xr_3}= 83$mm^2, use 2 08mm bars in the webs (top half)

from $A_{xr_4}= 47$mm^2, use 2 08mm bars in the webs (bottom half)

from $A_{xr_5}= 0$ and $A_{xp_5}= 40$mm^2, use 2 prestressing wires of 5mm diameter

from $A_{xr_6}= 151$mm^2 and $A_{xp_6}= 60$mm^2, use 2 10mm bars and 3 prestressing wires of 5mm diameter.

Transversal steel :

from $A_y = 474$mm^2, use 08mm stirrup at 105mm

Figure 3.11 shows details of partially prestressed concrete beam cross– sectional reinforcement.

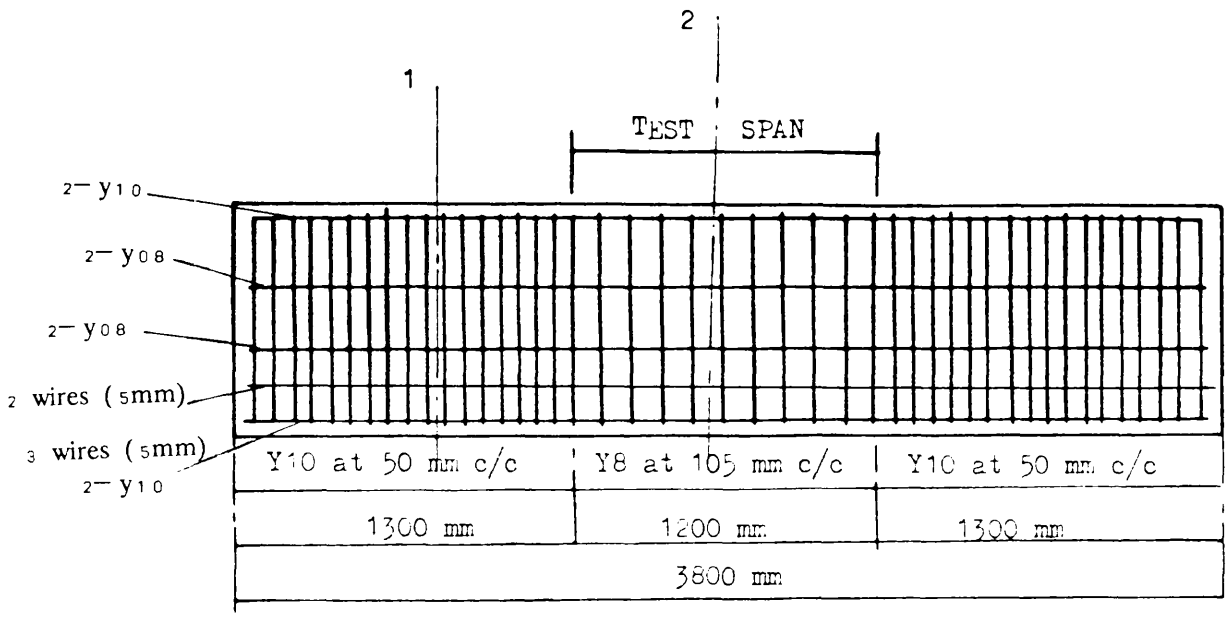

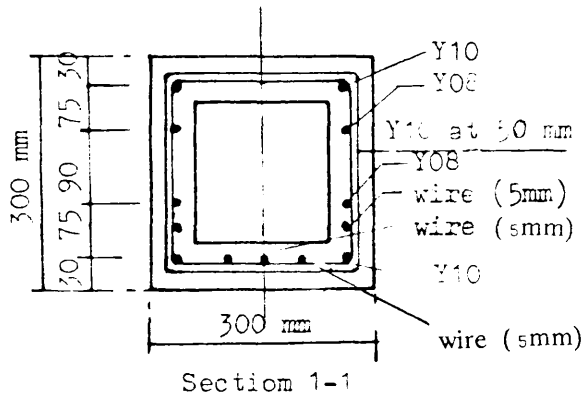

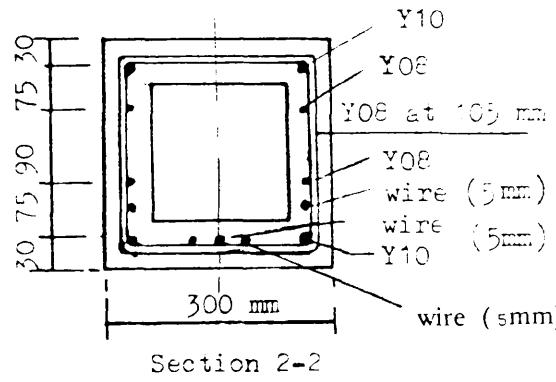

Figure 3.11 Reinforcement details of beams in series B.

CHAPTER 4

TESTING PROCEDURE

4.1 INTRODUCTION

The aim of this chapter is to explain the experimental set up, the determination of material properties and the test programme. The experimental set up was used to study the strength and behaviour of reinforced and partially prestressed concrete hollow beams subjected to multiple loading.

The investigation of the beams is carried out to study the following :

a) Load– deflection relationship.

b) Load– twist relationship.

c) Crack pattern and crack propagation.

d) Strain distribution.

e) Failure characteristics.

4.2 DESCRIPTION OF TEST RIG

The test rig shown in figures 4.1 and 4.2 is a three– dimensional frame designed for the independant application of torsion and bending moment. Bending moment was applied by means of a hydraulic jack fixed to the main frame. Load was transferred to the model through a speader beam mounted on the model by means of support bearings (details A and B). This type of support bearings allow rotational movement for torsion. Torsion was applied through the torsional arm fixed to each end of the model. The torsion arms consisted of a triangular frame with adjustement screws fixed to a 25mm steel plate with an inner face of aluminium. The torsional arm is mounted on an open box which is fixed to each end of the beam. On the open box is fixed a shaft which is linked to a bearing as shown in figure 4.1. This bearing rests on a steel stanchion stool fixed to the concrete floor. Torsional load was applied through the hydraulic jacks attached to

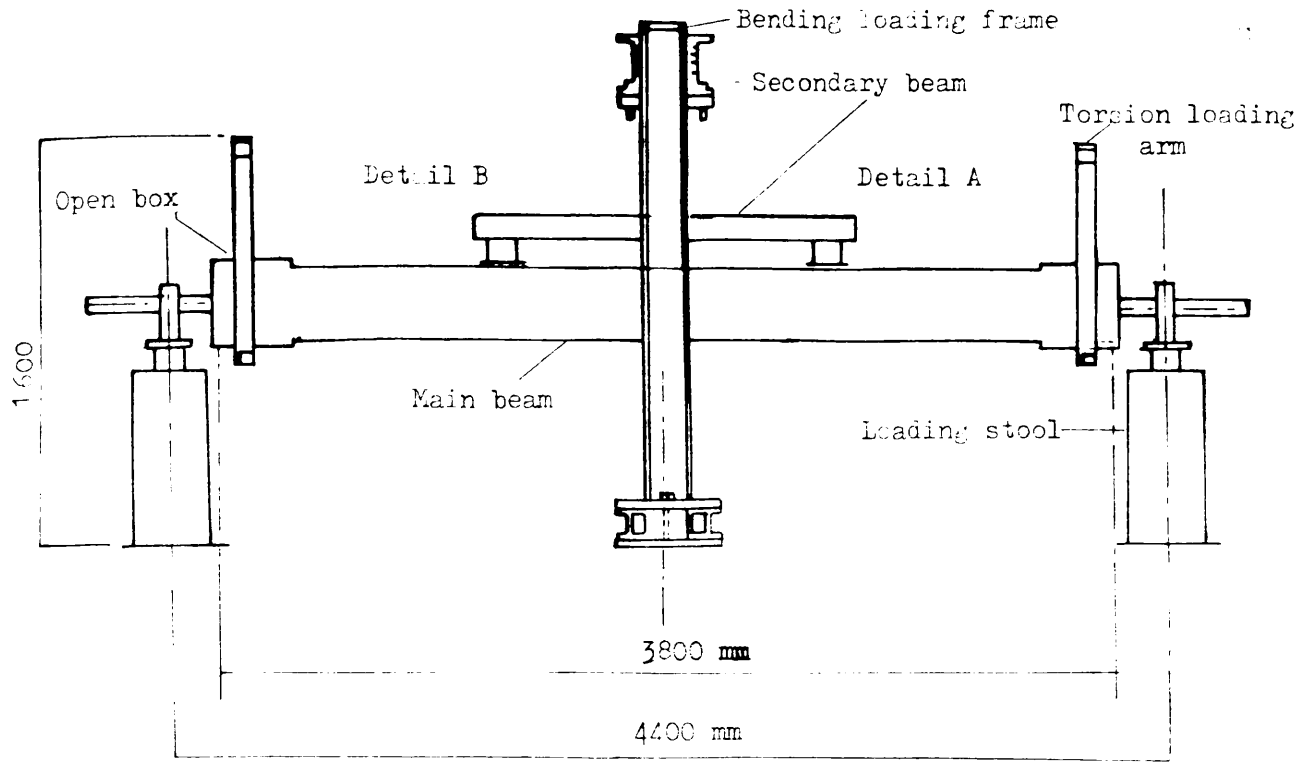

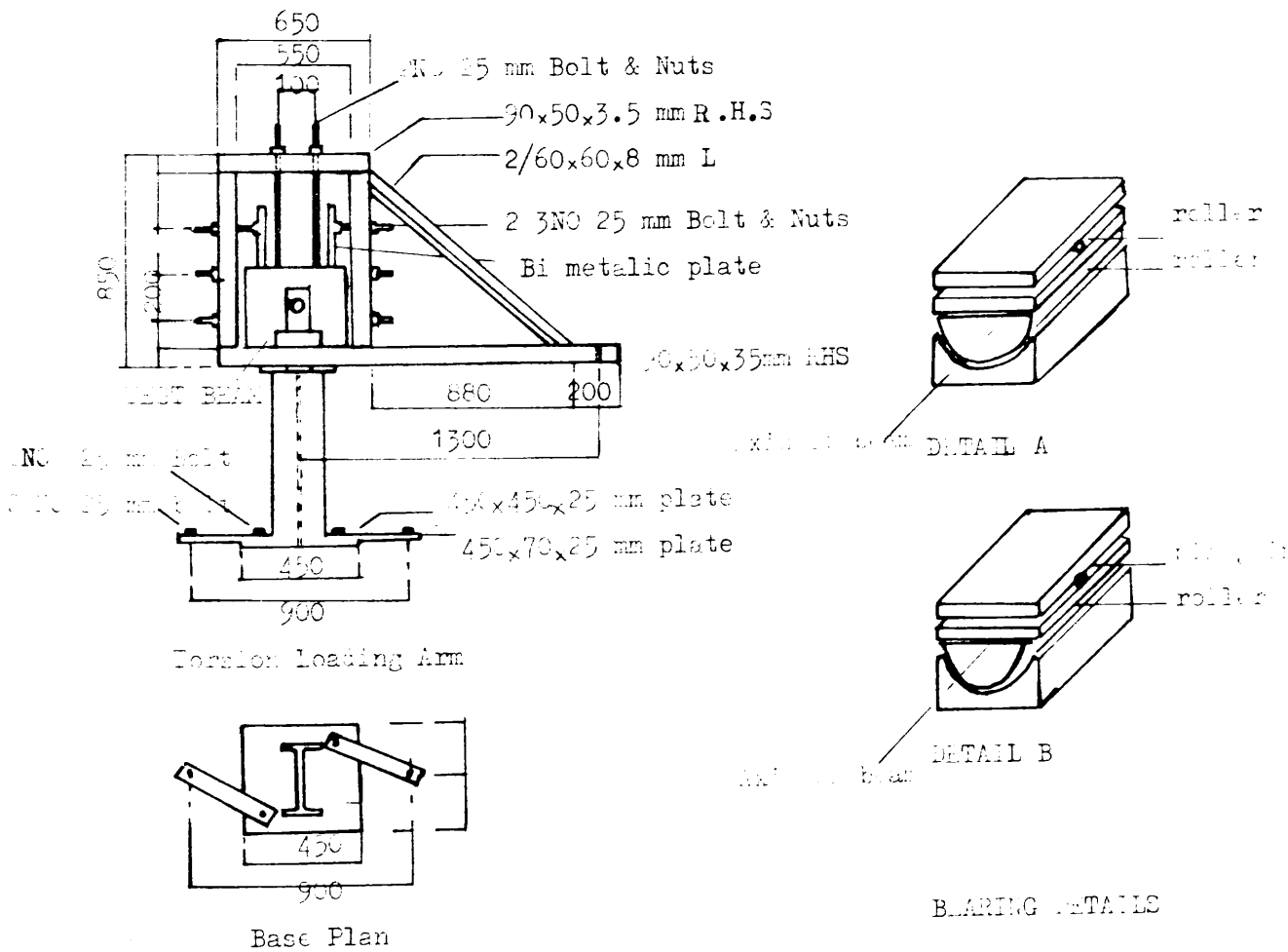

Figure (4.1) Experimental Testing Frame and Details

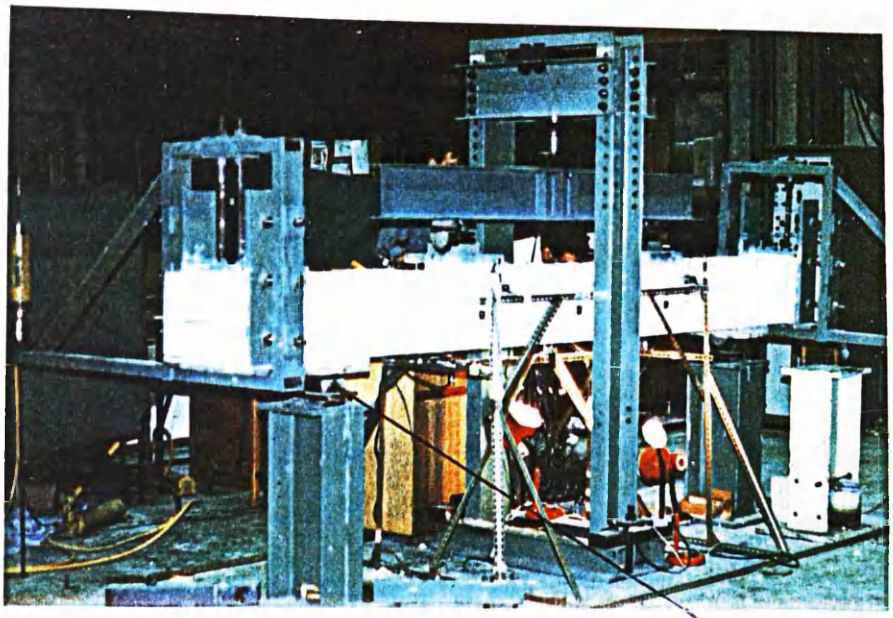

Figure(4.2a) Original Test Setup

Note: The Axis Of Rotation is Below the Beam .

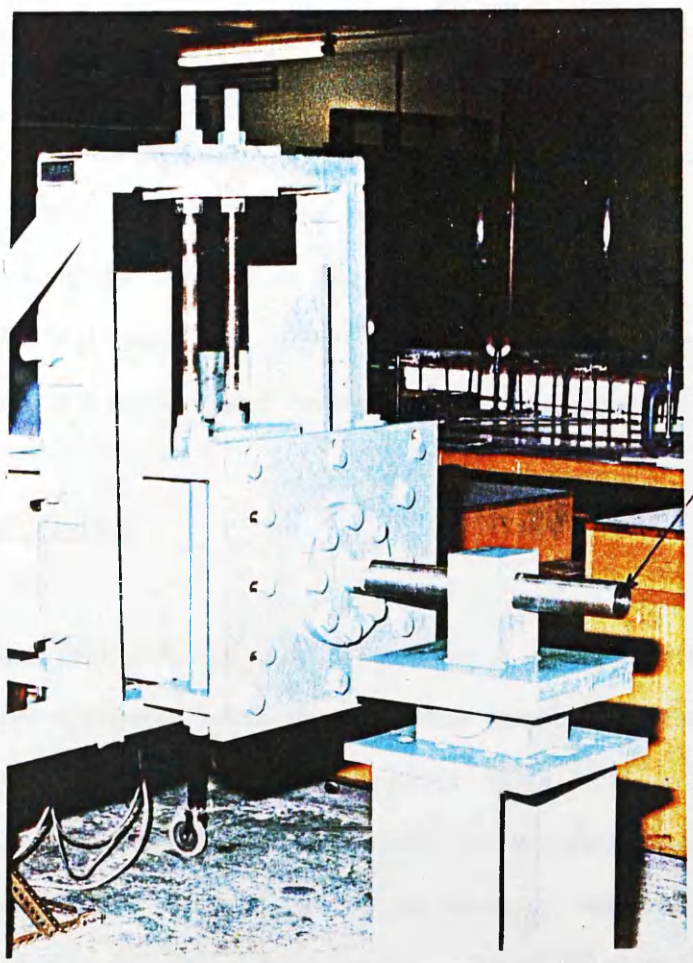

Figure (4.2.b) Improved Test Set Up

Note:The Axis Of Rotation Coincides with The Central Axis Of The Tested Beam.

each of the torsional arm. The applied load was measured by means of a load cell.

4.3 MATERIALS USED

4.3.1 *Concrete* :

The concrete mix consisted of rapid hardening cement, 10mm Hyndford gravels and zone 2 Hyndford sand obtained from Lanarkshire. A mix proportion of 1:1.5:2.5 was designed for an average cube strength of 45 N/mm^2 at 7 days, and a minimum slump of 100mm was specified for the mix. A 12mm diameter poker vibrator was used for compaction. After casting, the beams were cured under damp hessian for the first three days before removing the formwork for final curing under laboratory conditions.

For each test beam, control specimens included 6 Number 100mm cubes and 6 Number 150x300mm cylinders. The cube strength, cylinder compressive strenght, cylinder split tensile strength, and the static modulus of elasticity were determined at the time of testing the beam or at 28 days old as per BS 118, parts 116, 117 and 121[1]. Table 4.1 shows the properties of laboratory cured concrete for all the models. Figure 4.3 shows typical concrete stress– strain curve.

4.3.2 *Reinforcing steel* :

High yield deformed bars of diameter 8 and 10mm were used for both longitudinal and transverse reinforcement. Four samples for each diameter of bar were tested in an OLSEN testing machine fitted with a S– type electronic extensometer. The testing procedure followed the manufacturer's instruction manual. The yield stress of the bar was taken as the stress at which a line parallel to the initial slope of the curve from 0.2% proof strain intersects the curve. The yield strain was taken as the strain at yield stress assuming linear stress– strain

TABLE 4.1 – Properties of Concrete used in the Beams

Beam Mark	Compressive Strength (cube f_{cu}) N/mm^2	Compressive Strength (cylinder f_c') N/mm^2	split cyl Tensile Strength f_t N/mm^2	Modulus of elasticity E_c KN/mm^2
A0	47.5	34.2	3.1	23.2
A1	49.3	37.4	3.2	25.1
A2	46.0	33.5	3.7	22.3
A3	47.6	35.2	3.1	23.5
A4	54.9	41.2	3.3	24.6
B1	50.7	39.7	3.6	27.6
B2	57.6	40.9	3.7	28.7

* All the values given above are for laboratory cured specimens.

A0 : Corresponds to the pilot test beam.

A1 to A4 : are reinforced concrete beams.

B1 & B2 : are partially concrete beams.

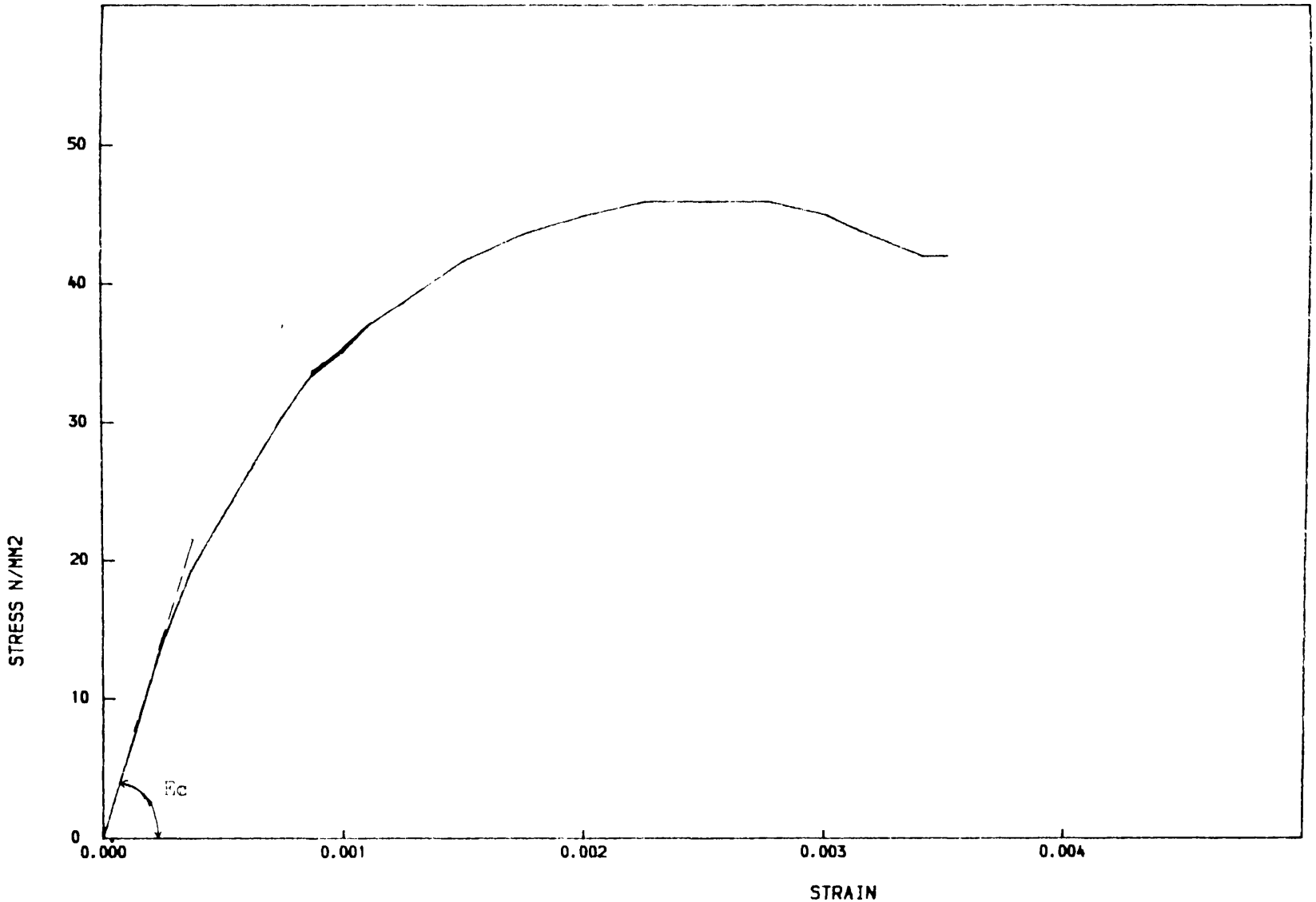

Figure (4.3) Typical stress-strain curve for concrete

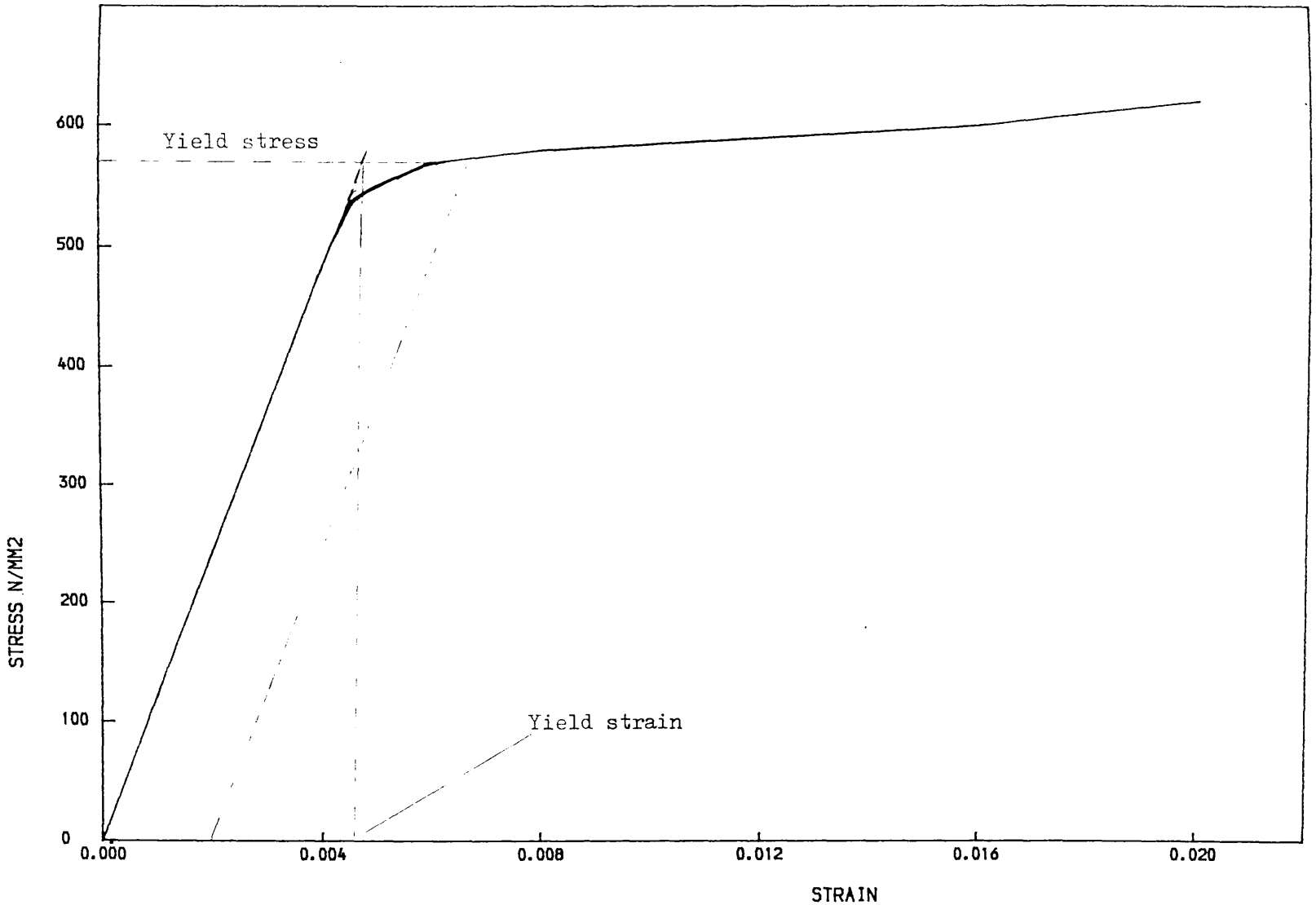

FIGURE (4.4) Definition of yield stress and strain of steel reinforcement

relationship as illustrated in figure 4.4. The mean value from four specimens for each diameter are presented in table 4.2 . Typical measured stress– strain curves for each diameter are presented in figures 4.5 and 4.6 .

Table 4.2 : Properties of steel reinforcement

Bar size mm	Yield stress N/mm^2	Yield strain 10^{-6} mm	Ultimate stress N/mm^2	Young's Modulus KN/mm^2
08	482	2446	592	201
10	525	2540	640	210

4.3.3 *Prestressing wires* :

Five prestressing wires of 5mm diameter were used in the two partially prestressed beams. Using a proof strain of 0.2% , the mean tensile yield stress was 1670 N/mm^2, mean yield strain was $8200x10^{-6}$, mean modulus of elasticity 203 KN/mm^2 and mean ultimate tensile stress of 1750 N/mm^2 ·

4.4 FORMWORK

The formwork was made up of two parts, an internal core and an open external box. The internal core was made up of 200mm thick polysterene sheet. The dimension of the polysterene was 200x200x2640mm. The open external box was made up of 20mm thick plywood strengthened by 50x50mm horizontal and vertical batterns. The external dimension was 300x300x3800mm. The ends of the external open box were solid. Figure 4.7 shows the formwork in elevation and in cross–section.

Since the wall thickness was only 50mm, maximum size of aggregate and the reinforcing bar diameter was restricted to 10mm.

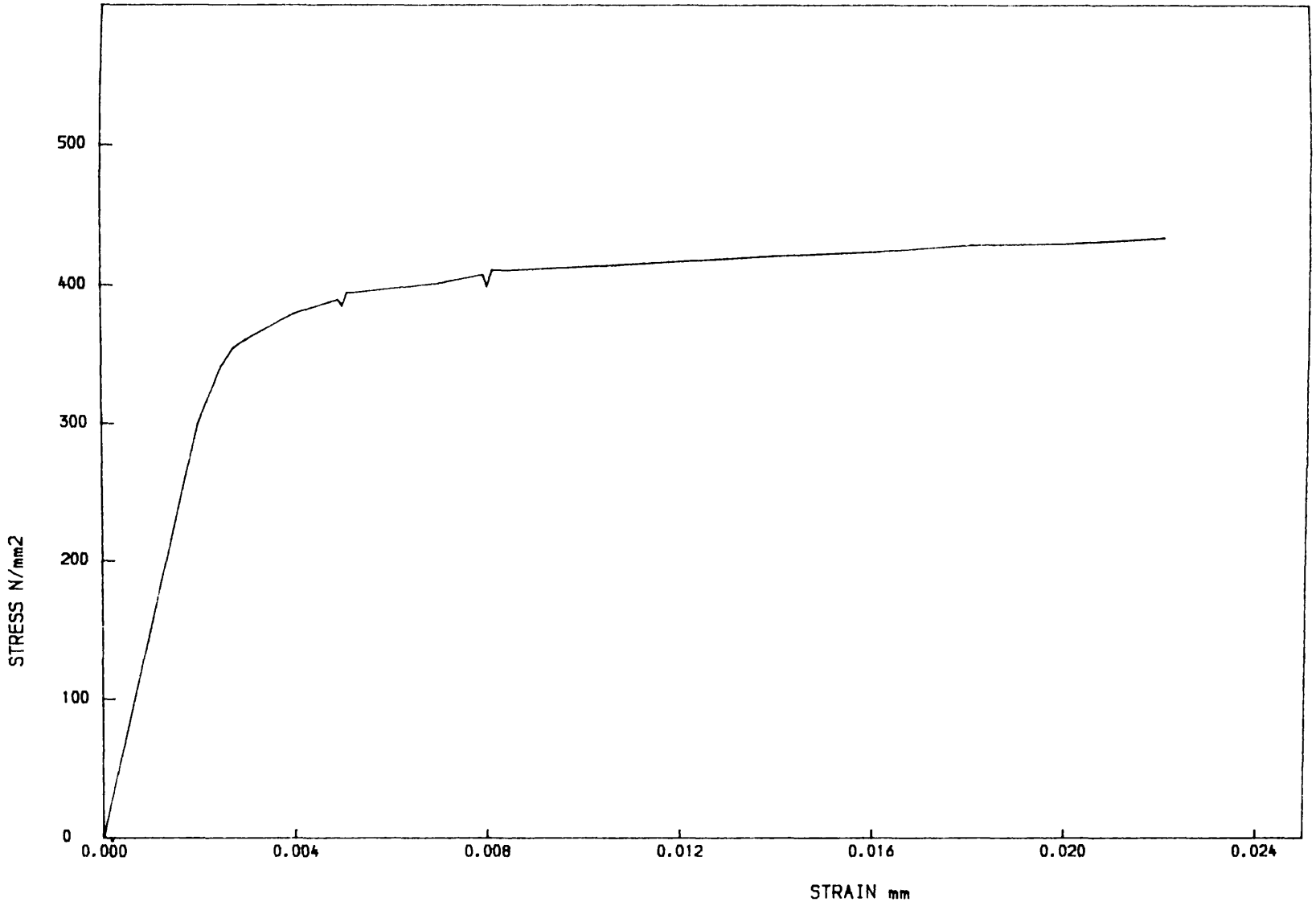

Figure (4.5) Typical stress-strain curve for a bar of 08 mm diameter

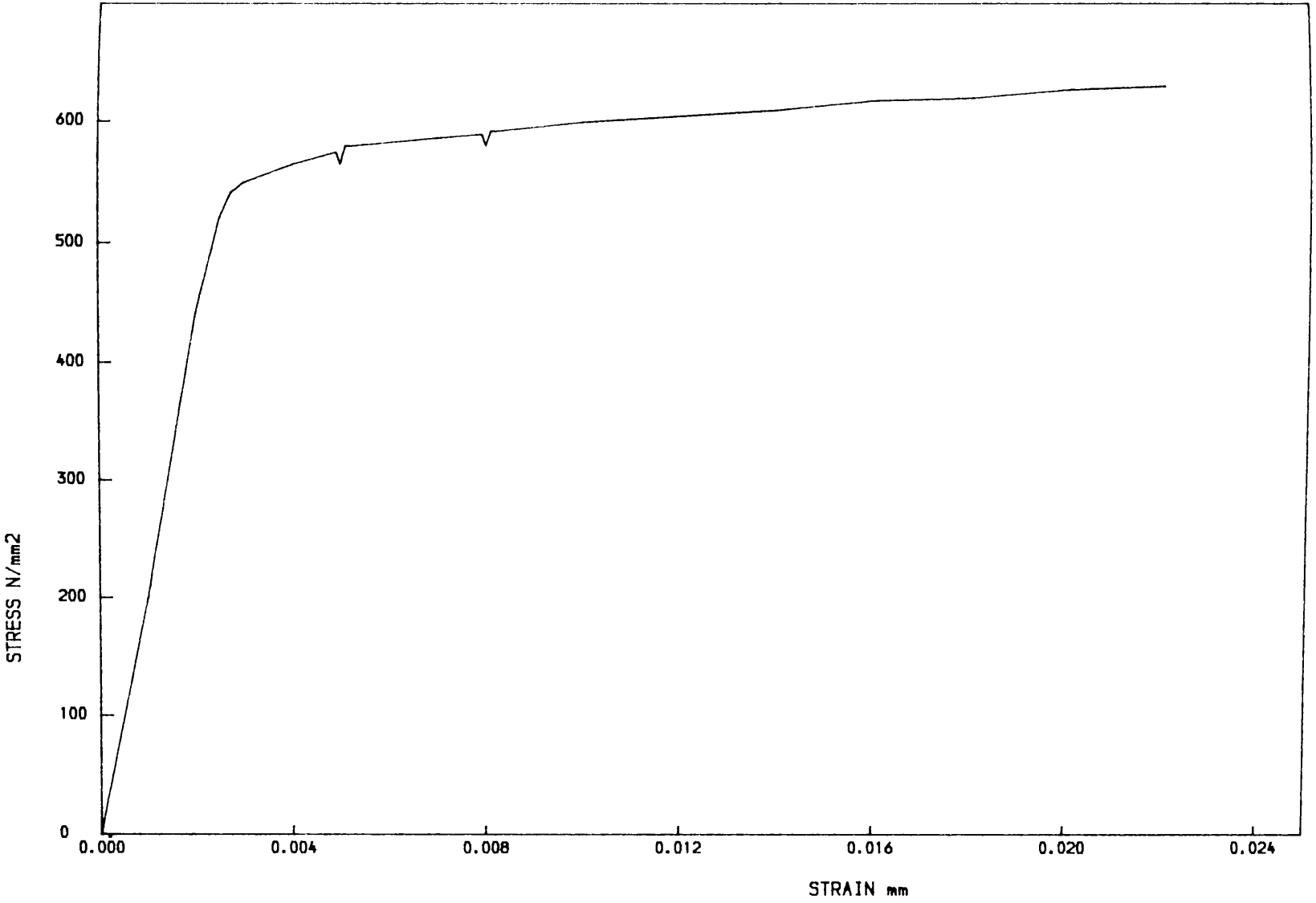

Figure (4.6) Typical stress-strain curve for a bar of 10 mm diameter

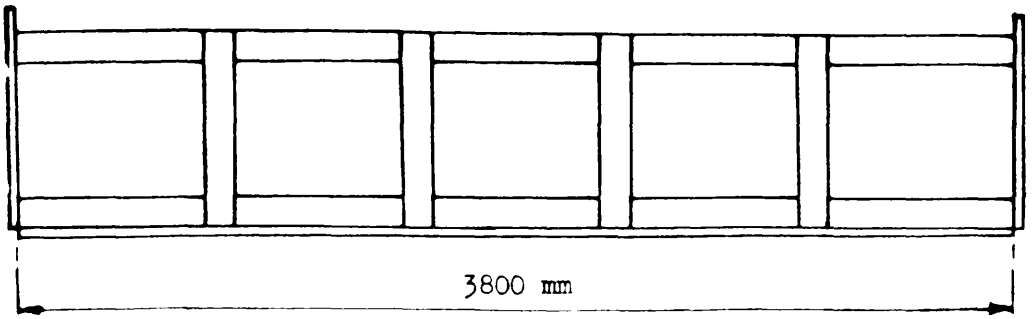

a) ELEVATION OF FORMWORK

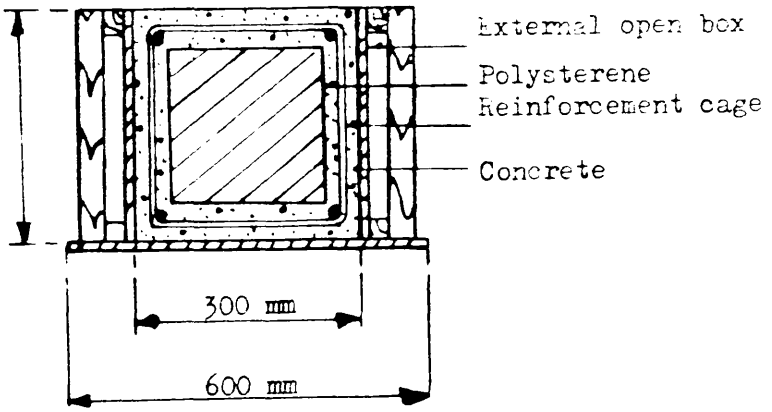

b) CROSS-SECTION OF FORMWORK

Figure (4.7) Typical Formwork for Models

4.5 INSTRUMENTATION

4.5.1 *Loads*

Hydraulic jacks were used to apply both torsion and bending moments, and load cells were used to measure the corresponding loads. Load cells were connected to a data logger. Figure 4.8 shows the loading arrangement.

4.5.2 *Global deformations*

Twist and deflection were measured at various points within the test span by means of a linear voltage displacement transducers (LVDT). The LVDT's were used in conjuction with an automatic data storing and processing system for the recording of results.

4.5.2.1 Deflection

The vertical deflection of the beam was measured by means of transducers located at midspan of the beam and at 600mm from the centre– line on both sides of the beam as shown in figure 4.9 . All the measurements were taken at the bottom face of the beam.

4.5.2.2 *Twist*

Twist was measured by means of transducers located along the horizontal centreline of beam on both webs as shown in figure 4.10. Rotation at any of the vertical points was obtained by dividing the vertical difference in displacement between directly opposite transducers by the respective horizontal distance between them, as shown in figure 4.11. Twist along the test span was obtained as the difference in rotation between two successives sections.

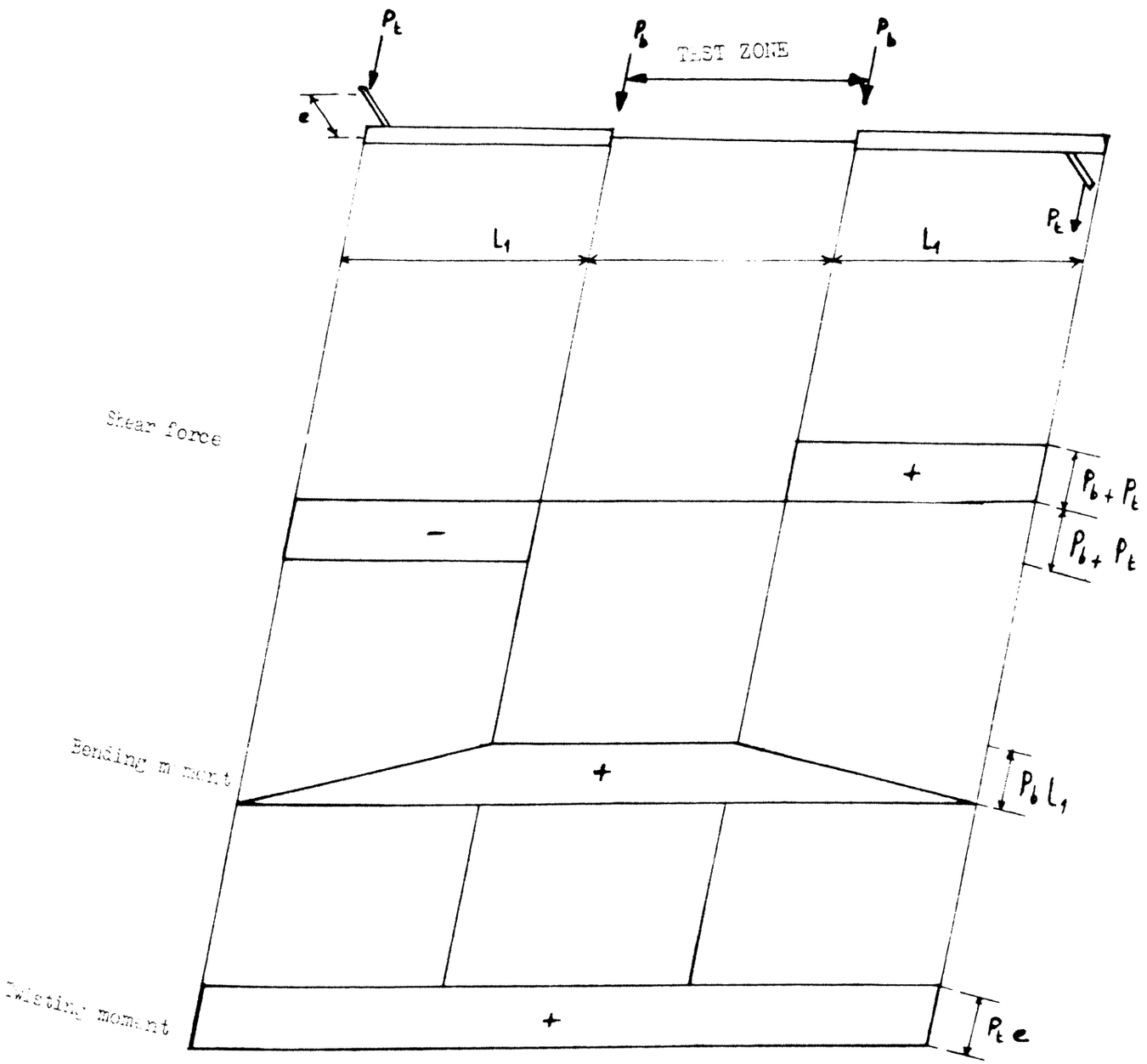

Figure (4.8) Loading arrangement for beams under Torsion and Bending

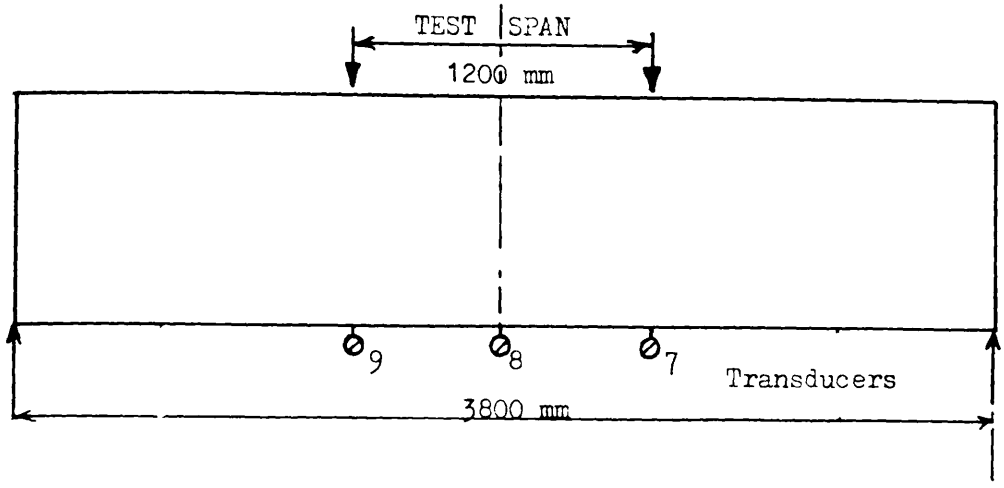

Figure (4.9) Transducers locations at bottom surface of beams

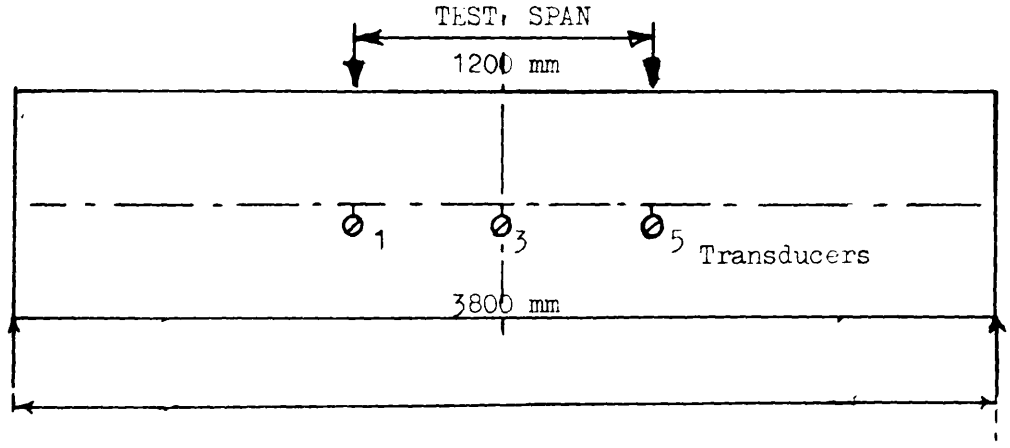

a) FRONT WEB

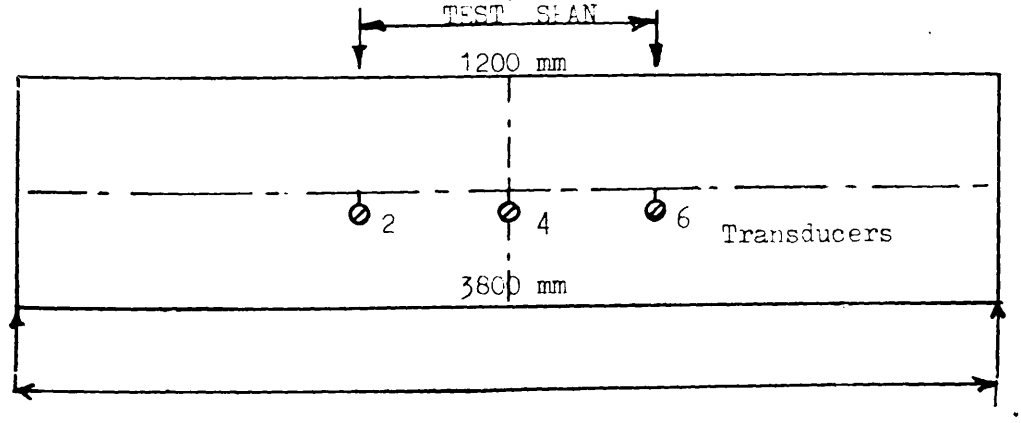

b) REAR WEB

Figure (4.10) Transducers locations on webs of beams.

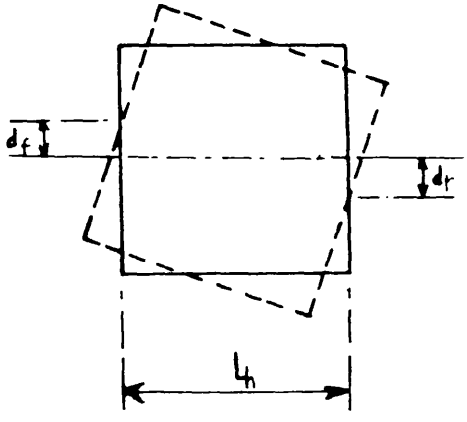

Figure (4.11) Deformation of Beam section under Torsional loading.

4.5.3 *Local deformations*

4.5.3.1 Strains

Strains in longitudinal and transverse steel bars were measured by means of 6mm long electrical resistance strain gauges type EA–06– 240LZ– 120 connected to a linear voltage processing mini–computer (data logger). To measure strain in reinforcement, a pair of strain gauges was fixed directly on to opposite face of the bar. Accordingly, the strain recorded at each load stage was taken as the average of the reading from two gauges. Figure 4.12 shows the location of strain gauges on reinforcement. 100mm demec gauges were used for measuring concrete surface strains.

4.5.3.2 Crackwidth and crack pattern

Crackwidths were measured by means of a crackwidth measuring microscope measuring to 0.02mm. The object of crackwidth measurement was to obtain a quantitative measure of the severity of the crack instead of arbitrary description being used and also for the purpose of monitoring the growth of cracks. At each load stage, crack pattern was traced on the beam by means of a marker.

4.6 TESTING PROCEDURE

The beams were tested under non–monotonic and non–proportional loading. The details of the loading procedure are shown in figures 4.13 to 4.18. One important feature of the load path used in these tests should be noted. For example comparing load paths in figures 4.13 to 4.16 and figures 4.17 to 4.18, One can see that the load steps are much larger in the case of figures 4.17 to 4.18 adopted for the series B (i.e partially prestressed beams) compared with figures 4.13 to 4.16 adopted for the series A (i.e reinforced concrete beams).

The nature of the beam supports and torsion loading arms were such that in the loading sequence, a uniform torque could be applied along the beam length. The uniform bending moment in the test span was applied by two points loads.

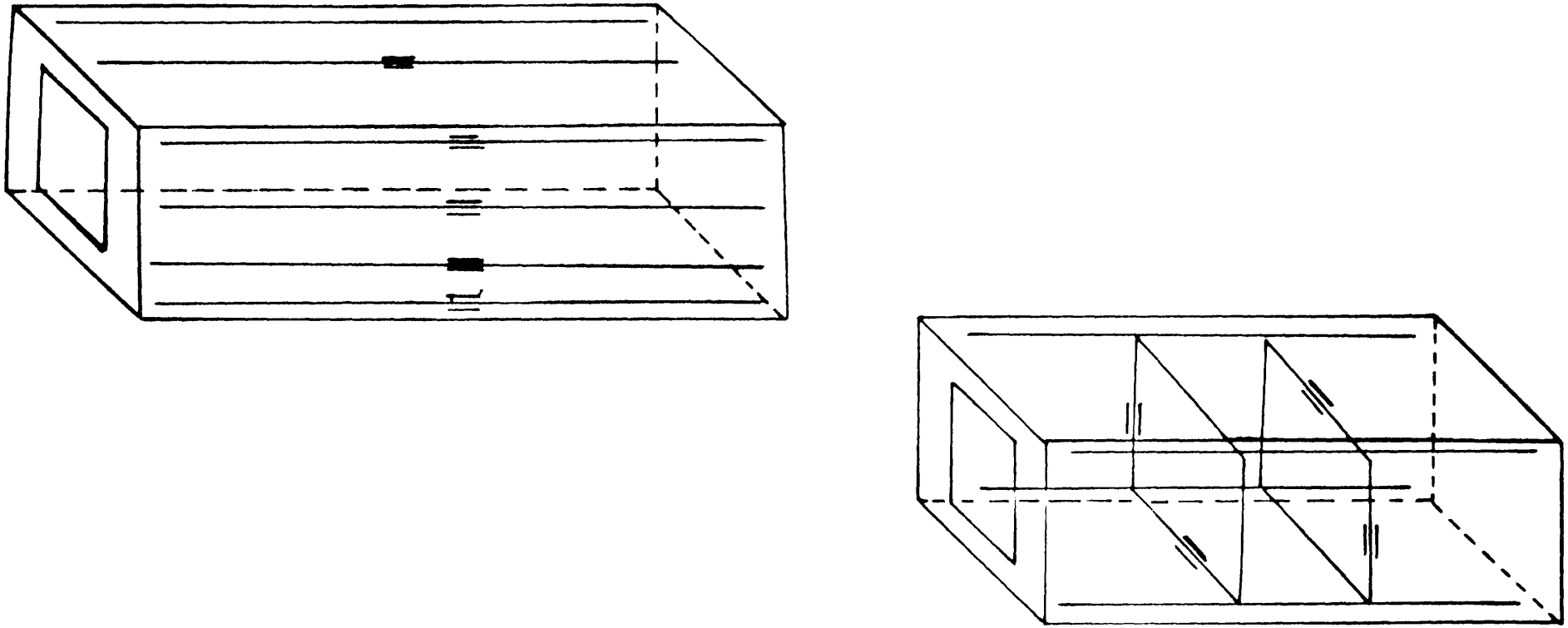

figure (4.12) Strain gauges location on reinforcement

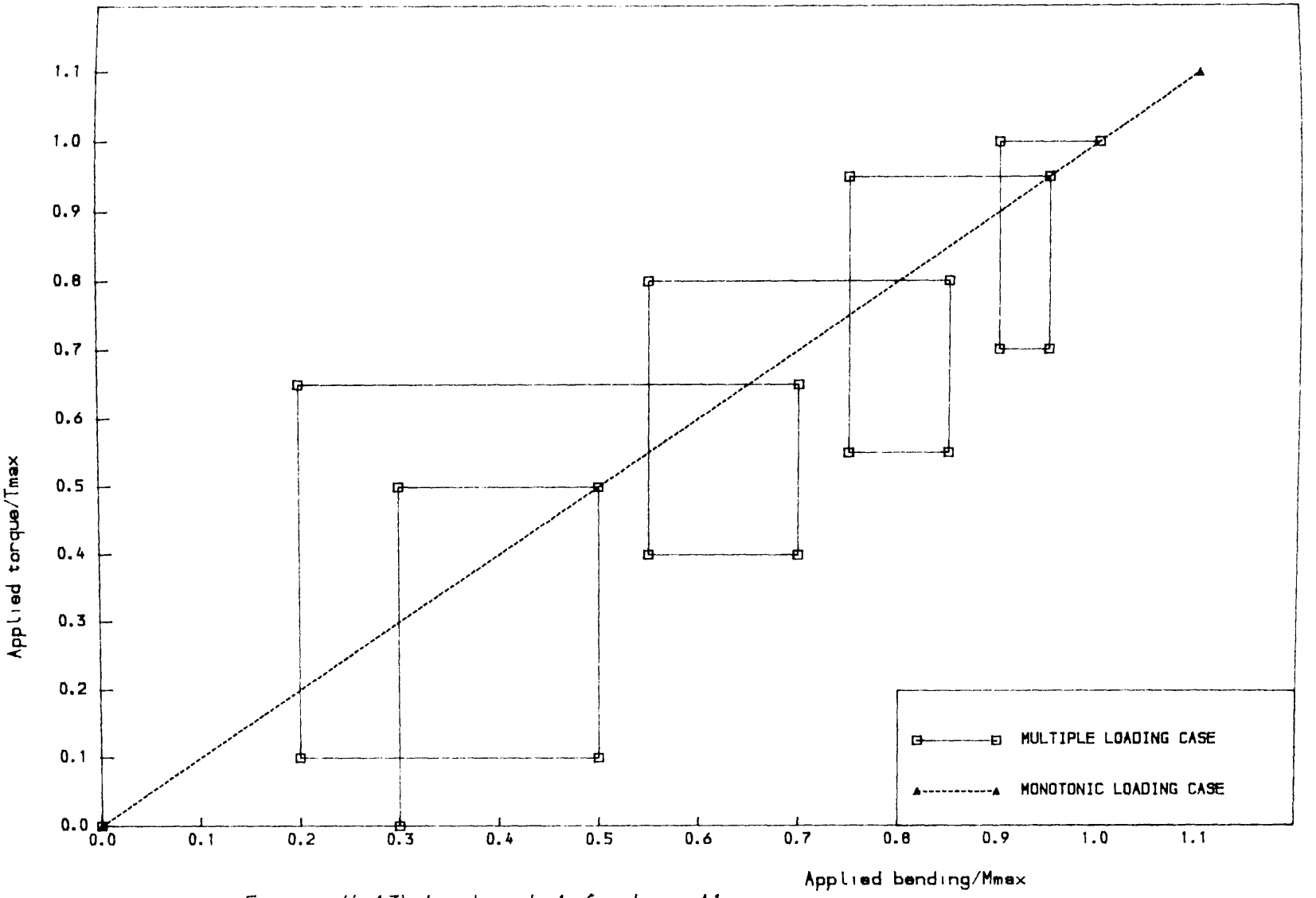

Figure (4.13) Load path 1 for beam A1

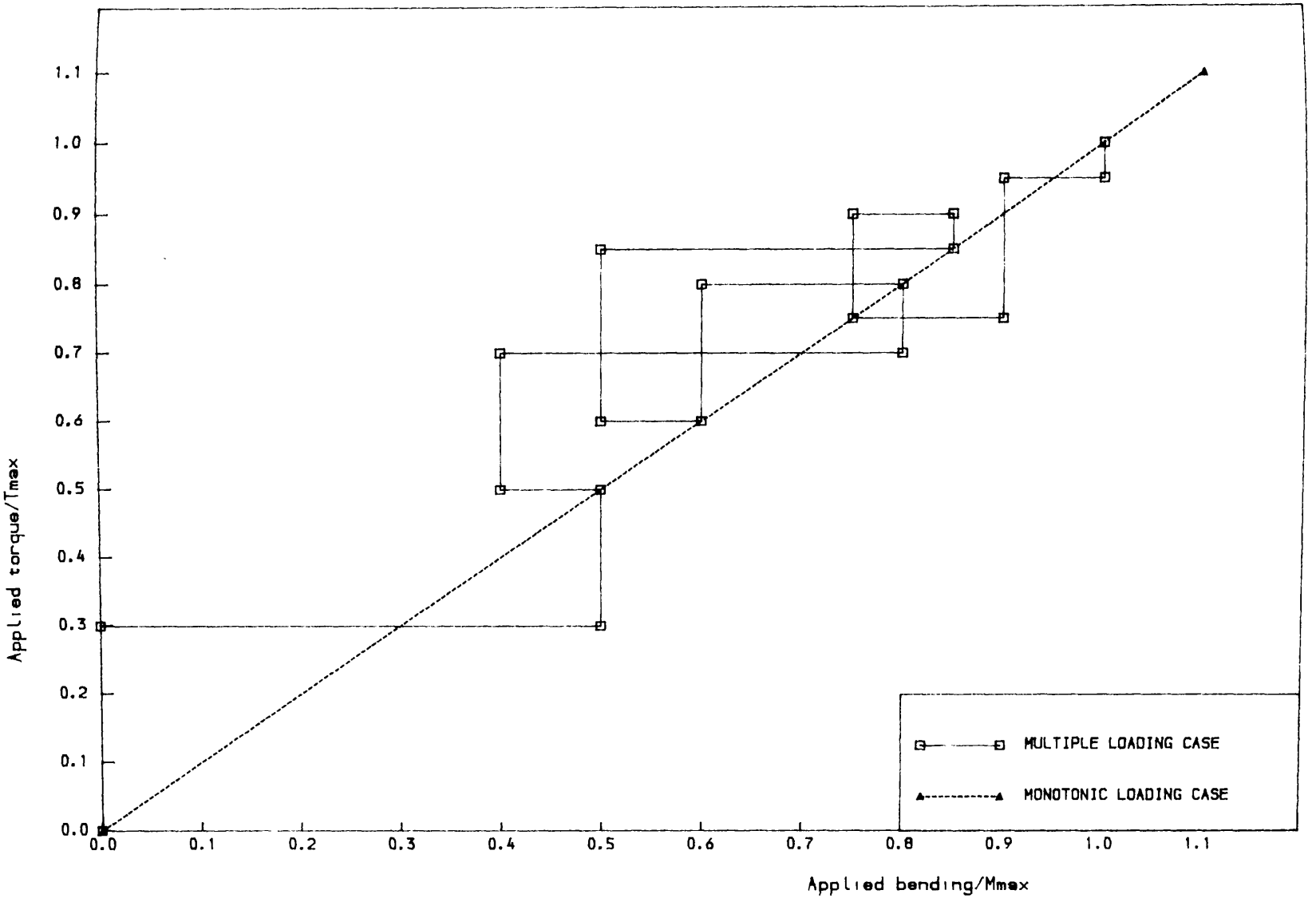

Figure (4.14) Load path 2 for beam A2

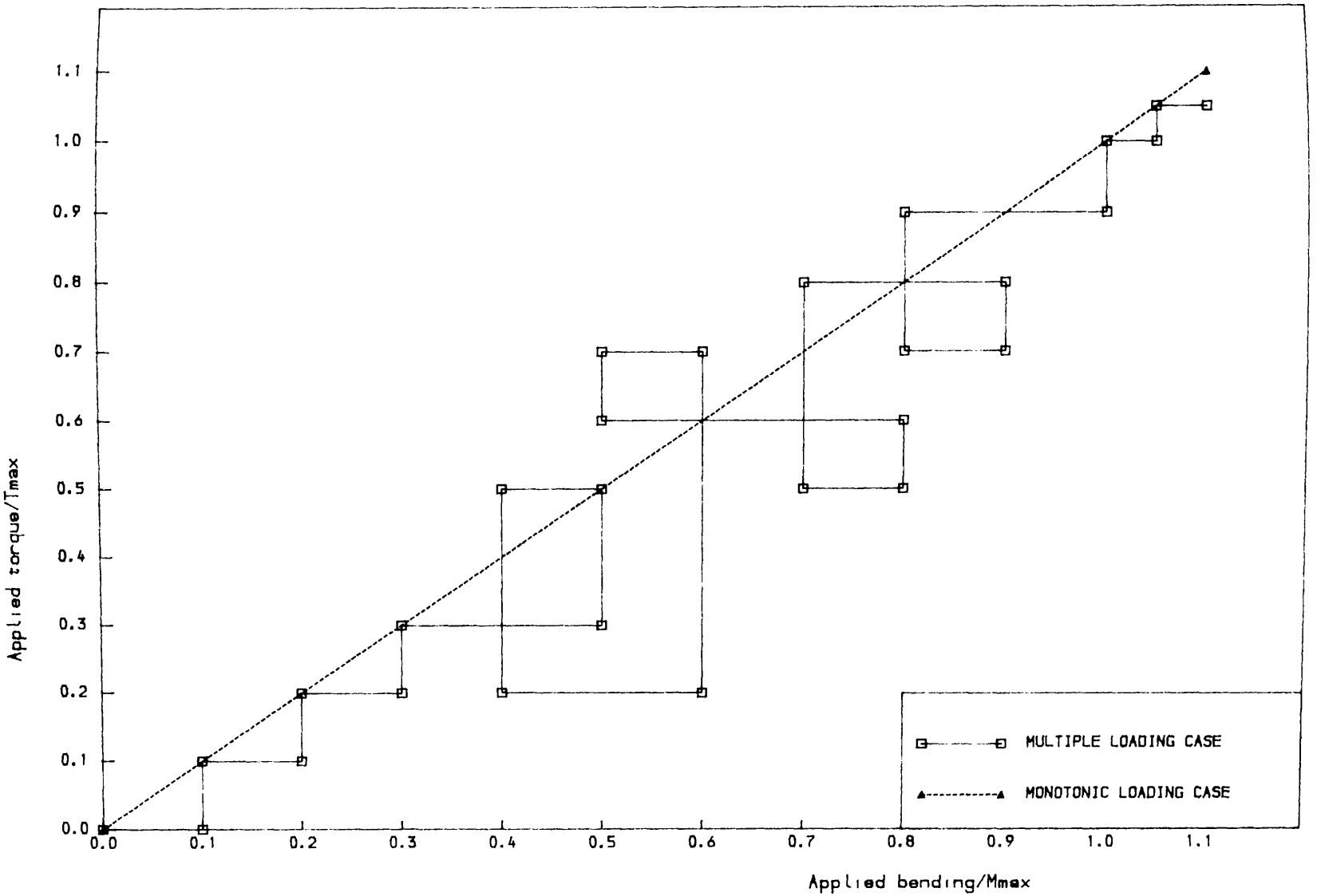

Figure (4.15) Load path 3 for beam A3

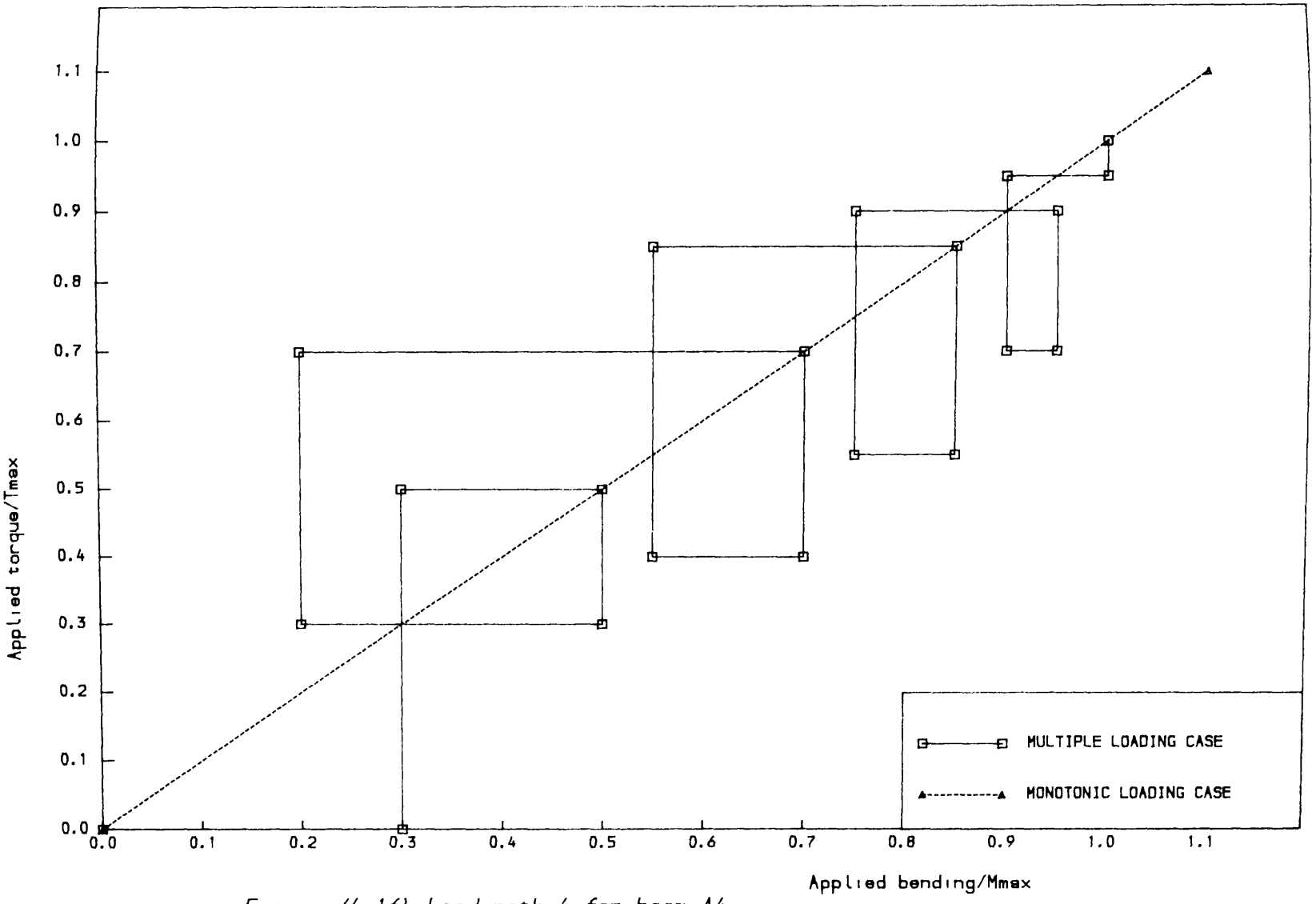

Figure (4.16) Load path 4 for beam A4

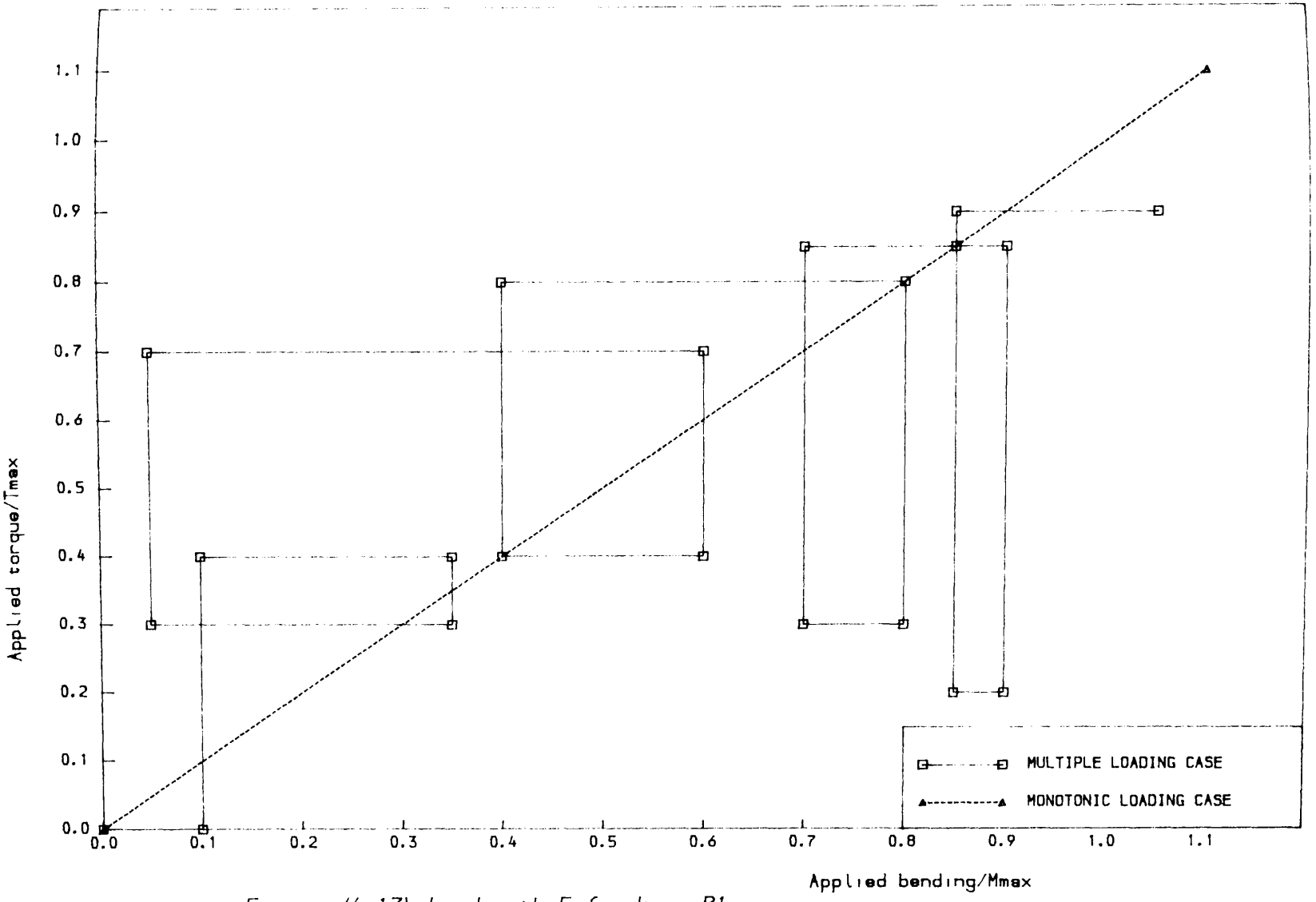

Figure (4.17) Load path 5 for beam B1

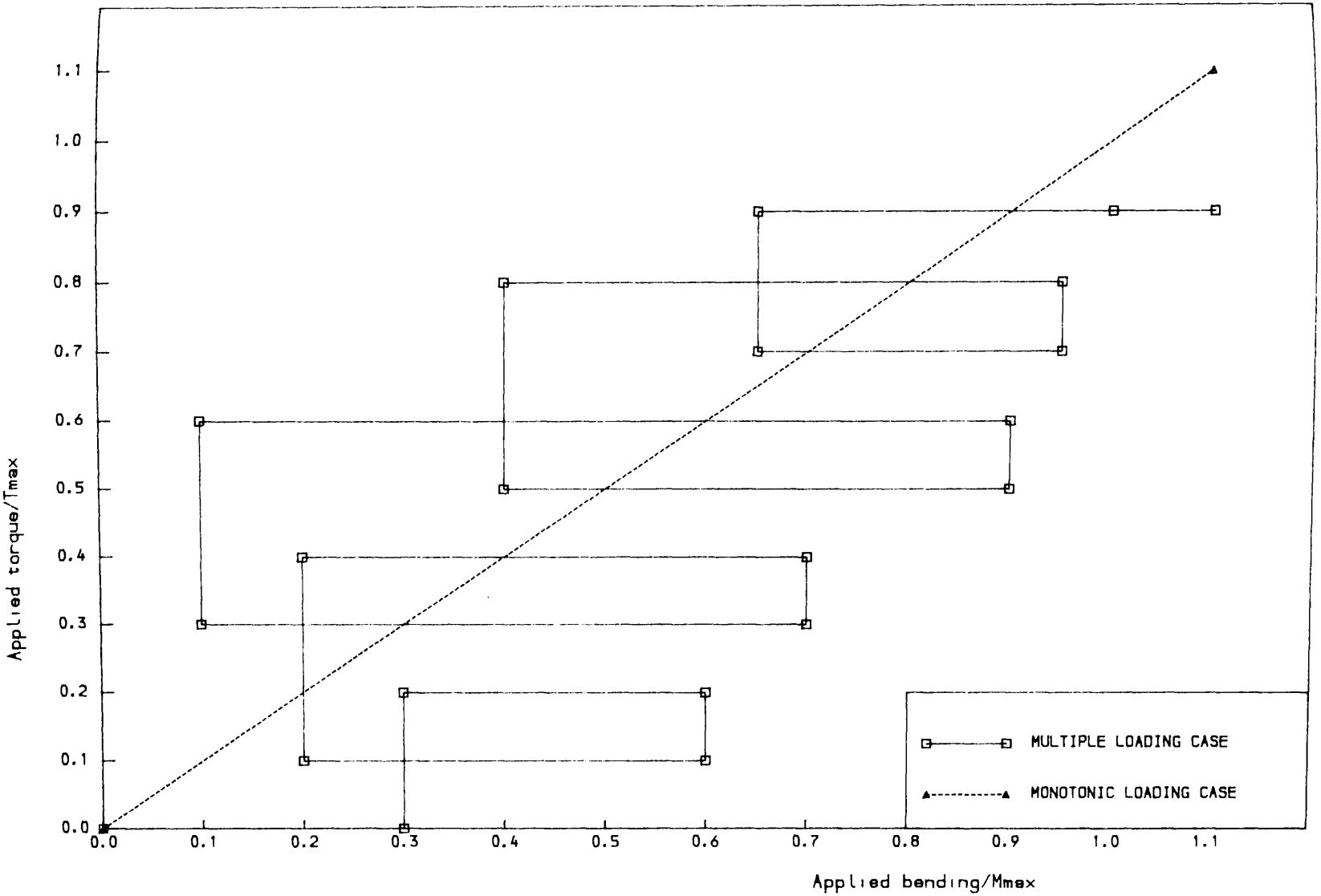

Figure (4.18) Load path 6 for beam B2

4.7 TEST PROGRAMME

Four reinforced and two partially prestressed concrete hollow beams were tested to destruction. The beams were designed according to the classical ultimate limit capacity concept to study the effect of multiple loading on reinforced concrete and partially prestressed concrete beams and to check the applicability of the proposed direct design method for multiple loading. All the beams were designed to withstand different load combinations with a maximum bending moment of M_{max}= 32.0 kN/m and a maximum torque of T_{max}= 32.0 kN/m. All the beams were square in section and of the same dimensions. The cross–sectional dimension is 300x300mm with a wall thickness of 50mm. The overall dimension of the beam was 3800mm; while the middle 1200mm was used as the test span. The areas outside the test zone were overreinforced in order to concentrate failure within the test span and the end sections were solid . The main variables studied are the loading history and the load combinations.

One of the objects of 'Direct Design' is to produce optimum designs, so that the steel consumption is minimised. In the case of prestressed beams many designs are possible using different eccentricities and amount of prestressing. The different case are presented in figure 4.19 and table 4.3. One has to choose between using ordinary steel which is less expensive than prestressing wires but its fabrication cost is higher, and also between using a maximum eccentricity for the case of bending and a minimum eccentricity for the case of torsion. One can see from figure 4.20 which represents the steel consumption versus prestressing force for different case of eccentricity that the optimum design is case 8B. However for reasons of technical constraints case 4A was the one adopted. Case 8B requires 8 load cells and a prestressing force of 21 kN, however in the department there were only 5 load cells and the maximum prestressing force we could get from the available jacking machine was 15 kN.

Table 4.3 : Different cases of prestressing

case	N⁰ wires	Jacking force (kN)	Eccentri-city (mm)	Stresses N/mm2	A_{xr} mm²	A_{xp} mm²
1A	4	15	- 60	σ_{pt}=0.26, σ_{pb}=1.6	537	80
1A	4	21	- 60	σ_{pt}=0.37, σ_{pb}=2.2	467	80
2A	6	15	- 65	σ_{pt}=0.30, σ_{pb}=2.5	417	120
2B	6	21	- 65	σ_{pt}=0.44, σ_{pb}=3.5	358	120
3A	5	15	- 72	σ_{pt}=0.16, σ_{pb}=2.2	445	100
3B	5	21	- 72	σ_{pt}=0.23, σ_{pb}=3.0	406	100
4A	5	15	- 102	σ_{pt}=0.26, σ_{pb}=2.6	425	100
4B	5	21	- 102	σ_{pt}=-0.37, σ_{pb}=3.7	387	100
5A	7	15	- 86	σ_{pt}=-0.05, σ_{pb}=3.3	343	140
5B	7	21	- 86	σ_{pt}=-0.05, σ_{pb}=4.6	282	140
6A	7	15	- 107	σ_{pt}=-0.46, σ_{pb}=3.7	335	140
6B	7	21	- 107	σ_{pt}=-0.66, σ_{pb}=5.3	263	140
7A	8	15	- 30	σ_{pt}=1.20, σ_{pb}=2.5	323	160
7B	8	21	- 30	σ_{pt}=1.68, σ_{pb}=3.6	275	160
8A	8	15	0	$\sigma_{pt} = \sigma_{pb} = 1.87$	295	160
8B	8	21	0	$\sigma_{pt} = \sigma_{pb} = 2.62$	242	160

A_{yr} = 474 mm² for all the cases

A_{xr} = total area of longitudinal steel

A_{yr} = total area of transverse steel

A_{xp} = total area of prestressing steel

σ_{pt}, σ_{pb} = prestressing stresses in top and bottom flange respectively

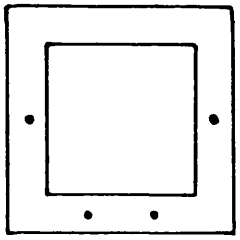

Case 1A & 1B

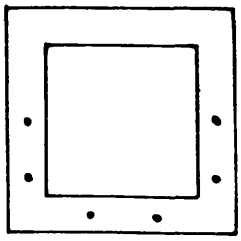

Case 2A & 2B

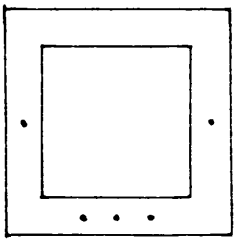

Case 3A & 3B

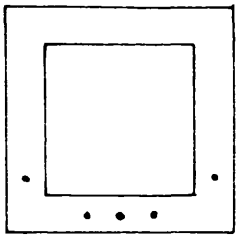

Case 4A & 4B

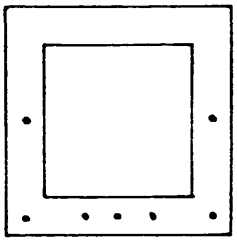

Case 5A & 5B

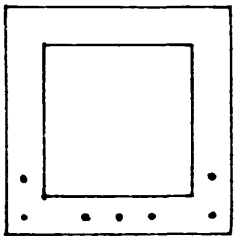

Case 6A & 6B

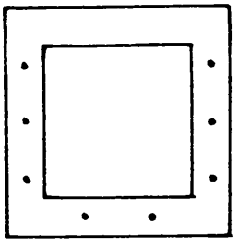

Case 7A & 7B

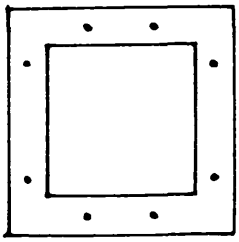

Case 8A & 8B

Figure (4.19) The different cases of prestressing design proposed.

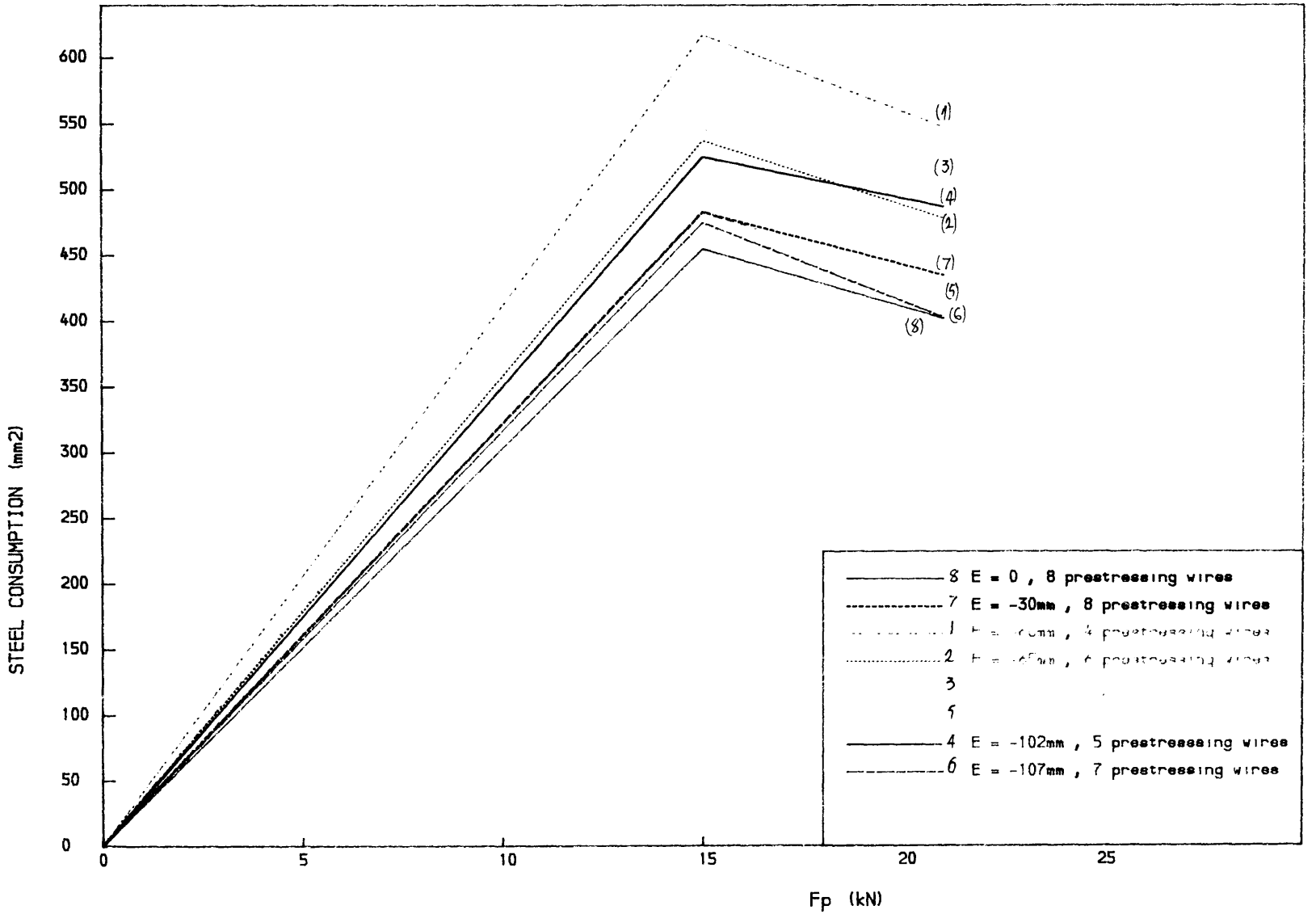

FIGURE 4.20 STEEL CONSUMPTION-PRESTRESSING FORCE CURVES

CHAPTER 5

EXPERIMENTAL RESULTS AND DISCUSSION

5.1 INTRODUCTION

This chapter presents the results of the experimental investigation on four reinforced concrete beams and two partially prestressed concrete beams subjected to multiple combination of bending and torsional loads. The test procedure used and the material properties for each beam are given in chapter 4.

The experiments were conducted to :

a) Verify the validity of the proposed direct design approach based on classical limit capacity concept[5,6,31] .

b) Study the behaviour of reinforced and partially prestressed concrete beams under such multiple loading cases.

c) Compare the behaviour of beams designed to resist multiple loading cases to the beams designed to resist monotonically increasing proportional loading.

5.2 RESULTS

This section summarises the observed behaviour in the test span of the beams tested. All the models were designed to withstand different load combinations with a maximum bending moment of M_{max} = 32 kN.m and a maximum torque moment of T_{max} = 32 kN.m . The load increments for the 6 models are shown in table 5.1.

5.2.1 *Series A* – *Reinforced concrete beams*

Four hollow reinforced concrete beams designed according to direct design method based on classical limit capacity concept[5] were tested under various load combinations. The different load paths followed in these tests are shown in figures

Table 5.1 Load increments for the 6 models

Inc N°	Beam A1		Beam A2		Beam A3		Beam A4		Beam B1		Beam B2	
	M	T	M	T	M	T	M	T	M	T	M	T
1	0.06	0	0	0.09	0.05	0	0.06	0	0.05	0	0.06	0
2	0.10	0	0	0.16	0.10	0	0.10	0	0.10	0	0.11	0
3	0.17	0	0	0.24	0.10	0.10	0.17	0	0.10	0.09	0.17	0
4	0.22	0	0	0.30	0.15	0.10	0.22	0	0.10	0.16	0.22	0
5	0.30	0	0.06	0.30	0.20	0.10	0.30	0	0.10	0.24	0.30	0
6	0.30	0.09	0.11	0.30	0.20	0.20	0.30	0.09	0.10	0.30	0.30	0.10
7	0.30	0.16	0.17	0.30	0.25	0.20	0.30	0.16	0.10	0.40	0.30	0.20
8	0.30	0.24	0.22	0.30	0.30	0.20	0.30	0.24	0.15	0.40	0.40	0.20
9	0.30	0.34	0.30	0.30	0.30	0.30	0.30	0.32	0.20	0.40	0.45	0.20
10	0.30	0.40	0.35	0.30	0.35	0.30	0.30	0.40	0.25	0.40	0.50	0.20
11	0.30	0.45	0.40	0.30	0.40	0.30	0.30	0.45	0.30	0.40	0.55	0.20
12	0.30	0.50	0.45	0.30	0.45	0.30	0.30	0.50	0.35	0.40	0.60	0.20
13	0.40	0.50	0.50	0.30	0.50	0.30	0.35	0.50	0.35	0.30	0.60	0.10
14	0.45	0.50	0.50	0.40	0.50	0.40	0.40	0.50	0.25	0.30	0.50	0.10
15	0.50	0.50	0.50	0.50	0.50	0.50	0.45	0.50	0.15	0.30	0.40	0.10
16	0.50	0.32	0.40	0.50	0.40	0.50	0.50	0.50	0.05	0.30	0.30	0.10
17	0.50	0.16	0.40	0.56	0.40	0.40	0.50	0.40	0.05	0.40	0.20	0.10
18	0.50	0.10	0.40	0.64	0.40	0.30	0.50	0.30	0.05	0.48	0.20	0.16
19	0.40	0.10	0.40	0.70	0.40	0.20	0.40	0.30	0.05	0.56	0.20	0.24
20	0.20	0.10	0.50	0.70	0.50	0.20	0.30	0.30	0.05	0.64	0.20	0.32
21	0.20	0.25	0.60	0.70	0.55	0.20	0.20	0.30	0.05	0.70	0.20	0.40
22	0.20	0.40	0.70	0.70	0.60	0.20	0.20	0.40	0.15	0.70	0.30	0.40
23	0.20	0.48	0.80	0.70	0.60	0.32	0.20	0.48	0.25	0.70	0.40	0.40
24	0.20	0.56	0.80	0.75	0.60	0.40	0.20	0.56	0.35	0.70	0.50	0.40
25	0.20	0.65	0.80	0.80	0.60	0.48	0.20	0.64	0.45	0.70	0.60	0.40
26	0.30	0.65	0.70	0.80	0.60	0.56	0.20	0.70	0.50	0.70	0.65	0.40
27	0.35	0.65	0.60	0.80	0.60	0.65	0.30	0.70	0.55	0.70	0.70	0.40
28	0.43	0.65	0.60	0.70	0.60	0.70	0.40	0.70	0.60	0.70	0.70	0.30
29	0.57	0.65	0.60	0.60	0.50	0.70	0.50	0.70	0.60	0.60	0.60	0.30
30	0.65	0.65	0.55	0.60	0.50	0.60	0.55	0.70	0.60	0.50	0.50	0.30
31	0.70	0.65	0.50	0.60	0.60	0.60	0.60	0.70	0.60	0.40	0.40	0.30
32	0.70	0.56	0.50	0.70	0.65	0.60	0.65	0.70	0.50	0.40	0.30	0.30

Table 5.1 (continued 1) Load increments for the 6 models

Inc N°	Beam A1		Beam A2		Beam A3		Beam A4		Beam B1		Beam B2	
	M	T	M	T	M	T	M	T	M	T	M	T
33	0.70	0.40	0.50	0.78	0.70	0.60	0.70	0.70	0.40	0.40	0.20	0.30
34	0.65	0.40	0.50	0.85	0.75	0.60	0.70	0.60	0.40	0.48	0.10	0.30
35	0.55	0.40	0.60	0.85	0.80	0.60	0.70	0.50	0.40	0.56	0.10	0.40
36	0.55	0.48	0.65	0.85	0.80	0.50	0.70	0.40	0.40	0.65	0.10	0.48
37	0.55	0.56	0.70	0.85	0.70	0.50	0.60	0.40	0.40	0.72	0.10	0.55
38	0.55	0.64	0.75	0.85	0.70	0.56	0.55	0.40	0.40	0.80	0.10	0.60
39	0.55	0.72	0.80	0.85	0.70	0.64	0.55	0.48	0.50	0.80	0.20	0.60
40	0.55	0.80	0.85	0.85	0.70	0.72	0.55	0.64	0.60	0.80	0.30	0.60
41	0.60	0.80	0.85	0.90	0.70	0.80	0.55	0.72	0.65	0.80	0.40	0.60
42	0.65	0.80	0.80	0.90	0.75	0.80	0.55	0.80	0.70	0.80	0.50	0.60
43	0.70	0.80	0.75	0.90	0.80	0.80	0.55	0.85	0.75	0.80	0.60	0.60
44	0.75	0.80	0.75	0.85	0.85	0.80	0.60	0.85	0.80	0.80	0.70	0.60
45	0.80	0.80	0.75	0.80	0.90	0.80	0.65	0.85	0.80	0.70	0.75	0.60
46	0.85	0.80	0.75	0.75	0.90	0.70	0.70	0.85	0.80	0.60	0.80	0.60
47	0.85	0.72	0.80	0.75	0.80	0.70	0.75	0.85	0.80	0.50	0.85	0.60
48	0.85	0.64	0.85	0.75	0.80	0.80	0.80	0.85	0.80	0.40	0.90	0.60
49	0.85	0.55	0.90	0.75	0.80	0.85	0.85	0.85	0.80	0.30	0.90	0.50
50	0.80	0.55	0.90	0.80	0.80	0.90	0.85	0.75	0.75	0.30	0.70	0.50
51	0.75	0.55	0.90	0.85	0.85	0.90	0.85	0.65	0.70	0.30	0.50	0.50
52	0.75	0.64	0.90	0.90	0.90	0.90	0.85	0.55	0.70	0.40	0.40	0.50
53	0.75	0.72	0.90	0.95	0.95	0.90	0.80	0.55	0.70	0.48	0.40	0.56
54	0.75	0.80	0.95	0.95	1.00	0.90	0.75	0.55	0.70	0.56	0.40	0.64
55	0.75	0.88	1.00	0.95	1.00	0.95	0.75	0.64	0.70	0.64	0.40	0.72
56	0.75	0.95	1.00	1.00	1.00	1.00	0.75	0.72	0.70	0.72	0.40	0.80
57	0.80	0.95			1.05	1.00	0.75	0.80	0.70	0.80	0.50	0.80
58	0.85	0.95			1.05	1.05	0.75	0.85	0.70	0.85	0.60	0.80
59	0.90	0.95			1.10	1.05	0.75	0.90	0.75	0.85	0.70	0.80
60	0.95	0.95					0.80	0.90	0.80	0.85	0.80	0.80
61	0.95	0.80					0.85	0.90	0.85	0.85	0.90	0.80
62	0.95	0.70					0.90	0.90	0.90	0.85	0.95	0.80
63	0.90	0.70					0.95	0.90	0.90	0.75	0.95	0.70
64	0.90	0.80					0.95	0.80	0.90	0.65	0.85	0.70
65	0.90	0.90					0.95	0.70	0.90	0.55	0.75	0.70

Table 5.1 (continued 2) Load increments for the 6 models

Inc N°	Beam A1		Beam A2		Beam A3		Beam A4		Beam B1		Beam B2	
	M	T	M	T	M	T	M	T	M	T	M	T
66	0.90	1.00					0.90	0.70	0.90	0.45	0.65	0.70
67	0.95	1.00					0.90	0.80	0.90	0.35	0.65	0.80
68	1.00	1.00					0.90	0.88	0.90	0.20	0.65	0.90
69							0.90	0.95	0.85	0.20	0.75	0.90
70							0.95	0.95	0.85	0.30	0.85	0.90
71							1.00	0.95	0.85	0.40	0.90	0.90
72							1.00	1.00	0.85	0.60	0.95	0.90
73							1.05	1.00	0.85	0.80	1.00	0.90
74							1.05	1.05	0.85	0.90	1.05	0.90
75									0.90	0.90	1.10	0.90
76									0.95	0.90		
77									1.00	0.90		

M = applied bending/M_{max}

T = applied torsion/T_{max}

4.13– 4.16. The object of these series was to study the behaviour of reinforced concrete beams under different load combinations. In the load paths shown in figures 4.13 and 4.16, bending was applied first, whereas in the load path shown in figure 4.14 torsion was applied first. The load steps followed in theses three load path are far from the monotonic case. In the load path shown in figure 4.15 torsion and bending were applied alternatively and the load steps followed were close to the monotonic loading case.

Model A1 – Load path 1 (see fig 4.13)

During the experiment the load was applied in small increments of $0.05xM_{max}$ and $0.08xT_{max}$. Figure 5.1 shows crack development on the model at each load stage, and the numbers on the photograph show the increment stages. Bending was first applied; the first cracks located at the bottom flange were noticed at a load of $0.3xM_{max}$. These cracks were approximately 90° to the beam axis. Keeping $M = 0.3xM_{max}$, torsion was increased till load $0.5xT_{max}$ was reached. At this load stage, inclined cracks developed on the webs. Keeping $T = 0.5xT_{max}$, bending was increased till a load of $0.5xM_{max}$ was reached. At this load level, the existing cracks widened further and the maximum displacement at midspan was 6mm. Then torsion and bending were successively decreased till a load of $(0.2xM_{max},0.3xT_{max})$ was reached. Keeping $M = 0.2xM_{max}$, torsion was increased till a load of $0.7xT_{max}$ was reached. Several inclined cracks developed on all sides of the beam. Most of the cracks extended through the height and joined at the corners to become spiral. When the load was decreased, the crack width narrowed and then widened when load is increased. Keeping $T = 0.7xT_{max}$, bending was increased till a load of $0.7xM_{max}$ was reached. Maximum displacement at the centre of the beam at this stage was 12mm. Then the load was decreased and increased three times as shown in figure 4.13 till failure occured. Figures 5.2, 5.3 shows the load/strain curves, while figure 5.4 shows the load/displacement curve for beam A1.

The deflection limit of span/250 according to BS8110[26] was attained at a load of $(0.7xM_{max},0.65xT_{max})$. The first yield of longitudinal steel was recorded at

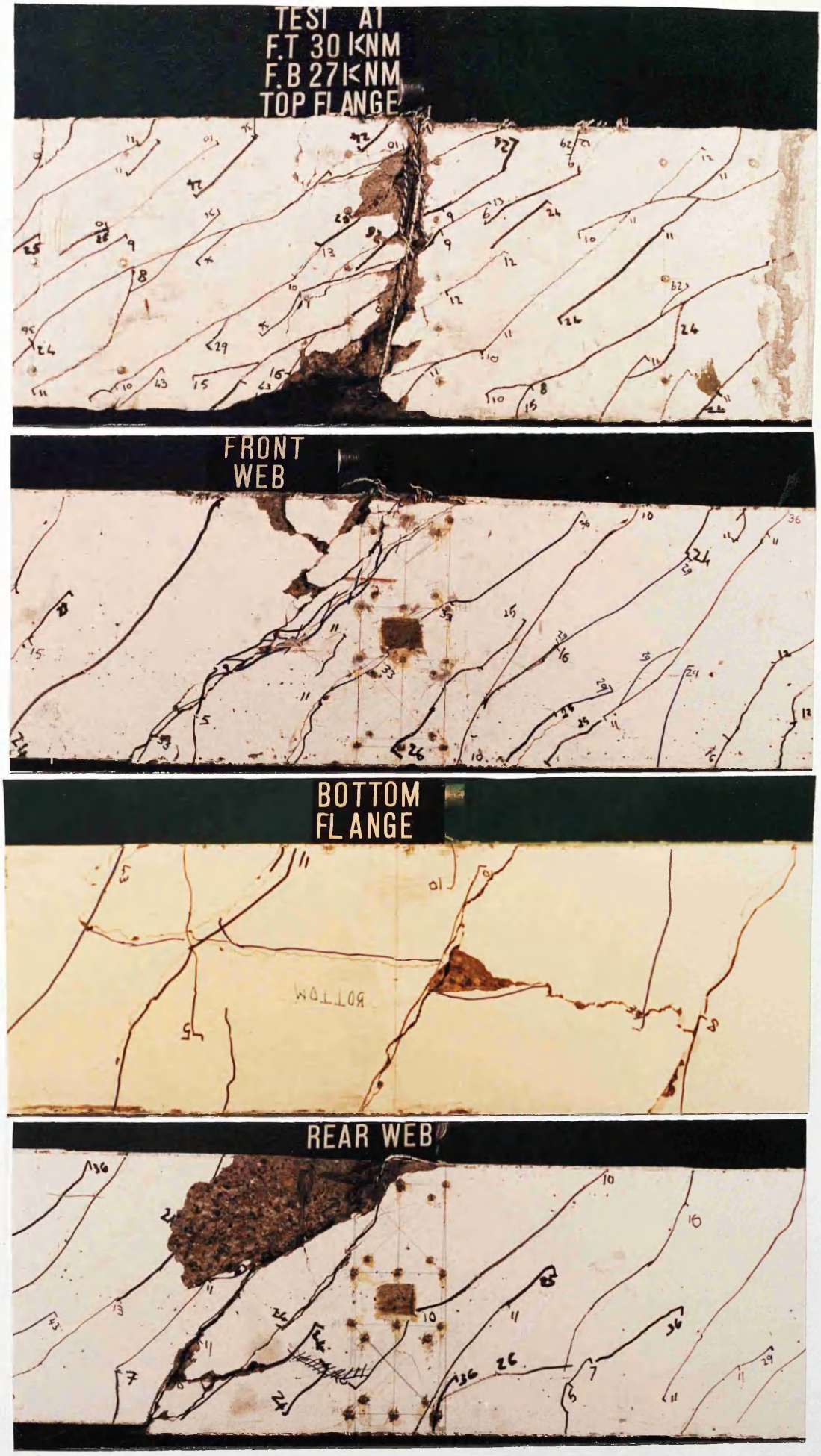

Fig 5.1 Crack development at each load stage.

(Beam A1 : Reinforced Concrete beam)

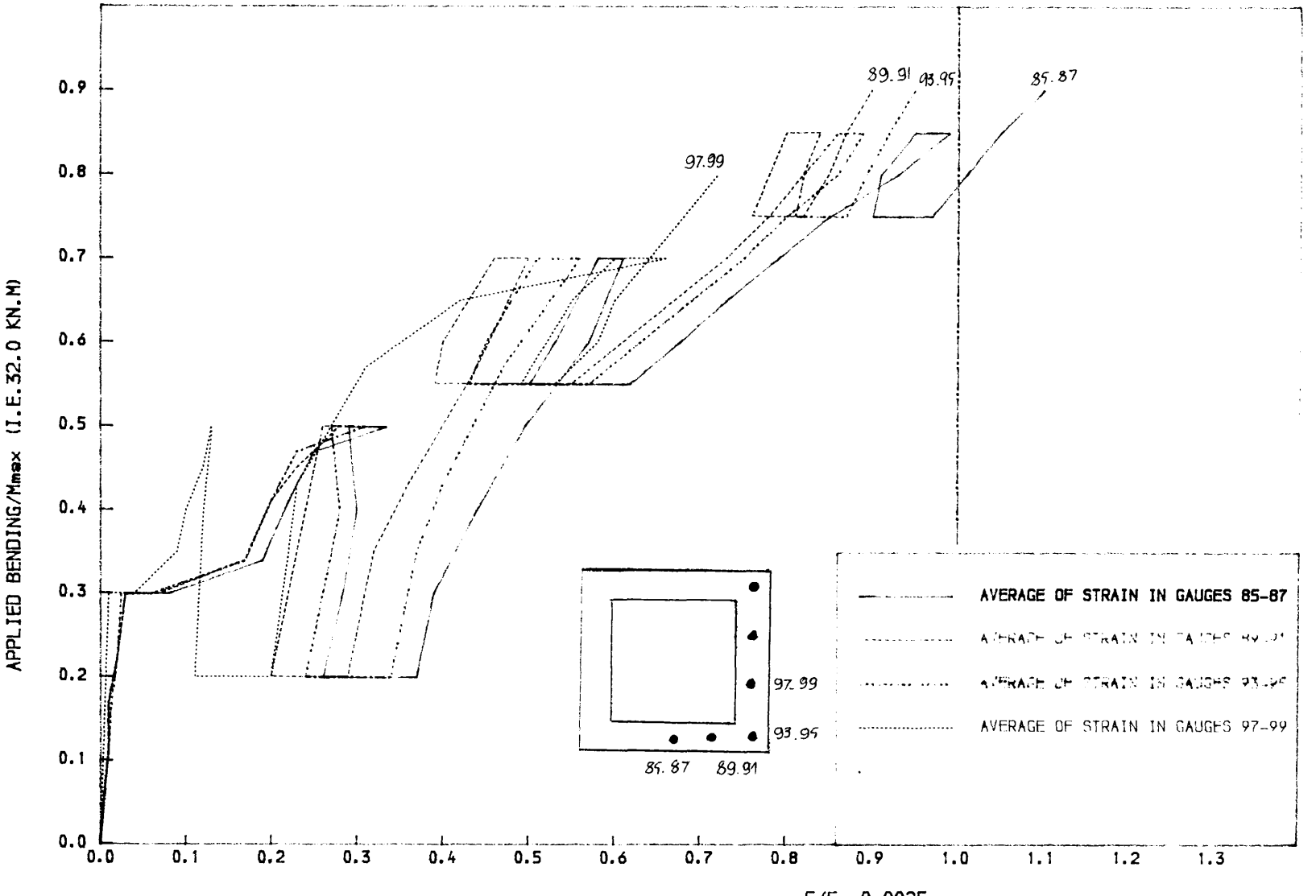

FIG 5.2 LOAD-STEEL STRAIN CURVE IN THE LONGITUDINAL BARS FOR BEAM A1

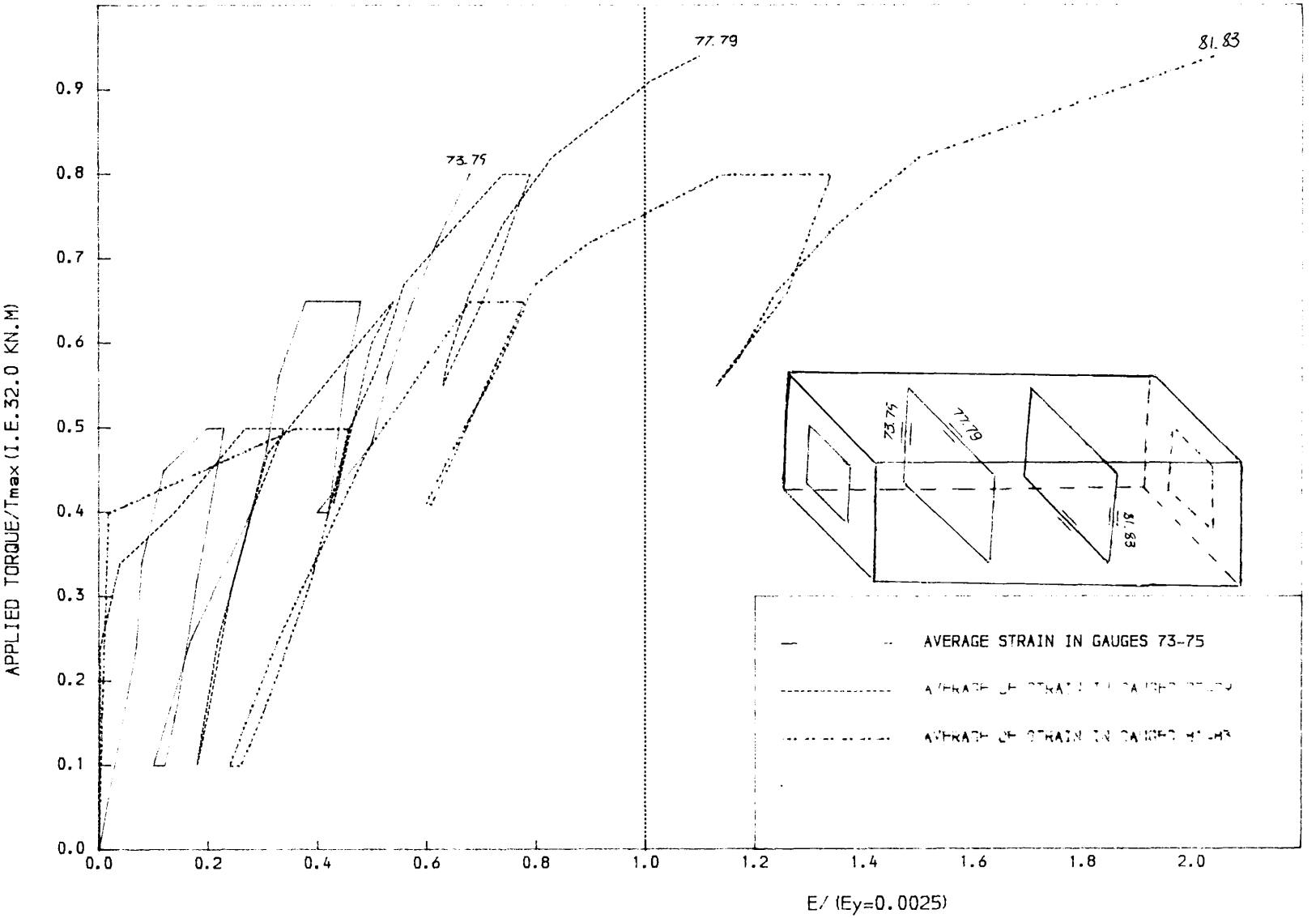

FIG 5.3 LOAD-STEEL STRAIN CURVE IN THE STIRRUPS FOR BEAM A1

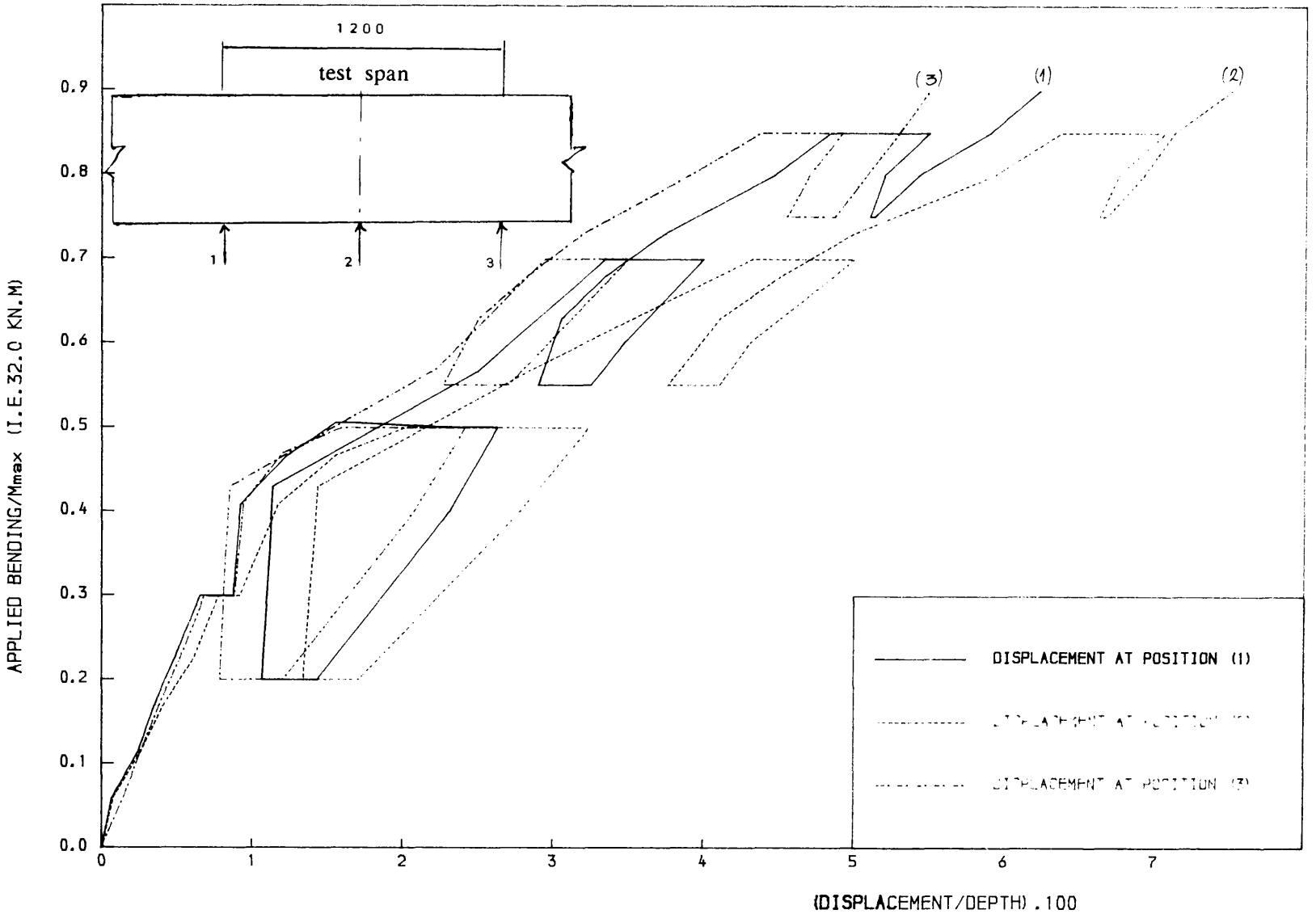

FIG 5.4 LOAD-DISPLACEMENT CURVE FOR BEAM A1

a load of ($0.75xM_{max}$,$0.8xT_{max}$) at the bottom longitudinal steel bar, while the first yield of transverse steel was recorded at a load of ($0.6xM_{max}$,$0.8xT_{max}$).

The beam failed after a load of ($0.9xM_{max}$,$0.95xT_{max}$) was reached. At that load, a major spiral crack opened up and the beam collapsed. The maximum displacement at the centre of the beam before failure was 18mm. The torsion loading system used in this test probably caused the early failure of the beam. It was impossible to get the same amount of torque at the ends of the beam. The system was altered and maximum load combinations were reached more or less conveniently for the other models.

Model A2 – Load path 2 (fig 4.14)

During the experiment, the load was applied in small increments of $0.05xM_{max}$ and $0.08xT_{max}$. Figure 5.5 shows crack development on the model at each load stage. Torsion was applied first and the first cracks were observed at a load of $0.3xT_{max}$. These cracks were approximately at 45° to the beam axis. The width of the crack measured on the front web was 0.08mm. Keeping $T= 0.3xT_{max}$, bending was increased till a load of $0.5xM_{max}$ was reached. Crack developed on the webs and on the bottom flange, and these two different cracks joined at the corners. The width of the crack measured on the front web was 0.14mm. Keeping $M = 0.5xM_{max}$, torsion was increased till a load of $0.5xT_{max}$ was reached. The main observations made at that stage were the spreading of the web cracks towards the top flange, and the 0.18mm wide crack measured on the front web. Keeping $T= 0.5xT_{max}$, bending was decreased till a load of $0.4xM_{max}$ was reached. Then keeping $M = 0.4xM_{max}$, torsion was increased till a load of $0.7xT_{max}$ was reached. At that load level, the maximum deflection at midspan was 18mm. Keeping $T= 0.7xT_{max}$, the bending moment was increased till a load of $0.8xM_{max}$ was reached. At that load stage, cracks developed on all sides of the beam. The crack width on the front web was 0.32mm and on the top flange 0.14mm. Then the beam was subjected to other load combinations as shown in figure 4.14 till failure happened. Figure 5.6 and 5.7 shows the load/strain curves, while figure 5.8 shows the load/displacement curve.

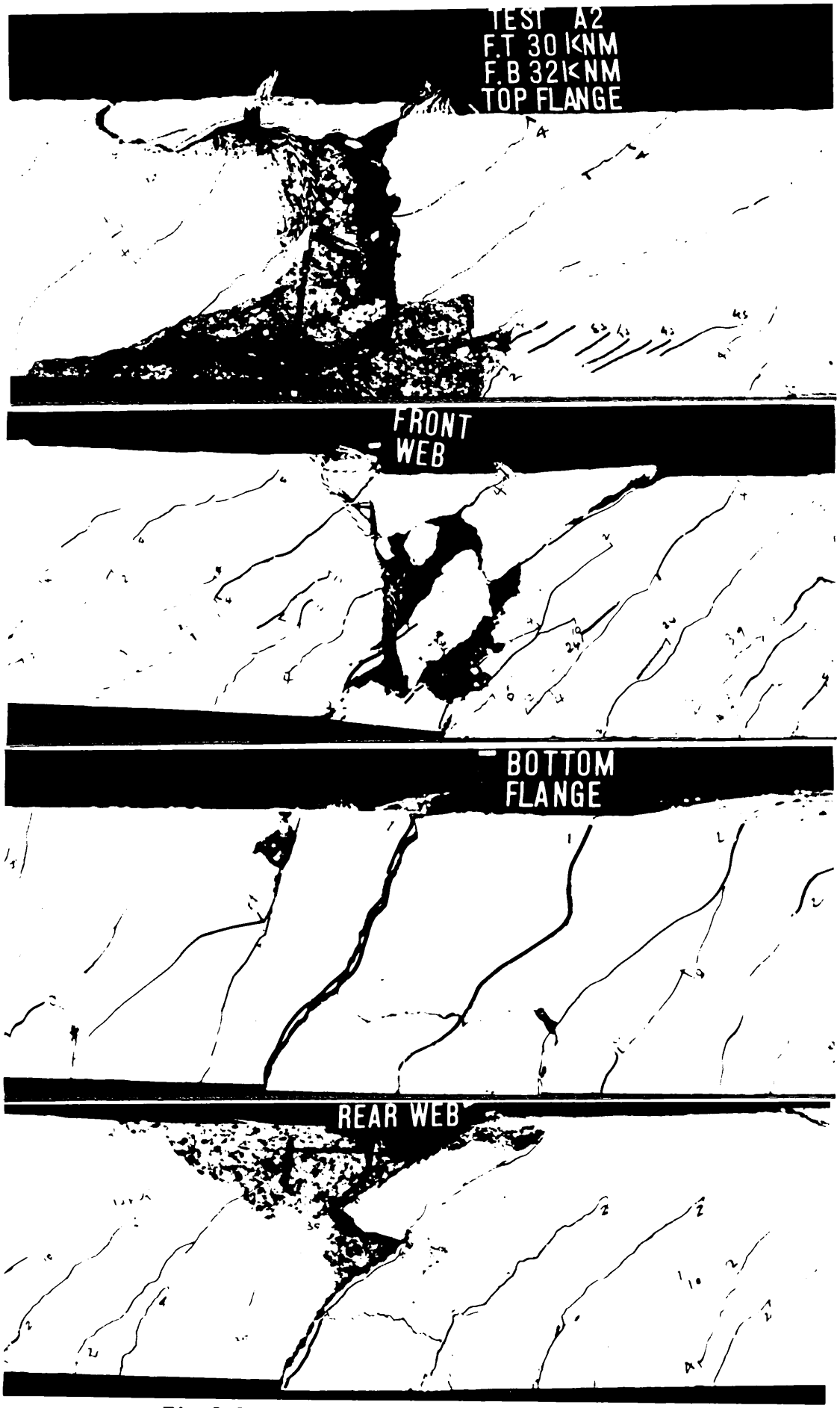

Fig 5.5 Crack development at each load stage.

(Beam A2 : Reinforced Concrete beam)

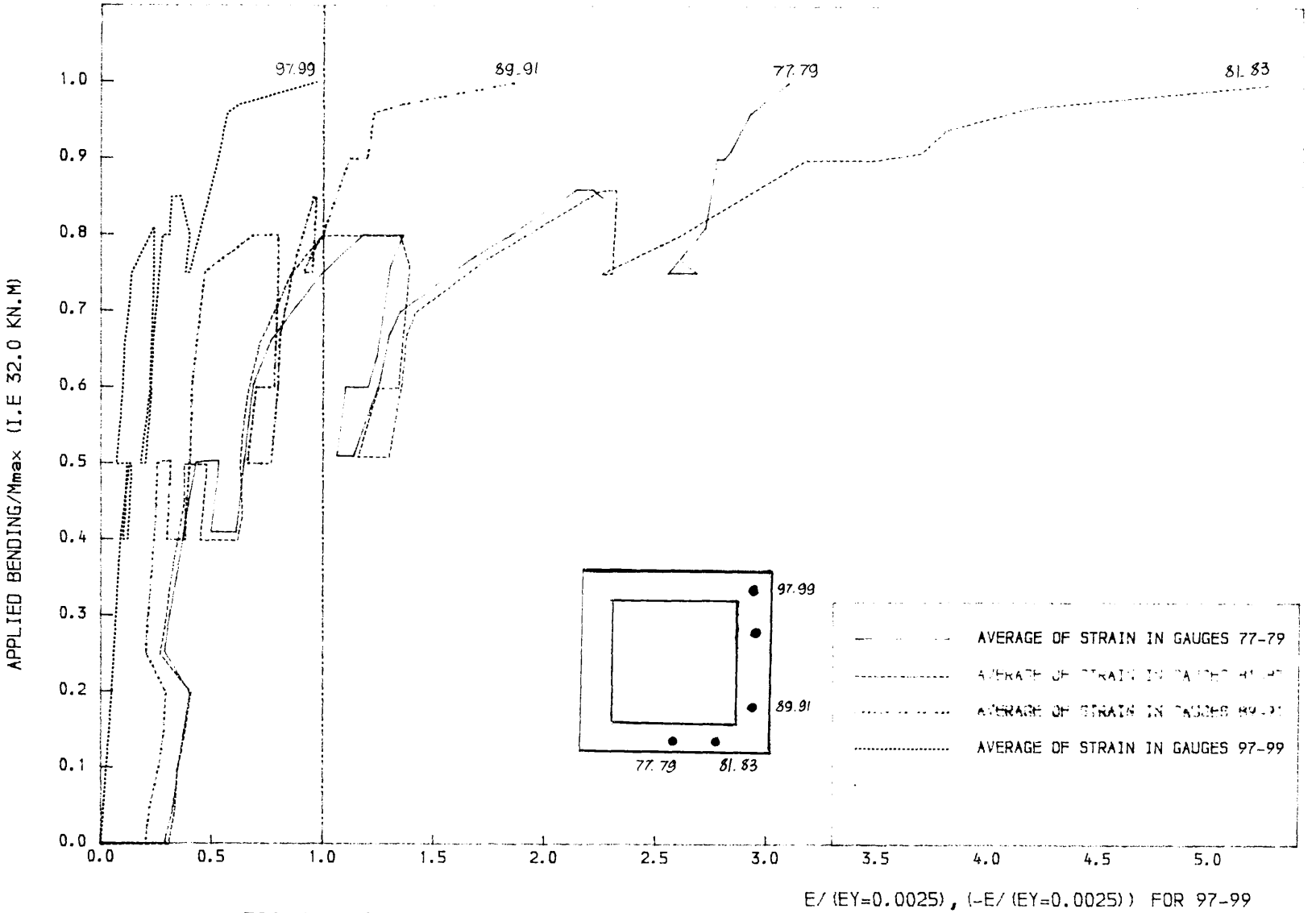

FIG 5.6 LOAD-STEEL STRAIN CURVE IN THE LONGITUDINAL BARS FOR BEAM A2

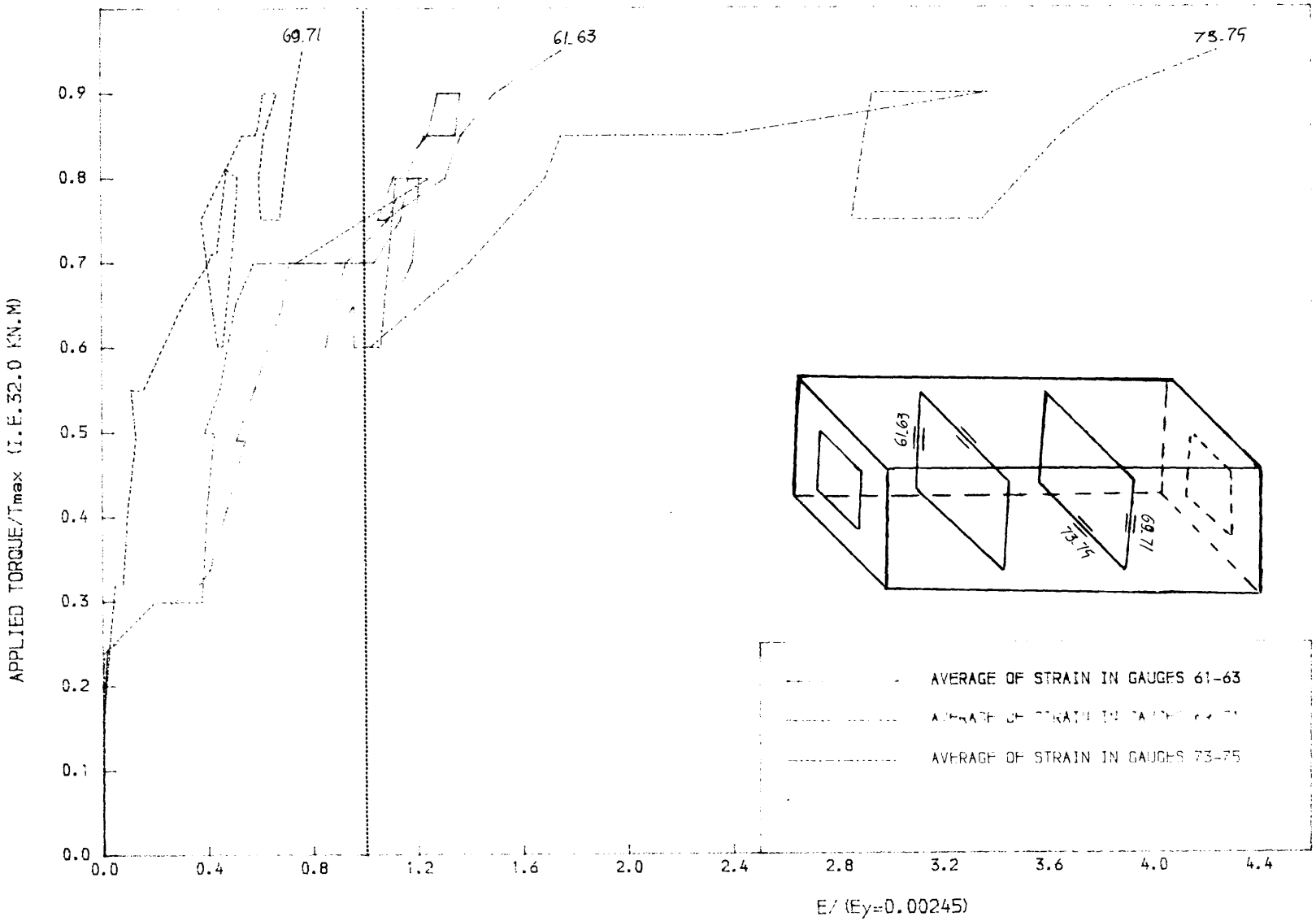

FIG 5.7 LOAD-STEEL STRAIN CURVE IN THE STIRRUPS FOR BEAM A2

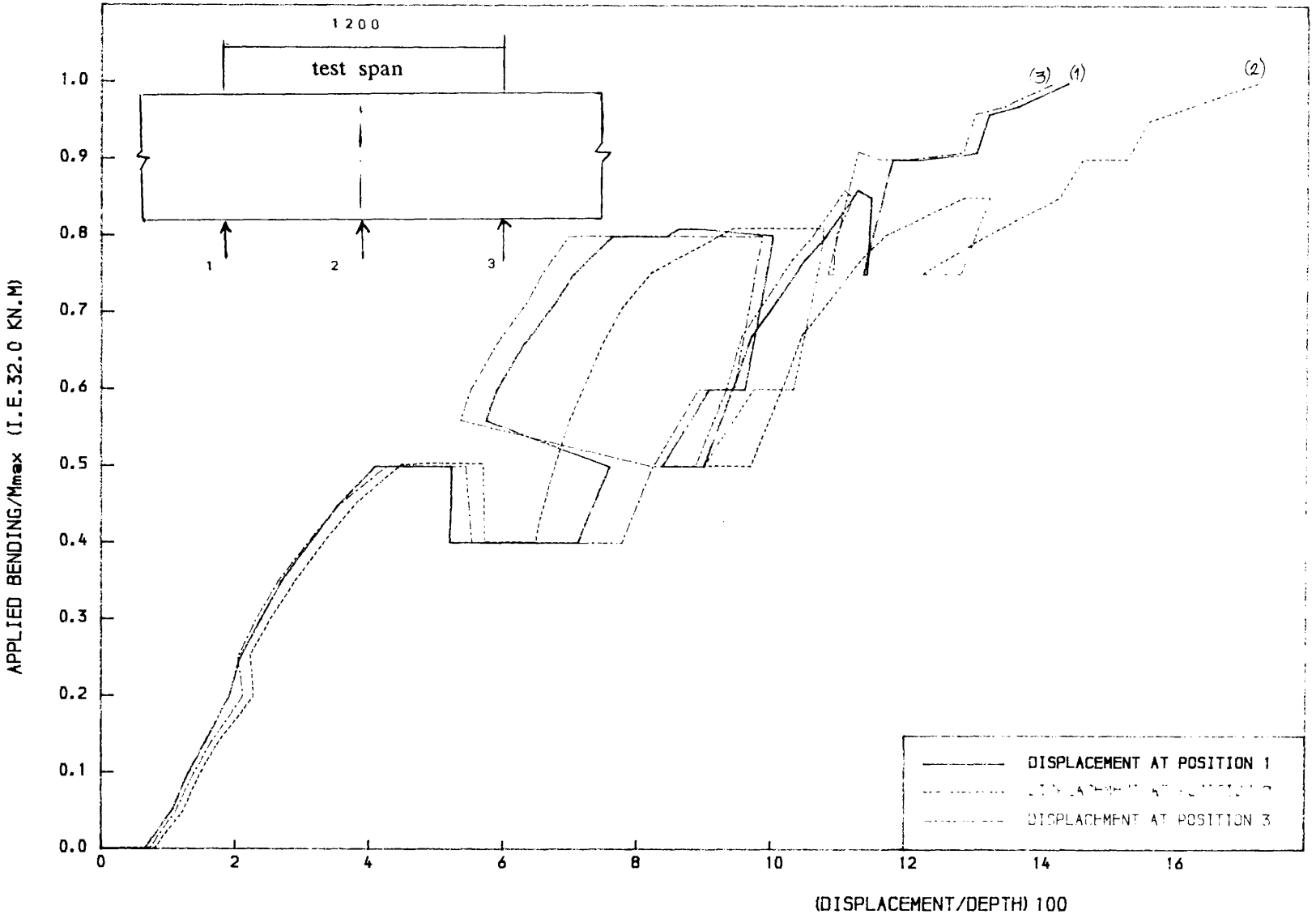

FIG 5.8 DISPLACEMENT CURVE FOR BEAM A2

The deflection limit of span/250 was attained at a load of ($0.5xM_{max}$,$0.7xT_{max}$). The first yield of longitudinal steel was recorded at a load of ($0.75xM_{max}$,$0.7xT_{max}$) at the bottom longitudinal steel bar and the first yield of transverse steel was recorded at the same load.

Under the last increment in torsion, the spalling of the concrete along the top flange was noticed. Then a major spiral crack at midspan opened up and the beam collapsed at a load of ($1.0xM_{max}$,$0.95xT_{max}$). Most of the steel were at yield. The top steel reinforcement had twisted. Before failure, the maximum displacement at midspan was 48mm.

Model A3 – Load path 3 (see fig 4.15)

The new set up shown in fig 4.2.b was used to test the next models (A3,A4,B1 and B2). The load was applied in small increments of $0.05xM_{max}$ and $0.08xT_{max}$. The beam was loaded alternatively in torsion and bending till a load of ($0.3xM_{max}$,$0.3xT_{max}$) was reached. The first cracks on both the webs and the bottom flange occured very early at load of ($0.15xM_{max}$,$0.1xT_{max}$). Between the load at cracking and a load of a ($0.3xM_{max}$,$0.3xT_{max}$), more cracks developed on both the webs and the bottom flange. As the load increased, these cracks spread towards the top flange but no cracks were noticed on the top flange. Maximum recorded displacement at the centre of beam was 6mm. Keeping $T = 0.3xT_{max}$, bending was increased till a load of $0.5xM_{max}$ was reached. At that stage more inclined cracks developed on the bottom flange. Keeping $M = 0.5xM_{max}$, torsion was increased till a load of $0.5xT_{max}$ was reached. Maximum recorded displacement at the centre of the beam was 12mm. Between loads of ($0.5xM_{max}$,$0.5xT_{max}$) and ($1.0xM_{max}$,1.0xTmax) more inclined cracks developed on all the sides of the beam, and existing cracks extended and widened. Figure 5.9 shows crack development on beam A3, and the crack width values are shown in table 5.2 . Figure 5.9.A shows the specific cracks where crack widths were measured. Most of the cracks joined up at the corners of the beam to become spiral. This was directly accompanied by a rapid increase in deformation. At a load of ($0.8xM_{max}$,$0.9xT_{max}$) the first cracks on the top flange were noticed.

Fig 5.9 Crack development at each load stage.

(Beam A3 : Reinforced Concrete beam)

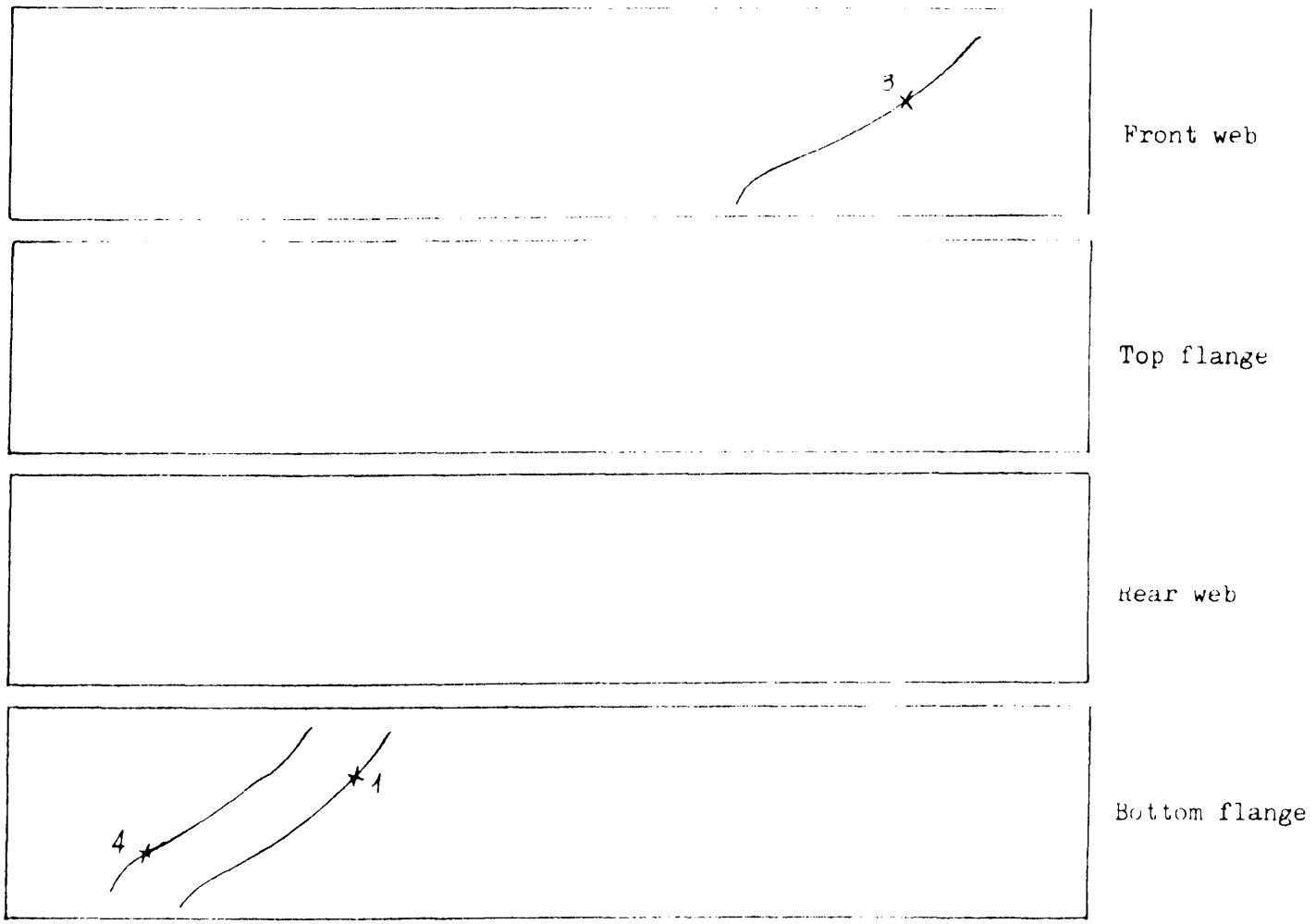

Figure [illegible] Location of cracks where the measurements were taken for beam A3

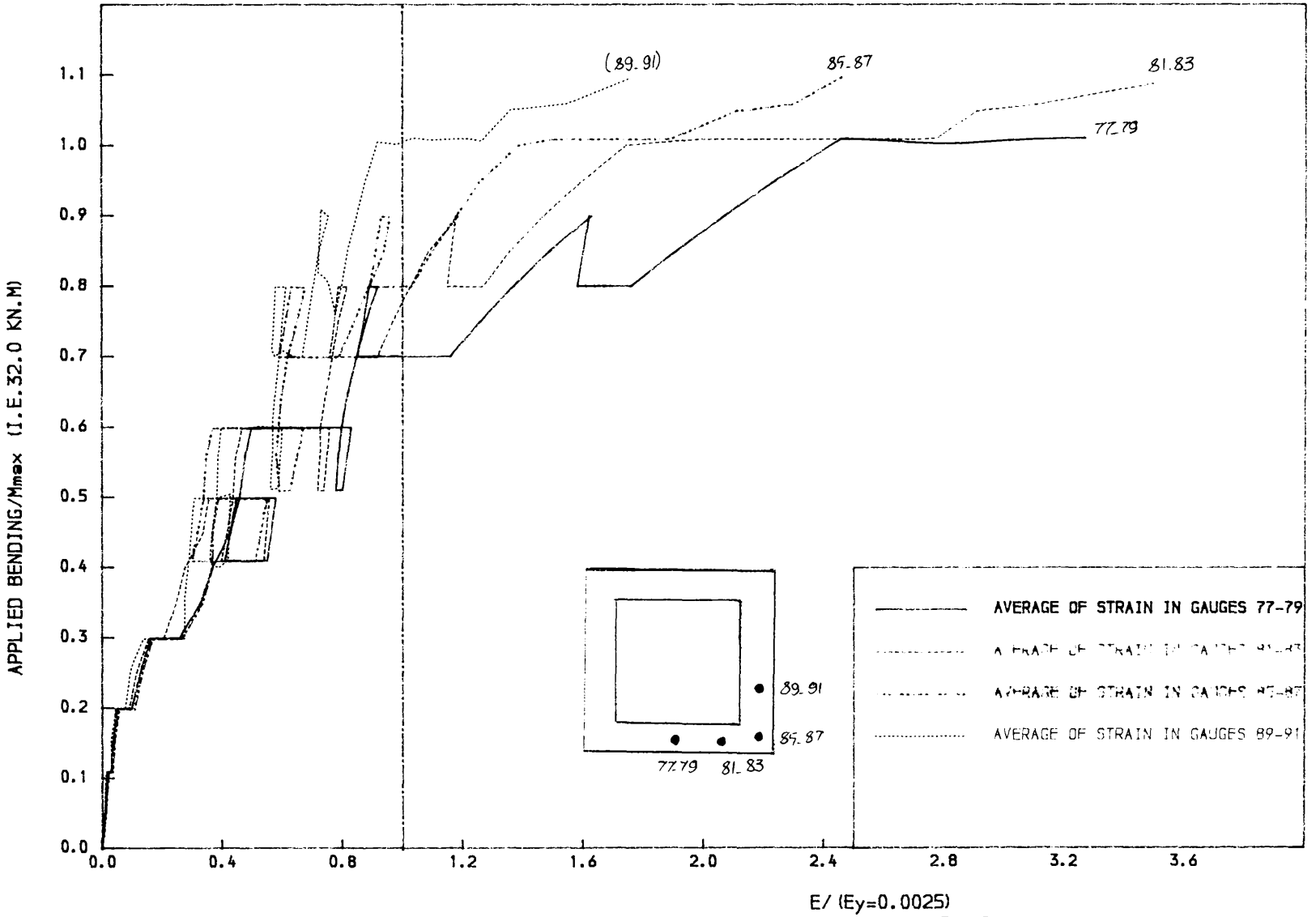

FIG 5.10 LOAD-STEEL STRAIN CURVE IN THE LONGITUDINAL BARS FOR BEAM A3

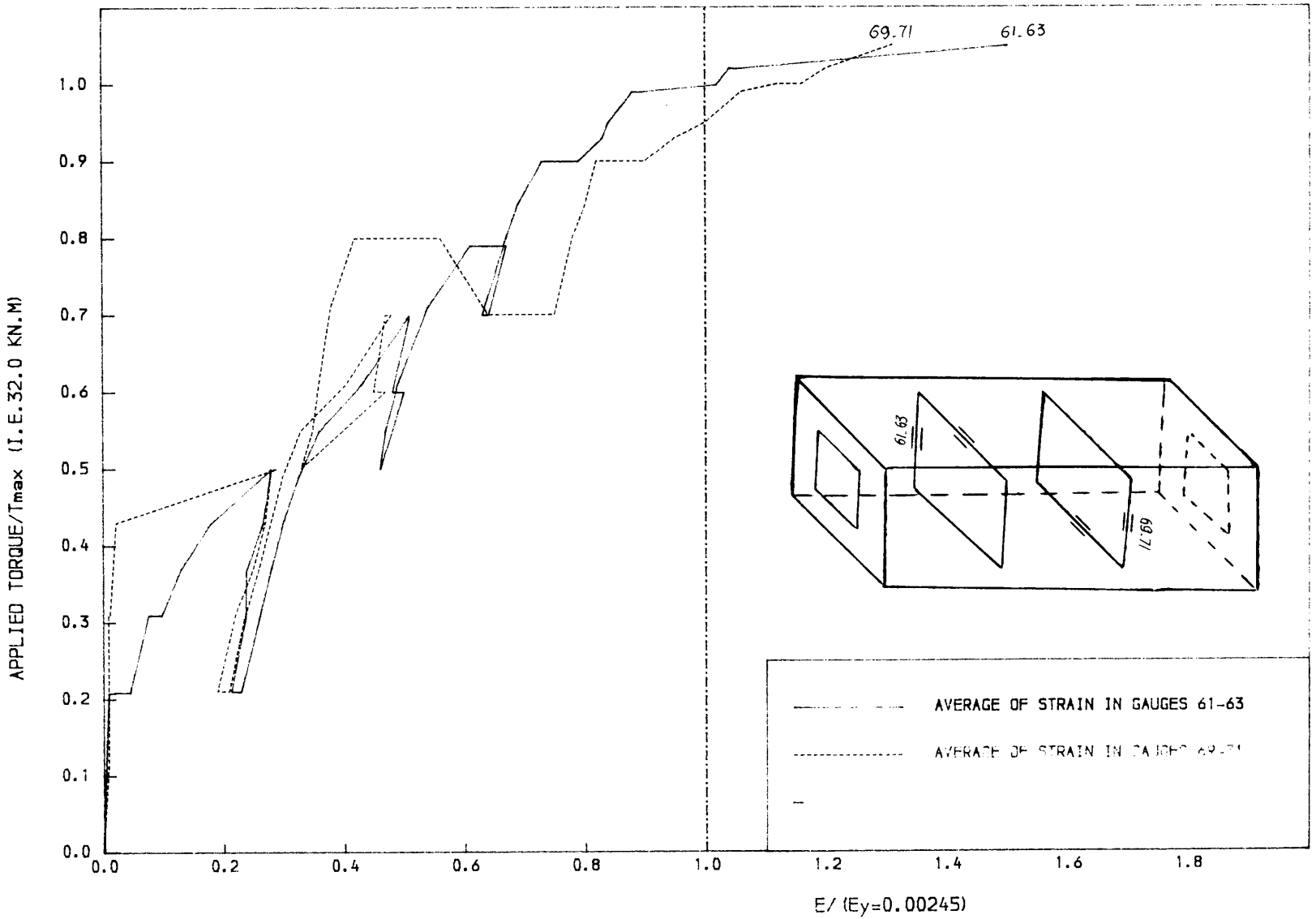

FIG 5.11 LOAD-STEEL STRAIN CURVE IN THE STIRRUPS FOR BEAM A3

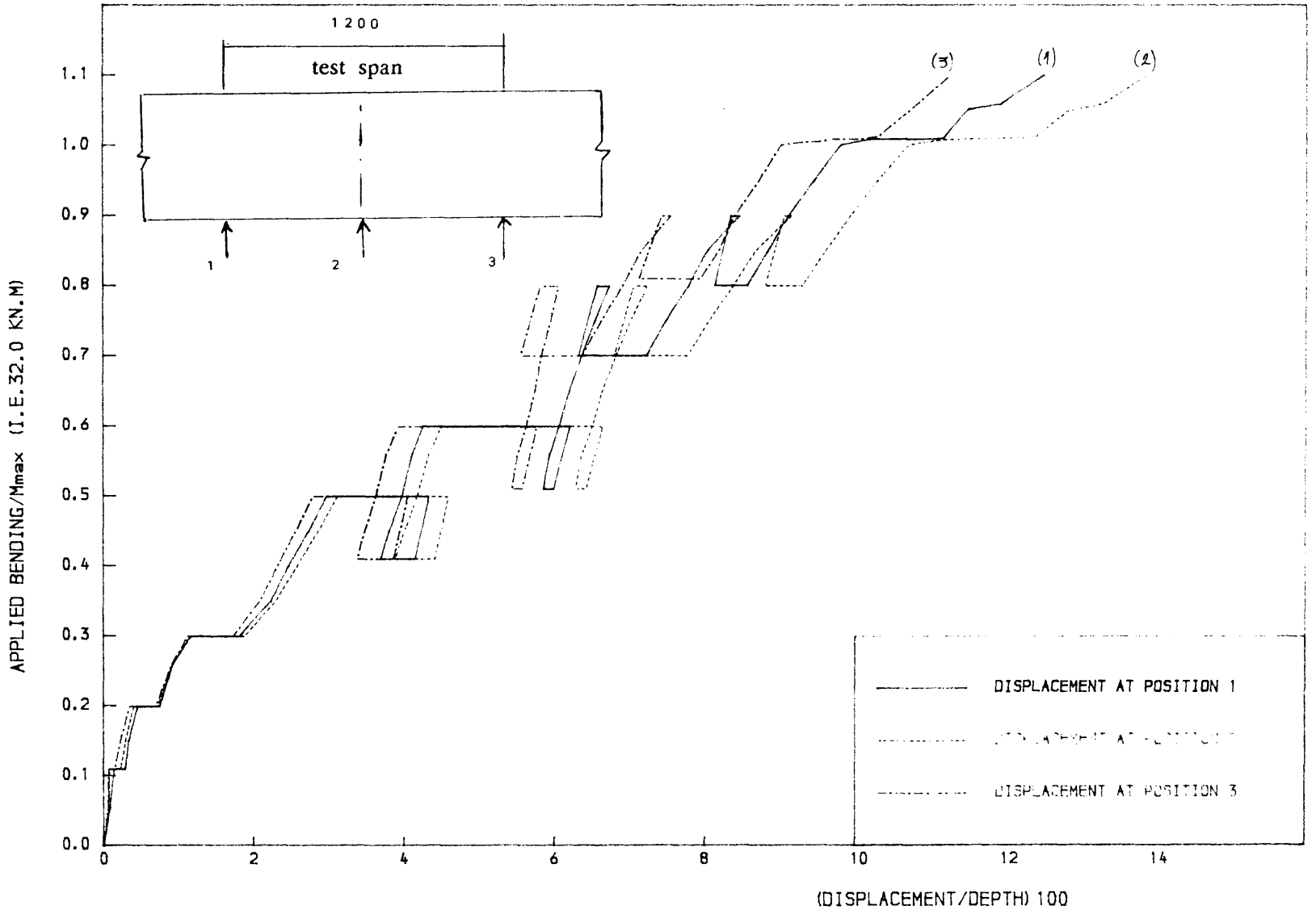

FIG 5.12 DISPLACEMENT CURVE AT MID-SPAN OF BEAM A3

Figure 5.10 and 5.11 shows the load/strain curves, while figure 5.12 shows the load/displacement curve for beam A3.

The deflection limit of span/250 was attained at a load of ($0.6xM_{max}$,$0.7xT_{max}$). The first yield of longitudinal steel was recorded at a load of ($0.7xM_{max}$,$0.8xT_{max}$) at the bottom longitudinal steel bar, while the first yield of transverse steel was recorded at a load of ($1.0xM_{max}$,$1.0xT_{max}$).

At a load of ($1.1xM_{max}$,$1.05xT_{max}$) a major spiral crack opened up and the beam collapsed. The strain in the longitudinal bars and stirrups either exceeded the yield strain or were near to yielding.

Table 5.2 Load/crack width for model A3

M/M_{max}	T/T_{max}	crack(1) (mm)	crack(2) (mm)	crack(*) (mm)
0.5	0.5	0.10	0.12	*
0.6	0.7	0.12	0.28	*
0.8	0.6	0.14	*	0.30
0.7	0.8	0.16	0.30	0.35
0.9	0.8	0.18	0.38	0.50
0.8	0.7	*	0.32	0.46
1.0	0.9	0.18	0.40	0.60

* missing data

Model A4 – Load path 4 (see fig 4.16)

The load was applied in small increments of $0.05xM_{max}$ and $0.08xT_{max}$. Bending was applied first. The first cracks appeared in the bottom flange at a load

of $0.3xM_{max}$. These cracks were approximately 90° to the beam axis. Keeping M = $0.3xM_{max}$, torsion was increased till a load of $0.5xT_{max}$ was reached. At that stage, inclined cracks developed on both the webs and the bottom flange. At a load of ($0.3xM_{max}$,$0.5xT_{max}$), the first inclined cracks occured on the top flange. Keeping T= $0.5xT_{max}$, bending was increased till a load of $0.5xM_{max}$ was reached. Maximum displacement at the centre of the beam at this stage was 15.4mm. Then torsion and bending were successively decreased till a load of $0.3xT_{max}$ and $0.2xM_{max}$ was reached. Keeping M = $0.2xM_{max}$, torsion was increased to $0.7xT_{max}$. At this stage more inclined cracks developed on all the sides of the beam. Most of the cracks joined up at the corners to become spiral. Keeping T = $0.7xT_{max}$, bending was increased to $0.7xM_{max}$. At that stage all the bottom flange longitudinal steel bars were at yield. Then torsion and bending were successively decreased to $0.4xT_{max}$ and $0.55xM_{max}$. Keeping M = $0.55xM_{max}$, torsion was increased to $0.85xT_{max}$. At that stage, the first yield of stirrup was recorded. Keeping T = $0.85xT_{max}$, bending was increased to $0.85xM_{max}$. At that stage; existing cracks extended and widened, but few new cracks developed. Figure 5.13 shows crack development on beam A4, and the crack width values are given in table 5.3. Figure 5.13.A shows the specific cracks where crack widths were measured. At a load of ($0.85xM_{max}$,$0.85xT_{max}$), the longitudinal steel bars in the top half of webs yielded. Then torsion and bending were successively decreased and increased twice as shown in figure 4.16 . At a load of ($1.0xM_{max}$,$1.0xT_{max}$), the longitudinal bars located in the bottom half of webs yielded. Near failure, spalling of concrete on the top flange was noticed, and stirrups and longitudinal steel bars were at yield. The beam failed at load ($1.1xM_{max}$,$1.05xT_{max}$). At that load a major spiral crack opened up and the beam collapsed. Kinking of the bars was noticed after the beam had failed.

The deflection limit of span/250 was attained at ($0.5xM_{max}$,$0.7xT_{max}$). The first yield of longitudinal steel was recorded at the same load, while the first yield of transverse steel was recorded at ($0.7xM_{max}$,$0.75xT_{max}$). Figure 5.14 to 5.17 shows the load/strain, load/deflection and load/twist curves for beam A4.

Fig 5.13 Crack development at each load stage.

(Beam A4 : Reinforced Concrete beam)

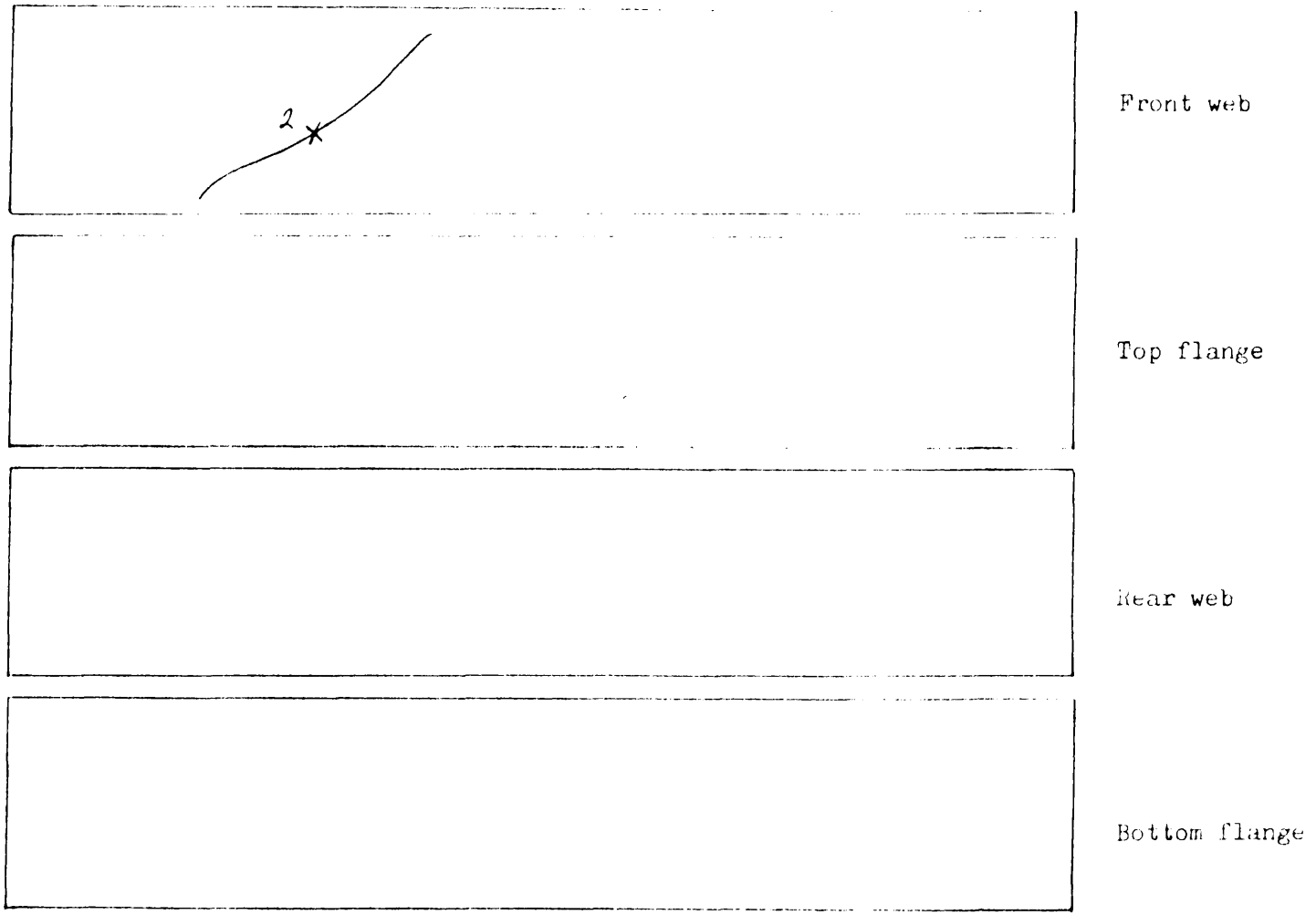

Figure [illegible].15.A location of cracks where the measurements were taken for beam A4

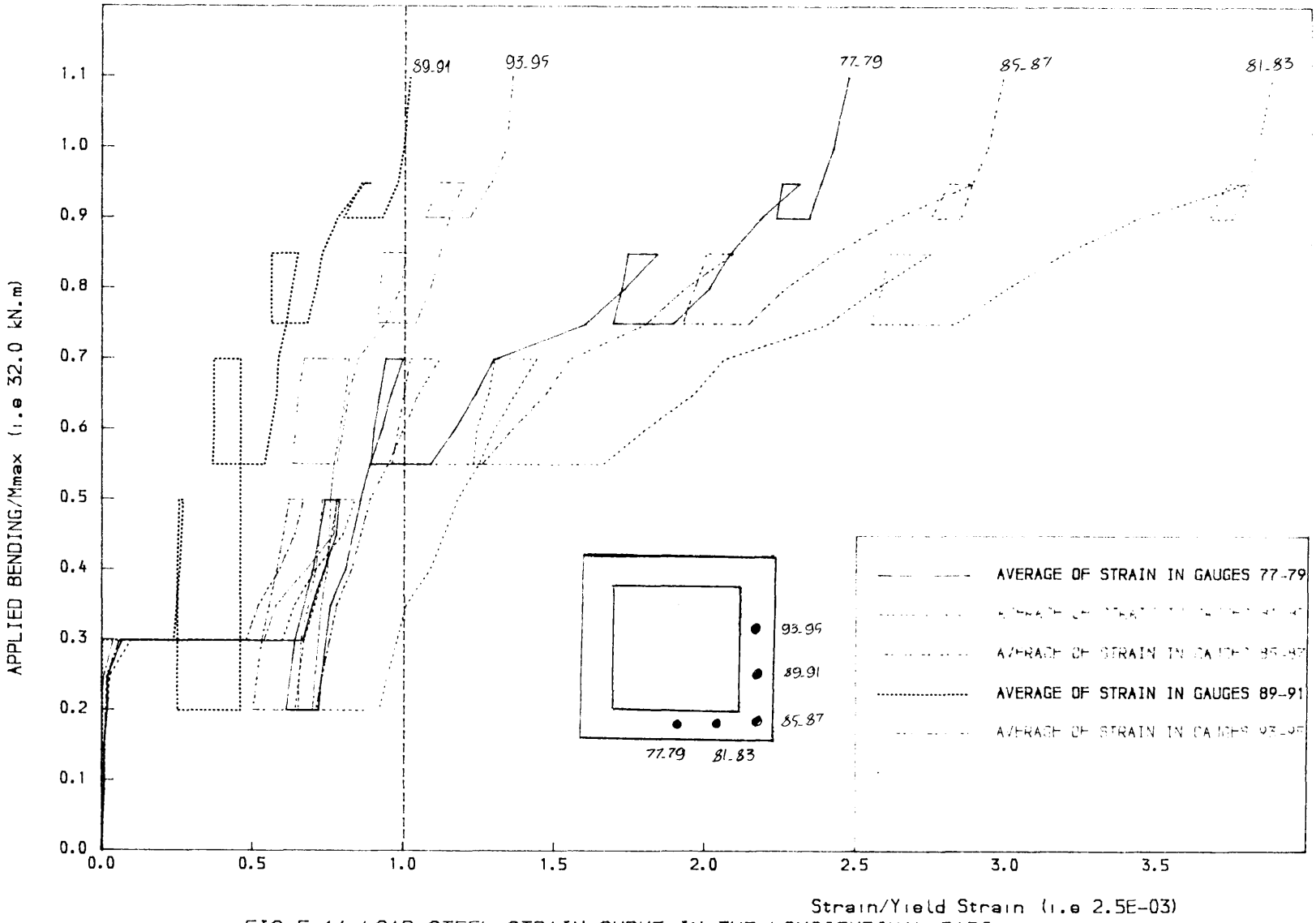

FIG 5.14 LOAD-STEEL STRAIN CURVE IN THE LONGITUDINAL BARS FOR BEAM A4

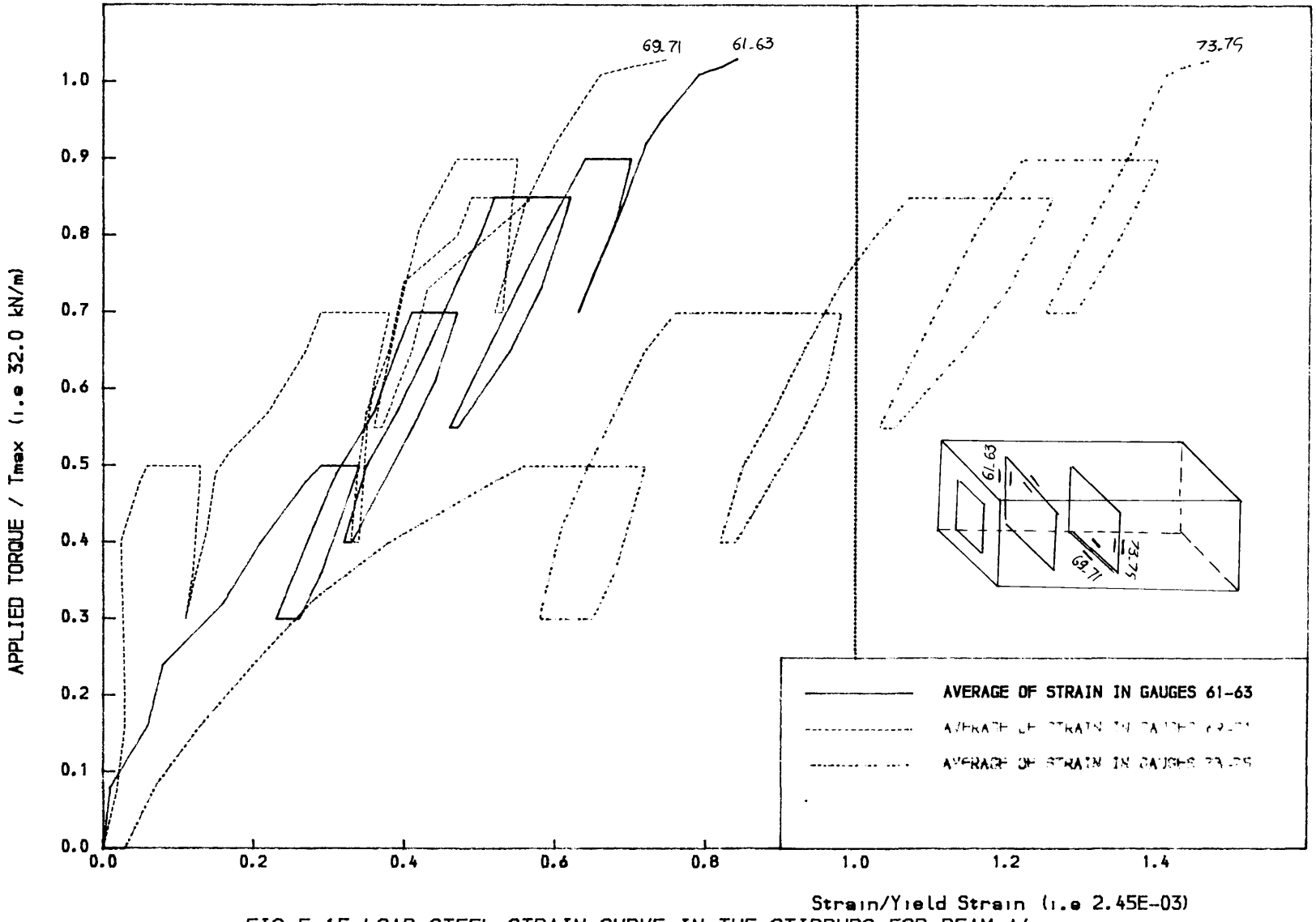

FIG 5.15 LOAD-STEEL STRAIN CURVE IN THE STIRRUPS FOR BEAM A4

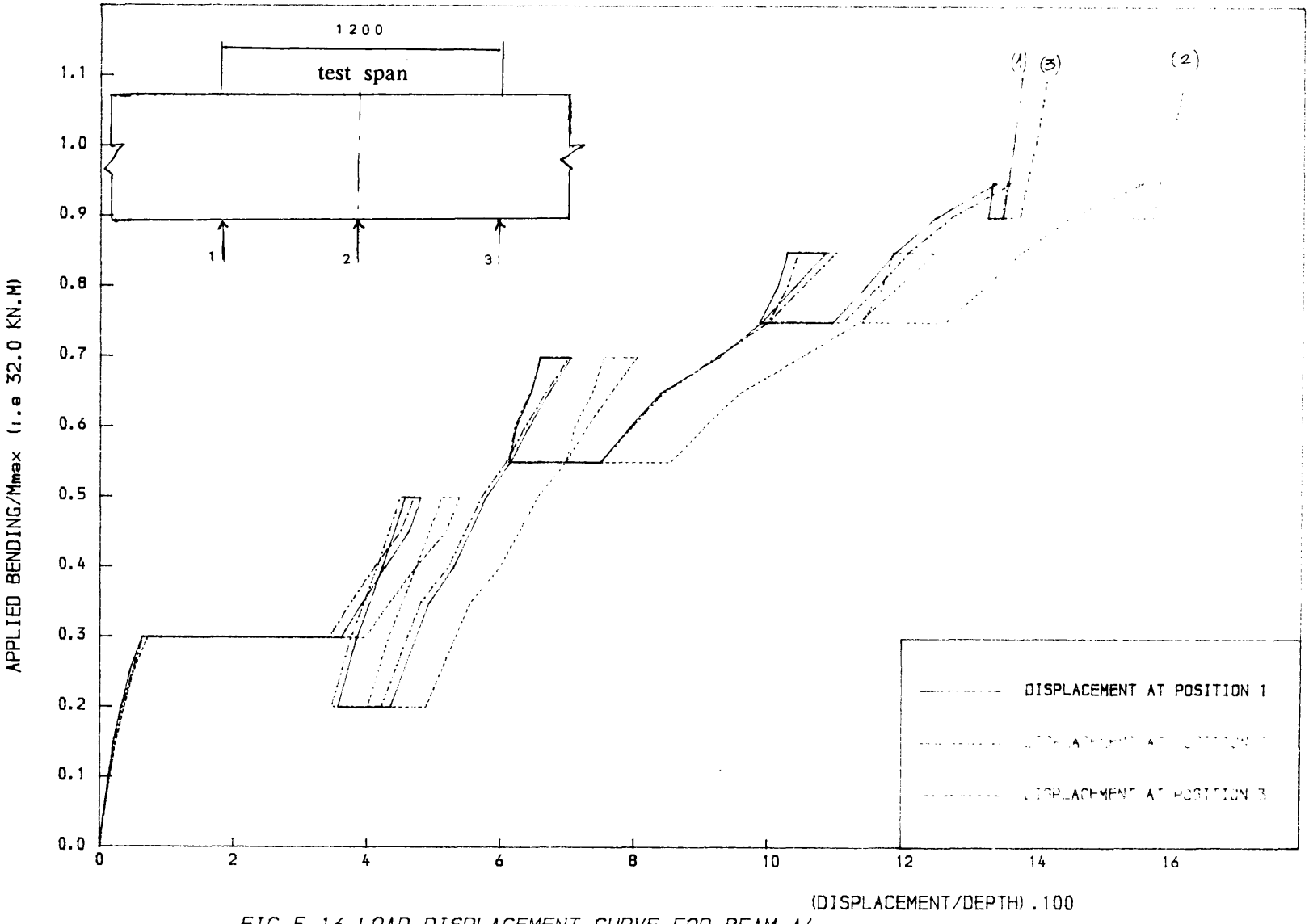

FIG 5.16 LOAD-DISPLACEMENT CURVE FOR BEAM A4

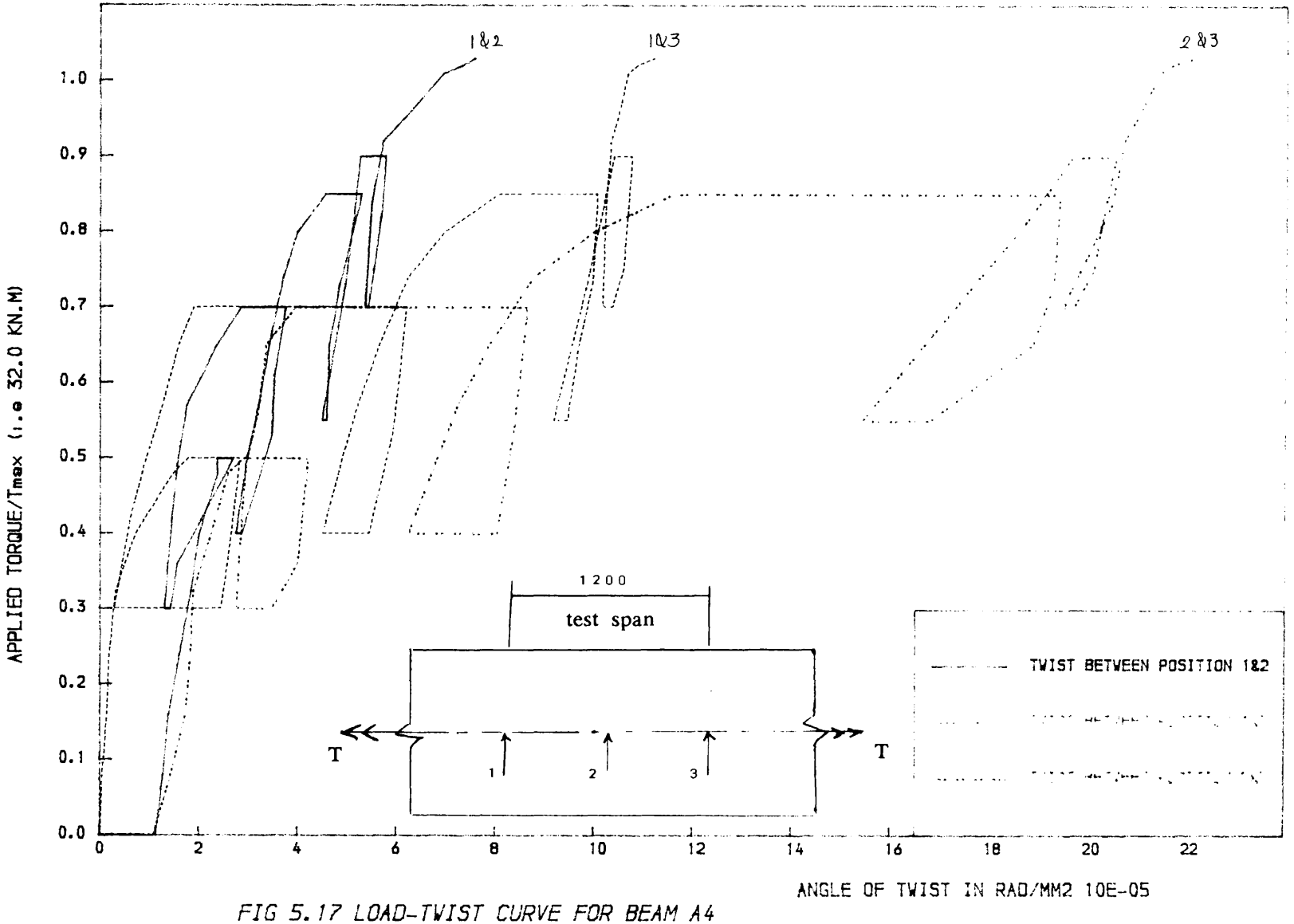

FIG 5.17 LOAD-TWIST CURVE FOR BEAM A4

In the case of series A cracks in the top flange appeared last.

Table 5.3 Load/crack width for model A4

M/M_{max}	T/T_{max}	crack(2) (mm)
0.50	0.7	0.12
0.55	0.7	0.15
0.65	0.7	0.20
0.55	0.8	0.25
0.55	0.85	0.30
0.65	0.85	0.35
0.80	0.85	0.40
0.85	0.85	0.45
0.85	0.90	0.50
0.90	0.90	0.55
0.95	0.90	0.60
0.90	0.95	0.60
1.00	1.00	0.70

5.2.2 *Series B – Partially prestressed concrete beams*

Two partially prestressed concrete hollow beams designed according to direct design method based on classical limit capacity concept[5] were tested under various load combinations. The load paths followed in these tests are shown in figures 4.17– 4.18 . The object of this series was to study the behaviour of

partially prestressed concrete beams under multiple loadcases. In these series, large decrease in loads were operated at higher load than in series A, in order to make the load history depart strongly from the monotonic loading case.

Model B1 – Load path 5 (see fig 4.17)

The load was applied in small increments of $0.05xM_{max}$ and $0.08xT_{max}$. Bending was applied first up to a load of $0.1xM_{max}$. Keeping $M = 0.1xM_{max}$, torsion was increased up to a load of $0.4xT_{max}$. At $(0.1xM_{max},0.3xT_{max})$ inclined cracks started to develop on the top flange. Torsional moment caused the development of these early cracks on the top flange. Keeping $T = 0.4xT_{max}$, bending was increased up to a load of $0.35xM_{max}$. At that load level, cracks developed on both the webs and the bottom flange as shown in figure 5.18. Then torsion and bending were successively decreased to $(0.05xM_{max},0.3xT_{max})$. Keeping $M= 0.05xM_{max}$, torsion was increased to $0.7xT_{max}$. At that stage more cracks developed on the top flange and the previously formed ones extended and widened, and the cracks on the webs spread towards the top flange. At $(0.05xM_{max},0.7xT_{max})$, cracks developed everywhere on the beam, most of them extended through the depth and joined at the corners to become spiral. Keeping $T= 0.7xT_{max}$, bending was increased to $0.6xM_{max}$. At that stage the crackwidth limit of 0.3mm according to BS8110[4] was reached. The span/250 limit displacement was reached at $(0.5xM_{max},0.7xT_{max})$. Then torsion and bending were successively decreased to $(0.4xM_{max},0.4xT_{max})$. Keeping $M = 0.4xM_{max}$, torsion was increased to $0.8xT_{max}$. At that load stage, the stirrups started yielding and the opening up of the cracks on both webs and bottom flange was noticed. Keeping $T= 0.8xT_{max}$, bending was increased to $0.8xM_{max}$. At $(0.6xM_{max},0.8xT_{max})$ yielding of bottom flange longitudinal steel bars was recorded. At a load of $(0.8xM_{max},0.8xT_{max})$, the longitudinal bars located in the webs yielded. Then the beam was subjected to other load combinations as shown in figure 4.17 till failure occured. The prestressing wires started yielding at a load of $(0.9xM_{max},0.8xT_{max})$. Figure 5.19 to 5.22 show the load/strain curves and load/displacement curves for beam B1. Near failure, spalling of concrete on the top

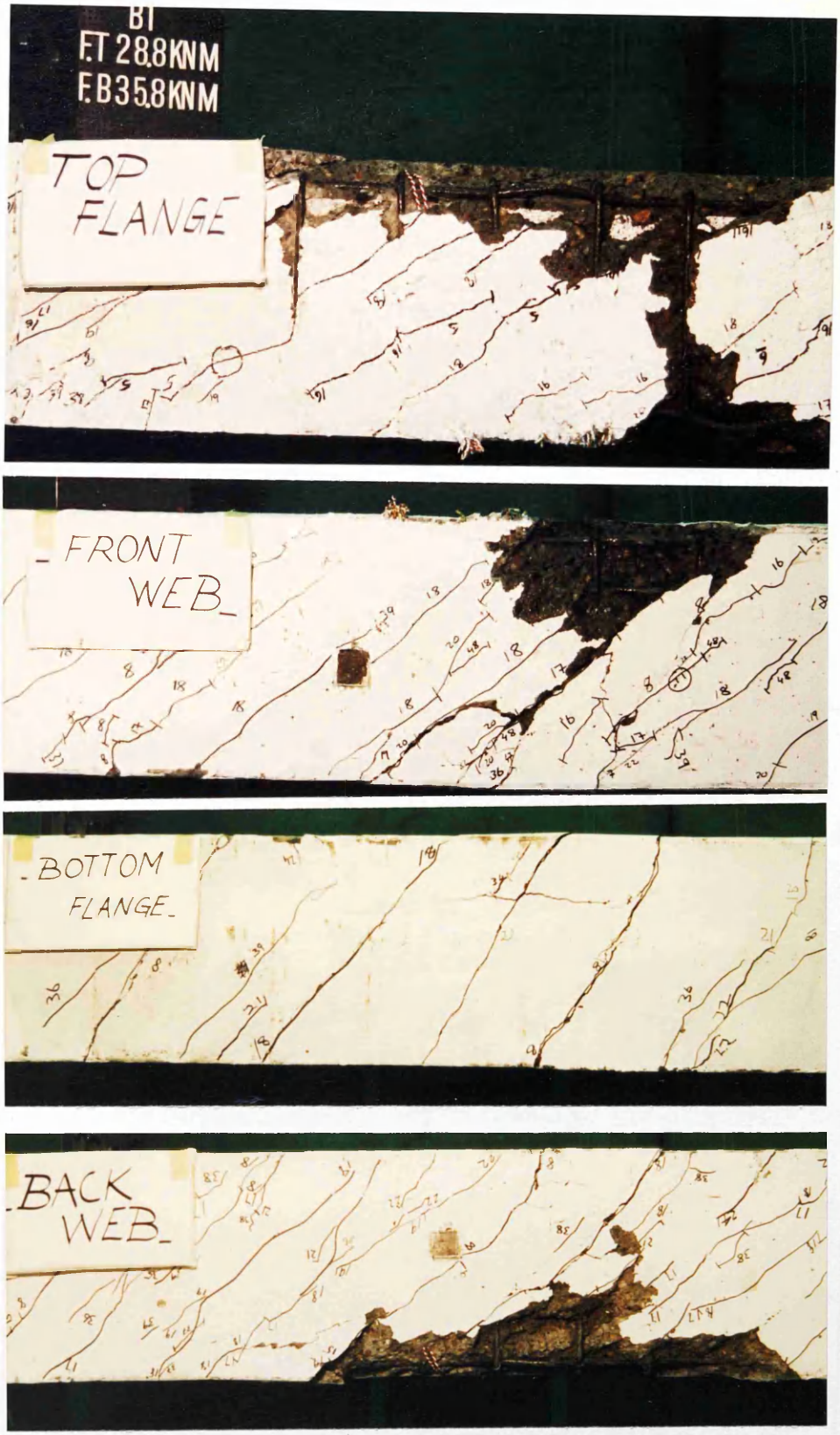

Fig 5.18 Crack development at each load stage.

(Beam B1 : Partially Prestressed Concrete beam)

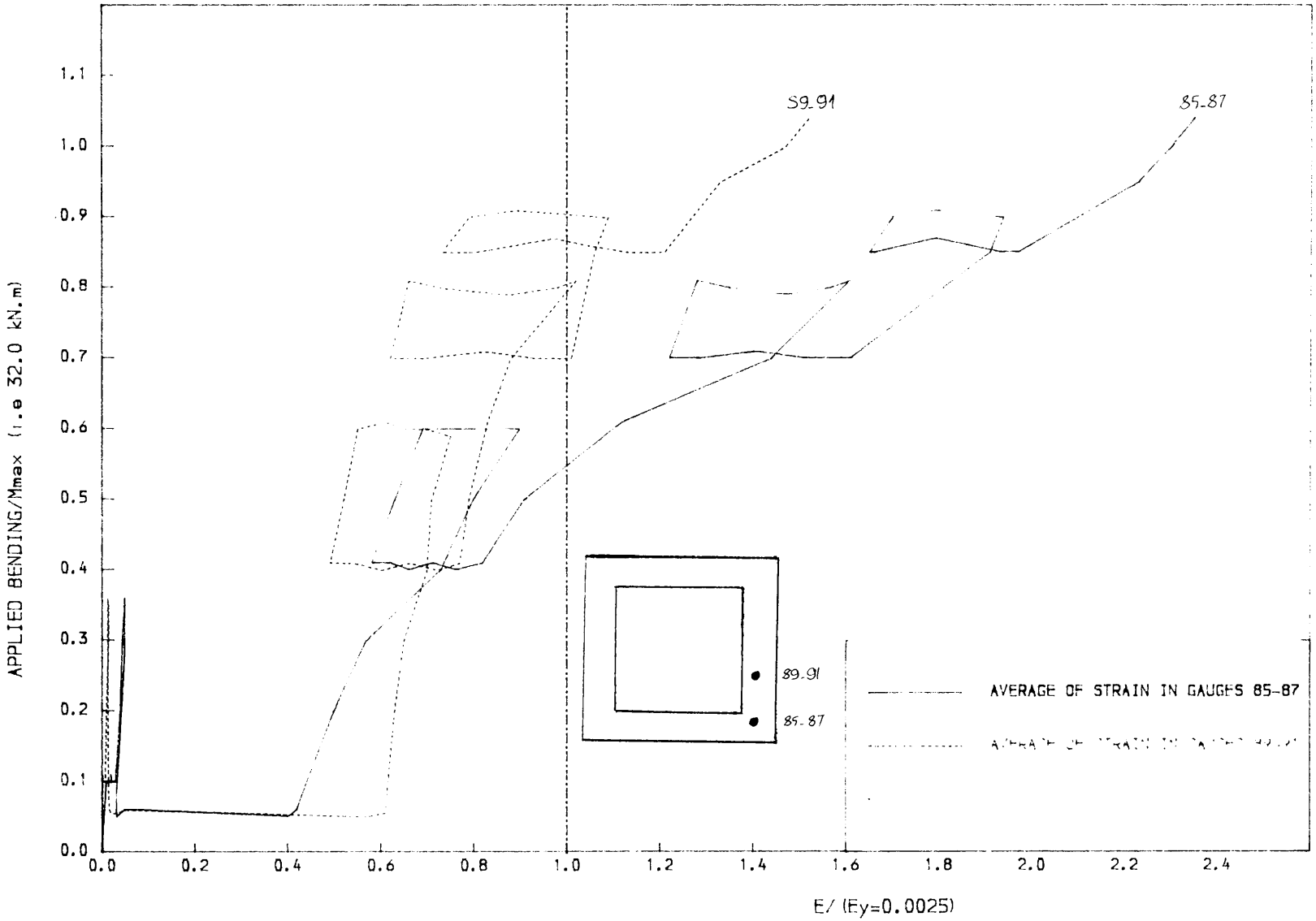

FIG 5.19 LOAD-STEEL STRAIN CURVE IN THE LONGITUDINAL BARS FOR BEAM B1

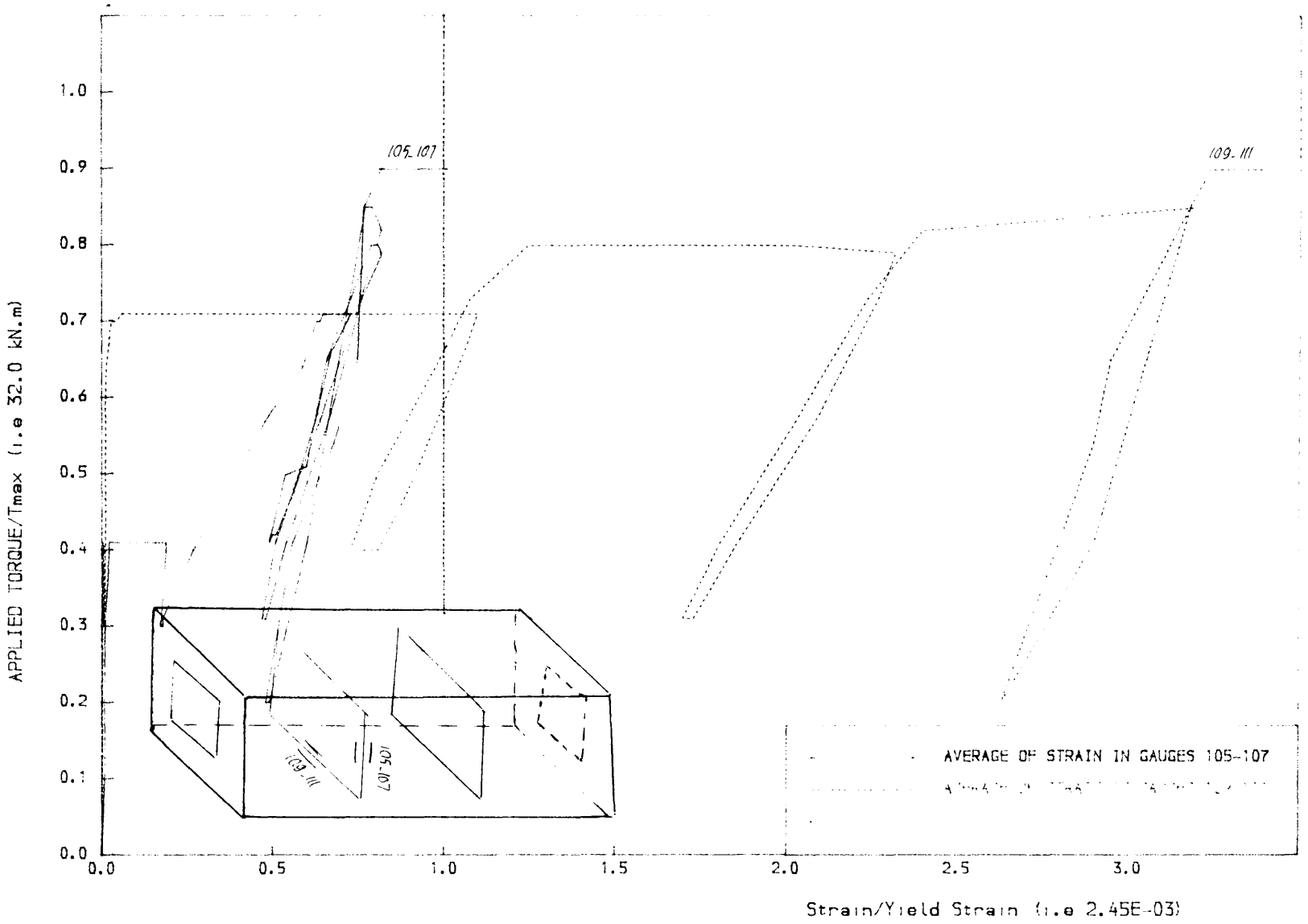

FIG 5.20 LOAD-STEEL STRAIN CURVE IN THE STIRRUPS FOR BEAM B1

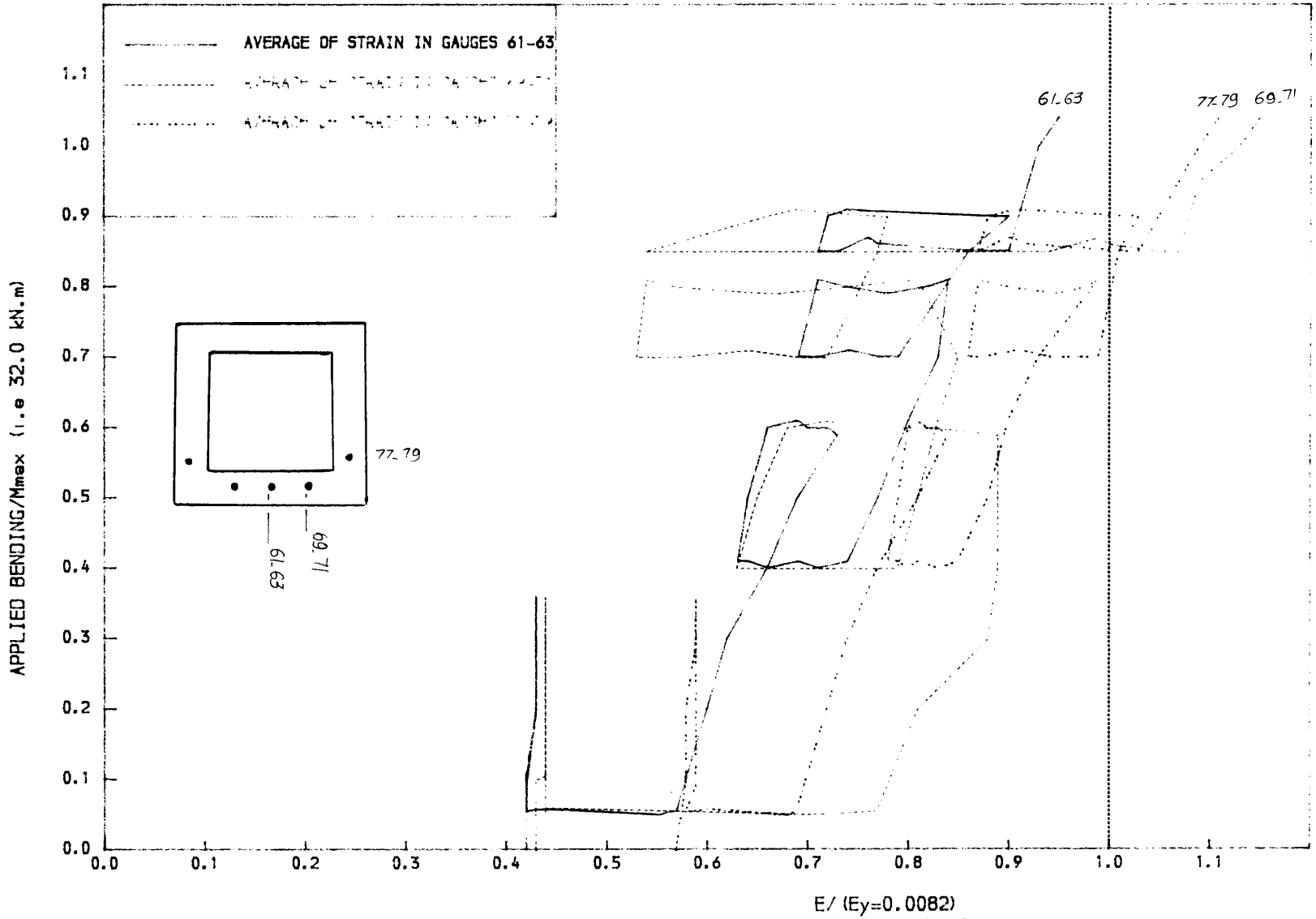

FIG 5.21 LOAD-STEEL STRAIN CURVE IN THE PRESTRESSING WIRES FOR BEAM B1

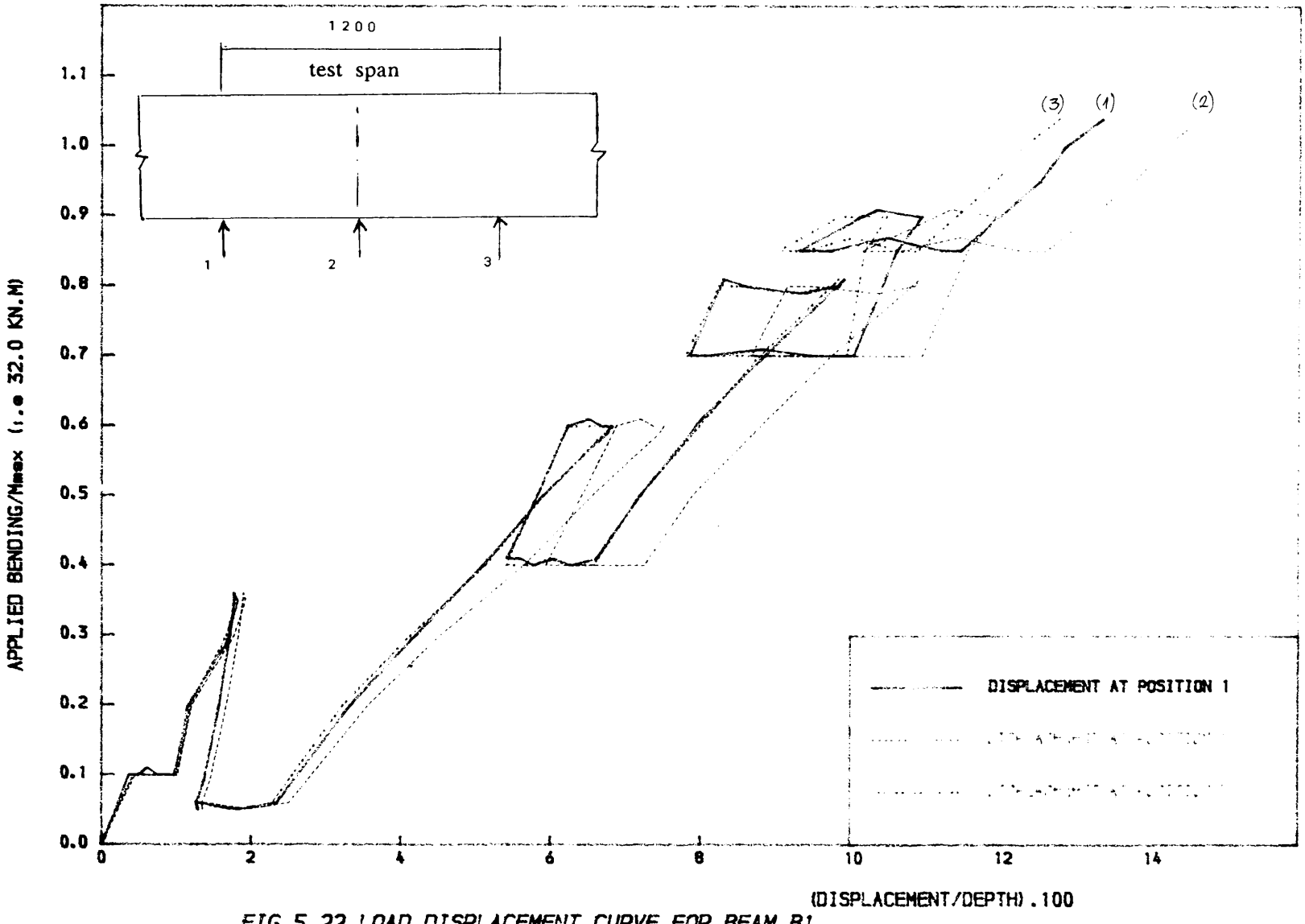

FIG 5.22 LOAD-DISPLACEMENT CURVE FOR BEAM B1

flange was noticed. The beam failed at ($1.05xM_{max}$,$0.9xT_{max}$). At that load, a major spiral crack opened up and the beam collapsed. Kinking of the bars and prestressing wires was noticed. The maximum value of torsion (T_{max}) was not reached, this might be due to the large decrease and increase of torsion operated at a stage where the reinforcing steel bars and stirrups were already at yield, and the concrete cracks were very quite wide (0.6mm).

Model B2 – Load path 6 (see fig 4.18)

The load was applied in small increments of $0.05xM_{max}$ and $0.08xT_{max}$. The first cracks occured at a load of ($0.4xM_{max}$,$0.2xT_{max}$) on both the webs and the bottom flange. After the initial load increments had been applied, bending was kept at $M= 0.2xM_{max}$ and torsion was increased to $0.4xT_{max}$. Then keeping $T= 0.4xT_{max}$, bending was increased to $0.7xM_{max}$. More inclined cracks developed on the bottom flange and both webs. At that stage, the cracks in the webs spread towards the top flange. At ($0.7xM_{max}$,$0.4xT_{max}$) the crackwidth limit of 0.3mm was reached. The crack development at each load stage is shown in figure 5.23 and the crack width values are given in table 5.4. Figure 5.23.A shows the specific cracks where crack widths were measured. Then torsion and bending were successively decreased to ($0.1xM_{max}$,$0.3xT_{max}$) and then they were successively increased to ($0.9xM_{max}$,$0.6xT_{max}$). The first inclined cracks on the top flange occured at ($0.2M_{max}$,$0.6xT_{max}$). Displacement limit of Span/250 was reached at ($0.5xM_{max}$,$0.7xT_{max}$). The first yield of longitudinal steel occured at the bottom longitudinal corner bar at a load of ($0.6xM_{max}$,$0.6xT_{max}$), while the first yield of transverse steel was recorded at a load of ($0.8xM_{max}$,$0.7xT_{max}$). Then the beam was subjected to other load combinations as shown in figure 4.18 till failure occured. At ($1.0M_{max}$,$0.85xT_{max}$) the spalling of concrete was noticed on the top flange and the failure surface was clearly noticed. The beam failed after load ($1.1xM_{max}$,$0.9xT_{max}$) was reached. At failure, the kinking of the steel reinforcement and prestressing wires which were near yield was noticed. Figure 5.24 to 5.27 show the load/strain curves, load/displacement and load/twist curves for beam B2.

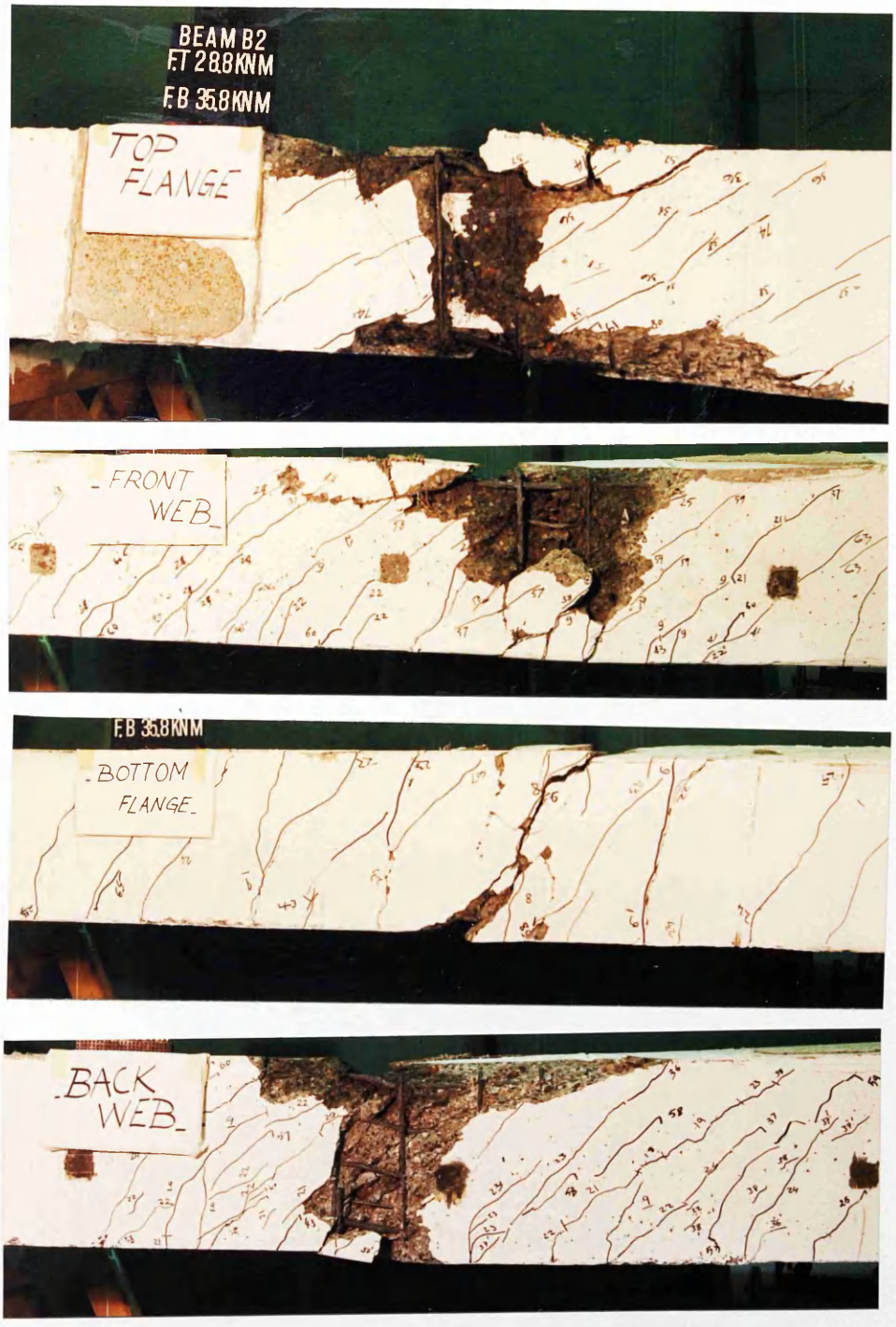

Fig 5.23 Crack development at each load stage.

(Beam B2 : Partially Prestressed Concrete beam)

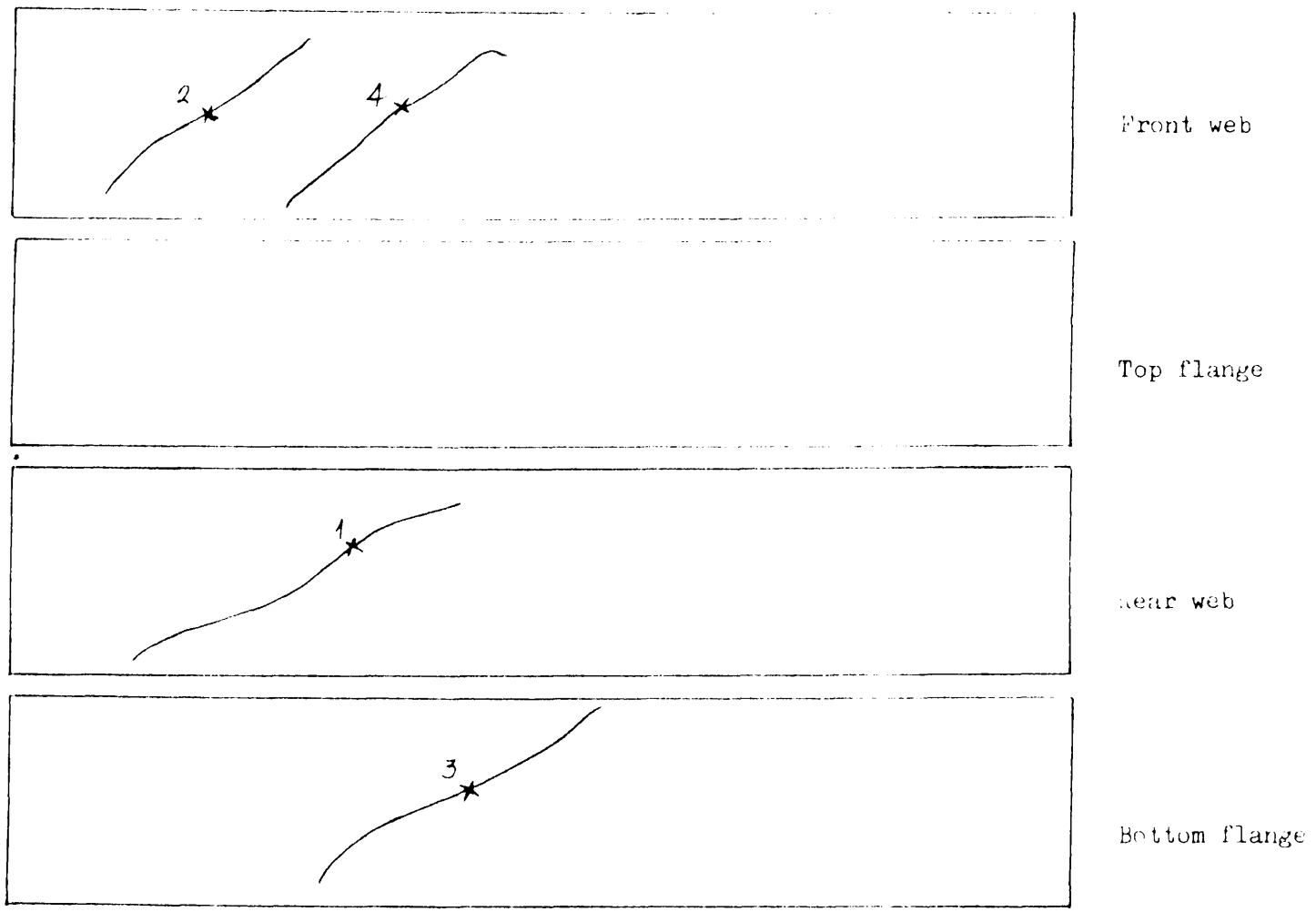

Figure 5.24.A Location of cracks where the measurements were taken for beam B2

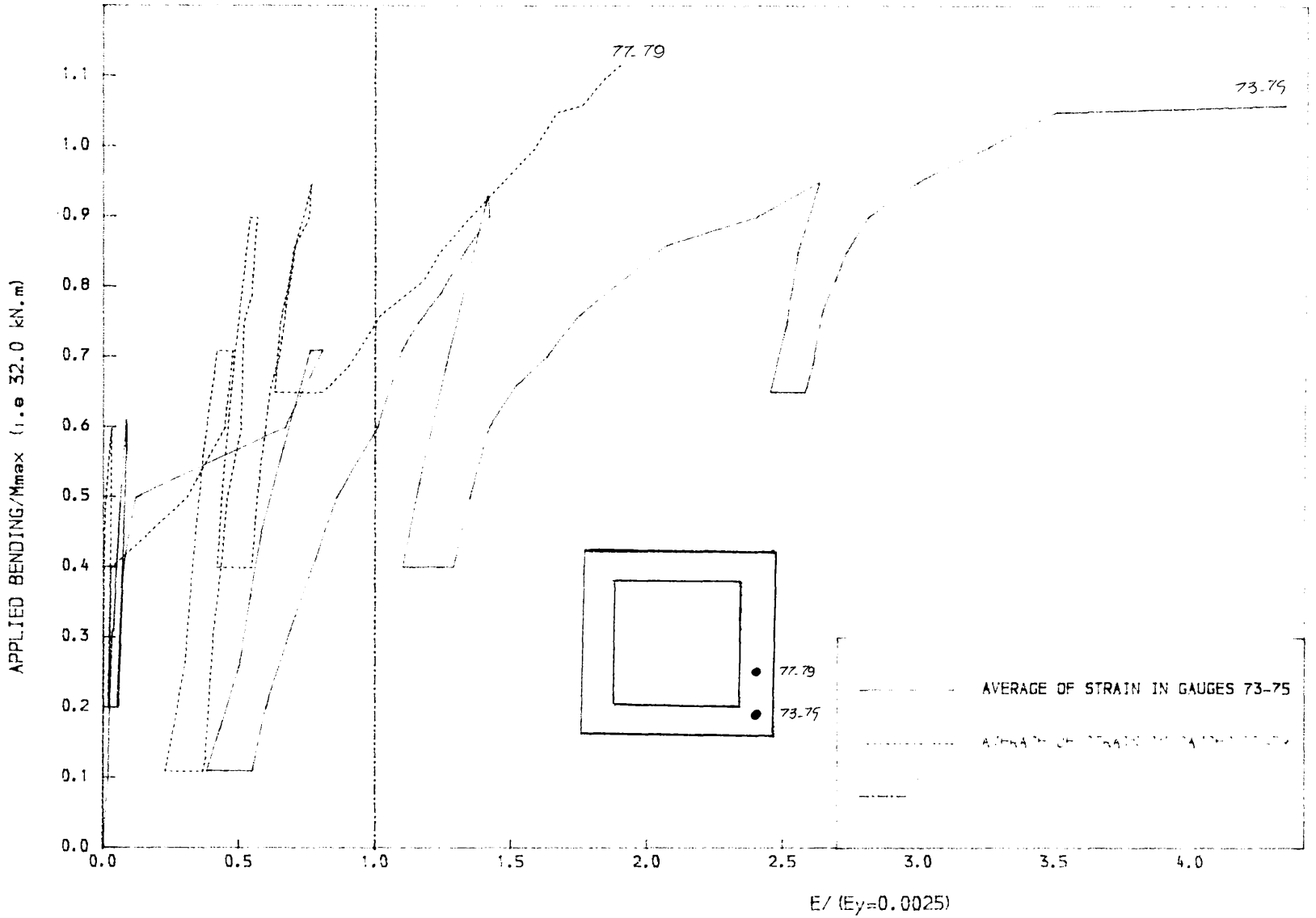

FIG 5.24 LOAD-STEEL STRAIN CURVE IN THE LONGITUDINAL BARS FOR BEAM B2

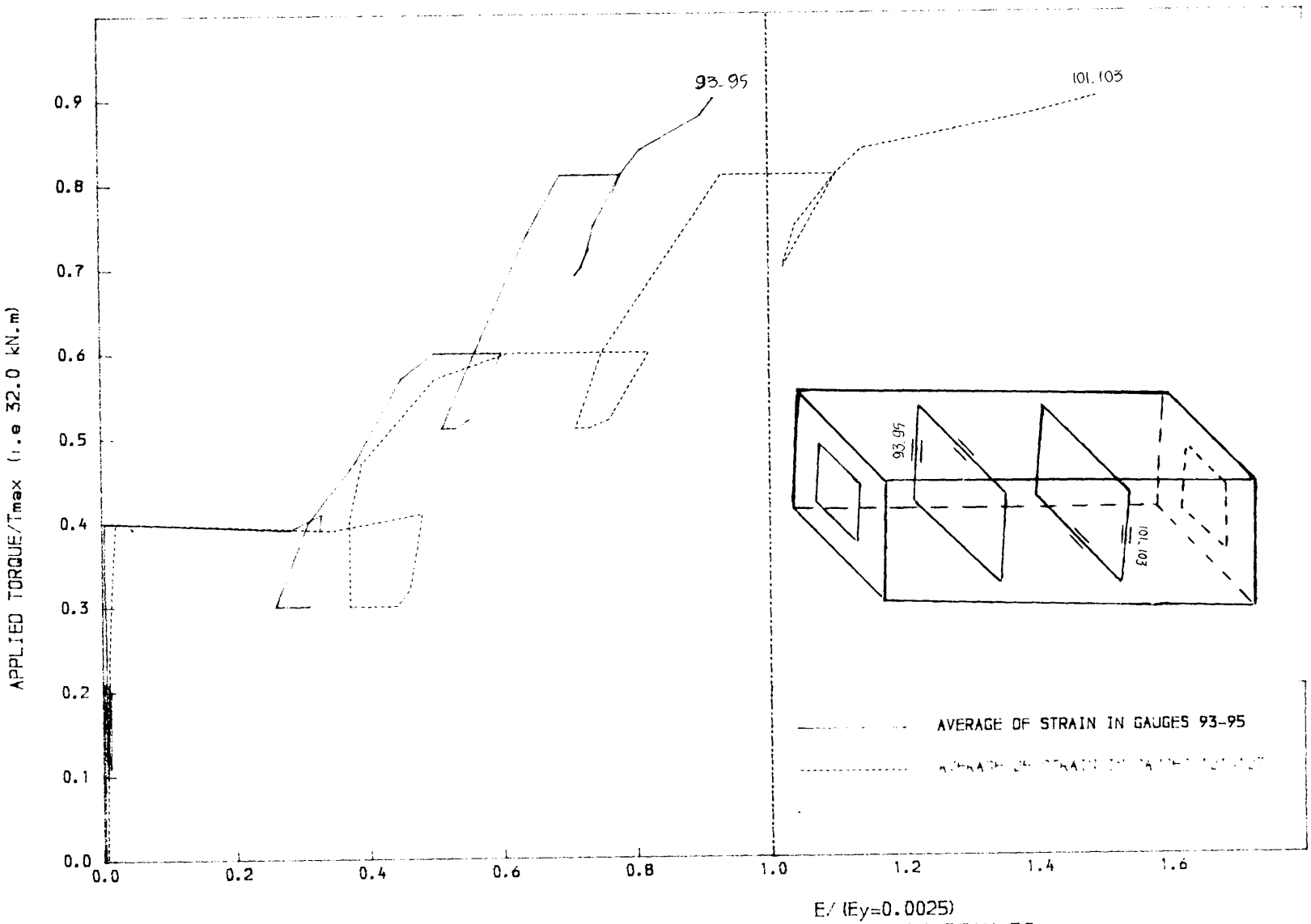

FIG 5.25 LOAD-STEEL STRAIN CURVE IN THE STIRRUPS FOR BEAM B2

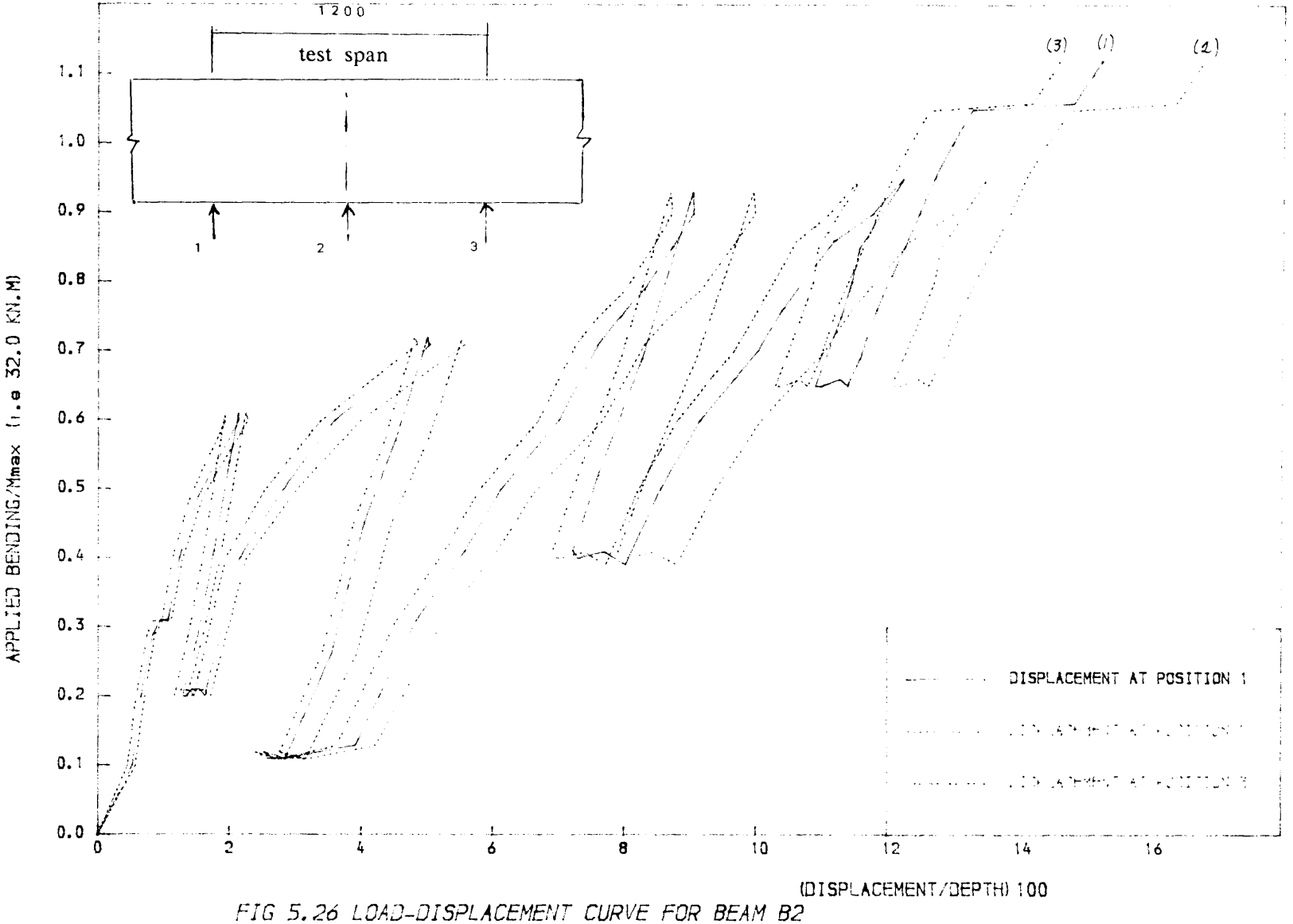

FIG 5.26 LOAD-DISPLACEMENT CURVE FOR BEAM B2

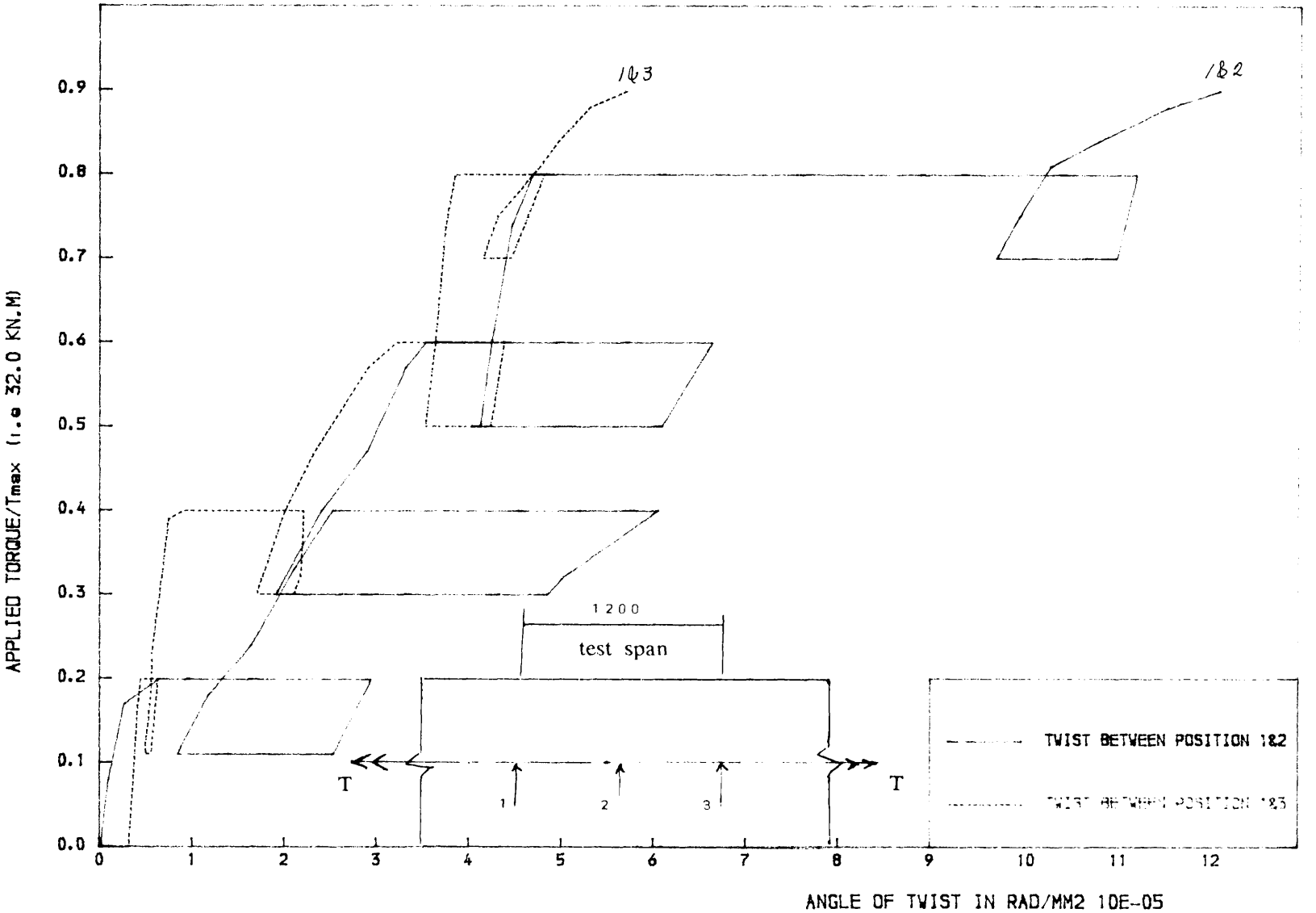

FIG 5.27 LOAD-TWIST CURVE FOR BEAM B2

Table 5.4 Load/crack width for model B2

M/M_{max}	T/T_{max}	crack(1) (mm)	crack(3) (mm)	crack(4) (mm)
0.40	0.20	0.05	0.40	*
0.80	0.60	0.10	0.60	*
0.80	0.70	0.15	*	0.25
0.85	0.80	0.20	0.80	0.30
1.00	0.85	0.25	0.95	0.35

* missing data

5.3 DISCUSSION

Detailed description of experimental behaviour of individual models was presented in section 5.2. The object of this section is to summarise the behaviour of all the models tested under the following headings.

a) Crack patterns

b) Deflection

c) Twist

d) Strains

5.3.1 *Crack patterns*

For reinforced concrete beams, under pure bending (first stages of tests A1,A4) cracks did not occur until a load of $0.3xM_{max}$ had been applied. Under pure Torsion (first stages of test A2) the first cracks occured at load of $0.3xT_{max}$. When the beam is loaded alternatively in torsion and bending (first stages of test

A3) cracks developed very early, at a load of ($0.15xM_{max}$,$0.1xT_{max}$). This might be due to the combined action of bending and torsion.

For partially prestressed concrete beams, the cracking load is at a much higher load than for reinforced concrete beams. For beam B1 the cracking load was ($0.1xM_{max}$,$0.3xT_{max}$), for beam B2 the cracking load was ($0.4xM_{max}$,$0.2xT_{max}$).

5.3.2 *Deflection*

The load/deflection curves follow generally the same variation as the load path, and for the different transducers locations the load/displacement curves are similar. When bending is increased, deflection increases and the load– deflection relationship is nearly linear. When bending is decreased, the deflection decreases too. When bending is kept constant and torsion is varied, deflection variation is minimal. The curves obtained by joining the peaks of the load/deflection curves from this investigation (reinforced and partially prestressed concrete beams under multiple loading cases) are compared to the load/deflection curves obtained under monotonically increasing proportional loading by J.Ebireri[2] (reinforced concrete beam subjected to combined bending and torsion) and R.Saadi[32] (partially prestressed concrete beams subjected to combined bending and torsion) in figures 5.28 and 5.29 .

5.3.3 *Twist*

Few conclusions can be drawn concerning twist, as the twist results presented are for models A4 and B2 only. It happened that the transducers used for the twist measurement repeatedly failed to function properly. However the load/twist curves (fig 5.17 and fig 5.27) obtained respectively from the testing of models A4 and B2 follow the same variations as the load path followed respectively in the testing of beams A4 (figure 4.16) and B2 (figure 4.18). When torsion is

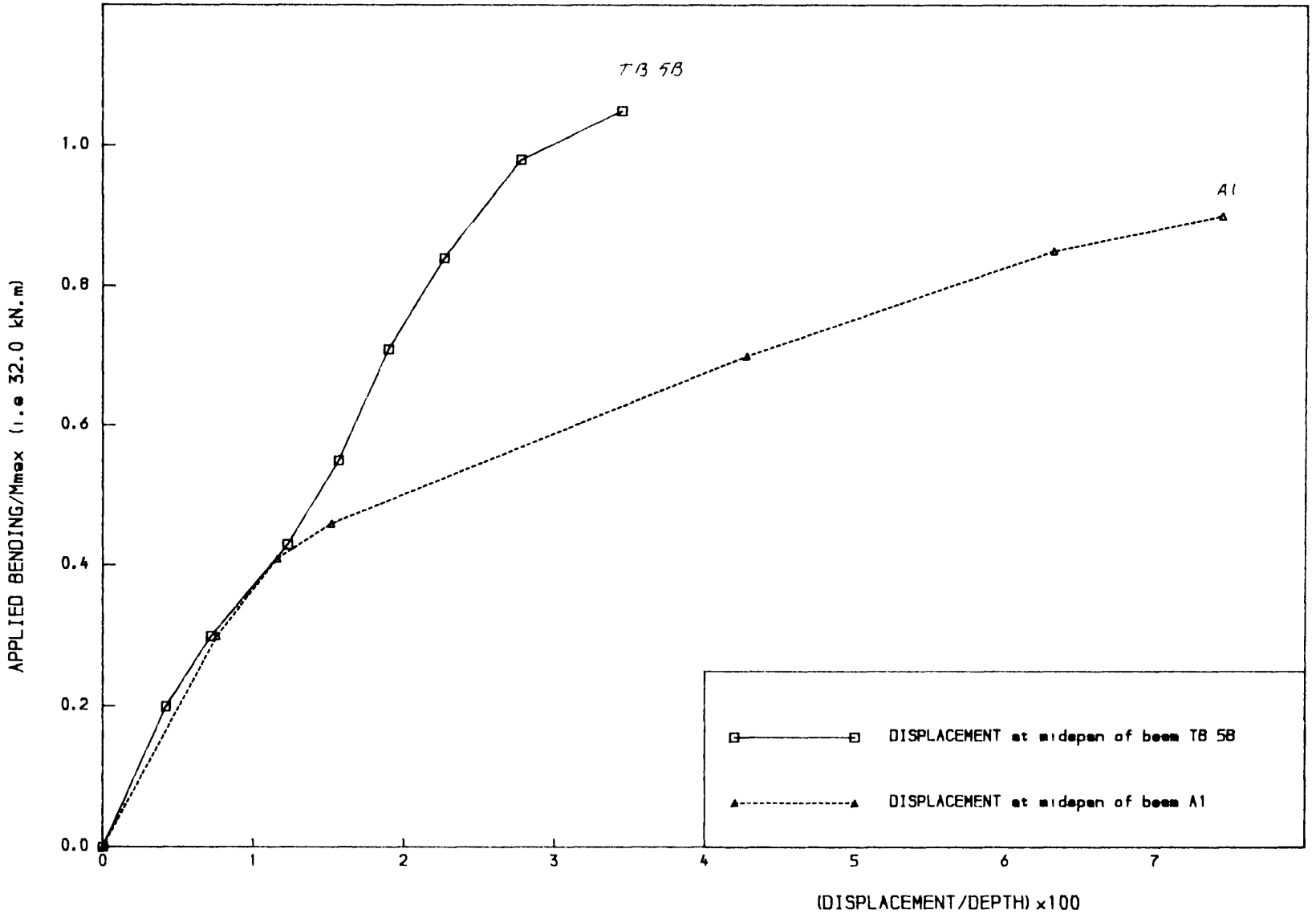

FIGURE 5.28 Load-Displacement curve for beams A1 & TB 5B (after J.Ebireri)

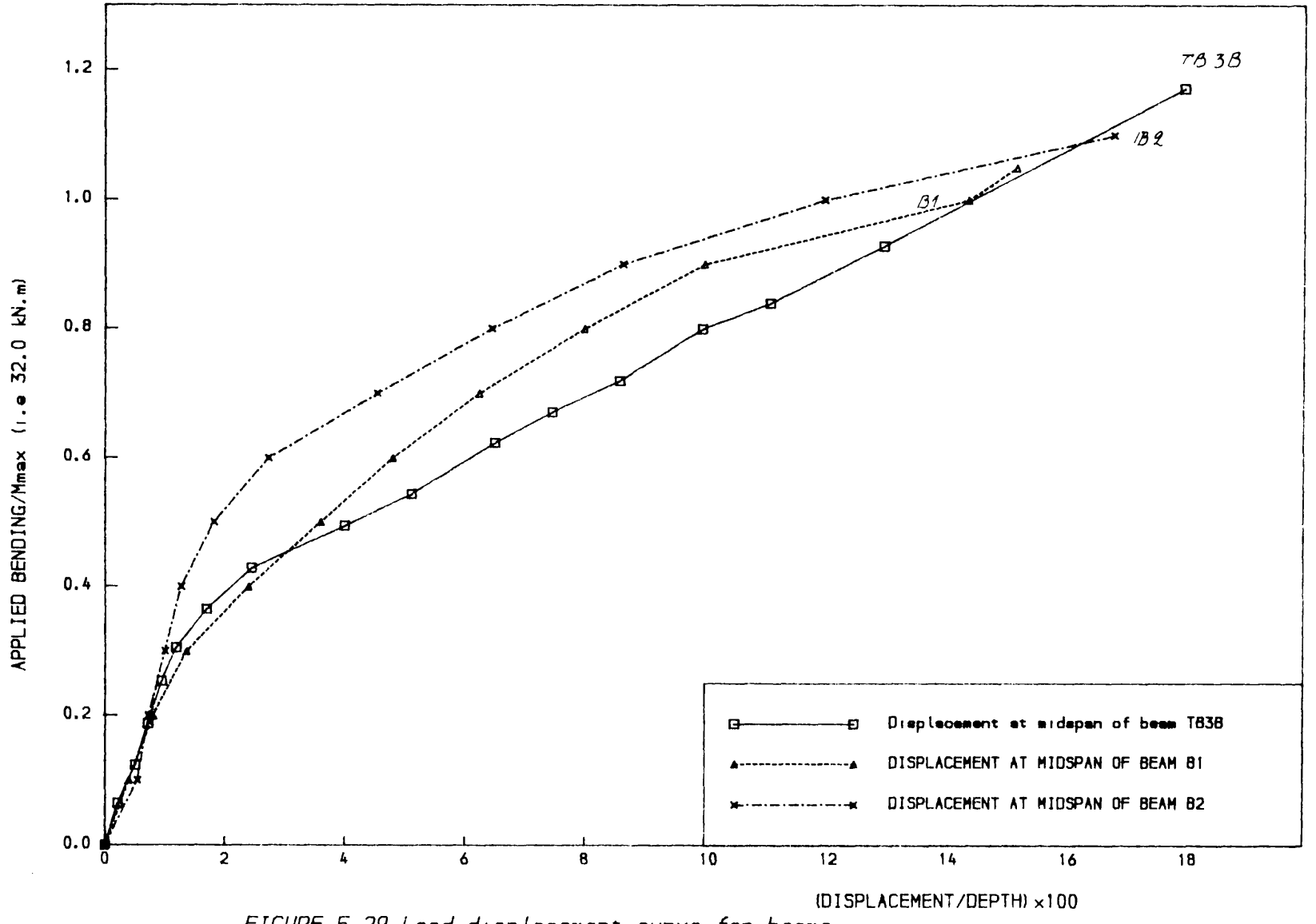

FIGURE 5.29 Load displacement curve for beams B1, B2 and TB3B (after R.Saadi)

increased, twist increases and the load–twist relationship is almost linear. When torsion is decreased the twist decreases too. When torsion is kept constant and bending is varied, twist changes very little.

5.3.4 *Strains*

The load/strain curves follow generally the same variation as the load path. When the load is increased, strain increases and the load–strain relationship is nearly linear. When the load is decreased the strain decreases too. When bending moment is kept constant and torsion is varied, both the strain in the longitudinal bars and prestressing wires varies very little. The torsion load/stirrups strain curve is nearly flat, when bending moment is varied and torsional moment is kept constant. The curves obtained by joining the peaks of the load/strain curves are compared to J.Ebireri[2] and R.Saadi[32] load/strain curves in figures 5.30 to 5.34 . It is clear from figure 5.30 to 5.34 that the general behaviour of the curves obtained in joining the peaks of the load/strain curves obtained for the case of multiple loadcases is similar to the load/strain curves obtained for the case of monotonically increasing proportional loading. The conclusion holds good for both reinforced concrete beams and partially prestressed beams. This general behaviour can be described as trilinear:

a) Behaviour before cracking

b) Behaviour after cracking

c) Behaviour after yielding of steel

Before the development of the first cracks, very little strain was normally observed in the reinforcing steel. As the applied load on the section is resisted mainly by concrete and steel is inactive.

After cracking, a gradual increase in strain was observed in all the steel bars and stirrups. The increase in strain is attributed to redistribution of stresses after cracking and subsequent progressive deterioration of concrete resistance.

After yielding, a rapid increase was recorded in strain with little or no

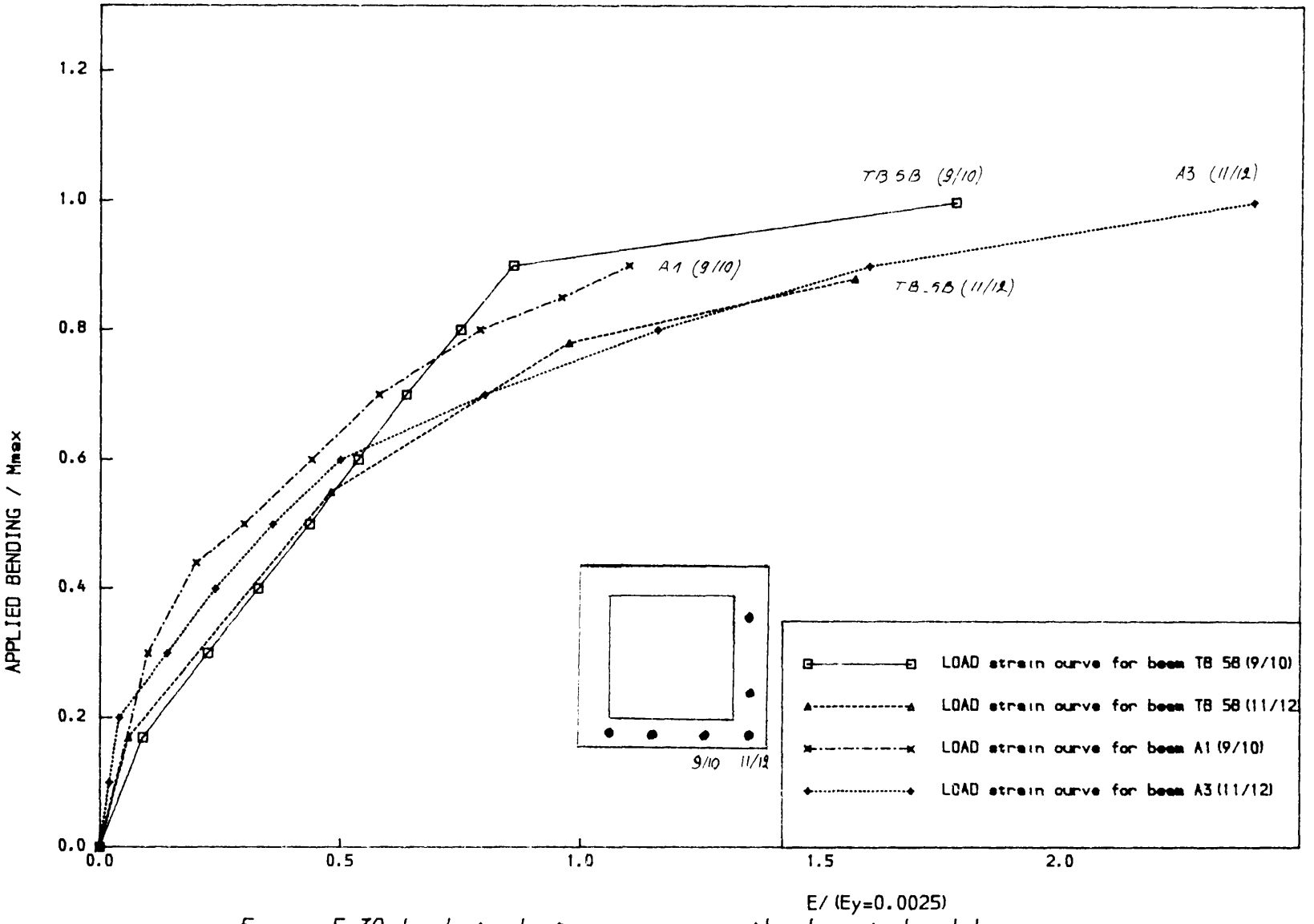

Figure 5.30 load-steel strain curve in the longitudinal bars for beams A1, A3 & TB 5B (after J.Ebireri)

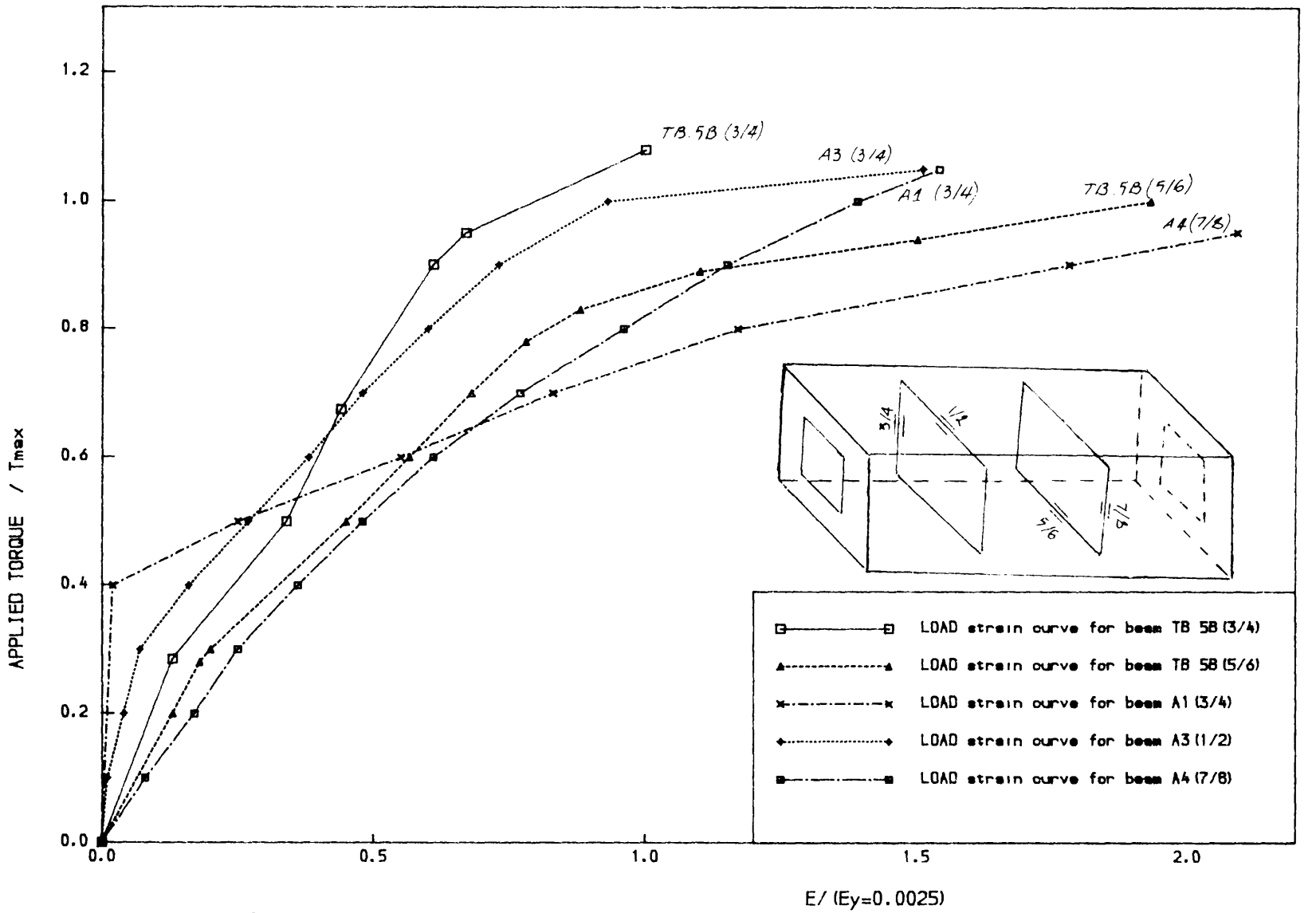

Figure 5.31 load-steel strain curve in the stirrups of beams A1, A3, A4 & TB 5B (after J.Ebireri)

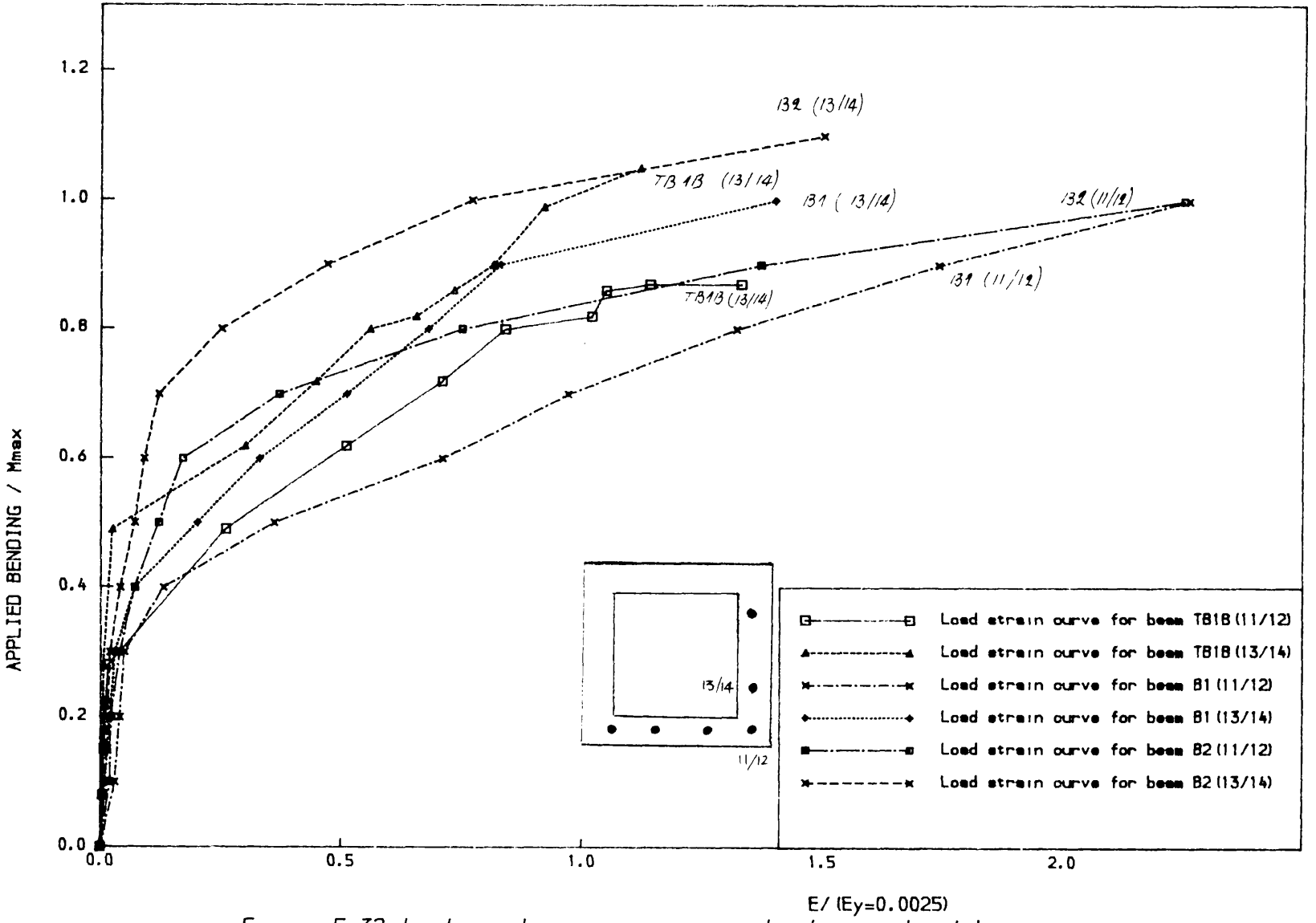

Figure 5.32 load-steel strain curve in the longitudinal bars for beams B1, B2 & TB 1B (after R. Saadi)

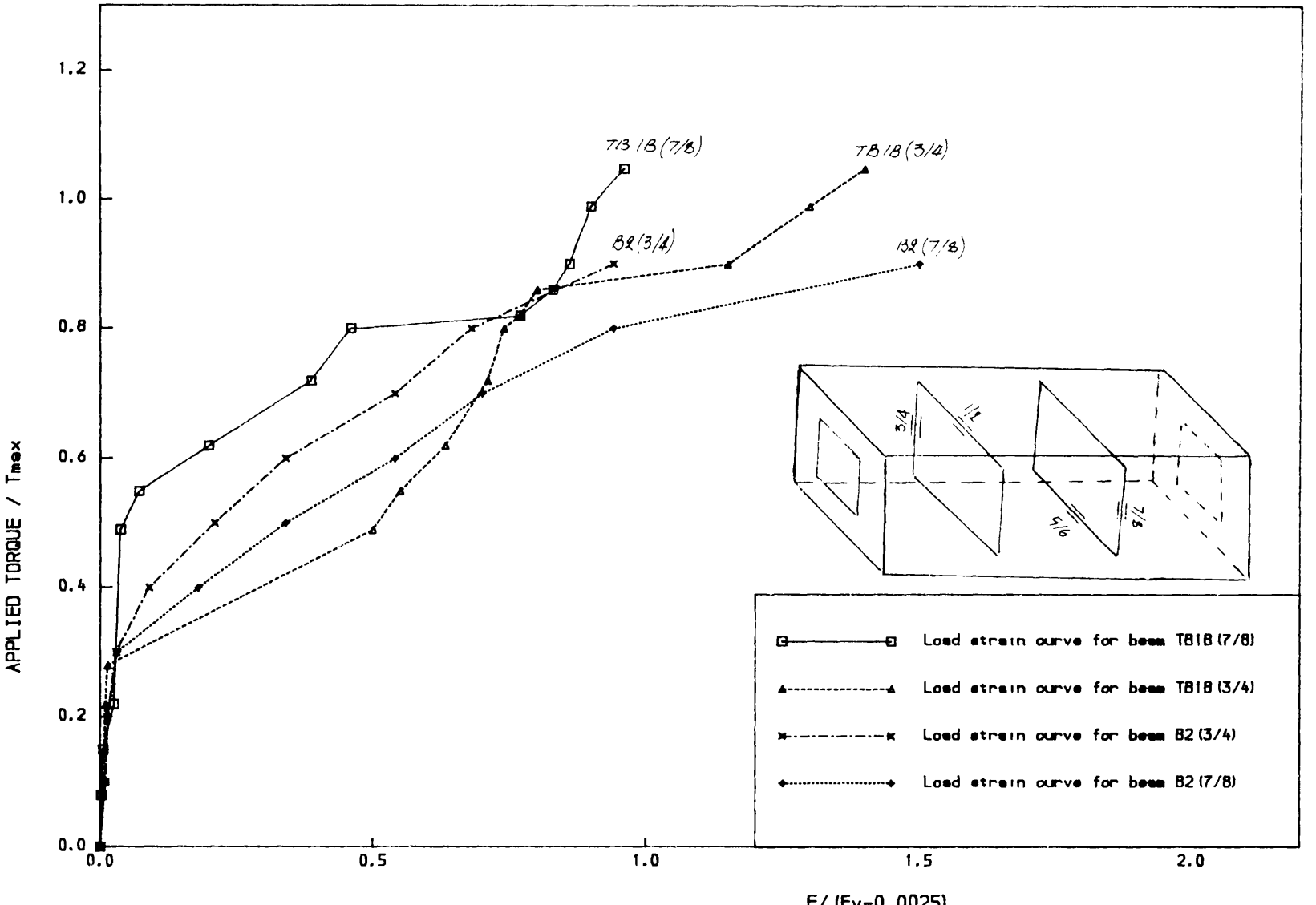

Figure 5.33 load-steel strain curve in the stirrups for beams B2 & TB 1B (after R. Saadi)

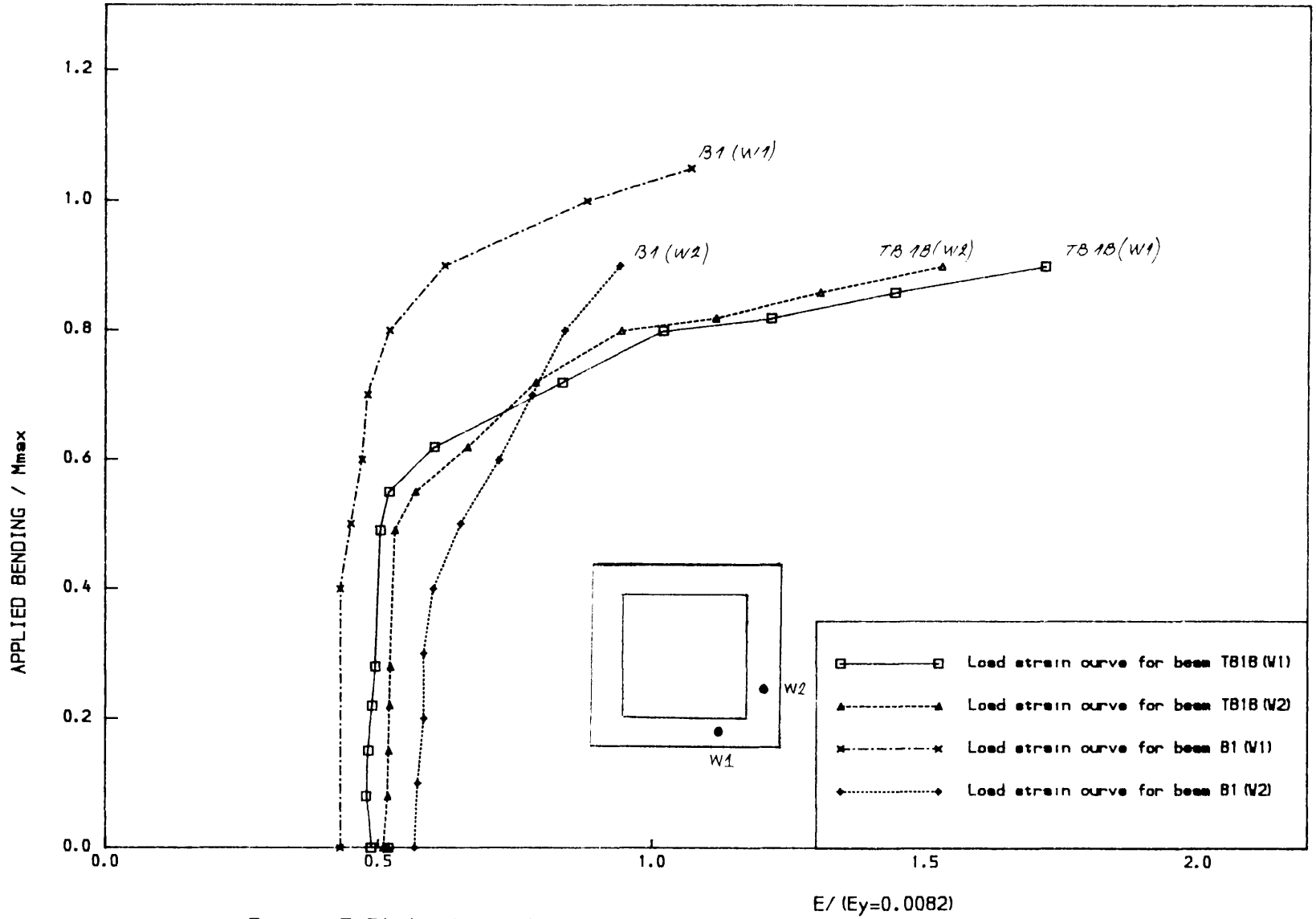

Figure 5.34 load-steel strain curve on the prestressed wires for beams B1 & TB 1B (after R. Saadi)

increase in load before failure. This represents the development of plastic strains. At ultimate load, most of the tension steel in the sections had yielded.

5.4 ANALYSIS OF TEST RESULTS

5.4.1 *Serviceability limit state*

Table 5.5 shows the summary of all the test results. The service load behaviour according to BS8110[26] is based on one of the following criteria.

a) Deflection limit of span/250

b) Maximum crackwidth limit of 0.3mm

From table 5.5, it is observed that all the beams reached the limiting service deflection at a low load–level. Average service deflection for the 6 beams tested is ($0.54xM_{max}$,$0.72xT_{max}$). The low service deflection load can be attributed to the presence of torsional moment. However, in the investigation reported in reference 2 , a very high service deflection load has been recorded in presence of torsional moment. This probably indicates that under non monotonic loading, deflection limit of span/250 cannot be used to determine serviceability limit state in the case of combined loadings. The deflection limit of span/250 recommended in BS8110[26] is normally intended for flexural moments only.

In the limit state theory, the general practice is to design for ultimate limit state and then check for serviceability. Considering that most of the loads on the beams tested are mainly live loads, by applying a load factor of 1.6 from BS8110[26] recommendations, the service load is obtained as :

$$\text{design load}/1.6 = 0.625xP_d \qquad (5.1)$$

Accordingly, the corresponding service deflection is obtained as deflection at a load level of 0.625 x design load from the test results.

Table 5.5 shows the ratio of load at maximum service crackwidth to maximum load for all the beams tested in this investigation. The maximum crackwidth was obtained as average crackwidth on the webs or flanges. From table

5.5 the load level corresponding to the maximum service crackwidth is fairly satisfactory. The average load level at service crackwidth of 0.3mm for all the beams is ($0.69xM_{max}$,$0.65xT_{max}$). This value is slightly higher than the working load of 0.625xdesign load, and nearly equal to the value obtained in the investigation reported in reference 2 (0.66xdesign load).

5.4.2 *Ultimate limit state*

Table 5.5 gives the summary of the ultimate behaviour of the beams tested in this investigation. The ultimate behaviour is classified into two stages for the purpose of analysis as :

a) First yield of steel

b) Final failure loads

a) First yield of steel

The average load at first yield of steel is equal to ($0.70xM_{max}$,$0.75xT_{max}$). This value is higher than the service load of 0.625xdesign load, but compared to the value obtained by J.Ebireri[2] (0.79xdesign load) it is slightly lower.

Comparison of the load at first yield of steel in the case of reinforced concrete and partially prestressed concrete beams shows that the yield load of reinforced concrete beams are higher than that of partially prestressed concrete beams when prestressing wires are excluded. The prestressing wires yield at very high load level or were only near yield at failure.

Comparison of the load at first yield of the longitudinal bars and stirrups shows that the yield load of stirrups is higher than that of the longitudinal bars.

b) Ultimate load

The ratio of experimental ultimate load to design load in table 5.5 shows that most of the beams tested in this investigation failed at the maximum bending load or in excess of the maximum bending load, but only two beams failed at the

maximum torsion load. Beams A1,A2,B1 and B2 failed at a load slightly less than the maximum torsion load. The reason for this may be attributed to the improper use of centre–line to calculate enclosed area of beam for shear stress. This has been discussed in section 2.2.2.2 and in appendix C. In appendix C is compared the differences in the alternative centreline location used for calculating enclosed area of section A_o . It was observed that the application of longitudinal bar centreline gives about +8.5% more torsional steel than the wall centreline approach adopted in this study. For beams with a small amount of torque, this difference is insignificant. However for high torsional loading, the difference could be very significant. For example, for a torque of 32 kN.m which is T_{max}, the beam is underreinforced by about 2.7 kN.m with centreline approach. This could be one of the main reasons for the early failure. The CEB–FIP[25] recommendation for the design of torsion is based on this concept.

The average ultimate failure loads for all the beams tested in this study is $(1.04xM_{max}, 0.97xT_{max})$. This result shows that the classical ultimate limit capacity concept gives very satisfactory failure loads under multiple load cases.

Table 5.5 Summary of experimental results

Test beam N°s	Cracking load maximum load		Load at displ span/250 maximum load		Load at 0.3mm crackwidth maximum load	
	M_c/M_{max}	T_c/T_{max}	M_{250}/M_{max}	T_{250}/T_{max}	$M_{0.3}/M_{max}$	$T_{0.3}/T_{max}$
A1	0.30	0.0	0.65	0.80	-	-
A2	0.0	0.30	0.50	0.70	0.80	0.70
A3	0.15	0.10	0.60	0.70	0.80	0.60
A4	0.30	0.0	0.50	0.70	0.55	0.85
B1	0.10	0.30	0.50	0.70	0.60	0.70
B2	0.40	0.20	0.50	0.70	0.70	0.40

Table 5.5 (continued) Summary of experimental results

Test beam N°s	Load at first yield of steel maximum load				Ultimate load maximum load	
	for long bars		for stirrups			
	$M_{ly}/Mmax$	$T_{ly}/Tmax$	$M_{sy}/Mmax$	$T_{sy}/Tmax$	$M_u/Mmax$	$T_u/Tmax$
A1	0.75	0.80	0.60	0.80	0.90	0.95
A2	0.75	0.70	0.75	0.70	1.00	0.95
A3	0.70	0.80	1.00	1.00	1.10	1.05
A4	0.50	0.70	0.70	0.75	1.10	1.05
B1	0.60	0.80	0.60	0.70	1.05	0.90
B2	0.60	0.60	0.80	0.70	1.10	0.90

CHAPTER 6

THEORETICAL INVESTIGATIONS

6.1 INTRODUCTION

The aim of this chapter is to analyse the beams tested using a non–linear finite element program. Before this a brief review of the non linear analysis and the finite element technique adopted are presented.

In problems of linear elastic stress analysis the differential equations governing the solution are linear. In numerical stress analysis, non–linear solution involves the solving of a series of linear problems. The phenomena introducing non linearity (e.g. plasticity, creep etc.,) are handled while satisfying basic laws of continum mechanics; equilibrium, compatibility and constitutive relationship of the materials.

The main causes of non–linearity in structures are :– [33,34]

a) Geometric non–linearity

b) Material non–linearity

Geometric non–linearity is caused by large displacement which alter the shape of the structure such that the equilibrium equations have to be considered in terms of the displaced position of the structure.

Material non–linearity occurs due to changes in the basic stress– strain relationship caused by plasticity, cracking, creep etc. In reinforced concrete structures, cracking and crushing of concrete and yielding of reinforcing steel are the main causes of non–linear behaviour. In this study, only the short term non–linear behaviour of reinforced concrete is considered.

Generally, the accuracy of a non–linear solution depends on the accuracy of the material law, numerical procedure used, and the basic finite element approximation. For economical but reasonably accurate solution, some degree of error is normally tolerated.

6.2 REVIEW OF NON—LINEAR ANALYSIS

6.2.1 Numerical appraoch for non–linear analysis (33,34)

In small strain linear elastic problems, using the displacement approach of the finite element technique, the external nodal force are related to the nodal displacement {d} through the element constant stiffness matrix [K] in the form

$$\{P\} = [K].\{d\} \qquad \text{.....(6.1)}$$

This relationship assumes a linear elastic constitutive law as:

$$\{\sigma\} = [D].[\{\epsilon\} - \{\epsilon_0\}] + \{\sigma_0\} \qquad \text{.....(6.2)}$$

where

$[D]$ = constant linear elastic material property matrix.

σ, ϵ = final stress and strain respectively.

σ_0, ϵ_0 = initial stress and strain respectively.

Generally, in structural analysis problems involving small displacement for which a varying constitutive relationship D applies, condition of displacement continuity and equilibrium must still be satisfied. Equa 4.2 is still valid provided that yield criterion $F(\sigma, \epsilon)$ is not violated i.e $F(\sigma, \epsilon) < 0$. However, if the material yields i.e.

$$F(\sigma, \epsilon) = 0 \qquad \text{.....(6.3)}$$

then a new material law has to be used. This relationship is generally non–linear. The solution of equa. 6.1 when [K] is not constant is obtained by a succession of linear approximations. This forms the basis of the non–linear approach.

The finite element method uses one of the following techniques for the solution of non–linear problems:

a) Incremental procedure

b) Iterative procedure

c) Incremental–Iterative procedure

The above techniques will not be described in this chapter. All the details of this techniques are given in references (33,34,35).

6.2.2 Procedures in non-linear analysis

The following are the basic steps of non-linear analysis.

1) Apply load increment and calculate trial incremental displacement.

$$\Delta\{d_n\} = [K]^{-1}.\{\Delta P\} \quad \text{.....(6.4)}$$

where ΔP = load increment

[K] = stiffness matrix based on material law at the start of loading.

2) Estimate total displacement and strains at this stage :

$$\{d_{n+1}\} = \{d_n\} + \Delta\{d_n\}$$

$$\Delta\epsilon_n = [B].\Delta d_n$$

$$\{\epsilon_{n+1}\} = \{\epsilon_n\} + \Delta\{\epsilon_n\} \quad \text{.....(6.5)}$$

3) Calculate the total stress σ_{n+1} from present material properties

$$\Delta\sigma_n = [D].\Delta\epsilon_n$$

$$\{\sigma_{n+1}\} = \{\sigma_n\} + \Delta\{\sigma_n\}$$

4) Check total stress against relevant yield surface.

$$F(\sigma_{n+1}, \epsilon_{n+1}) = 0$$

If total state of stress does not cause yielding, repeat steps 1 to 4.

5) If the state of total stress violates the yield criterion, modify the material constitutive matrix and then bring the state of stress back to the yield surface. Calculate excess force F^{ex} .

$$F^{ex} = \{P_{n+1}\} - \int B^T.\sigma_0.dv \quad \text{.....(6.6)}$$

6) Add excess force to present load vector, and reanalyse the structure

$$\Delta\{d_n\} = [K^{-1}].F^{ex} \quad \text{.....(6.7)}$$

Check for force and displacement convergence, if satisfied, proceed to step 1 and repeat.

7) Go back to step 2 and repeat process until convergence is achieved.

6.3 FINITE ELEMENT TECHNIQUE

The finite element method has been widely used in structural analysis. Its basic principles are well known [33–37]. The main advantage of this method is its versatility. However, the accuracy of any analysis greatly depends on the choice of the finite element model adopted.

In this investigation attention is concentrated on the analysis of "thin–walled" beams under bending and torsional loadings. Considering the complex behaviour of hollow beams, a detailed analysis would normally require a full three dimensional finite element model. A full three dimensional finite element analysis requires six degrees of freedom (three translations and three rotations) per node of the element. However, such models demand very large computer capacity and time, and therefore very expensive. Various simplified two dimensional finite element models have been proposed [2,38,39] with two main objectives in mind :

a) To reduce expensive computation associated with three dimensional analysis.

b) To produce a simple, acceptable analytical approach.

The model proposed in reference 2 was the one adopted in this study.

A study of the structural behaviour of thin–walled beams indicates that the main stress condition are those of inplane stresses in the plates of the box girder. In steel box girders, cross–sectional distortional stresses are also important. However, in the case of concrete box girders, this may not be the case, provided the individual plates are reasonably thick and there are sufficient diaphragm to prevent cross–sectional distortion. Therefore, it can be represented by an assemblage of plane stress elements to account for the major stresses and zero stiffness assumed for out of plane bending action of the component plates. Figure 6.1 shows the rectangular plane stress element with two degree of freedom per node adopted in this investigation. The two–dimensional idealisation of box girders is adequate provided compatibility of displacement between adjoining plates along the line of intersection is maintened and cross–sectional distortion is reduced to minimum.

The advantage of this approach over a full three–dimensional finite element

solution is that it leads to cheaper computations while at the same time the main stresses are obtained with reasonably accuracy.

To achieve these objectives, the following techniques has been adopted as shown in figure 6.2.

1) To ensure shear transfer between adjoining plates of the beam, compatibility of displacements along the line of intersection at the common edge of adjoining plates is maintained by introducing geometrical constraints, as shown in figure 6.3.

2) To reduce cross–sectional distortion, end diaphragms are introduced into the analysis.

The mesh and the boundary conditions adopted in this theoretical study are shown in figure 6.4.

6.4 NUMERICAL PROCEDURE ADOPTED IN THE PROGRAM

The procedure adopted in the program can be summarised as follows:

a) Read in the beam's geometrical properties, material properties, design loads and the exact quantity of steel used as input data.

b) Using the initial uncracked materials properties, the program performs an elastic analysis to obtain deflections and stress distribution ($\sigma_x, \sigma_y, \tau_{xy}$) at every Gauss point in each element.

c)An incremental non–linear analysis is then performed until failure.

d) The serviceability and ultimate behaviour of all the beams tested in this study are checked with respect to the following:

1) Deflections: – The program outputs deflections and stress distribution at each load increment. However, the initial deflection and stresses under the design load are obtained with the elastic stiffness of the section. Assuming that only live load is applied to the members, the service deflection is taken as the deflection corresponding to a load of $P_d/1.6$ (i.e. an ultimate load factor of 1.6 is assumed).

2) Yielding of steel: – The stress in the reinforcing steel is calculated during the non–linear analysis. A yield strain of 2.5×10^{-3} is assumed for steel.

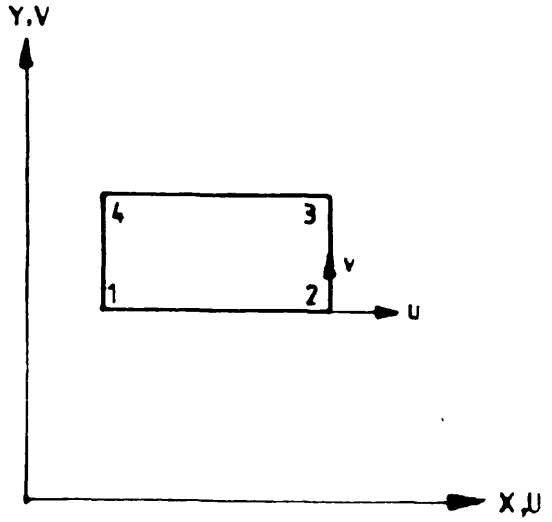

Figure 6.1 Improved simplified finite element model by J.Ettiredi

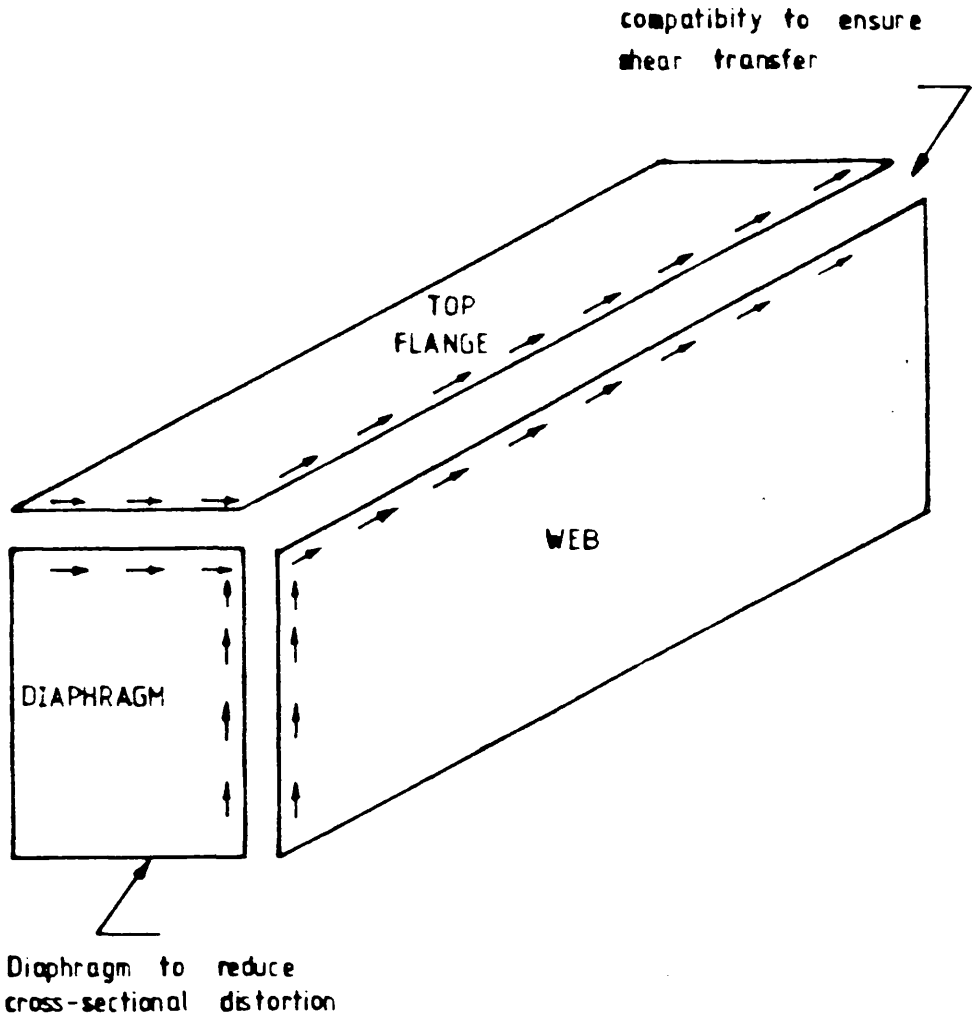

Figure 6.2 Idealisation of box beam in plane stress analysis

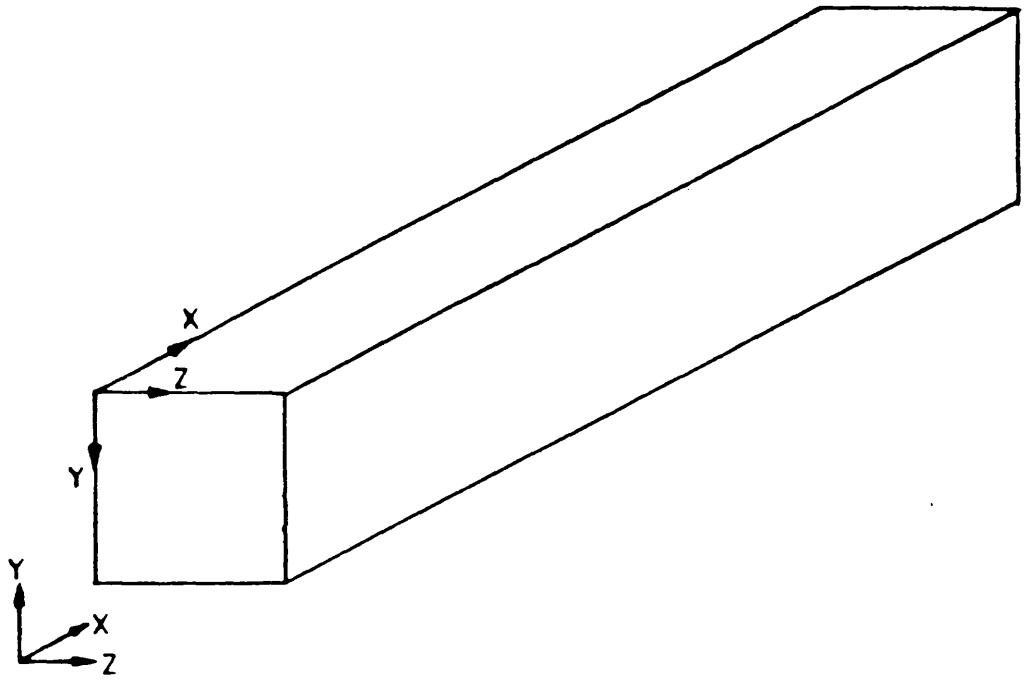

a) GENERAL VIEW OF RECTANGULAR BOX BEAM

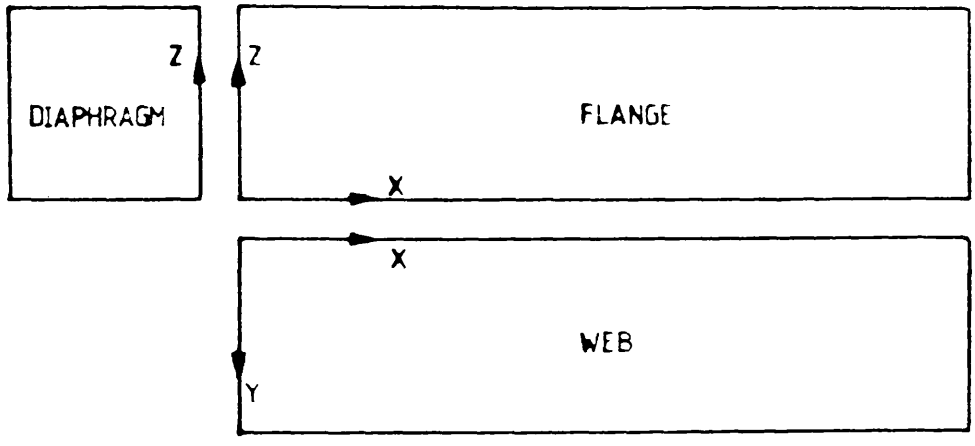

b) LAYOUT OF BOX BEAM UNITS FOR PLANE STRESS ANALYSIS

Figure 6.3 Two dimensional idealisation of a box beam.

Figure. 6.4 BOUNDARY CONDITIONS FOR SERIES A BEAMS UNDER COMBINED BENDING AND TORSION

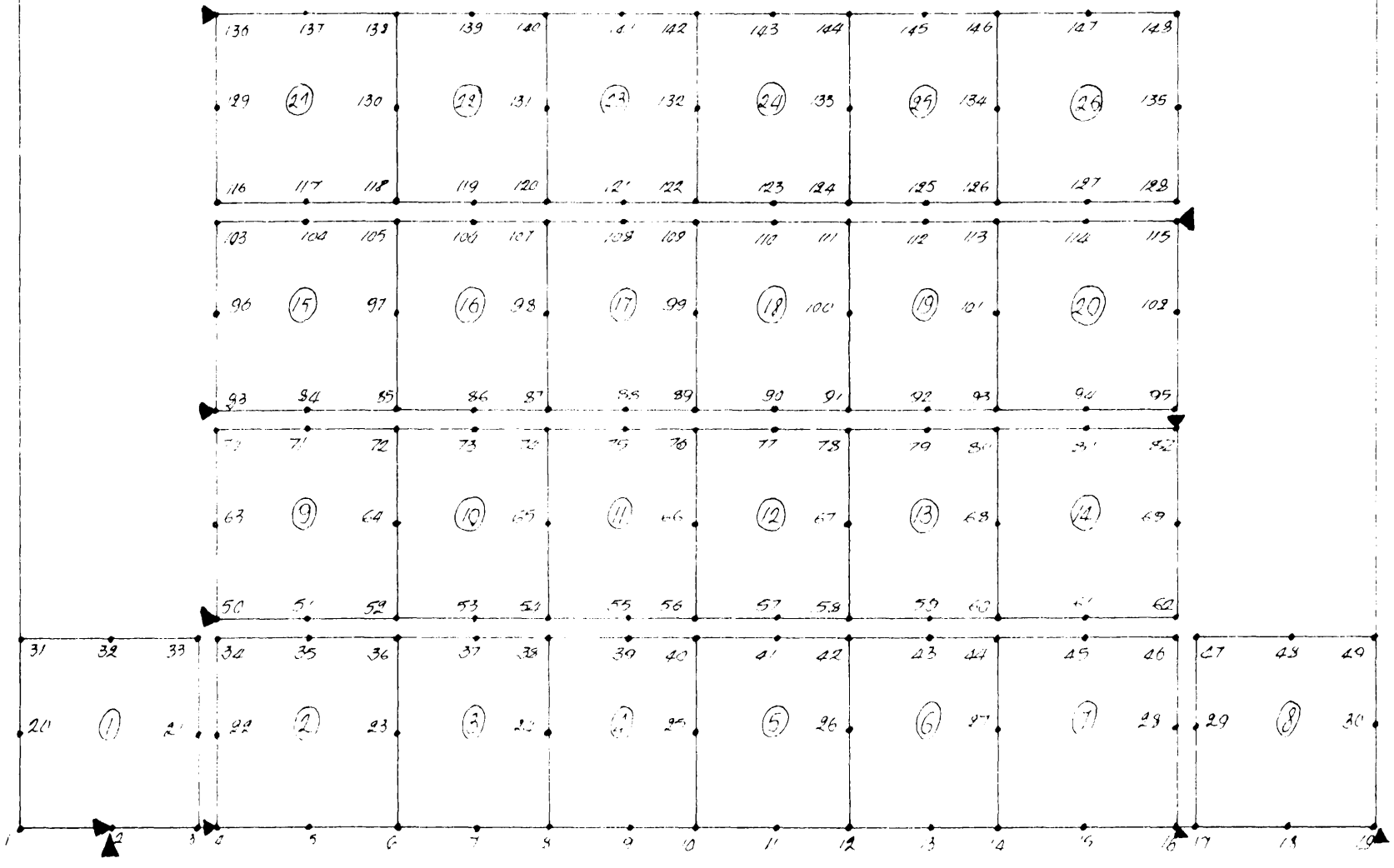

3) Cracking and crushing of concrete: – A crack is assumed to occur when the principal stress exceeds the tensile strength of concrete. The development of cracks is closely monitored during the analysis. A limit crack width of 0.3mm is assumed for serviceability ckeck.

4) Ultimate load: – The ultimate failure load of the beams tested and stress distribution are also considered. Failure is attained when reinforcing steel in many elements has yielded and very large displacements are obtained and it becomes impossible to obtain convergence.

Further details of the program used for the analysis are found in reference (30).

6.5 COMPARISON OF EXPERIMENTAL AND THEORETICAL RESULTS OF TESTED BEAMS

Only reinforced concrete beams were studied theoretically. For lack of time the partially prestressed beams were not analysed.

Table 6.1 and figures 6.5 to 6.7 show the results of the comparison between theoretical and experimental studies. The results are discussed under the two headings.

6.5.1 *Service behaviour*

The post–cracking region of the load–deflection relationship at the midspan of the beams shows good agreement between theory and experiment. At service load, the average ratio of theoretical to experimental deflection at midspan was 0.91. The maximum steel strain at service load was also examined. It was observed that both theoretical and experimental results show very good correlation. The average ratio of theoretical to experimental maximum steel strain at service load was 0.96.

In the theoretical analysis, it was observed that all the steel yielded outside the service load. The load at first yield of steel was higher for the case of theoretical analysis (0.9 design load) than for the case of experimental tests (0.7

design load). The average ratio of theoretical to experimental load at first yield of steel was 1.28.

6.5.2 *Ultimate load*

Comparison of final failure loads for both theoretical and experimental investigations shows very good agreement. The average ratio of theoretical to experimental ultimate load was 0.94.

From the above results, we conclude that both theoretical and experimental analysis agree satisfactorily at both service and ultimate load levels.

Table 6.1 Comparison of theoretical and experimental results of tested beams

Beam N^0	Cracking load P_{crT}/P_{crE}	Service load($0.625xP_d$)		Load at yield of steel P_{yT}/P_{yE}	Ultimate load P_{uT}/P_{uE}
		Displct δ_{sT}/δ_{sE}	Strains $\epsilon_{sT}/\epsilon_{sE}$		
A1	1.25	1.25	1.50	1.17	1.02
A2	1.66	0.71	0.94	1.25	0.97
A3	1.66	1.05	0.75	1.20	0.88
A4	1.43	0.67	0.75	1.50	0.83

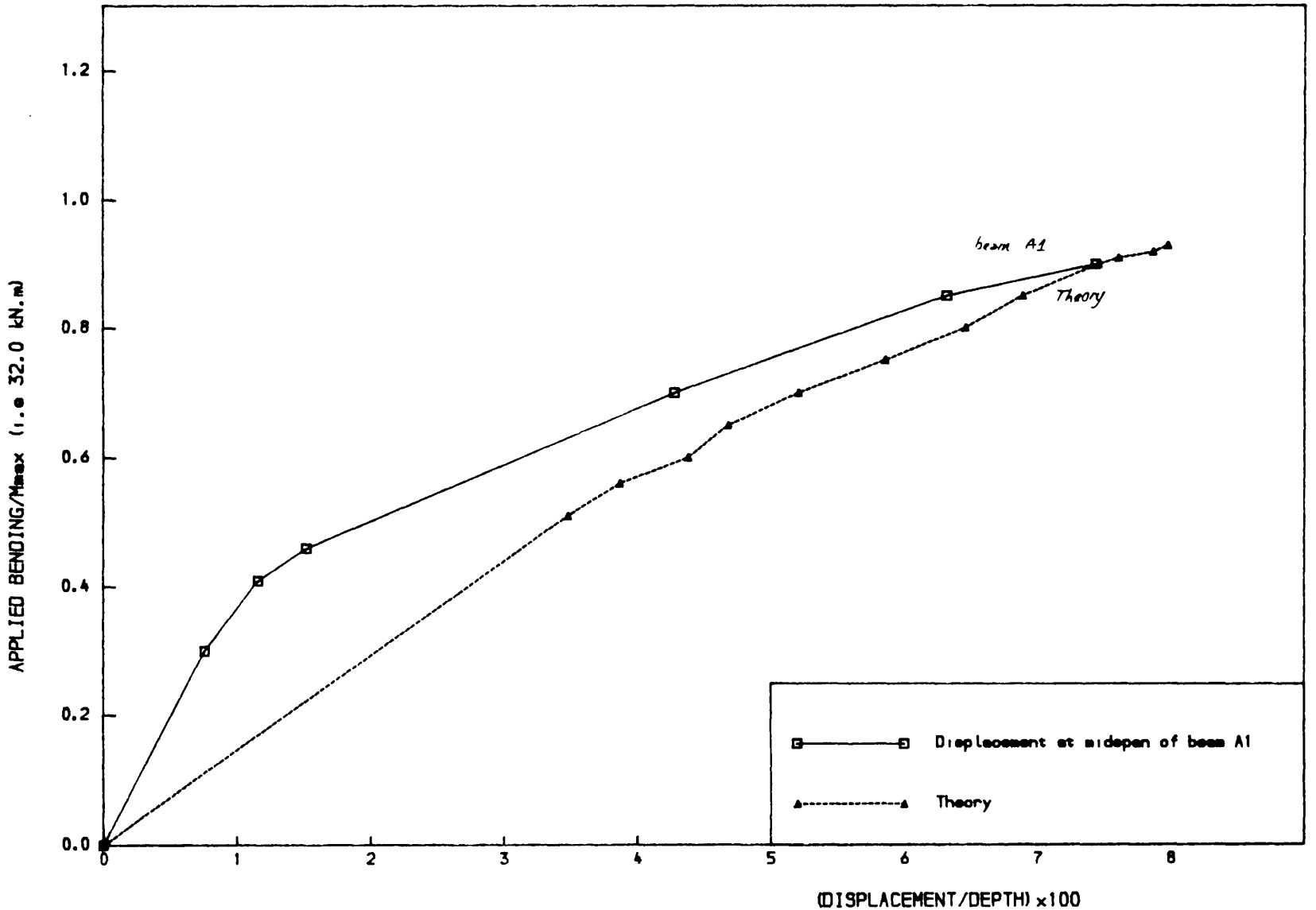

FIGURE 6.5 COMPARISON OF EXPERIMENTAL AND THEORETICAL DEFLECTION CURVES

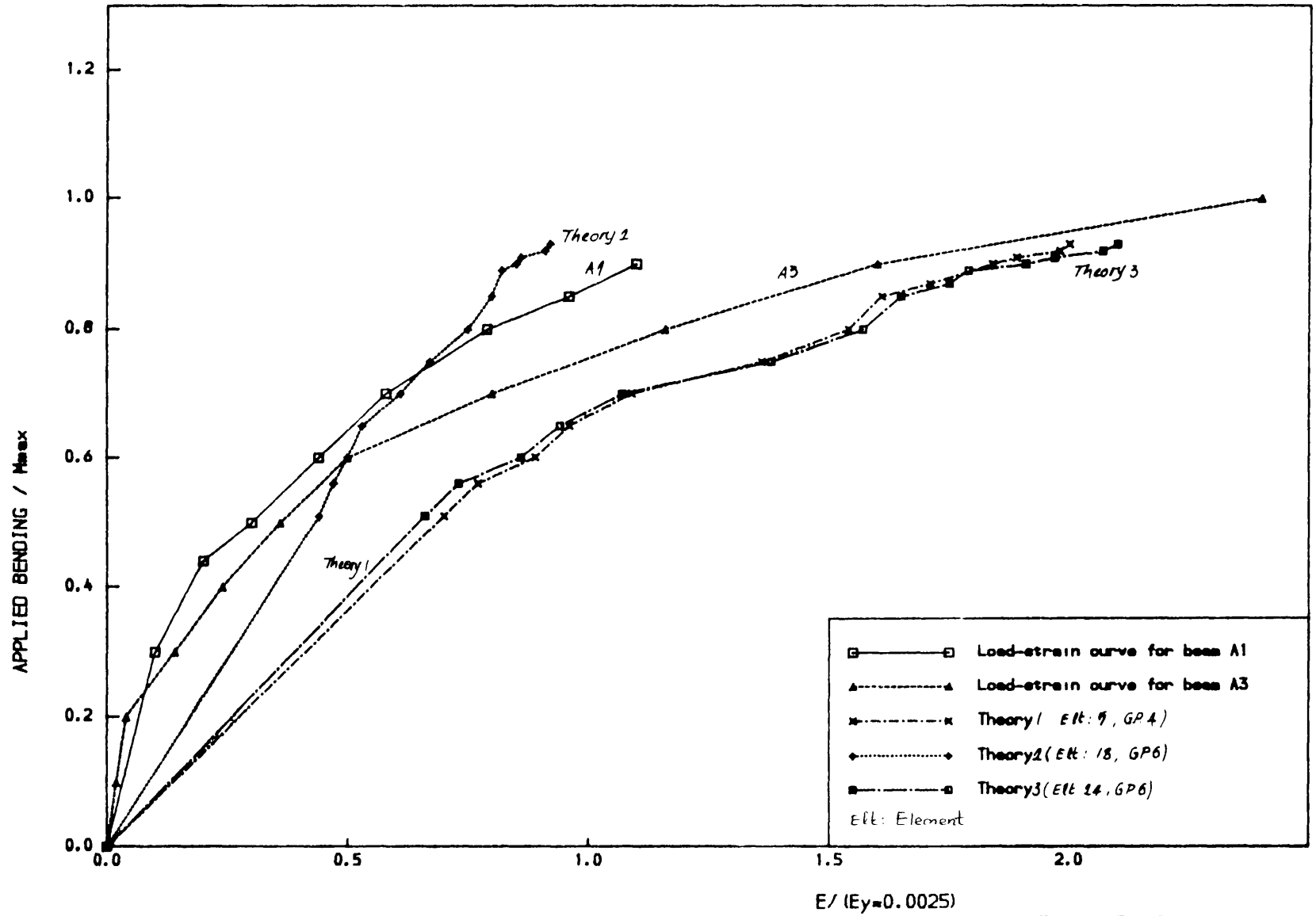

FIGURE 6.6 COMPARISON OF EXPERIMENTAL AND THEORITICAL LOAD-STEEL STRAIN CURVES FOR THE LONGITUDINAL BARS

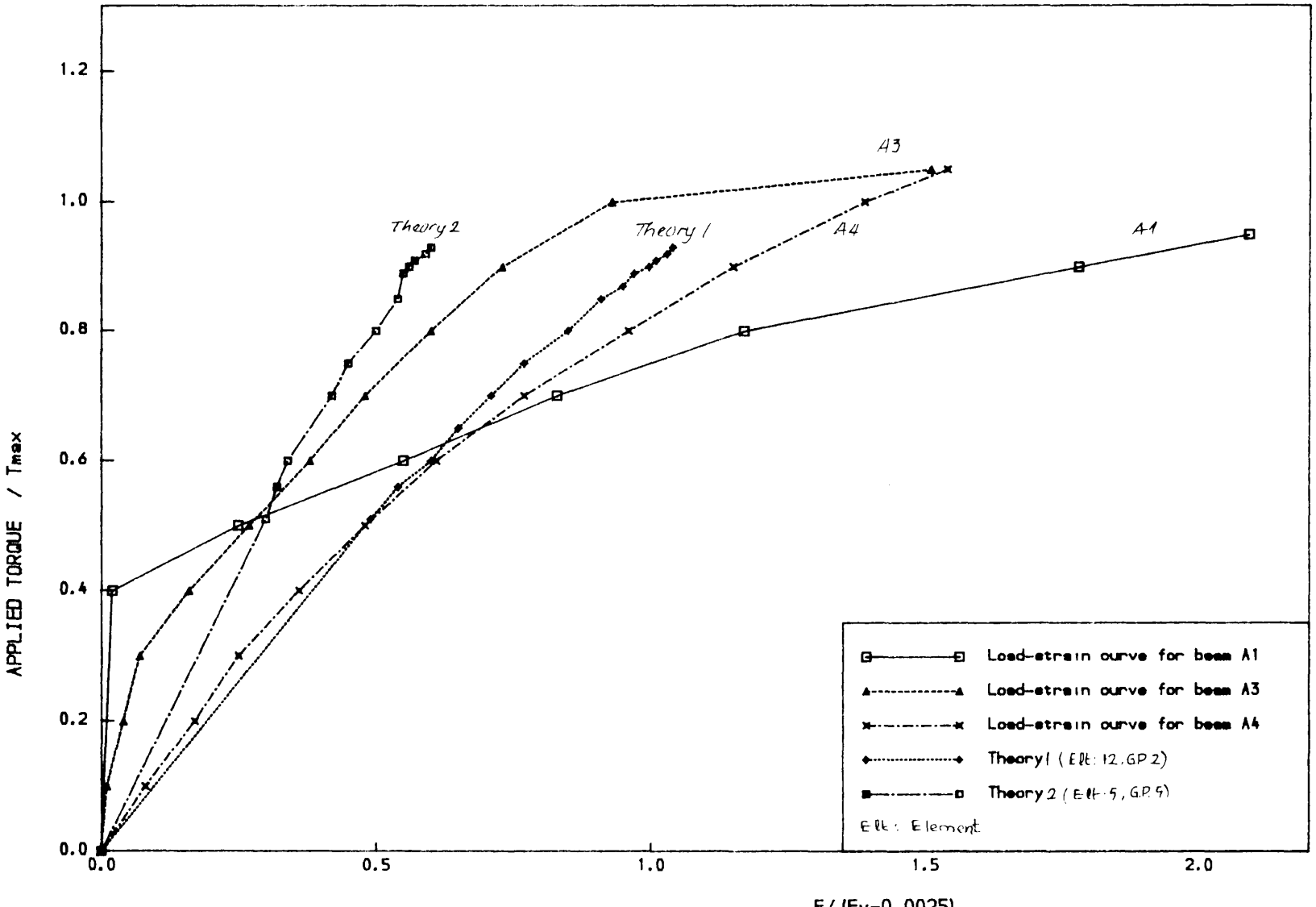

FIGURE 6.7 COMPARISON OF EXPERIMENTAL AND THEORETICAL LOAD-STEEL STRAIN CURVES FOR THE STIRRUPS.

CHAPTER 7

CONCLUSIONS AND RECOMMENDATIONS

7.1 CONCLUSION

From the experimental and theoretical investigations reported in this thesis, the following conclusions can be drawn:

1– The direct design method based on classical ultimate limit capacity concept[5,6,31] was used to design the beams tested in this study. It was observed that the approach predicted satisfactorily the behaviour of beams subjected to multiple combinations of bending and torsional loadings.

2– The results indicate that at service load (0.625xdesign load) both deflections and crack widths were within the limits recommended by the British Standard Code BS8110[26]. Average crackwidth of 0.3mm was reached at ($0.69xM_{max}$, $0.65xT_{max}$).

3– No steel yielded within the service load limit. The average load at first yield of steel for all the beams tested was ($0.70xM_{max}$, $0.75xT_{max}$).

4– The average ultimate load for all the beams was ($1.04xM_{max}$, $0.97xT_{max}$). However, four of the beams tested (A1,A2,B1,B2) failed at approximately 92% of the maximum torsional load. This behaviour is attributed to the use of a longer centreline in calculating the enclosed area of section A_o for torsional shear stress resulting in less steel area.

5– The general behaviour of the beams tested is similar to the behaviour of beams subjected to monotonic, increasing proportional loading.

6– The non linear finite element program used in this study proved to be a useful tool for the analysis of reinforced concrete hollow beams under multiple combinations of bending and torsional loadings. Good agreement was obtained between theoretical and actual behaviour of beams in almost all cases.

7– The use of polysterene has given satisfaction for the casting of the hollow beams tested. It is a cheap material and does not need any fabrication.

8– It is recommended (from the casting of the tested beams) to increase the wall thickness from 50mm to 60mm.

7.2 RECOMMENDATIONS FOR FURTHER WORK

1– The experimental and theoretical investigations presented in this thesis pertains only to beams. It is recommended to extend the study to other elements of structure such as slabs and columns.

2– The beams investigated in this study are subjected to only multiple combinations of bending and torsional loadings. It is recommended that multiple combinations of bending, shear force and torsional loadings should be studied in future investigations.

3– Only partially prestressed concrete beams were studied in this investigation. It is recommended to extend the study to fully prestressed concrete beams.

APPENDIX A

Appropriate centre– line for the calculation of torsion in beams.

The general equation for calculating torsional shear in beams is given as :

$$\tau = T/(2.A_o.t) \qquad \text{.....(A1)}$$

Where τ = shear stress

t = thickness of beam wall

T = applied torque

$A_o = (x_1.y_1)$, enclosed area of centre– line

The resulting shear stress from above equation depends on the exact enclosed area A_o adopted. Accordingly, the steel area required to resist the applied shear is directly influenced by the location of the centre– line. The following three types of alternative centre– line can be used.

a) Centre– line of thickness of beam wall.

b) Centre– line of stirrups.

c) Centre– line of longitudinal bars

Figure A1 shows part details of section 300x300x50mm .

Enclosed area A_o is then obtained as follows :

a) A_o from centre– line of beam wall

$A_o = (300 - 2(15 + 10))^2 = 250^2$ mm^2

b) A_o from centre– line of stirrups

$A_o = (300 - 2(15 + 5))^2 = 260^2$ mm^2

c) A_o from centre– line of longitudinal bars

$A_o = (300 - 2(15 + 10 + 5))^2 = 240^2$ mm^2

The centre– line of the beam wall was adopted in calculating the enclosed area A_o in this investigation. If the stirrup centre– line was used, an increased enclosed area A_o will be obtained resulting in a reduction of about 8.2% in the quantity of steel required to resist a similar loading. However, if the centre– line of longitudinal bars is adopted, a reduced enclosed area is obtained. Accordingly, more quantity of steel is required to resist

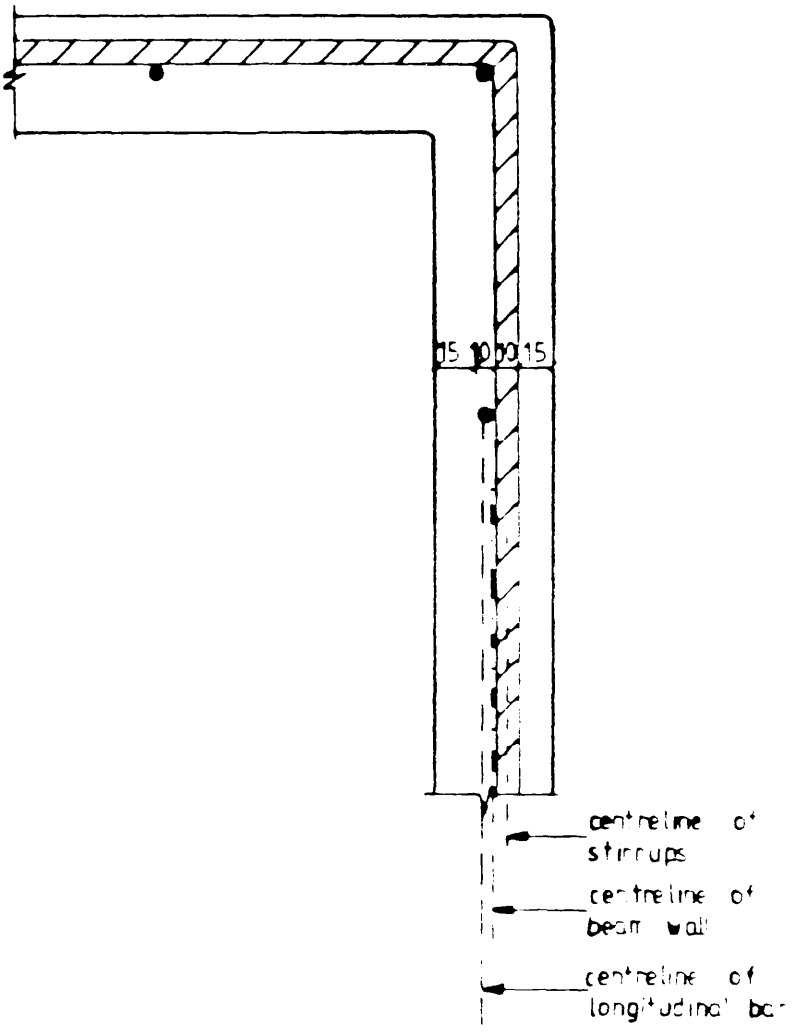

Figure A.1 Various centrelines locations for calculating enclosed area, Ao, of beams subjected to torsion.

similar loading. An increase of 8.5% is obtained compared to the centre–line approach adopted. This method is recommended in CEB–FIP model code[25].

APPENDIX B

Contribution of self weight and sundries to total moments on test beams.

Square sections (300mmx300mm)

1) Self weight of solid end of beam 580mm.

$0.3 \times 0.3 \times 24 = 2.16$ KN/M

2) Self weight of effective span of beam (hollow section)

$((0.3 \times 0.3) - (0.2 \times 0.2)) \times 24 = 1.2$ KN/M

3) Self weight of torsion arm = 3.0 KN

4) Self weight of secondary beam = 0.65 KN

Reaction $R_a = (2.16 \times 0.58) + 3.0 + 0.33 + (1.2 \times 1.32) = 6.17$ KN

Moment of midspan is

$(6.17 \times 1.9) - (1.2 \times 1.32^2/2) - (0.33 \times 0.6) - (3.0 \times 1.78)$

$- (2.16 \times 0.58 \times 1.61) = 3.12$ KN.M

This value represents 10% 0f the maximum bending applied. This means that the actual bending applied is M + 0.1M = 1.1M.

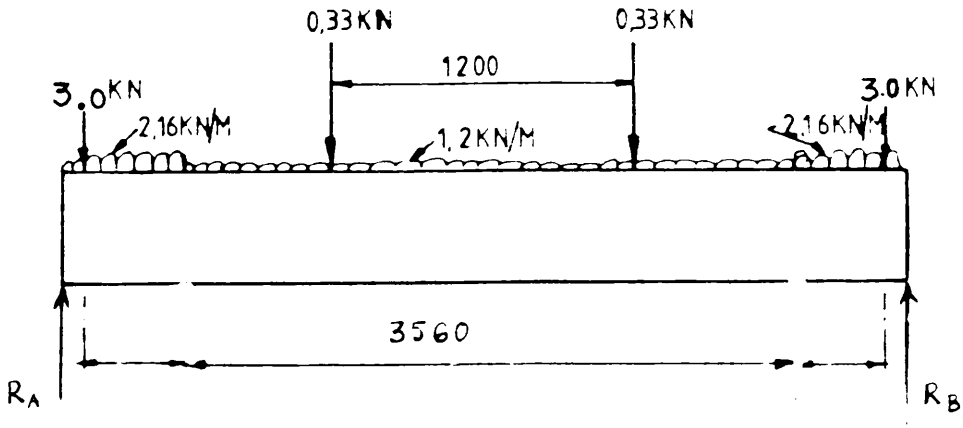

REFERENCES

1. Hsu, T.T.C., " Torsion of Reinforced Concrete ", Van.Nostrand Reinhold Company, 1984.

2. Ebireri, J.," Direct Design of Beams for Combined Bending and Torsion", Ph.D Thesis, Department of Civil Engineering, University of Glasgow, May 1985.

3. Wood, R.H.," The Reinforcement of Slabs in Accordance with a Pre-Determined Field of Moments", Concrete, Feb 1968, pp 69-76.

4. Armer, G.S.T., Correspondence on " The Reinforcement of Slabs in Accordance with a Pre-Determined Field of Moments", Concrete, Aug 1968, pp 319-320.

5. Nielsen, M.P., " Yield Conditions for Reinforced Concrete Shells in the Membrane State", Non classical shell problems, IASS Symposium, Warsaw 1963, pages 1030-1038.

6. Clark, L.A.," The Provision of Tension and Compression Reinforcement to resist in plane forces", Magazine of Concrete Research. Vol.28 (N^0 94), March 1976, pp 3-12.

7. Cowan, H.J. " Reinforced and Prestressed Concrete in Torsion. " Edward Arnold, 1965.

8. McHenry, D and Karni J., " Strength of concrete under combined tensile and compressive stresses", Journal of the American Concrete Institute, Proc.vol 54, April 1958 , pp 829-839 .

9. BS8110 : Part 2 . 1985
Code of practice for the structural use of concrete,
British Standards Institution , London 1985.

10. Lampert, P. and Collins, M.P. "Torsion, Bending and Confusion -an attempt to establish the facts", Journal of the American Concrete Institute. August 1972, pp 500-505 .

11. Kuyt, B. " A Theoretical Investigation of Ultimate Torque as calculated by Truss Theory and by the Russian Ultimate Equilibrium Method", Magazine of Concrete Research, vol 23, N° 77, December 1971 , pp 155-180 .

12. Thurlimann, B. " Shear Strength of Reinforced and Prestressed Concrete Beams -CEB Apprach", Journal of the American Concrete Institute, SP 59 , 1978, pp 93-115.

13. Thurlimann, B. " Torsional Strength of Reinforced and Prestressed Concrete Beams -CEB Approach", Journal of the American Concrete Institute , SP 59, 1978, pp 117-143.

14. Branson, D.E. " Design Procedures for Computing Deflections", Journal of the American Concrete Institute. Proc, vol 65, Septembre 1968, pp 730-742.

15. Gilbert,R.I. " Deflections of Reinforced Concrete Beams –a Design Approach", Dept of Civil Engineering, University of New South Wales Kensington, UNICIV Report, N° R-201, December 1981.

16. Beeby, A.W. " An Investigation in Slabs Spanning oneway", Cement and Concrete Association; Technical Report, TRA 433, April 1970.

17. Hsu, T.T.C., and Mo, Y.L., "Softening of Concrete in Torsional Members - Theory and Tests", ACI Journal, Proc, vol 82, May-June 1985, pp 290-303.

18. Hsu, T.T.C., and Mo, Y.L., "Softening of Concrete in Torsional Members –Design Recommendations", ACI Journal, Proc, vol 82, July-August 1985, pp 443-452.

19. Hsu, T.T.C., and Mo, Y.L., "Softening of Concrete in Torsional Members - Prestressed Concrete", ACI Journal, Proc, vol 82, September-October 1985 , pp 603-615 .

20. Stankowski, T and Gerstle, K.H "Simple Formulation of Concrete Behaviour under Multiaxial Load Histories", ACI Journal, Proceedings, V.82, N^0 2, March-April 1985, pp 213-221.

21. Park, R and Paulay, T., " Reinforced Concrete Structures ", Wiley, New York, 1975.

22. Collins, M.P and Mitchell, D., " Shear and Torsion Design of Prestressed and Non–Prestressed Concrete Beams ", Journal of the Prestressed Concrete Institute, V.25, N°5, Sept–Oct 1980,pp32-100.

23. Nawy, E.G., " Crack Control in Reinforced Concrete Structures ", ACI Journal, Proceedings V.65, N° 10, Oct 1968, pp 825–836

24. Cook, N.E and Gerstle, K. H., " Load History Effects on Structural Members ", Journal of Structural Engineering, ASCE, Vol.111, N° 3, Mar 1985, pp 628-640

25. CEB–FIP Model Code for Concrete Structures, 3rd Edition, Comite Euro–International du Beton/Federation Internationale de la Precontrainte, Paris, 1978, 348pp.

26. BS 8110 : Part 1, 1985
Code of practice for the structural use of concrete
British Standards Institution, London 1985 .

27. Hago, A.W.," Direct Design of Reinforced Concrete Slabs", Ph.D Thesis, Department of Civil Engineering, University of Glasgow, May 1982.

28. Memon, M.," Strength and Stiffness of Shear Wall-Floor Slab Connections", Ph.D Thesis, Department of Civil Engineering, University of Glasgow, Jan 1984.

29. El-Nounou, G.F.R.," Design of Shear Wall -Floor Connections", Ph.D Thesis, Department of Civil Engineering, University of Glasgow, Aug 1985.

30. Abdelhafiz, L.," Direct Design of Reinforced Concrete Skew Slabs", Ph.D Thesis, Department of Civil Engineering, University of Glasgow, Oct 1986.

31. Nielsen, M.P.
Optimum design of reinforced concret shell and slabs
Structural Research laboratory, Technical University of Denmark.
Report, NR.R44 , 1974 , pages 190-200 .

32. Saadi, R.
Direct design of partially prestressed beams for combined bending and torsion. Msc thesis in preparation, civil engineering dept, University of Glasgow, 1988.

33. Owen, D.R.J and Hinton, E., " Finite Element in Plasticity ", Prineridge press, 1980

34. Zienkiewicz, O.C., " Finite Element Method in Engineering Science", Mc Graw– Hill, London, 1976.

35. Phillips, D.V., "Non Linear Analysis of Structural Concrete by Finite Element Method". Ph.D thesis, University of Wales, 1973.

36. Hinton, E and Owen, D.R.J., "Finite Element Programming". Academic press, 1977.

37. Cheung, Y.K and Yeo, M.F., " A Practical Introduction to Finite Element Analysis", Pitman, London, 1979.

38. Scordelis, A.C., "Analytical Solutions for Box Girders Bridges." Development in Bridge Design and Construction. Edited by K.C Rockey et al. University of Cardiff Crosby Lockwood, 1971

39. Sawko, F and Cope, R.J., "Analysis of Multi-Cell Bridges Without Transverse Diaphragms, a Finite Element Approach", The structural Engineer, Vol.47, N^{0} 11, Nov 1969.